AD_____

Award Number: DAMD17-98-1-8246

TITLE: Nuclear Tubulin: A Novel Target for Breast Cancer Chemotherapy

PRINCIPAL INVESTIGATOR: Richard F. Luduena, Ph.D.

CONTRACTING ORGANIZATION: The University of Texas
Health Science Center at San Antonio
San Antonio, Texas 78284-7828

REPORT DATE: May 2001

TYPE OF REPORT: Final

PREPARED FOR: U.S. Army Medical Research and Materiel Command
Fort Detrick, Maryland 21702-5012

NOTICE

USING GOVERNMENT DRAWINGS, SPECIFICATIONS, OR OTHER DATA INCLUDED IN THIS DOCUMENT FOR ANY PURPOSE OTHER THAN GOVERNMENT PROCUREMENT DOES NOT IN ANY WAY OBLIGATE THE U.S. GOVERNMENT. THE FACT THAT THE GOVERNMENT FORMULATED OR SUPPLIED THE DRAWINGS, SPECIFICATIONS, OR OTHER DATA DOES NOT LICENSE THE HOLDER OR ANY OTHER PERSON OR CORPORATION; OR CONVEY ANY RIGHTS OR PERMISSION TO MANUFACTURE, USE, OR SELL ANY PATENTED INVENTION THAT MAY RELATE TO THEM.

LIMITED RIGHTS LEGEND

Award Number: DAMD17-98-1-8246
Organization: The University of Texas Health Science Center

Those portions of the technical data contained in this report marked as limited rights data shall not, without the written permission of the above contractor, be (a) released or disclosed outside the government, (b) used by the Government for manufacture or, in the case of computer software documentation, for preparing the same or similar computer software, or (c) used by a party other than the Government, except that the Government may release or disclose technical data to persons outside the Government, or permit the use of technical data by such persons, if (i) such release, disclosure, or use is necessary for emergency repair or overhaul or (ii) is a release or disclosure of technical data (other than detailed manufacturing or process data) to, or use of such data by, a foreign government that is in the interest of the Government and is required for evaluational or informational purposes, provided in either case that such release, disclosure or use is made subject to a prohibition that the person to whom the data is released or disclosed may not further use, release or disclose such data, and the contractor or subcontractor or subcontractor asserting the restriction is notified of such release, disclosure or use. This legend, together with the indications of the portions of this data which are subject to such limitations, shall be included on any reproduction hereof which includes any part of the portions subject to such limitations.

THIS TECHNICAL REPORT HAS BEEN REVIEWED AND IS APPROVED FOR PUBLICATION.

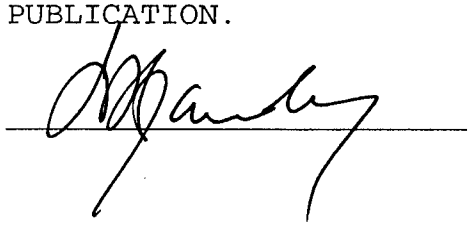

12/15/99

REPORT DOCUMENTATION PAGE

Form Approved
OMB No. 074-0188

1. AGENCY USE ONLY (Leave blank)	2. REPORT DATE	3. REPORT TYPE AND DATES COVERED
	May 2001	Final (1 May 98 - 30 Apr 01)

4. TITLE AND SUBTITLE
Nuclear Tubulin: A Novel Target for Breast Cancer Chemotherapy

5. FUNDING NUMBERS
DAMD17-98-1-8246

6. AUTHOR(S)
Richard F. Luduena, Ph.D.

7. PERFORMING ORGANIZATION NAME(S) AND ADDRESS(ES)
The University of Texas
Health Science Center at San Antonio
San Antonio, Texas 78284-7828
Email - luduena@uthscsa.edu

8. PERFORMING ORGANIZATION REPORT NUMBER

9. SPONSORING / MONITORING AGENCY NAME(S) AND ADDRESS(ES)
U.S. Army Medical Research and Materiel Command
Fort Detrick, Maryland 21702-5012

10. SPONSORING / MONITORING AGENCY REPORT NUMBER

11. SUPPLEMENTARY NOTES
Report contains color graphics

12a. DISTRIBUTION / AVAILABILITY STATEMENT
Distribution authorized to U.S. Government agencies only (proprietary information, May 2001). Other requests for this document shall be referred to U.S. Army Medical Research and Materiel Command, 504 Scott Street, Fort Detrick, Maryland 21702-5012.

12b. DISTRIBUTION CODE

13. ABSTRACT *(Maximum 200 Words)*

Our research is based on our observation that the β_{II} isotype of tubulin is found in the nuclei of cultured breast cancer cells. Our goals are to learn the function of β_{II} and to design a novel anti-tumor drug that will target β_{II}. We have found that the process by which β_{II} enters the nucleus is specific for that isotype and that nuclear β_{II}, while very rare in normal cells, is a characteristic of 80% of all tumors, including 100% of breast tumors. We have found that successful anti-tumor drugs (taxol, vinblastine) expel β_{II} from the nuclei of tumor cells. We have also found that the β_{III} isotype may be involved in making tumor cells resistant to oxidation, while the β_{IV} isotype can interact with actin filaments in a process regulated by the β_{I} isotype. We also synthesized a peptidyl-colchicine derivative designed to target the nucleus. Our results indicate that nuclear β_{II} may be very important in the diagnosis, prognosis, biology and treatment of breast cancer.

14. SUBJECT TERMS
Breast Cancer, Tubulin Isotypes, Cell Nucleus, Cancer Chemotherapy, Anti-tumor Drugs

15. NUMBER OF PAGES
272

16. PRICE CODE

17. SECURITY CLASSIFICATION OF REPORT	18. SECURITY CLASSIFICATION OF THIS PAGE	19. SECURITY CLASSIFICATION OF ABSTRACT	20. LIMITATION OF ABSTRACT
Unclassified	Unclassified	Unclassified	Unlimited

TABLE OF CONTENTS

INTRODUCTION

The research reported here is based on the observation that one of the isotypes of tubulin, β_{II}, is found in the nuclei of a wide variety of cancer cells, including breast, prostate, and lung. We have found nuclear β_{II} not only in cultured cancer cells but also in breast cancer *in situ*. We have also found β_{II} in the nuclei of cultured rat kidney mesangial cells. In contrast, we do not see nuclear β_{II} in normal cells. We have had two overall aims in this research: 1) to identify the function of nuclear β_{II}; and 2) to design a drug that will target nuclear β_{II}. Our overall hypothesis in the first aim is that nuclear β_{II} somehow aids in rapid cell proliferation; our objective is to find out how. As we originally proposed, we have microinjected monoclonal antibodies specific for individual tubulin isotypes into both breast cancer and rat kidney mesangial cells and we have found that they have no apparent effect on cell viability and function. Microinjection of antibodies into mesangial cells gave similar results. Accordingly, we developed a variety of approaches to test this hypothesis. This included addressing the mechanism of nuclear β_{II} localization, surveying other cancer cells, including tumors from patients, to see if nuclear β_{II} is a widespread phenomenon, examining the effects of drugs on nuclear β_{II}, and investigating the functions of the β_I, β_{III} and β_{IV} isotypes. We have found that the localization of β_{II} in nuclei does not require that it enter the intact nucleus; rather, nuclear β_{II} binds to a nuclear component during mitosis when the nucleus has disintegrated. As the nucleus re-forms it incorporates β_{II} into it. The process, whatever it is, is specific for β_{II}; neither β_I, β_{III} nor β_{IV} will enter the nucleus. We have also found strong evidence that entry of β_{II} into the nuclei may require tyrosine phosphorylation, possibly of the β_{II}. We have also surveyed a variety of cancer cells in culture and also cancer excisions and observed that all of the former and 80% of the latter contain nuclear β_{II}. We have found that successful anti-tumor drugs that target tubulin (e.g., taxol and vinblastine) expel β_{II} from the nuclei of cells, whereas drugs that target tubulin equally well, but which are less successful against cancer, do not expel nuclear β_{II}. Finally, we have found evidence that β_{III} is involved in protecting cancer cells from oxidation, that β_{IV} interacts with actin and that β_I may regulate the actin-β_{IV} interaction. The hypothesis underlying the second aim is that an anti-tubulin drug that has been modified by addition of a moiety that would be directed toward the nucleus may be particularly toxic to cancerous cells that contain nuclear tubulin. Accordingly, we have attempted to link the anti-tubulin drug colchicine to such a moiety, in one case to estradiol, in the other to a peptide containing a nuclear localization sequence. We were unable to demonstrate synthesis of the former product, but we made the second one, a peptide-colchicine derivative. We were unsuccessful, however, in demonstrating that this peptide targets the nucleus.

BODY

TASK 1: MICROINJECTION OF ISOTYPE-SPECIFIC ANTIBODIES INTO BREAST CANCER AND NORMAL CELLS

Rationale:

The research described here is based on the finding that the β_{II} isotype of tubulin occurs in the nuclei of a variety of cancer cells, including breast cancer cells. The specific goal for Task 1 is to determine the function of nuclear β_{II}. The idea is to microinject antibodies specific for each tubulin isotype into cells and see what cellular functions are disrupted. As it happened, microinjection did not give unequivocal results, hence we decided to address this question using a variety of approaches.

Experimental Results:

Microinjection of the Isotype-Specific Antibodies

We microinjected breast cancer cells with monoclonal antibodies specific for the β_I, β_{II}, β_{III} and β_{IV} isotypes. We saw no change in their viability. In order to carry out this experiment in a system more focused on nuclear β_{II}, we turned to rat kidney mesangial cells. The reason is that the mesangial cells contain β_{II} almost entirely in their nuclei, whereas breast cancer cells contain β_{II} in both the nuclei and the cytoplasm (1). Our rationale was that if microinjection of anti-β_{II} into mesangial cells had an effect, then that effect was likely to be attributable to interfering with nuclear β_{II} as opposed to cytoplasmic β_{II}. We microinjected them during interphase and mitosis. Microinjection was done into the cytoplasm and the nuclei. We found that microinjection of anti-β_{II} had no effect at all on the mesangial cells, including not only their viability and ability to form mitotic spindles but also their ability to undergo cAMP-induced shape change, a process that can be blocked by microtubule-inhibitory drugs. Microinjection of antibodies against β_{III} and β_{IV} had no effect either. The only effect was seen with micro-injection of anti-β_I, which caused the cells to undergo unusual shape changes when cAMP was added. This is likely to reflect the fact that β_I is the most abundant isotype in the cytoplasm of mesangial cells rather than arising from a specific function of β_I.

The fact that microinjection of isotype-specific antibodies into cells did not have any major effect does not mean that specific isotypes do not have particular functions, nor that nuclear β_{II} has no significance. It is possible that the microinjected antibodies were not sufficiently concentrated to interact with their isotypes. There could also be a question of timing, since the antibodies can only last for a certain length of time before the cell degrades them. There may be specific times during the cell cycle during which the isotype differences become important; perhaps the effective concentration of the antibody at those times in the vicinity of its antigen is not sufficiently high to interact

with the isotypes. At any rate, we decided to address the question of the functional significance of nuclear β_{II}-tubulin using other approaches, including determination of the occurrence of nuclear bII in normal and cancer cells and, for purposes of comparison, investigating the functions of the other isotypes.

Confocal Microscopy of Breast Cancer and Normal Breast Epithelial Cells

Our results, using normal immunofluorescence microscopy, have shown that β_{II} occurs in the nuclei of breast cancer cells and in lesser amounts in the nuclei of MCF-10F cells, that are supposedly non-transformed breast cancer cells (Figure 1). Even in our best micrographs, however, it was not clear that, in breast cancer cells, the other isotypes were absent from the nucleus. It took us a long time to locate a viable system for confocal microscopy, but we now have an arrangement with Dr. Victoria Froehlich, Assistant Professor in the Department of Cellular and Structural Biology at the Health Science Center who supervises the Optical Imaging Core Facility. This facility has an Olympus FV500 Confocal Scanning System equipped with argon and red and green helium-neon lasers, based on an IX70 inverted microscope. Very recent results using this microscope has shown clearly that the β_{I}, β_{III} and β_{IV} isotypes, all of which are expressed by MCF-7 breast cancer cells, are absent from their nuclei (Figure 2). They are also absent from the nuclei of MCF-10F cells (Figure 1). Thus, it appears very clear that the nuclear localization of β_{II} is specific for that isotype.

Characterization of Nuclear β_{II} in Cancer Cells

The basis for this grant was our earlier finding that β_{II} occurs in the nuclei of breast cancer cells. We decided to characterize it further. First, we found that β_{II} occurred with α-tubulin, indicating that nuclear β_{II} is almost certainly in the form of an $\alpha\beta_{II}$ dimer (Figure 3). Second, we treated the cells with fluorescent colchicine and found that this colchicine derivative labeled the nuclei in a pattern indistinguishable from that of β_{II} (Figure 4). Third, we treated cells with a fluorescent derivative of taxol and found that it also labeled the nuclei. In short, even though nuclear β_{II} did not form microtubules, it appeared to be an $\alpha\beta_{II}$ dimer and was otherwise normal, at least in its drug-binding properties.

We saw that β_{II} accumulated in structures that we assumed were nucleoli. However, we had not directly demonstrated that. We found that fluorescein-colchicine appeared to label the nucleoli in extracted cells (Figure 5). We thus co-labeled our cancer cells with anti-β_{II} and with acridine orange, a fluorescent dye specific for RNA (nucleoli are very rich in RNA). We found that β_{II} does indeed co-localize with nucleoli (Figure 6). To make doubly certain, we also co-labeled cells with anti-β_{II} and nucleolin, a nucleolar marker (Figure 7) and also with fluorescent colchicine and acridine orange (Figure 8), obtaining the same results each time.

Microinjection of Fluorescently Labeled Tubulin Isotypes into Mesangial Cells

Since mesangial cells have only low levels of cytoplasmic β_{II}, we have begun this approach using these cells. As previously reported, we microinjected these cells with fluorescently labeled $\alpha\beta_{II}$ tubulin. $\alpha\beta_{II}$ is isotypically purified tubulin, that is, a tubulin dimer whose β subunit is β_{II}, as opposed to isotypically unfractionated tubulin, which, in our source of bovine brain, is a mixture of $\alpha\beta_{I}$, $\alpha\beta_{II}$, $\alpha\beta_{III}$ and $\alpha\beta_{IV}$ dimers (2). As previously reported (1), the fluorescently labeled $\alpha\beta_{II}$ localized to the nucleus, and in the same pattern as we found for the cell's own $\alpha\beta_{II}$, namely, concentrated in the nucleoli (Figure 9). We found, however, that a mitotic cycle had to pass before the $\alpha\beta_{II}$ entered the nuclei. $\alpha\beta_{II}$ that was microinjected during mitosis also entered the nucleus. These results imply that the process by which $\alpha\beta_{II}$ does not involve entering the intact nucleus, but rather that it must bind to a nuclear component during mitosis, when the nucleus has disintegrated, and that $\alpha\beta_{II}$ is present in the re-forming nucleus.

We then went on to microinject the cells with fluorescently labeled $\alpha\beta_{III}$ and $\alpha\beta_{IV}$. These did not enter the nucleus, no matter when they were injected (Figure 9). Thus, this implies that the mechanism of nuclear entry is specific for $\alpha\beta_{II}$. Presumably, therefore, there is a nuclear component that binds only to β_{II} and not to the other isotypes.

Post-translational Modification of Nuclear β_{II}-Tubulin

One possible explanation for how β_{II} localizes to the nucleus is that it undergoes a different type of post-translational modification than does non-nuclear β_{II}. This is not a trivial possibility since the tubulin molecule undergoes more post-translational modifications than most other proteins; these include detyrosinolation and retyrosinolation of α, removal of the last two residues from α, acetylation of α, phosphorylation, palmitoylation, and polyglutamylation of both α and β, and polyglycylation of β (3). We have previously shown that the α in nuclear $\alpha\beta_{II}$ is tyrosinolated (1). We subjected a nuclear extract to gel electrophoresis followed by immunoblotting using antibodies against polyglutamylated and phosphorylated proteins. We found very clear evidence that nuclear β_{II} is not polyglutamylated; our results also suggested that nuclear β_{II} may be phosphorylated at a tyrosine residue. This latter result was not unequivocal, however, since we could not be sure that the phosphorylated protein was β_{II}.

We approached this question in another manner, by incubating the cells with genistein, an inhibitor of tyrosine phosphorylation (4). We obtained some inhibition of nuclear β_{II} localization in MCF-7 breast cancer cells, rat kidney mesangial cells and T98G glioma cells, most dramatically in the latter (Figures 10-13). This finding implies that, in order for the $\alpha\beta_{II}$ dimer to enter the nuclei, tyrosine phosphorylation is necessary, although whether the phosphorylated protein is β_{II} is not yet clear.

Identification of Nuclear Proteins Binding to β_{II}

This has so far been disappointing. We have used co-localization and immunoprecipitation to attempt to identify proteins that bind to β_{II}. We previously reported that vault ribonucleoprotein co-localized with β_{II} in the nuclei of mesangial cells. We have now found that our anti-vault antibody may also bind to tubulin, casting the results of the co-localization experiments into doubt. We also looked for co-localization of nuclear β_{II} with tau, microtubule-associated protein 4 (MAP4), and adenomatous polyposis coli protein (APC). None of these proteins co-localized with nuclear β_{II}.

We also attempted to approach this question by immunoprecipitation of a nuclear extract with anti-β_{II}. We found that 4 bands were obtained; however, the same bands were obtained by immunoprecipitation with anti-β_{I} and anti-β_{IV}, so there was no specificity with β_{II}.

Double-label Immunofluorescence of the Mitotic Spindle

We have been exploring the hypothesis that the tubulin isotypes play different roles during mitosis and that nuclear localization of β_{II} allows it to play a unique role during mitosis. We have occasionally observed that β_{I}, β_{II} and β_{IV} do not co-localize exactly in the spindle and midbody. We intend to carry out some confocal microscopy experiments to examine this at higher resolution. One specific hypothesis that we wish to test is that the different isotypes distribute differently among the microtubules of the mitotic spindle. If one isotype is clustered around the kinetochore, for example, it could help attract microtubules from the centrosome to the kinetochore; this would make the process of mitosis more rapid and accurate and would allow for faster cell proliferation. We intend to test this hypothesis.

Survey of Nuclear β_{II} in Cultured Cancer Cells

In order to better understand the role of nuclear β_{II}, we surveyed other cell types to see if they also had nuclear β_{II}. We found that relatively few normal cell types contained nuclear β_{II}. Mesangial cells were actually an exception in that they are normal cells and their nuclei clearly contain β_{II}. In contrast, osteoblasts, fibroblasts and certain smooth muscle cell lines do not contain nuclear β_{II} (Figure 14). However, every cultured cancer cell line that we have examined contains nuclear β_{II}. These include breast, glioma, prostate, ovarian and colon cancer cell lines (Figure 15).

Survey of Nuclear β_{II} in Excised Tumors

We extended our survey to actual cancers excised from patients. These samples were treated with anti-β_{II} and stained using the immunoperoxidase approach. The results are shown in Table 1.

Table 1. Presence of Nuclear β_{II} in Human Cancer Excisions

Type of Cancer Examined	Fraction of Cancers with Nuclear β_{II}		
Breast	**18/18**		
Prostate	16/16		
Colon	14/14		
Stomach	13/14		
Ovary	10/13		
Bone[a]	16/18		
Brain[b]	5/17		
Liver (hepatocellular carcinoma)	1/7		
Bile duct	1/1		
Melanoma	1/1		
Retroperitoneal carcinoma	1/1		
Basal cell carcinoma	1/1	**TOTAL:**	**97/121 = 80%**

[a]Includes osteosarcoma and giant cell carcinoma. [b]Includes astrocytoma, ependymoma, chordoma, meningioma and medulloblastoma.

If the table is revised to reflect only cancers of epithelial origin, then the percentage of cancers with nuclear β_{II} is 90%. This is a very high percentage, that suggests that nuclear β_{II} may serve some particularly important function for the cancer cell, although it does not tell us what that function may be.

Nuclear β_{II} in Excised Breast Tumors

We examined 18 excisions from breast tumors. All of these had nuclear β_{II}. The pattern was quite variable (Figure 16). The intensity of staining of nuclear β_{II} did not appear to be correlated with any variable such as the grade of the tumor or how differentiated it was. Some tumors showed weak nuclear β_{II} staining; others had nuclei that stained very strongly for nuclear β_{II}. Some had β_{II} mainly in the cytoplasm, some in both the nuclei and the cytoplasm, and some largely in the nuclei (Figure 16). Perhaps the most striking pattern was in the cases of mucinous or colloid carcinoma that we observed; these had very intense nuclear β_{II} staining and very little in the cytoplasm (Figure 16).

We also examined 14 samples of benign breast hyperplasia. There was a great deal of variation. A sample of stromal fibrosis had some nuclear β_{II}, as did one fibroadenoma, but not another fibroadenoma. Cysts showed little or no nuclear β_{II}, and apocrine metaplasia showed very little. Hyperplasia usually showed little nuclear β_{II}, although there were some exceptions. One pattern observed in hyperplasia was that epithelial cells had very little nuclear β_{II}, while myoepithelial cells had considerable nuclear β_{II}. These results raise the possibility of using nuclear β_{II} as a diagnostic and/or prognostic factor in breast biopsies.

Effect of Drugs on Nuclear β_{II}

We have found that nuclear β_{II} is very sensitive to certain drugs; the effect of drugs, however, is surprising. We have found that vinblastine causes disappearance of cellular microtubules and also of nuclear β_{II} (Figure 17). Taxol causes disappearance of nuclear β_{II} but also induces bundling of microtubules in the cytoplasm (Figure 18). The effect of taxol on expulsion of β_{II} from cancer cell nuclei is dose-dependent (Figure 19). Interestingly, there is a group of drugs, all potent against tubulin, that have no effect on nuclear β_{II}. These include combretastatin A-4, colchicine, nocodazole, and estramustine. Even though all of these drugs inhibit microtubule assembly *in vitro* and depolymerize cellular microtubules in the cytosol and also, in some cases cause apoptosis, yet they are unable to expel β_{II} from the nuclei (Figures 20-21). It is interesting that certain anti-tubulin drugs expel β_{II} from the nucleus and certain others do not. We could divide the drugs into two groups, as follows: group A, consisting of taxol and vinblastine, and group B, consisting of the other drugs we examined. One could summarize the observed differences by saying that, although drugs from each group can cause apoptosis, those from group A will expel β_{II} from nuclei even from non-apoptotic cells. The drugs from group B do not affect nuclear β_{II} even in apoptotic cells. These results are best summarized in tabular form (Table 2).

Table 2. Effect of Anti-tubulin Drugs on Nuclear β_{II} in Cells

Drug	Expulsion of Nuclear β_{II}[a]	Effect on Tubulin Polymerization[b]	Isotype Specificity[c]	Anti-Cancer Usefulness
Group A				
Taxol	Yes	Promotes[d]	$\alpha\beta_{II}$[e]	High[f]
Vinblastine	Yes	Promotes[g]	$\alpha\beta_{II}$[h]	High[i]
Group B				
Colchicine	No	Inhibits	$\alpha\beta_{IV}$[j]	Low[k]
Combretastatin A-4	No	Inhibits	$\alpha\beta_{II}$[j]	Indirect[l]
Nocodazole	No	Inhibits	$\alpha\beta_{II}$[j]	Low[m]
Estramustine	No	Inhibits	$\alpha\beta_{II}$?[n]	Medium[o]

[a]Based on our data (described in this Report). [b]Effect on microtubule assembly *in vitro*. [c]Various approaches were used to compare the binding of each drug to the isotypically purified $\alpha\beta_{II}$, $\alpha\beta_{III}$ and $\alpha\beta_{IV}$ dimers; these are detailed after each drug. [d]Taxol induces microtubule assembly and bundling of microtubules (5). [e]Measured by the effect on the dynamics of microtubules assembled from isotypically purified dimers (6). [f]Taxol has been very useful in treatment of ovarian and prostate cancers; its analogue, taxotere, is highly useful in breast cancer (7,8). [g]Although vinblastine inhibits microtubule assembly, it is unusual in that it induces the polymerization of tubulin into non-microtubule structures, typically spiral protofilaments (9). [h]Measured by the effect on microtubule assembly and polymerization into spiral-type aggregates (10). [i]Vinblastine is the

treatment of choice for Hodgkins' disease (11). [j]Measured by a fluorescence binding assay (12). [k]Although repeatedly examined, colchicine has not proved a useful anti-tumor drug (13,14). [l]Combretastatin A-4 is a potentially very useful-anti-tumor agent. However, it does not attack cancer cells directly; rather it inhibits angiogenesis by acting on endothelial cells (15). [m]Although first synthesized in hopes that it would prove a useful anti-tumor drug, nocodazole has been disappointing (16). [n]The binding of estramustine to tubulin isotypes has not been directly measured. However, when brain tubulin is incubated with radioactive estramustine and treated to bind covalently to tubulin, the label co-migrates with the β_1, rather than the β_2 band (17). On polyacrylamide gels containing Na dodecyl sulfate, the β_2 band consists only of the β_{III} isotype, while the β_1 band of tubulin contains of the β_I, β_{II} and β_{IV} isotypes (18). Since β_{II} accounts for 77% of the β_1 band, it is very likely that estramustine reacts preferentially with the $\alpha\beta_{II}$ isotype. [o]Estramustine was once used to treat hormone-refractory prostate cancer (19), but it is now being superseded by taxol, that is considered to be at least equally effective (20).

What do the drugs in group A have in common that the drugs in group B do not? As mentioned above, the drugs in group A expel $\alpha\beta_{II}$ from the nucleus; they also are the most effective against cancer. They also induce tubulin polymerization, either normal or abnormal. It is conceivable that their ability to induce tubulin to polymerize may lower the free tubulin concentration in the cytosol and thus, induce tubulin to exit the nucleus. This is unlikely to explain the results, however, for the following reasons: 1. If nuclear tubulin were in equilibrium with cytoplasmic tubulin, that would imply a great deal of porosity in the nuclear membrane, a porosity that would contradict our finding that $\alpha\beta_{II}$ cannot cross the nuclear membrane. 2. If nuclear tubulin were in equilibrium with cytoplasmic tubulin, then it is difficult to imagine that all the nuclear tubulin would be expelled by the drugs, yet our results suggest that this is exactly what happens. In short our results suggest that there must be a way for β_{II} to exit the intact nucleus even if it cannot enter it. Most importantly, however, our results raise the possibility that nuclear β_{II} may serve as a target for anti-tubulin drugs. Granted that the concentrations of drug required to expel $\alpha\beta_{II}$ from the nucleus are higher than those that inhibit microtubule dynamics in the cell, it is quite reasonable to postulate that expulsion of nuclear $\alpha\beta_{II}$ be only a terminal effect, that at very low concentrations, drugs of group A may actually have a novel effect, inhibiting the ability of nuclear $\alpha\beta_{II}$ from performing its as yet unknown function.

Effect of Ionizing Radiation on Tubulin Isotype Composition in Breast Cancer Cells

In collaboration with Dr. Mohan Natarajan of the Radiology Department, we are looking at the effect of ionizing radiation on MCF-7 breast cancer cells. MCF-7 cells were subjected to a burst of ionizing radiation and then allowed to incubate for 24 hours. Cell proliferation was not markedly affected, compared to control cells that had not been irradiated. The colchicine binding activity of the cell extract at 3 hours increased by 13%, however, at 24 hours, the irradiated cells had 44% less colchicine binding activity than did the control (Table 3). This suggests that the MCF-7 cells have switched isotypes in response to the irradiation, perhaps switching to one that binds less colchicine, such as

$\alpha\beta_{III}$. We will be examining nuclear β_{II} localization and also isotype composition of the irradiated breast cancer cells. One hypothesis about nuclear β_{II} is that the nucleus acts as a storehouse for tubulin to protect it from free radicals that are likely to be generated by ionizing radiation.

Table 3. Effect of Ionizing Radiation on Colchicine-Binding Activity of MCF-7 Breast Cancer Cell Extracts

Ionizing Radiation (units)	After Three Hours in Culture Total Prot (μg)	DPM	After 24 Hours in Culture Total Prot (μg)	DPM
0	504	4650 ± 416	802	6600 ± 132
1	459	5400 ± 44	882	6801 ± 252
10	377	5264 ± 794	725	3723 ± 118

Batches of MCF-7 breast cancer cells were treated subjected to either 0, 1 or 10 units of ionizing radiation. They were then allowed to grow in culture for either 3 or 24 hours. At the indicated times, cells were harvested and homogenized in the presence of a cocktail of protease inhibitors (benzamidine (5 mM), TAME (2 mM), SBT1 (0.1 mg/mL), aprotinin (0.2 μg./mL), leupeptin (1 μg/mL), antipain (1 μg/mL), and PMSF (1% (v/v)). In each cell homogenate the total protein was determined. An aliquot of each homogenate was diluted to 0.75 mg protein/mL and was incubated with 50 μM [^{3}H]colchicine for 1 hour at 37 °C. Reactions were filtered and the radioactivity of the filters determined (21).

A Function for the β_{III} Isotype: Protecting Tubulin in Cancer Cells from Oxidation

In another approach to test the function of the β_{III} isotype, we compared two lines of breast cancer cells---MDA and BT5492---and measured the concentration of free radicals. BT5492 contains a very high concentration of β_{III}. MDA cells contain very little β_{III}. A-10 cells were used as a control; these are smooth muscle cells that contain no detectable β_{III}. As seen in Figure 22, the level of free radicals appeared much higher in the BT5492 cells than in the MDA cells, and somewhat higher in the latter than in the A-10 cells. This has led us to hypothesize that the β_{III} isotype, whose sequence lacks the easily oxidizable, yet assembly-critical cys^{239}, may serve to protect the microtubules of cancer cells from oxidation. This is consistent with the fact that β_{III} is found in tissues likely to be exposed to free radicals such as the colon and nasal epithelia (22,23). We are formulating for future research a strategy for breast cancer in which we treat with a drug such as taxol, that tends to bind very well to β_{II}; this would force the cancer cell to shift to making more β_{III}. We would then treat with a drug, perhaps an antisense nucleotide, specific for β_{III}, to eradicate the cancer.

Functional Significance of the β_I and β_{IV} Isotypes

We have also characterized the other antibodies that we have made. We found that, in various cell types, there appears to be co-localization between the β_{IV} isotype of tubulin and actin filaments. This is particularly apparent when the cells are treated so as to remove microtubules. We hypothesize that one function of β_{IV} is to interact with actin filaments. Perhaps if a cell needs to have interaction between microtubules and actin filaments, it expresses β_{IV}. This is described in an attached manuscript (24). In a related project, adhesion of MDCK cells was studied. In these cells, the periphery contains the actin filaments involved in adhesion. These cells express the β_I, β_{II} and β_{IV} isotypes. However, the β_{II} and β_{IV} isotypes occur throughout the entire microtubule network, including the periphery, while the β_I isotype occurs in all the microtubule network, except the periphery. It is reasonable to speculate, based on our results with β_{IV} (24) that the β_{IV} in the periphery is interacting with actin. However, if these cells are made to over-express β_{IV}, then adhesion is inhibited. It is possible, therefore, that the role of β_I is to regulate the actin/β_{IV} interaction. These results are described in the attached manuscript by Lezama *et al.* (25).

Molecular Modeling of the Tubulin Isotypes

In collaboration with Dr. Peddaiahgari of BioNumerik Pharmaceuticals, Inc., we modeled the $\alpha\beta_{II}$, $\alpha\beta_{III}$ and $\alpha\beta_{IVb}$ dimers by in essence mutagenizing the β-tubulin sequence used by Nogales *et al.* (26). We found that the conformations of all three dimers are likely to be different (Figure 23). Three conclusions can readily be drawn from these models. First, each dimer differs in the conformation of the α subunit as well as the β subunit even though in the modeling no changes in the α sequence were assumed. These results raise the possibility that the β subunit may exert a powerful effect on the conformation of the entire tubulin molecule and therefore control its response to drugs. Second, $\alpha\beta_{III}$ clearly has the most, and $\alpha\beta_{IV}$ the least, compact configuration of the three dimers. This is consistent with our previous published work indicating that $\alpha\beta_{III}$ is the most rigid and $\alpha\beta_{IV}$ the least rigid of the dimers (27-29). Third, our results suggest that drugs could be designed to be isotype-specific.

TASK 2: SYNTHESIS AND CHARACTERIZATION OF A STEROID-COLCHICINE DERIVATIVE THAT TARGETS THE NUCLEUS AND BINDS TO TUBULIN

This task was scheduled to be performed in the first year of the grant, but the reviewers were very skeptical about its feasibility, so we postponed it. However, in view of the previous finding that the distribution of β_{II} within the nucleus was correlated with resistance to estrogen, we decided to go ahead and attempt to make this compound (Scheme 1). The procedure was as follows: a slurry of β-estradiol (12.6 mg, 0.05 mmol), triphosgene (14.8 mg, 0.05 mmol) and potassium carbonate (4 mg, 0.03 mmol) in dichloromethane (4 mL) was stirred at room temperature under nitrogen for 2 hours. A

solution of deacetylcolchicine (18 mg, 0.05 mmol) in dichloromethane (2 mL) was added and stirring of the resulting yellow slurry was continued overnight. The slurry was partitioned between dichloromethane and water, the organic layer separated, washed with water, dried over sodium sulfate, filtered and evaporated to give a brown residue. Proton NMR indicated formation of the NHC(O) bond but further analysis using high resolution mass spectrometry gave a molecular weight of 643.3027. The calculated molecular weight should have been 654.3069. The 11 mass units difference indicates that there was a problem with the synthesis.

TASK 3: SYNTHESIS AND CHARACTERIZATION OF A PEPTIDYL-COLCHICINE DERIVATIVE THAT TARGETS THE NUCLEUS AND BINDS TO TUBULIN

Background:

We synthesized the following peptide:

KRPRPCGMNK*EARKTKK

(* indicates that this lysine residue is labeled with fluorescein).

We showed in an earlier report that the peptide, when microinjected into rat kidney mesangial cells, began to accumulate in the nucleus within two hours after microinjection. After 20 hours, most of the peptide was in the nucleus.

We intended to make the peptidyl-colchicine derivative by reacting the peptide with deacetylcolchicine, but deacetylcolchicine is no longer commercially available. We therefore had to devise a synthesis for the peptide, beginning with colchicine (Scheme 2). The synthesis was as follows:

Synthesis of Peptidyl-Colchicine Derivative:

Synthesis of Trimethylcolchicinic Acid

A solution of colchicine (3.01 g, 8 mmol) in 4:3 concentrated HCl and methanol (70 mL) was refluxed for 48 hours. The solution was allowed to cool to room temperature after which a rinsing of the reaction flask was added. Neutralization of the pH with solid sodium carbonate gave a yellow flocculent precipitate which was extracted with dichloromethane. The aqueous layer was extracted and the combined organics dried by passage through sodium sulfate and evaporated to give crude trimethylcolchicinic acid. The structure was confirmed by ^{1}H NMR.

Synthesis and Purification of Deacetylcolchicine

The next step was to methylate the trimethylcolchicinic acid with diazomethane. For this, trimethylcolchicinic acid (2.277 g) in dichloromethane (50 mL) cooled to 0-5 °C was mixed with a solution of KOH (16 g, 0.29 mol)) in 16:13 ethanol/water, and a solution of diazald™ (16g, 0.075 mol) in ether (144 mL). The reaction was distilled until the distillate was colorless. The reaction was allowed to come to room temperature and evaporated to give a brown residue that was dissolved in dichloromethane and evaporated again to remove excess diazomethane. The product was identified by ^{1}H NMR. This method gave a 1:2.5 mixture of deacetylcolchicine and isodeacetylcolchicine. Several procedures were used in order to purify the deacetylcolchicine. All of them involved chromatography on silica gel (30,31).

Synthesis of N-4-Maleimidobutyroyldeacetylcolchicine

Once the deacetylcolchicine was purified it was derivatized to generate *N*-4-maleimidobutyroyldeacetylcolchicine. In one method, deacetylcolchicine was reacted with γ-maleimidobutyric acid in oxalyl chloride. The second method involved reacting deacetylcolchicine with γ-maleimidobutyric acid N-hydroxysuccinimide ester. The first two methods gave the purest product. The other methods involved using 1-hydroxybenzotriazole as a catalyst with or without dicyclohexylcarbodiimide. These generated the desired product, but with some by-products as well.

Synthesis of the Peptidyl-deacetylcolchicine Derivative

The next step was to couple *N*-4-maleimidobutyroyldeacetylcolchicine to the above-mentioned peptide. For this, acetic acid (10%, 50 μL) was added to a solution of the peptide (0.5 mg, 0.2 μmol) in water (0.4 mL) and the resulting solution stirred for five minutes at room temperature. A solution of *N*-4-maleimidobutyroyldeacetylcolchicine (0.11 mg, 0.2 μmol) in acetonitrile (150 μL) was then added. Samples were withdrawn at various times and analyzed by HPLC. Analysis by MALDI indicated that the products were not pure. The largest product was identified as:

PRPC$^{\#}$GMNK*EARKTKK,

where # corresponds to the deacetylcolchicine attached to the cysteine residue and * is the fluorescein. It is clear that the peptide underwent partial hydrolysis during the coupling reaction, losing the first two residues. However, the truncated peptide still retains a nuclear localization sequence and should be able to localize to the nucleus.

Microinjection of the Peptidyl-Colchicine Derivative into Rat Kidney Mesangial Cells:

We microinjected the peptidyl-deacetylcolchicine derivative into cultured rat kidney mesangial cells, having first made it as concentrated as possible, while still

remaining soluble. Unfortunately, the microinjected derivative was not sufficiently fluorescent to be visible in the fluorescence microscope.

TASK 4: CREATION OF A TUBULIN-BINDING NUCLEAR-LOCALIZING PEPTIDE USING A COMBINATORIAL LIBRARY

This task was going to be done in collaboration with Dr. David Edwards of Ceres Technology, a San Antonio-based company. However, Dr. Edwards moved away, his company apparently folded, and the combinatorial library was not available, so we could not pursue this aim.

TASK 5: ATTACHMENT OF FOLIC ACID TO THE MOST SUCCESSFUL PEPTIDE

We intended to attach folic acid to the peptide-colchicine derivative made in Task 3. We decided to use the approach shown in Scheme 3: to couple the folic acid to *N*-hydroxysuccinimide, which would then be linked to the peptidyl-colchicine derivative. Our first attempt was carried out using the coupling reagent dicyclohexyl carbodiimide in dichloromethane. However, severe solubility problems were encountered. Hence, we switched to using 1-ethyl-3-(3-dimethylaminopropyl)carbodiimide (EDAC) and 1-hydroxybenzotriazole (HOBt), a well-known coupling reagent mixture; instead of dichloromethane, we used dimethylformamide as the solvent to increase solubility of the reactants. The reaction appeared to be successful, however, it was likely to yield two isomers (**1** and **2**). We attempted to monitor the reaction by thin-layer chromatography, but the reactants appeared to be changing in a manner other than predicted initially. Hence, we used ion-exchange chromatography on DEAE-cellulose to separate the isomers (the chromatography solvent was 0.08 M NH_4CO_3 in methanol:water (20:80). Mass spectrometric analysis of the reaction products suggested that there was considerable degradation and hence that we were not getting the desired products. Attempts to attach ethylenediamine, as a spacer, to the folic acid were also unsuccessful.

In view of the unexpected difficulties encountered in the synthesis, and because we were unable to demonstrate that the peptide-colchicine derivative had entered the nucleus in the micro-injected cells, and since Dr. Michael Moore, the chemist, had left to seek another job, it did not seem worthwhile to hire another chemist to attempt to complete this one aim, since the success of the drug was problematical.

We concentrated our efforts instead on increasing our understanding of the role of nuclear β_{II}, as described above.

KEY RESEARCH ACCOMPLISHMENTS

- The process by which β_{II}-tubulin enters the nucleus of cells does not involve transportation into the nucleus but rather that it binds to a nuclear component during mitosis after nuclear disintegration; β_{II} then remains in the nucleus after the nucleus reforms.

- The process by which β_{II} enters the nucleus is specific for β_{II}. Neither β_{III} nor β_{IV} enter the nucleus.

- Nuclear β_{II}-tubulin is not polyglutamylated; in that respect it differs greatly from brain tubulin.

- The process by which β_{II} enters the nuclei appears to require tyrosine phosphorylation.

- Ionizing radiation causes a large change in tubulin properties in breast cancer cells. This could reflect a change in tubulin isotype composition.

- There is a correlation between the presence of β_{III} in a tumor cell and the oxidation state, suggesting that the function of β_{III} may be to constitute a population of microtubules resistant to oxidation.

- Nuclear β_{II} occurs in a variety of cultured cancer cells and in 80% of human cancer excisions, including 100% of the breast cancers that we have examined.

- Vinblastine and taxol induce disappearance of nuclear β_{II}-tubulin. Colchicine, estramustine, and nocodazole do not. The fact that, of the tubulin-specific drugs, the ones that are most successful against tumors are the ones that expel β_{II} from the nuclei, raises the possibility that nuclear β_{II} may be a promising target to investigate further.

- One function of β_{IV} is to interact with actin filaments.

- The function of β_{I} appears to be to regulate the actin-β_{IV} interaction.

- We have synthesized a derivative of colchicine attached to a peptide containing a nuclear localization sequence.

REPORTABLE OUTCOMES

1. Manuscripts, abstracts, presentations, degrees obtained:

Manuscripts:

Walss-Bass, C., Prasad, V., Kreisberg, J.I. and Ludueña, R.F. (2001) Interaction of the β_{IV}-tubulin isotype with actin stress fibers in cultured rat kidney mesangial cells. *Cell Motility and the Cytoskeleton*, in press (**Appendix 2**)

Walss-Bass, C., Kreisberg, J.I. and Ludueña, R.F. (2001) Mechanism of localization of β_{II}-tubulin in the nuclei of cultured rat kidney mesangial cells. *Cell Motility and the Cytoskeleton*, in press (**Appendix 3**).

Lezama, R., Castillo, A., Luduena, R.F. and Meza, I. Over-expression of βI tubulin in MDCK cells and incorporation of exogenous βI tubulin into microtubules interferes with adhesion and spreading. *Cell Motility and the Cytoskeleton*, submitted for publication (**Appendix 4**).

Khan, I.A. and Ludueña, R.F. Different effects of vinblastine on the polymerization of isotypically purified tubulins from bovine brain. *Biochemistry*, submitted for publication (**Appendix 5**).

Walss-Bass, C., Kreisberg, J.I. and Ludueña, R.F. Effect of the anti-tumor drug vinblastine on nuclear β_{II}-tubulin cultured rat kidney mesangial cells. To be submitted for publication (**Appendix 6**).

Walss-Bass, C. and Ludueña, R.F. Nuclear β_{II}-tubulin as a marker for rapid cell proliferation. To be submitted for publication (**Appendix 7**).

Woo, K., Ludueña, R.F. and Hallworth, R. Differential expression of β tubulin isotypes in gerbil nasal epithelia. To be submitted for publication (**Appendix 8**).

Abstracts (Appendix 9):

Verdier-Pinard, P., Bai, R., Luduena, R.F., Banerjee, A., Sausville, E.A. and Hamel, E. (2000) Tubulin content and β-tubulin isotype distribution in cell lines used in the NCI in vitro drug screen. *Proc. Amer. Assoc. Cancer Res.* **41**, 142.

Walss, C., Barbier, P., Banerjee, M., Bissery, M.C., Ludueña, R.F. and Fellous, A. (2000) Nuclear tubulin as a possible marker for breast cancer cells. *Proc. Amer. Assoc. Cancer Res.* **41**, 553.

Ludueña, R.F., Banerjee, M., Moore, M., Walss, C., Barbier, P., Bissery, M.C. and Fellous, A. (2000) Nuclear β_{II}-tubulin as a marker and therapeutic target in breast cancer. *Era of Hope*, p.687.

Walss, C., Xu, K., Prasad, V., Kasinath, V., and Luduena, R.F. (2000) Effect of taxol and vinblastine on the βII isotype of tubulin in the nuclei of normal and transformed cells. *Mol. Biol. Cell* **11**, 198a.

Luduena, R.F., Banerjee, M., Centonze, V., Yeh, I-T., and Pressley , O. (2001) Occurrence of the βII isotype of tubulin in the nuclei of ovarian cancer cells. *Proc. Amer. Assoc. Cancer Res.* **42**, 404.

Xu, K. and Ludueña, R.F. (2001) Effect of taxol on the β_{II} isotype of tubulin in the nuclei of cancer cells. *French-American Colloquium on the Cytoskeleton and Human Disease*, page 83.

Presentations:

Walss, C., Barbier, P., Banerjee, M., Bissery, M.C., Ludueña, R.F. & Fellous, A. Nuclear tubulin as a possible marker for breast cancer cells. *American Association for Cancer Research*, San Francisco, CA, April 4, 2000. Although originally intended to be presented as a poster, we were invited to present it as a platform talk in a minisymposium session.

Ludueña, R.F., Banerjee, M., Moore, M., Walss, C., Barbier, P., Bissery, M.C. & Fellous, A. Nuclear β_{II}-tubulin as a marker and therapeutic target in breast cancer. *Era of Hope Meeting*.Atlanta, GA, on June 11, 2000. (poster)

Ludueña, R.F., Hallworth, R., Chaudhuri, A.R., Walss, C., Banerjee, M., Khan, I., Xu, K. and Barnes, L. Function and distribution of tubulin isotypes. *International Symposium on Cellular and Molecular Aspects of the Birth, Life and Death of the Nervous System*, Pucon, Chile, October 4-7, 2000 (symposium talk)

Luduena, R.F., Banerjee, M., Centonze, V., Yeh, I-T., and Pressley , O. (2001) Occurrence of the βII isotype of tubulin in the nuclei of ovarian cancer cells. *American Association for Cancer Research*, New Orleans, LA, March 26, 2001 (poster).

Xu, K. and Ludueña, R.F. Effect of taxol on the β_{II} isotype of tubulin in the nuclei of cancer cells. *French-American Colloquium on the Cytoskeleton and Human Disease*, Marseilles, France, April 17-20, 2001. (poster)

Ludueña, R.F. The β_{II} isotype of tubulin is located in the nuclei of a wide variety of cancer cells. *French-American Colloquium on the Cytoskeleton and Human Disease*, Marseilles, France, April 18, 2001. (platform session)

Chaudhuri, A.R., Natarajan, M., Herman, T.S. and Thomas, C.R. Ionizing radiation generates drug resistance to tubulin-directed antiproliferative agents in MCF-7 human adenocarcinoma breast cancer cells. *American Society for Therapeutic*

Radiology and Oncology, San Francisco, November 4-8, 2001. (poster).

Degrees Obtained:

Consuelo Walss-Bass, The Functional Significance of the Mammalian β-Tubulin Isotypes β_I, β_{II} and β_{IV} in Cultured Cells. Ph.D. Dissertation, defended January 5, 2001. Degree awarded May 25, 2001. Mentor: Richard F. Ludueña, Ph.D.

Keliang Xu, Investigations of Nuclear β_{II}-Tubulin in Tumor Cells. M.S. Thesis, to be defended in July, 2001. Degree to be awarded May, 2002. Mentor: Richard F. Ludueña, Ph.D.

2. Funding Applied for Based on Work Supported by this Award

Applied for and Funded:

Title: The Role of Nuclear β_{II}-Tubulin in Breast Cancer Cells
Funding Agency: US Army Breast Cancer Research Program
PI: Richard F. Ludueña
Dates: March 1, 2001-February 29, 2004 **Amount of Funding**: $429,352

Title: Epothilones and Tubulin Isotypes
Funding Agency: Schering AG, Berlin, Germany
PI: Richard F. Ludueña
Dates: July 1, 2001-June 30, 2002 **Amount of Funding**: $64,834

Applied for and Not Funded:

Title: Nuclear β_{II}-Tubulin and the β_{IV}-Actin Link
Funding Agency: National Institutes of Health
PI: Richard F. Ludueña

Title: β_{VII}-Tubulin, a Novel Target for Cancer Chemotherapy
Funding Agency: San Antonio Cancer Institute.
PI: Richard F. Ludueña
Dates: March 1, 2000-February 28, 2001 **Amount of Funding:** $19,961

Title: Nuclear β_{II}-Tubulin in Prostate Cancer
Funding Agency: US Army Prostate Cancer Research Program
PI: Richard F. Ludueña
Dates: April 1, 2001-March 31, 2004 **Amount of Funding**: $288,704

Title: Nuclear β_{II}-Tubulin in Ovarian Cancer Diagnosis, Biology and Treatment
Funding Agency: US Army Ovarian Cancer Research Program
PI: Richard F. Ludueña

Dates: June 1, 2001-May 31, 2004 **Amount of Funding**: $373,524

Pending:

Title: The Role of the β_{II} Isotype of Tubulin in the Diagnosis and Development of Prostate Cancer
Funding Agency: US Army Prostate Cancer Research Program
PI: Richard F. Ludueña
Dates: November 1, 2001-October 31, 2004 **Amount of Funding**: $537,933

Title: β_{III}-Tubulin: A Novel Approach to the Biology and Treatment of Prostate Cancer
Funding Agency: US Army Prostate Cancer Research Program
PI: Asish R. Chaudhuri
Dates: November 1, 2001-October 31, 2004 **Amount of Funding**: $319,391

Personnel Receiving Salary from this Grant:

Robert Williams, Associate Professor
Michael Moore, Post-doctoral Fellow
Asish R. Chaudhuri, Research Instructor
Mohua Banerjee, Research Assistant

CONCLUSIONS

This project has centered on the β_{II} isotype of tubulin, which is unusual in that, in breast cancer cells, it is located in the nuclei. We have found that none of the other β-tubulin isotypes (β_I, β_{III} and β_{IV}) occur in the nuclei, and, in fact, they appear unable to enter the nuclei. We have found that nuclear β_{II} is present in every cultured cancer cell we have examined, but not in most normal cells. However, nuclear β_{II} occurs in 80% of excised cancers and in 100% of breast cancers. Future work may indicate whether the presence of nuclear β_{II} in a breast biopsy could provide guidelines for the diagnosis, prognosis and treatment of cancer. In addition, in the future we would like to pursue the actual function of nuclear β_{II} in cancer cells. In order to clarify the role of β_{II} in cancer cells, we have attempted to determine the role of the other β isotypes. We have found that β_{IV} is involved in interacting with actin filaments and that β_I may regulate this interaction. Most interesting is that β_{III}, which is known to be more resistant to oxidation, is greatly increased in breast cancer cell lines that have a higher concentration of oxygen-derived free radicals, and, in fact, are more resistant to anti-tumor drugs.

A major focus of this project was to examine the possible utility of nuclear β_{II} as a drug target. We synthesized a derivative of colchicine that should have targeted the nucleus, but its fluorescence was not sufficient to permit its subcellular location to be determined. However, we then observed that certain drugs (taxol, vinblastine) were able to cause cells to expel β_{II} from their nuclei, by a mechanism that remains to be determined. In contrast, other drugs that are equally effective at binding to tubulin, such as colchicine or nocodazole, are unable to expel β_{II} from the nuclei. The interesting aspect of this finding is that the drugs of the first group are successful anti-tumor agents, while drugs of the second group are not. Conceivably, what we need is a more refined taxol or vinblastine, capable of binding even better to β_{II}, and less well to the other isotypes. We are formulating for future research a strategy for breast cancer in which we treat with a drug, perhaps derived from taxol, that binds specifically to β_{II}; this would either kill the cancer cell or else force it to shift to making more β_{III}. We would then treat with a drug, perhaps an antisense nucleotide, specific for β_{III}, to eradicate the cancer. To aid in this project, we have made models of the different isotypes. Our hope is to use the models to design drugs specific for the β_{II} and β_{III} isotypes.

REFERENCES

1. Walss C, Kreisberg JI & Ludueña RF (1999) Presence of the β_{II}-isotype of tubulin in the nuclei of cultured rat kidney mesangial cells. *Cell Motil. Cytoskeleton* **42**, 274-284.
2. Banerjee A, Roach MC, Wall KA, Lopata MA, Cleveland DW & Ludueña RF (1988) A monoclonal antibody against the type II isotype of β-tubulin. Preparation of isotypically altered tubulin. *J. Biol. Chem.* **263**, 3029-3034.
3. Ludueña RF (1998) Multiple forms of tubulin: different gene products and covalent modifications. *Int. Rev. Cytol.* **178**, 207-275.
4. Kim H, Peterson TG, Barnes S (1998) Mechanisms of action of the soy isoflavone genistein: emerging role for its effects via transforming growth factor β signaling pathways. *Am. J. Clin. Nutrition.* 68(Suppl **6**), 1418S-1425S.
5. Schiff PB, Fant J & Horwitz SB (1979) Promotion of microtubule assembly in vitro by taxol. *Nature* **277**, 665-667.
6. Derry WB, Wilson L, Khan IA, Ludueña RF & Jordan MA (1997) Taxol differentially modulates the dynamics of microtubules assembled from unfractionated and purified β-tubulin isotypes. *Biochemistry* **36**, 3554-3562.
7. Hardman JG & Limbird LE (1996) *Goodman & Gilman's The Pharmacological Basis of Therapeutics*, 9th Ed., pp. 1228, 1257-1261, 1603, McGraw-Hill, New York.
8 *Physicians' Desk Reference*, 54th Edition (2000) Medical Economics Co., Montvale, NJ.
9. Erickson HP (1975) Negatively stained vinblastine aggregates. *Ann. N.Y. Acad. Sci.* **253**, 51-52.
10. Khan IA & Ludueña RF. Different effects of vinblastine on the polymerization and aggregation of isotypically purified tubulins from bovine brain. Submitted to *Biochemistry.*
11. Goodman LS & Gilman A (1970) *The Pharmacological Basis of Therapeutics* (4th Edn) Macmillan, New York.
12. Chaudhuri AR, Tomita I, Mizuhashi F, Murata K & Ludueña RF (1998) Tubulin stability and decay. Mediation by two distinct classes of IKP104-binding sites. *J. Prot. Chem.* **17**, 303-309.
13. Amoroso EC (1935) Colchicine and tumor growth. *Nature* **135**, 226-267.
14. Osieka R (1986) Colchicine in der tumortherapie? *Deutsche Medizinische Wochenschrift* **111**, 1985.
15. Dark GG, Hill SA, Prise VE, Tozer GM, Pettit GR & Chaplin DJ (1997) Combretastatin A-4, an agent that displays potent and selective toxicity toward tumor vasculature. *Cancer Res.* **57**, 1829-1834.
16. Hoebeke J, van Nijen G & de Brabander M (1976) Interaction of nocodazole (R 17934), a new anti-tumoral drug, with rat brain tubulin. *Biochem. Biophys. Res. Commun.* **69**, 319-324.
17. Laing N, Dahllöf B, Hartley-Asp B, Ranganathan S & Tew KD (1997) Interaction of estramustine with tubulin isotypes. *Biochemistry* **36**, 871-878.
18. Ludueña RF, Zimmermann HP & Little M (1988) Identification of the phosphorylated β-tubulin isotype in differentiated neuroblastoma cells. *FEBS Lett.*

230, 142-146.
19. Janknegt RA, Boon TA, van de Beek C & Grob P (1997) Combined hormono/chemotherapy as primary treatment for metastatic prostate cancer: a randomized, multicenter study of orchiectomy alone versus orchiectomy plus estramustine phosphate. *Urology* **49**, 411-420.
20. Picus J & Schultz M (1999) Docetaxel (taxotere) as monotherapy in the treatment of hormone-refractory prostate cancer: preliminary results. *Semin. Oncol.* **26 (Suppl 17)**, 14-18.
21. Borisy GG (1972) A rapid method for quantitative determination of microtubule protein using DEAE-cellulose filters. *Anal. Biochem.* **50**, 373-385.
22. Roach MC, Boucher VL, Walss C, Ravdin PM & Ludueña RF (1998) Preparation of a monoclonal antibody specific for the class I isotype of β-tubulin: the β isotypes of tubulin differ in their cellular distributions within human tissues. *Cell Motil. Cytoskeleton* **39**, 273-285.
23. Woo K, Ludueña RF & Hallworth R Differential expression of β tubulin isotypes in gerbil nasal epithelia. Unpublished manuscript (see Appendices).
24. Walss-Bass C, Prasad V, Kreisberg JI & Ludueña RF (2001) Interaction of the β_{IV}-tubulin isotype with actin stress fibers in cultured rat kidney mesangial cells. *Cell Motility and the Cytoskeleton*, in press (see Appendices).
25. Lezama R, Castillo A, Luduena RF & Meza I Over-expression of βI tubulin in MDCK cells and incorporation of exogenous βI tubulin into microtubules interferes with adhesion and spreading. *Cell Motility and the Cytoskeleton*, submitted for publication (see Appendices).
26. Nogales E, Wolf SG & Downing KH (1998) Structure of the αβ tubulin dimer by electron crystallography. *Nature* **391**, 199-203.
27. Banerjee A, D'Hoore A & Engelborghs Y (1994) Interaction of desacetamidocolchicine, a fast binding analogue of colchicine with isotypically pure tubulin dimers $\alpha\beta_{II}$, $\alpha\beta_{III}$, and $\alpha\beta_{IV}$. *J. Biol. Chem.* **269**, 10324-10329.
28. Sharma J & Ludueña RF (1994) Use of *N,N'*-polymethylenebis(iodoacetamide) derivatives as probes for the detection of conformational differences in tubulin isotypes. *J. Prot. Chem.* **13**, 165-176.
29. Schwarz PM, Liggins JR & Ludueña RF (1998) β-Tubulin isotypes purified from bovine brain have different relative stabilities. *Biochemistry* **37**, 4687-4692.
30. Williams RF, Mumford CL, Williams GA, Floyd LJ, Aivaliotis MJ, Martinez RA, Robinson AK & Barnes LD (1985) A photoaffinity derivative of colchicine: 6'-(4'-azido-2'-nitrophenylamino)hexanoyldeacetylcolchicine. *J. Biol. Chem.* **260**, 13794-
31. Aivaliotis MJM (1983) *Synthesis of Derivatives of Colchicine: the Interaction of Colchicine and Colchicine Analogs with Renal Tubulin.* M.S. Thesis, University of Texas Health Science Center at San Antonio, San Antonio, TX.
32. Banerjee A, Roach MC, Trcka P, Ludueña RF. 1992. Preparation of a monoclonal antibody specific for the class IV isotype of β-tubulin. Purification and assembly of $\alpha\beta_{II}$, $\alpha\beta_{III}$, and $\alpha\beta_{IV}$ tubulin dimers from bovine brain. J BiolChem 267:5625-5630.

APPENDICES

Appendix 1: Figures 1-23; Schemes 1-2

Figure 1. Subcellular Localization of the β_I, β_{II}, β_{III} and β_{IV} Isotypes of Tubulin in MCF-10F Breast Epithelial Cells. MCF-10F cells, since they are not transformed, are considered as a control for MCF-7 breast cancer cells. We find them to be imperfect controls. Cells were prepared and stained for immunohistochemistry with the isotype-specific antibodies as described by Walss *et al.* (1). Cells were treated with the following antibodies: β_I (upper left), β_{II} (upper right), β_{III} (lower left) and β_{IV} (lower right). Notice that there is very little, if any, β_I, β_{III} or β_{IV} in the nuclei, but that they are abundant in the cytoplasm. In contrast, there are low levels of β_{II} in the nuclei, but not as much as in the cytoplasm.

Figure 2. Subcellular Localization of the β_I, β_{II}, β_{III} and β_{IV} Isotypes of Tubulin in Carcinoma Cell Lines. Cells were treated with antibodies to the four isotypes as follows: β_I (panels A, E, I, M and Q), β_{II} (panels B, F, J, N and R), β_{III} (panels C, G, K, O, S), β_{IV} (panels D, H, L, P and T). Cells were C6 glioma (panels A, B, C, and D), T98G glioma (panels E, F, G and H), MCF-7 breast cancer (panels I, J, K and L), MDA breast cancer (panels M, N, O and P), and HeLa (panels Q, R, S and T). Samples were examined by confocal fluorescence microscopy. Note the complete absence of β_I, β_{III} and β_{IV} in all the nuclei and the presence of β_{II} in the nuclei of each cancer cell.

Figure 3. Co-localization of α- and β_{II}-Tubulin in Carcinoma Cell Nuclei. Cells on glass cover slips were incubated on ice for 5 min with cold CSK-100 buffer, which removes all soluble cytoplasmic and nucleoplasmic proteins, to prepare the cytosol-extracted cells. Cells were then incubated with anti-α primary antibody followed by FITC-conjugated secondary antibody. The same cells were then incubated with rhodamine-conjugated anti-β_{II}. Cells are as follows: C6 glioma (panels A and B), T98G glioma (panels C and D), MCF-7 breast cancer (panels E and F), MDA breast cancer (panels G and H), HeLa (panels I and J). Cells incubated with anti-α are in the top row (panels A, C, E, G and I), those incubated with anti-β_{II} are in the bottom row (panels B, D, F, H and J). Note the coincidence of α and β_{II} in the nuclei of each cell, suggesting that the nuclei contain the $\alpha\beta_{II}$ dimer.

Figure 4. Localization of Colchicine to the Nuclei of Carcinoma Cells. Cells were treated with fluorescein-colchicine after fixing and then examined by fluorescence microscopy. Cells are as follows: C6 glioma (panel A), T98G glioma (panel B), MCF-7 breast cancer (panel C), MDA breast cancer (panel D), and HeLa (panel E). The accumulation of colchicine in the nuclei indicates that nuclear tubulin is a functionally viable form of tubulin.

Figure 5. Sub-nuclear Localization of Fluorescein-Colchicine in the Nuclei of Carcinoma Cells. Cells were extracted as in Figure 3 and the, to prepare the nuclear matrix, these cells were further incubated at room temperature for 1 h in CSK-50 buffer

containing 100 μg/ml of DNAse I. The chromatin was removed by addng 2 M $(NH_4)_2SO_4$ drop-wise to a final concentration of 0.25 M. Cells were then fixed and incubated with 0.1 mg/ml fluoresceine-colchicine. Fluorescent micrographs are shown in panels A, C, E, G and I. Phase contrast micrographs to indicate the nuclei and nucleoli are shown in panels B, D, F, H and J. Cells are as follows: C6 glioma (panels A and B), T98G glioma (panels C and D), MCF-7 breast cancer (panels E and F), MDA breast cancer (panels G and H), HeLa (panels I and J).

Figure 6. Co-Localization of β_{II}-Tubulin and Acridine Orange in Carcinoma Cells. Cells were treated with anti-β_{II} followed by fluorescein-conjugated secondary antibody (top row) and also with acridine orange (middle row). The figures are superimposed in the bottom row. From left to right, cells were C6 glioma, T98G glioma, MCF-7 breast cancer, MDA breast cancer, and HeLa. Note the coincidence of β_{II} and acridine orange, a marker for RNA.

Figure 7. Co-Localization of β_{II}-Tubulin and Nucleolin in Carcinoma Cells. Cells were treated with rhodamine-conjugated anti-β_{II} (top row) and also with anti-nucleolin followed by a fluorescein-conjugated goat anti-mouse IgG (middle row).
The figures are superimposed in the bottom row. From left to right, cells were C6 glioma, T98G glioma, MCF-7 breast cancer, MDA breast cancer, and HeLa. Note the coincidence of β_{II} and nucleolin.

Figure 8. Co-Localization of Fluorescein-Colchicine and Acridine Orange in Carcinoma Cells. Cells were treated with fluorescein-colchicine (top row) and acridine orange (middle row). The figures are superimposed in the bottom row. From left to right, cells were C6 glioma, T98G glioma, MCF-7 breast cancer, MDA breast cancer, and HeLa. Note the coincidence of colchicine and RNA.

Figure 9. Microinjection of Fluorescently Labeled $\alpha\beta_{II}$, $\alpha\beta_{III}$ and $\alpha\beta_{IV}$ Dimers in Rat Kidney Mesangial Cells. The $\alpha\beta_{II}$, $\alpha\beta_{III}$ and $\alpha\beta_{IV}$ dimers were purified from bovine brain as previously described (32) and polymerized and reacted with 5-(4,6-dichlorotriazin-2-yl)aminofluorescein (DTAF). Microtubules were washed and each fluorescent dimer was shown to be capable of polymerization in vitro. The $\alpha\beta_{II}$, $\alpha\beta_{III}$ and $\alpha\beta_{IV}$ dimers were microinjected into rat kidney mesangial cells which were then permitted to undergo a cycle of mitosis. Cells were microinjected as follows: $\alpha\beta_{II}$ (top), $\alpha\beta_{III}$ (middle) and $\alpha\beta_{IV}$ (bottom). Note that only the $\alpha\beta_{II}$ entered the nucleus; the $\alpha\beta_{III}$ and $\alpha\beta_{IV}$ dimers remain in the cytoplasm.

Figure 10. Effect of Genistein on Nuclear β_{II} in MCF-7 Breast Cancer Cells. MCF-7 cells were treated with the following concentrations of genistein: 0 μM (left), 5 μM (middle) and 25 μM (right). Top row: β_{II}. Bottom row: DAPI, to show the nuclei. Note a slight fading of nuclear β_{II} at the highest concentration of genistein.

Figure 11. Effect of Genistein on Nuclear β_{II} in Rat Kidney Mesangial Cells. Rat kidney mesangial cells were treated with the following concentrations of genistein: 0 μM (left), 5 μM (middle) and 50 μM (right). Top row: β_{II}. Bottom row: DAPI, to show the nuclei. Note very little fading of nuclear β_{II} at the highest concentration of genistein, but an increase in cytoplasmic β_{II}, suggesting that less β_{II} is entering the nuclei.

Figure 12. Effect of Genistein on Nuclear β_{II} in T98G Glioma Cells. T98G glioma cells were treated with the following concentrations of genistein: 0 μM (left), 5 μM (middle) and 10 μM (right). Top row: β_{II}. Bottom row: DAPI, to show the nuclei. Note some fading of the nuclei at the higher concentration of genistein.

Figure 13. Effect of Genistein on Nuclear β_{II} in T98G Glioma Cells. T98G glioma cells were treated with the following concentrations of genistein: 15 μM (left), 20 μM (middle) and 25 μM (right). Top row: β_{II}. Bottom row: DAPI, to show the nuclei. Note considerable fading of the nuclei compared to the control in Figure 12, at the higher concentration of genistein.

Figure 14. Distribution of β_{II} in Non-transformed Cell Lines. The following cells were stained for β_{II}: MCF-10F breast endothelial cells (upper left); osteoblasts (upper right); HSK fibroblasts (lower left); 506 smooth muscle cells (lower right). Note the relative absence of β_{II} in the nuclei, especially when compared to the transformed cells in Figure 15.

Figure 15. Nuclear β_{II} in Some Transformed Cell Lines. The following cells were stained for β_{II}: LNCaP prostate cancer cells (upper left); MCF-7 breast carcinoma cells (upper right); MDA breast carcinoma cells (lower left); Calc 18 breast carcinoma cells (lower right). Note the presence of β_{II} in the nuclei of all the cancer cells. In Calc 18 cells, the pattern is somewhat different with β_{II} being clearly absent from the nucleoli.

Figure 16. Distribution of β_{II} in Breast Cancers. *Top*: ductal hyperplasia, with most of the β_{II} in the cytoplasm. *Center*: ductal carcinoma, with β_{II} staining largely in the nuclei. *Bottom*: colloid carcinoma, with β_{II} staining almost entirely in the nuclei.

Figure 17. Effect of Vinblastine on Nuclear β_{II} in Rat Kidney Mesangial Cells. Rat kidney mesangial cells were treated with vinblastine as follows: no vinblastine (top);15 nM vinblastine for 1 hour (middle); 30 nM vinblastine for 1 hour (bottom). Cells were either stained for β_{II} (left) or with DAPI to show the nuclei (right). Note how, in the presence of 15 nM vinblastine, several nuclei no longer contain β_{II}, while even more have lost it in the presence of 15 nM vinblastine.

Figure 18. Effect of Taxol on Nuclear β_{II} in MDA Cells. MDA cells were treated with the following concentrations of taxol: 0, 30 nM, 1 μM and 5 μM. They were then stained with anti-β_{II} (top row) and with DAPI to visualize the nuclei (bottom row). Note how taxol causes removal of β_{II} from the nuclei and its bundling in the cytoplasm.

Figure 19. Effect of Taxol on Nuclear β_{II} and Apoptosis in C6 Glioma Cells. *Left*: cells were treated for 24 hours with the indicated concentrations of taxol and, for each set, about 500 cells were measured to determine the percentage of cells lacking nuclear β_{II}. Standard deviations are shown. *Right*: Multiple nuclei, taken as an indication of apoptosis, were measured in the same cells. Note that as the taxol concentration increases, apoptosis declines and nuclear β_{II} expulsion increases. It appears that apoptosis and expulsion of β_{II} from the nuclei are not correlated.

Figure 20. Effect of Colchicine, Estramustine and Nocodazole on Nuclear β_{II} in MDA Breast Cancer Cells. MDA cells were treated with the indicated concentrations of colchicine, estramustine or nocodazole and either stained for β_{II} (top row) or with DAPI to show the DNA (bottom row). Notice how β_{II} is not expelled from the nuclei even though the drugs induce apoptosis (colchicine, nocodazole).

Figure 21. Effect of Colchicine and Estramustine on Nuclear β_{II} in MCF-7 Breast Cancer Cells. MCF-7 cells were treated with the indicated concentrations of colchicine, or estramustine and either stained for β_{II} (top row) or with DAPI to show the DNA (bottom row). Notice how β_{II} is not expelled from the nuclei even though the drugs induce apoptosis.

Figure 22. Reactive Oxygen Species in Cells of Different β_{III} Content. Cells were treated with the indicated concentrations of 2,7-dichlorofluorescein diacetate and the fluorescence was measured. Higher fluorescence indicates a higher concentration of reactive oxygen species.

Figure 23. Molecular Models of the $\alpha\beta_{II}$, $\alpha\beta_{III}$, and $\alpha\beta_{IV}$ Tubulin Dimers. Models were generated of $\alpha\beta_{II}$ (top), $\alpha\beta_{III}$ (center) and $\alpha\beta_{IVb}$ (bottom). Mammals express two forms of β_{IV}: β_{IVa} and β_{IVb}. Our monoclonal antibody against β_{IV} cannot distinguish between β_{IVa} and β_{IVb} (32). We chose to model the more widespread β_{IVb}. Each model includes GDP bound to β and GTP bound to α. In addition, several of the key cysteine residues are shown. Note that the conformations of the three dimers are different and that this is true not only for the β but for the α subunit as well.

Scheme 1. Synthesis of Steroid-Colchicine Derivative. The scheme shows the mechanism by which deacetylcolchicine (**DAC**) can be added to estradiol to generate the derivative **DAC-Estradiol**.

Scheme 2. Synthesis of Peptidyl-Colchicine Derivative. The scheme shows how colchicine is converted into trimethylcolchicinic acid (**TMCA**), which is in turn methylated to give a mixture of deacetylcolchicine (**DAC**) and isodeacetylcolchicine (**IDAC**). The **DAC** is separated from the **IDAC** and then converted into *N*-4-maleimidobutyroyldeacetylcolchicine (**DAC-GMB**). The **DAC-GMB** is then reacted with the peptide to generate the peptidyl-colchicine derivative.

Scheme 3. Coupling of Folic Acid to *N*-Hydroxysuccinimide. The scheme shows the attempt to react **folic acid** with *N*-hydroxysuccinimide and the subsequent generation of two isomers (**1** and **2**).

Appendix 2: Walss-Bass, C., Prasad, V., Kreisberg, J.I. and Ludueña, R.F. (2001) Interaction of the β_{IV}-tubulin isotype with actin stress fibers in cultured rat kidney mesangial cells. *Cell Motility and the Cytoskeleton*, in press.

Appendix 3: Walss-Bass, C., Kreisberg, J.I. and Ludueña, R.F. (2001) Mechanism of localization of β_{II}-tubulin in the nuclei of cultured rat kidney mesangial cells. *Cell Motility and the Cytoskeleton*, in press.

Appendix 4: Lezama, R., Castillo, A., Luduena, R.F. and Meza, I. Over-expression of βI tubulin in MDCK cells and incorporation of exogenous βI tubulin into microtubules interferes with adhesion and spreading. *Cell Motility and the Cytoskeleton*, submitted for publication.

Appendix 5: Khan, I.A. and Ludueña, R.F. Different effects of vinblastine on the polymerization of isotypically purified tubulins from bovine brain. *Biochemistry*, submitted for publication.

Appendix 6: Walss-Bass, C., Kreisberg, J.I. and Ludueña, R.F. Effect of the anti-tumor drug vinblastine on nuclear β_{II}-tubulin cultured rat kidney mesangial cells. To be submitted for publication.

Appendix 7: Walss-Bass, C. and Ludueña, R.F. Nuclear β_{II}-tubulin as a marker for rapid cell proliferation. To be submitted for publication.

Appendix 8: Woo, K., Ludueña, R.F. and Hallworth, R. Differential expression of β tubulin isotypes in gerbil nasal epithelia. To be submitted for publication.

Appendix 9: Abstracts

Richard F. Ludueña, Ph.D.
DAMD17-98-1-8246

Appendix 1

Figures and Schemes

10 F β_1

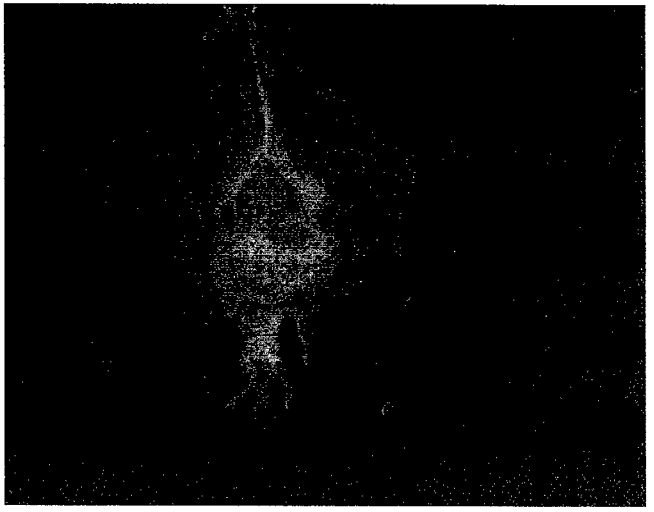

β_2

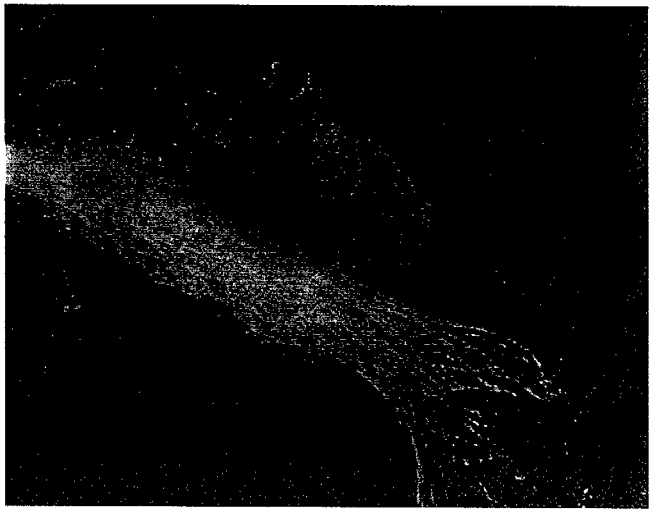

β_3

β_4

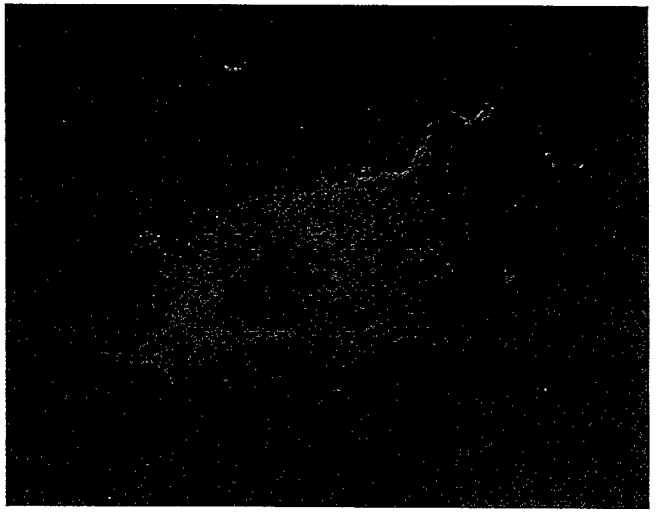

Figure 1

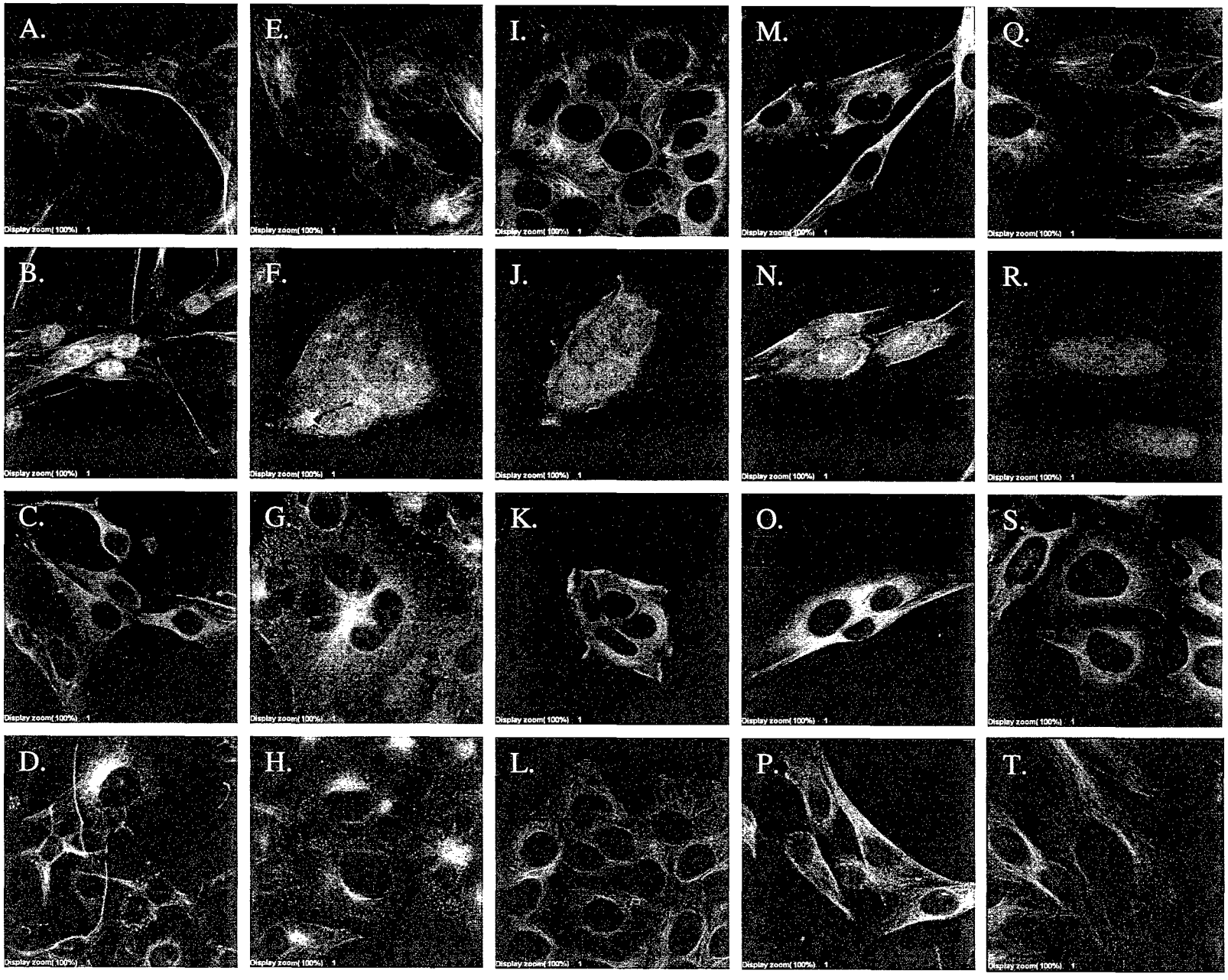

Figure 2

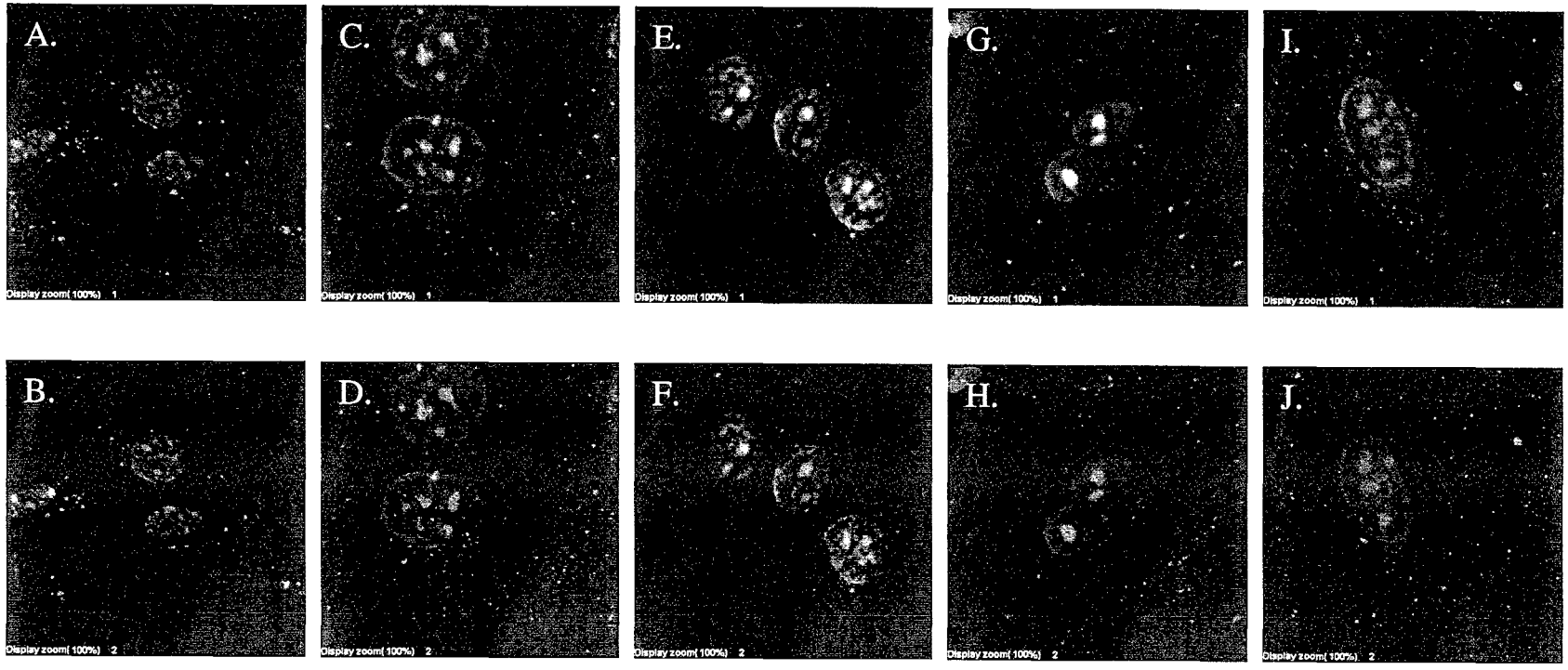

Figure 3

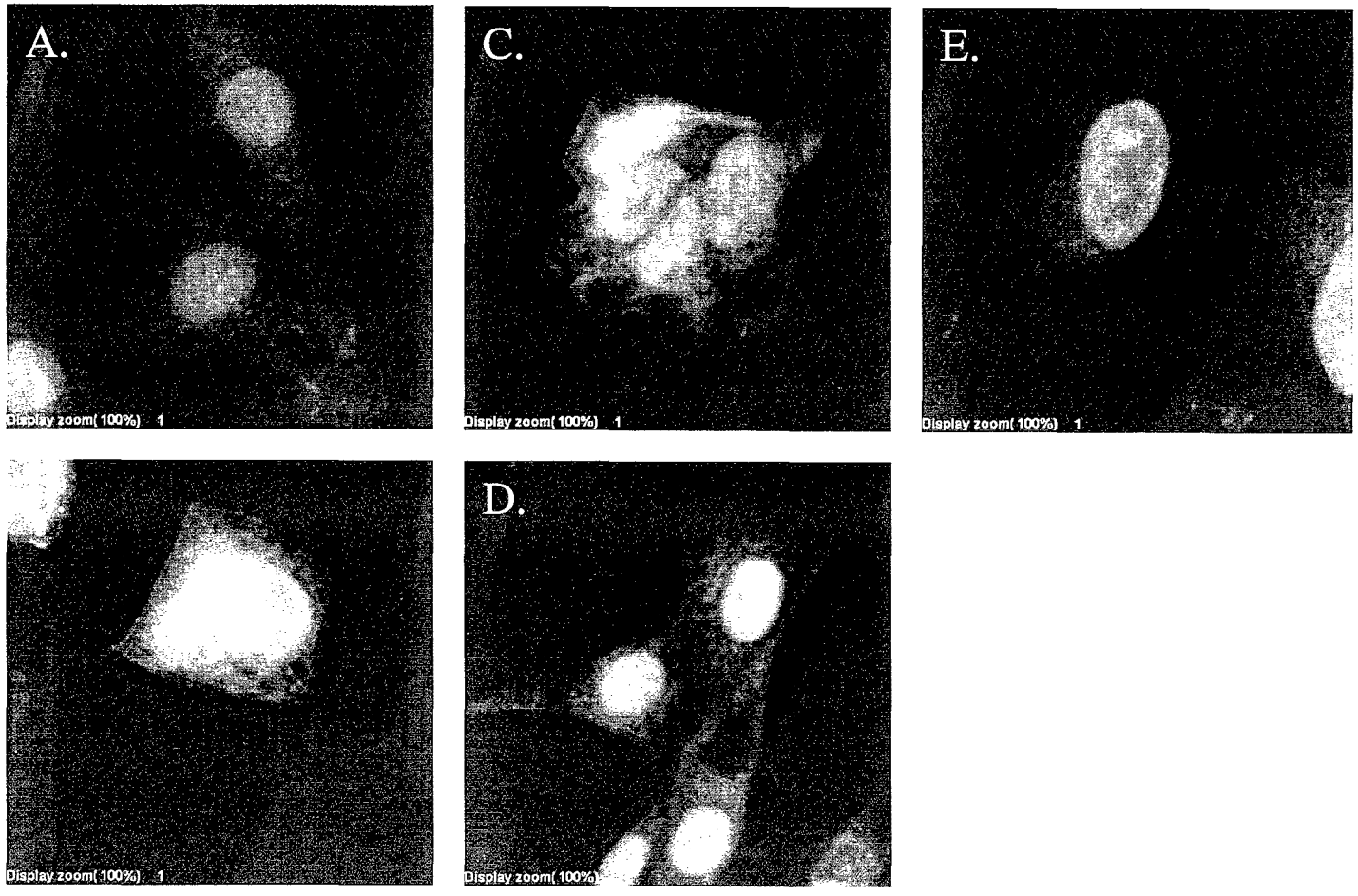
A.
Display zoom(100%) 1
C.
Display zoom(100%) 1
E.
Display zoom(100%) 1
Display zoom(100%) 1
D.
Display zoom(100%)

Figure 4

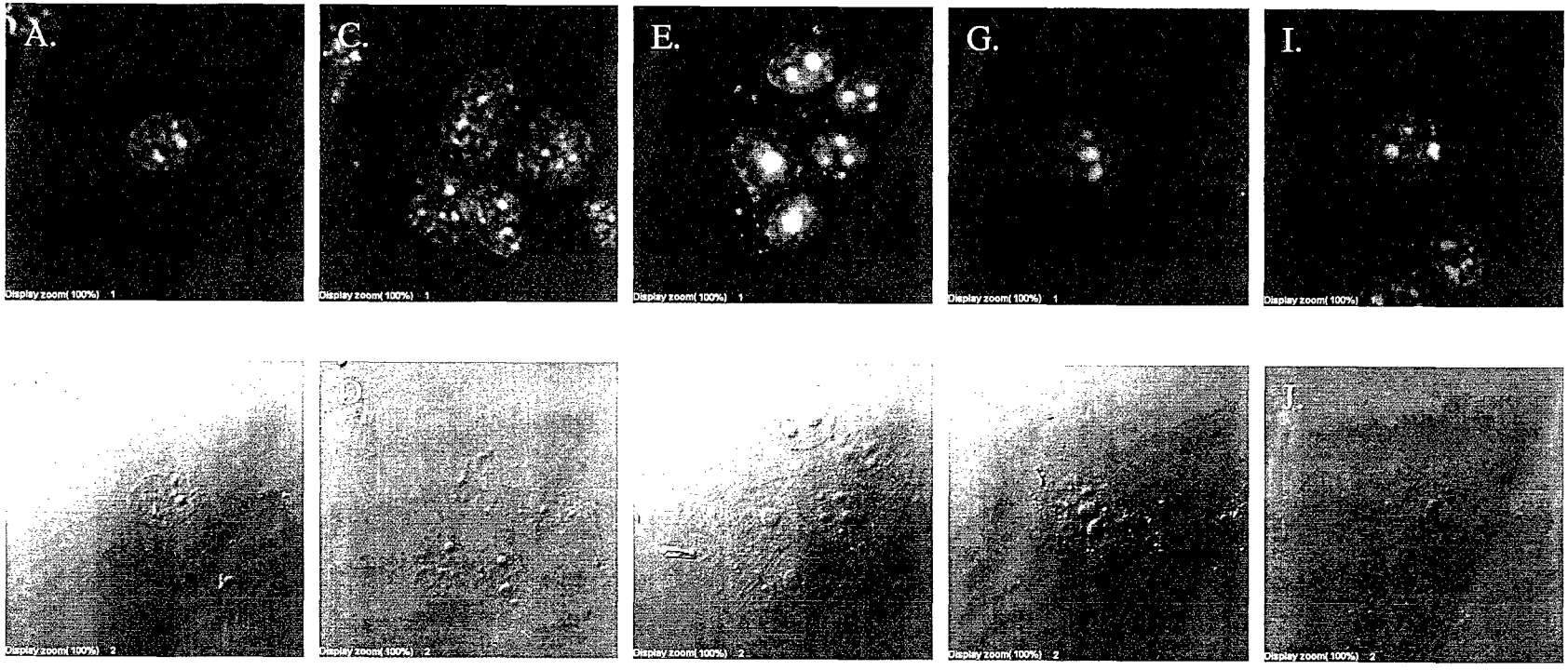

Figure 5

Cells Stained with Anti-βII and Acridine Orange

Primary antibody: anti-βII (1:100); secondary antibody: fluorescein-conjugated goat anti-mouse IgG (1:50)

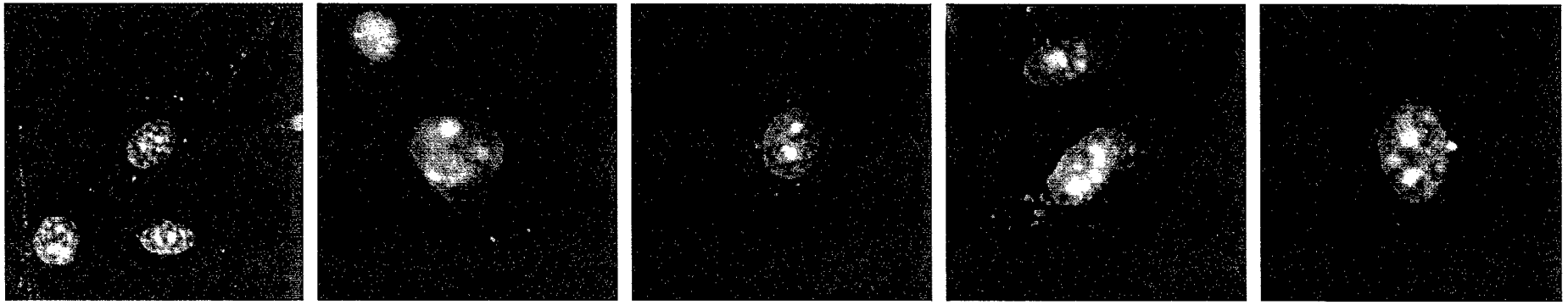

Acridine orange (10 ug/ml)

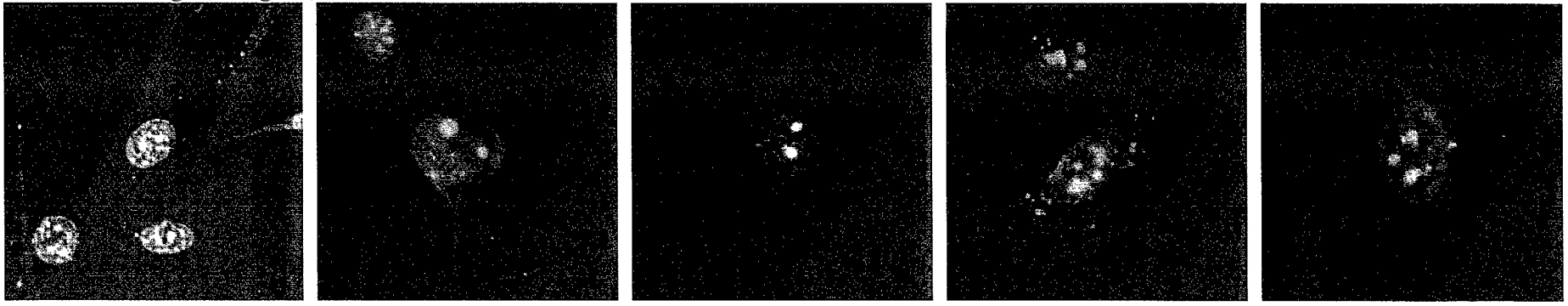

Combined pictures

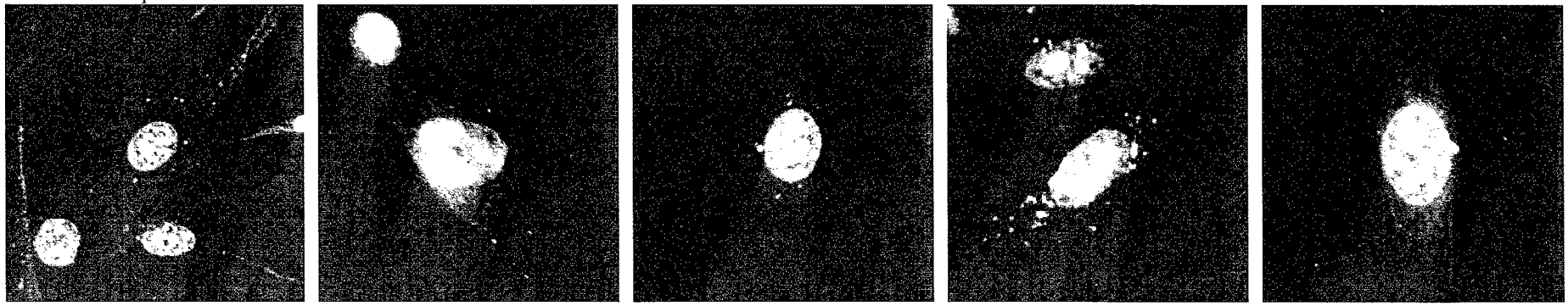

C6 T98G MCF-7 MDA Hela

Figure 6

Colocalization of βII Tubulin and Nucleolus

βII tubulin staining (using rhodamine-conjugated anti-βII, 0.1mg/ml)

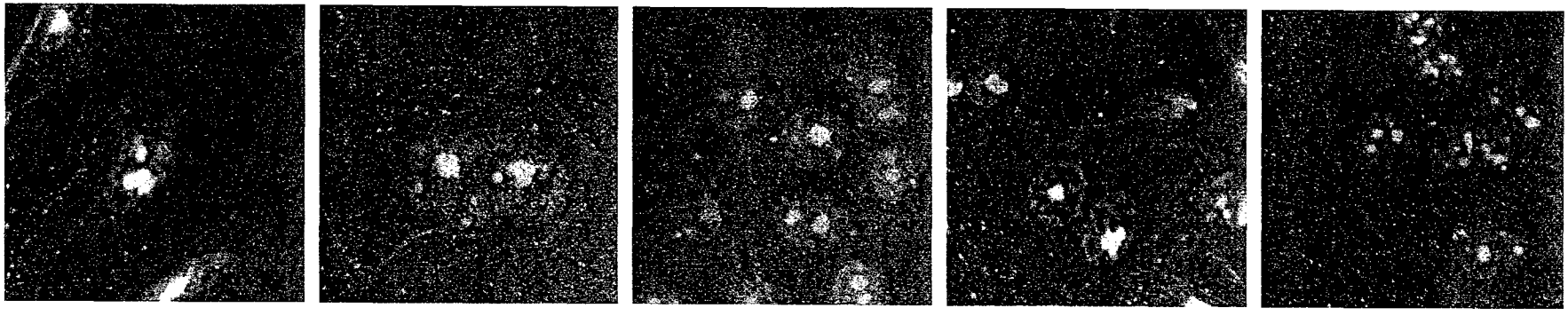

Nucleolin staining (primary antibody: monoclonal anti-nucleolin; secondary antibody: fluorescein-conjugated goat anti-mouse Ig-G)

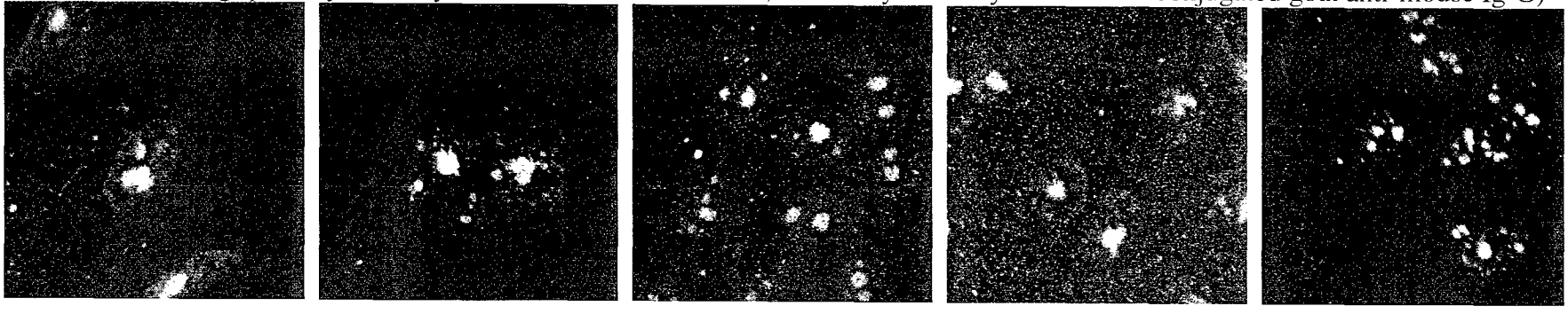

Combined pictures

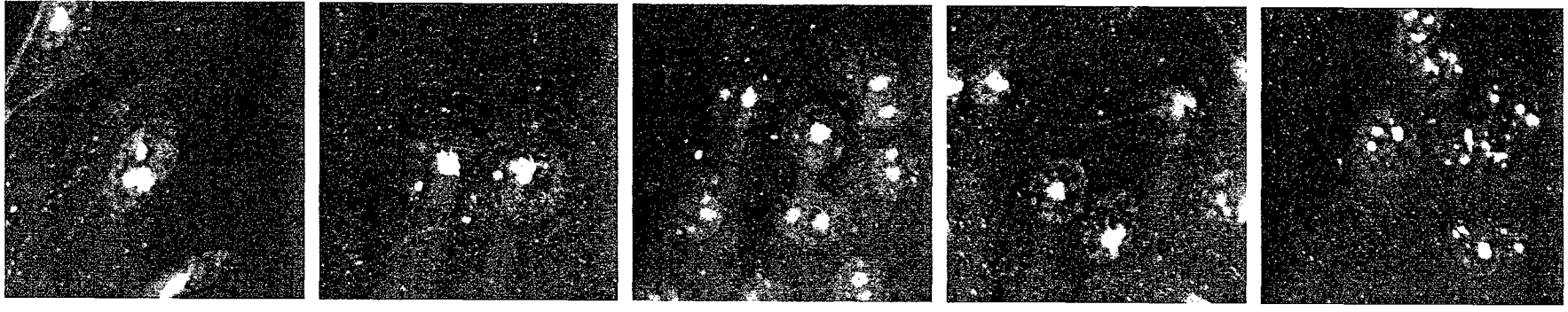

C6 T98G MCF-7 MDA Hela

Figure 7

Extracted Cells Stained with Fluorescein-colchicine and Acridine Orange

Fluorescein-colchicine (0.1 mg/ml)

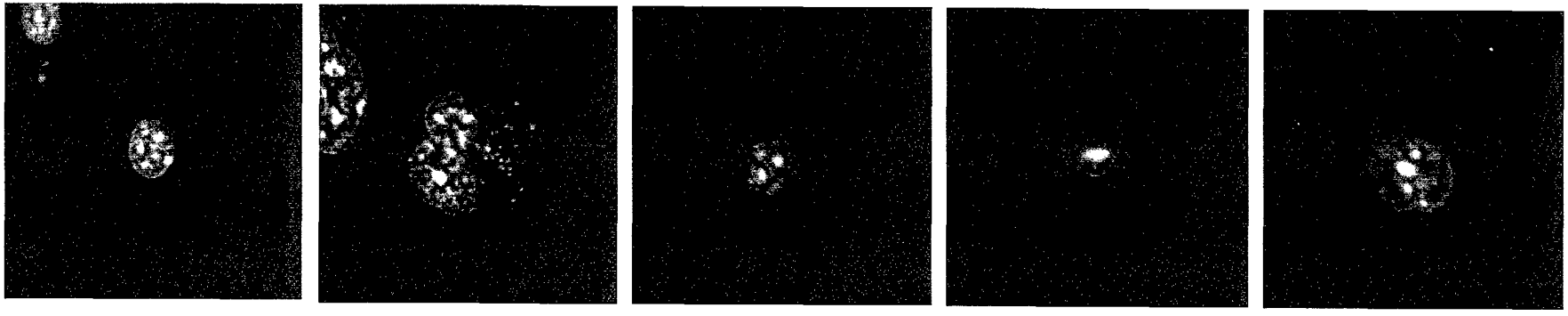

Acridine orange (10 ug/ml)

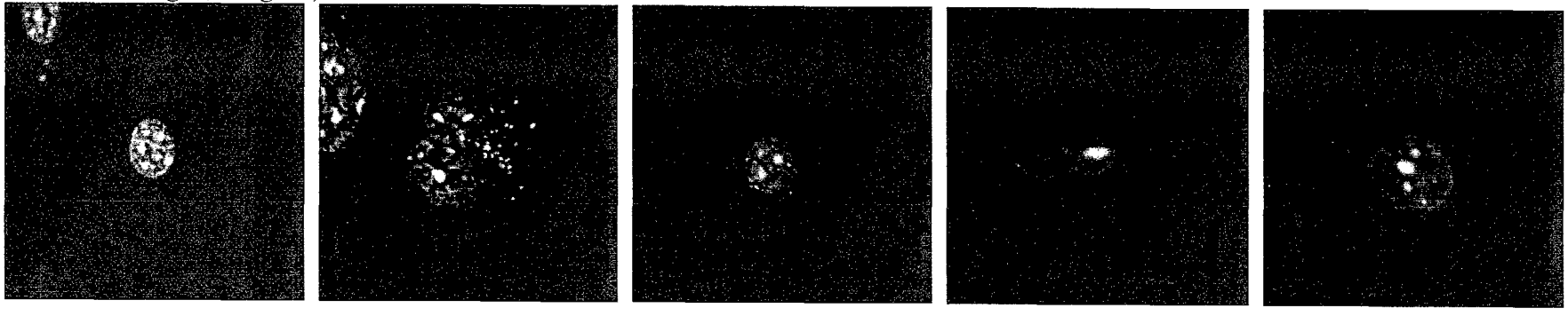

Combined pictures

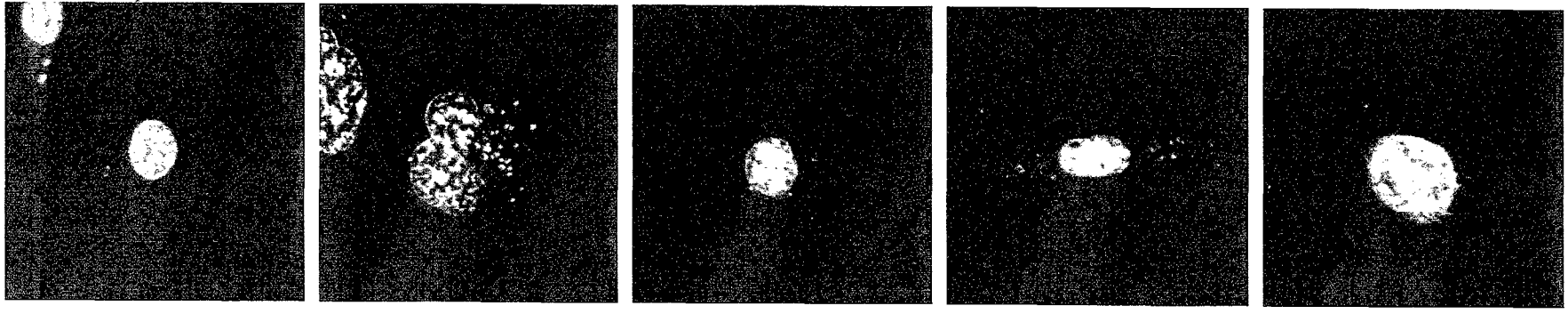

C6 T98G MCF-7 MDA Hela

Figure 8

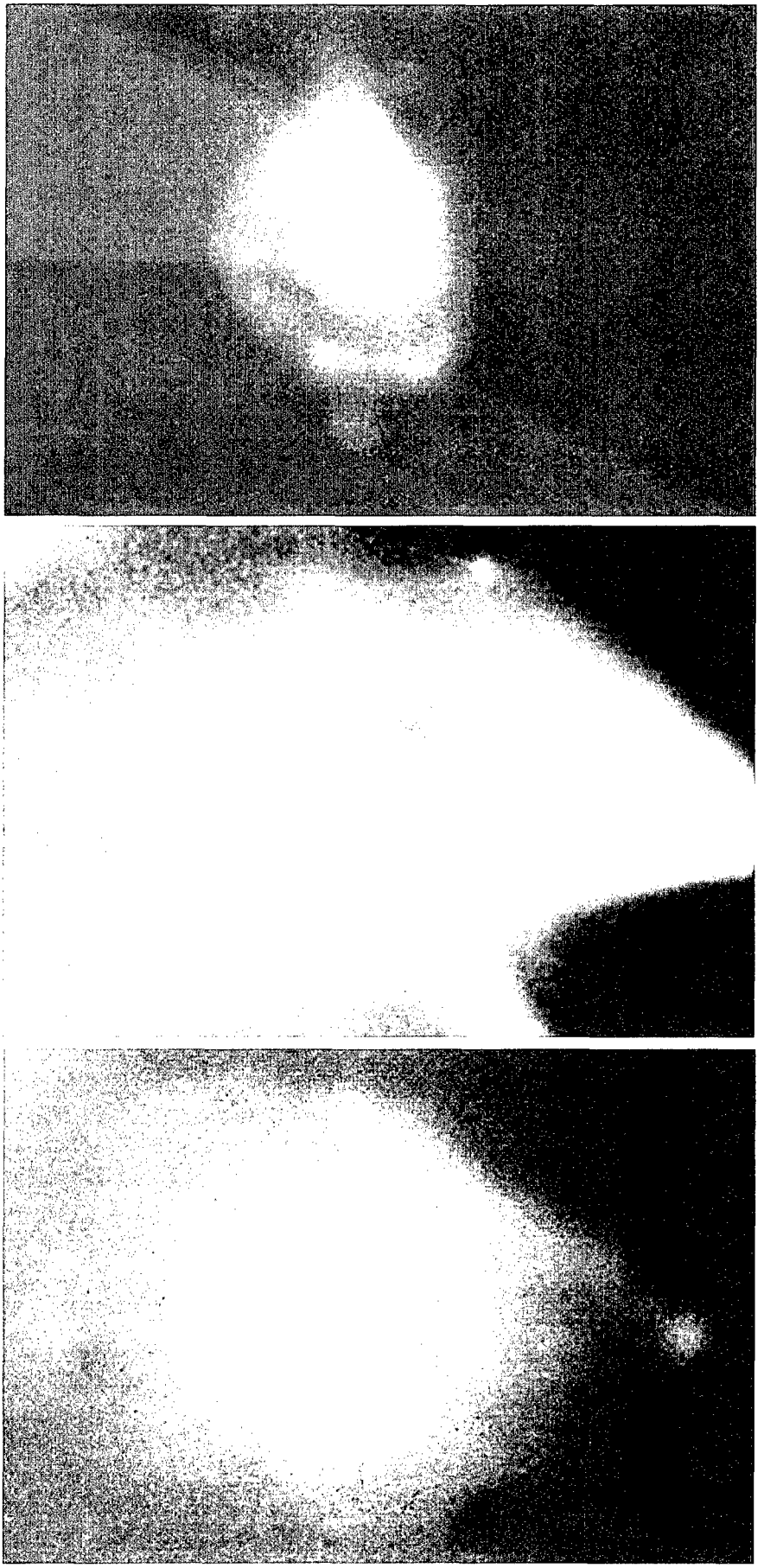

Figure 9

MCF7 +5uM Genistein + 25 uM Genistein

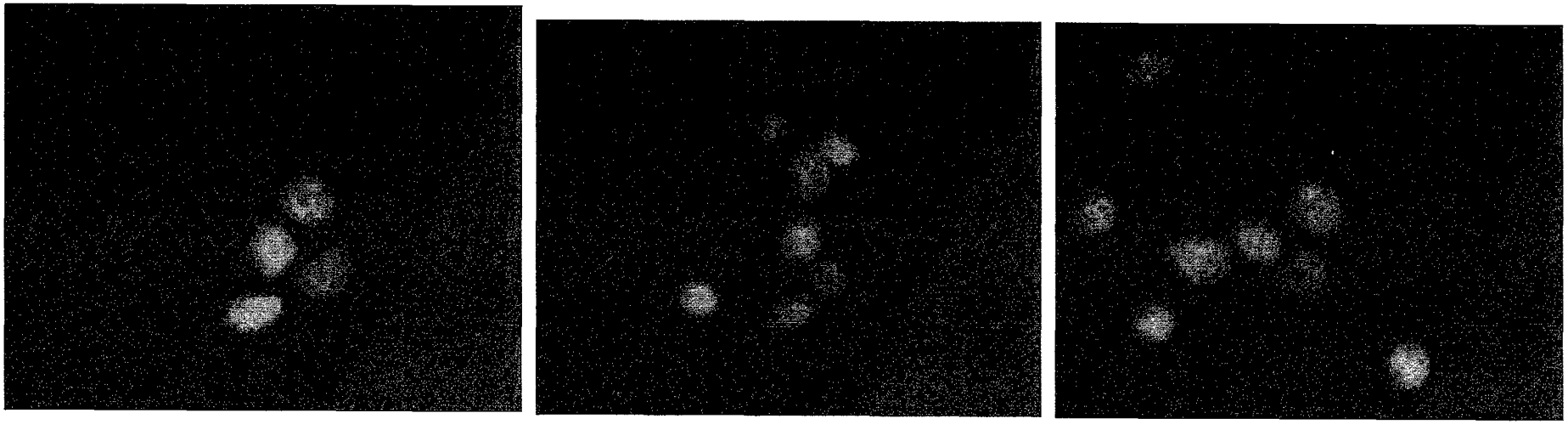

Figure 10

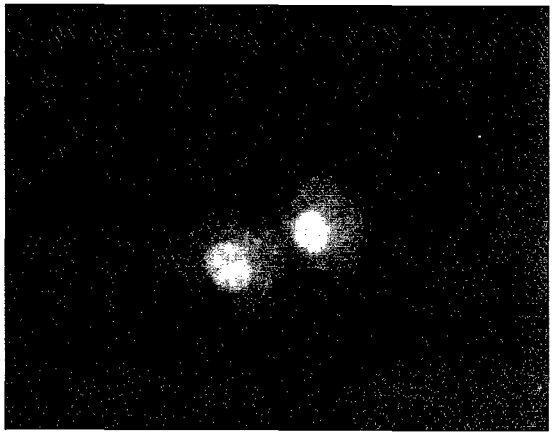

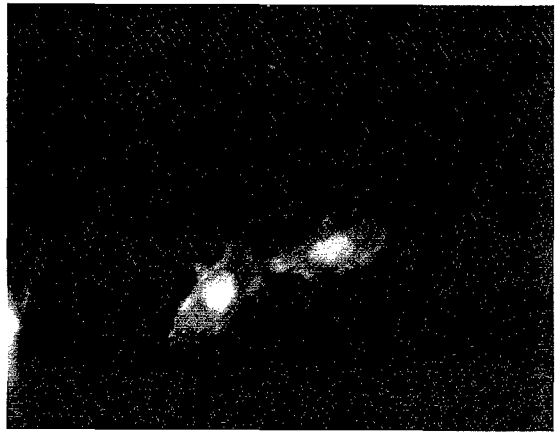

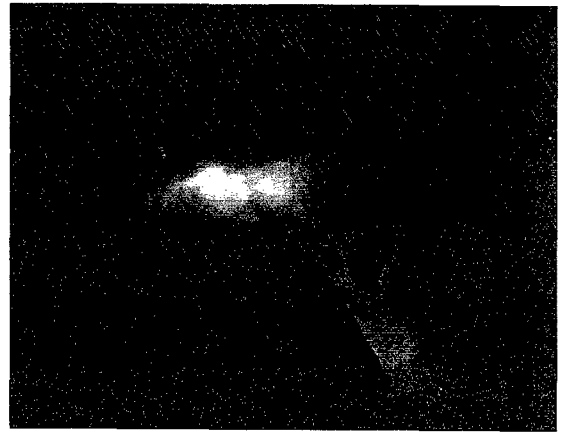

CTL MSN

5umGenistein

50uM Genistein

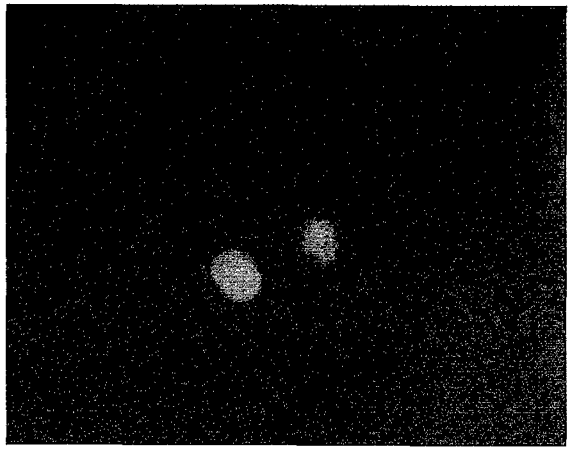

Figure 11

T98G cells treated with Genistein(24 hours)

Control(β2)

5uM Genistein

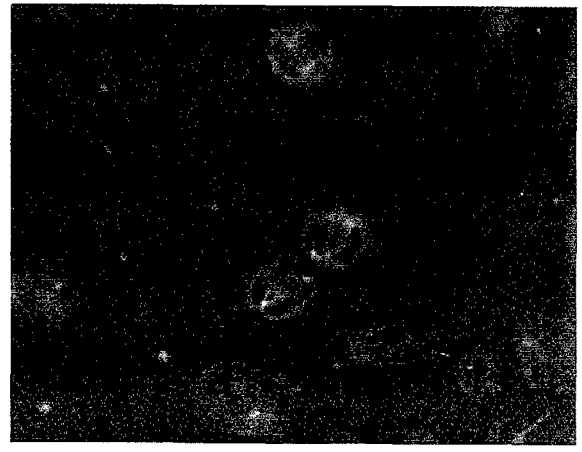

10 uM Genistein

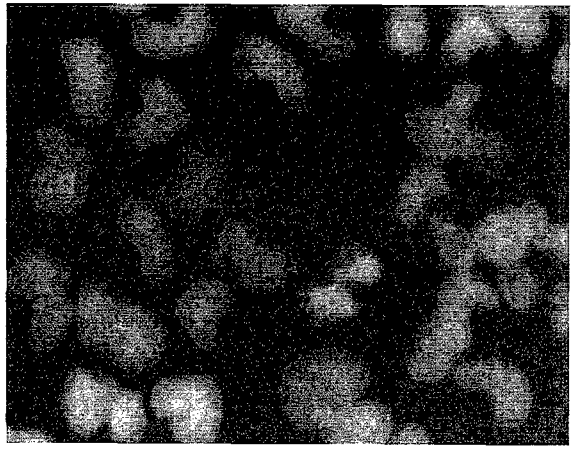

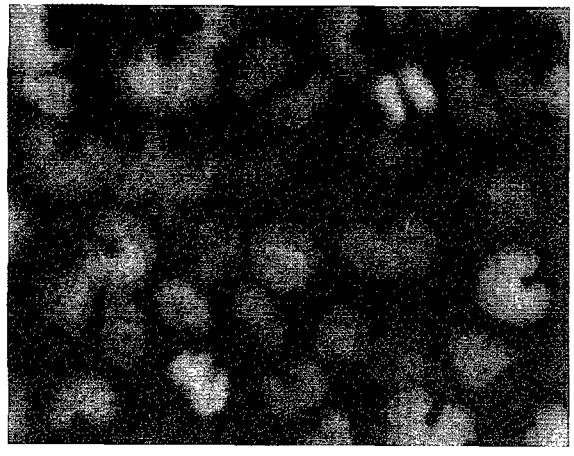

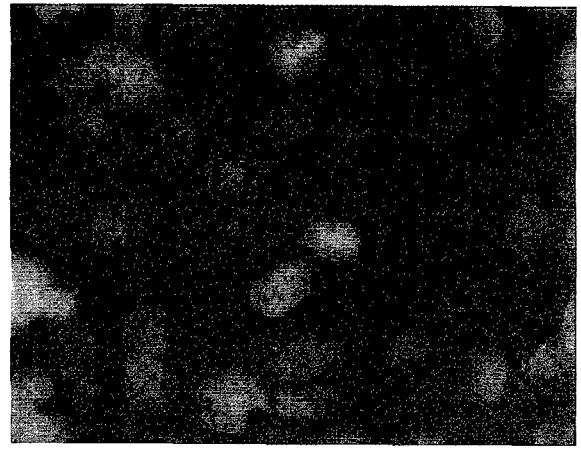

Figure 12

T98 G cells + Genistein (24 hrs)

15 uM 20 uM 25 uM

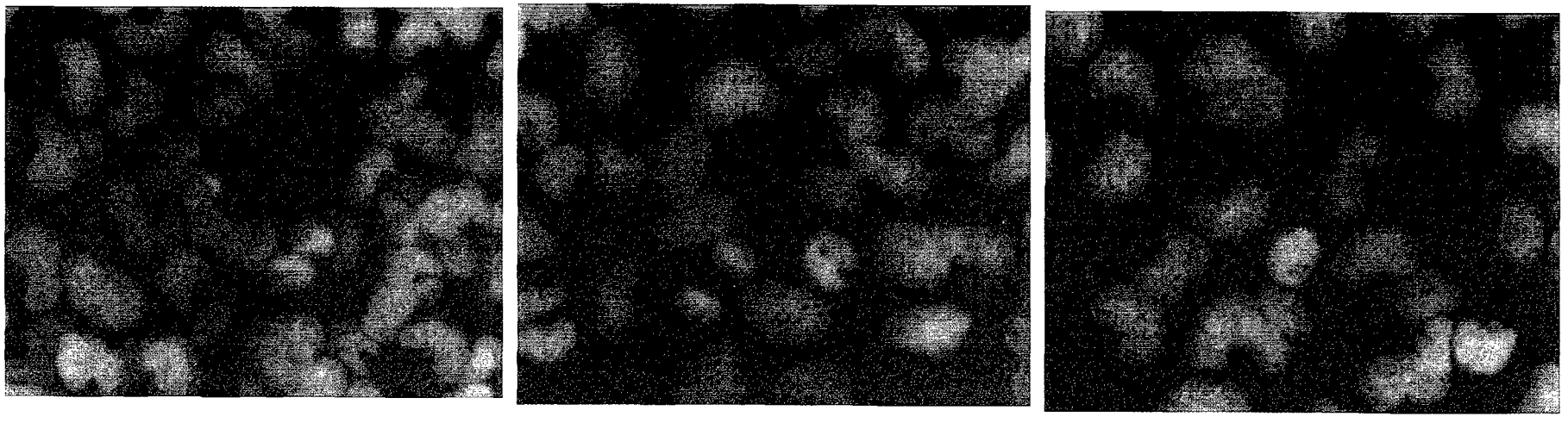

Figure 13

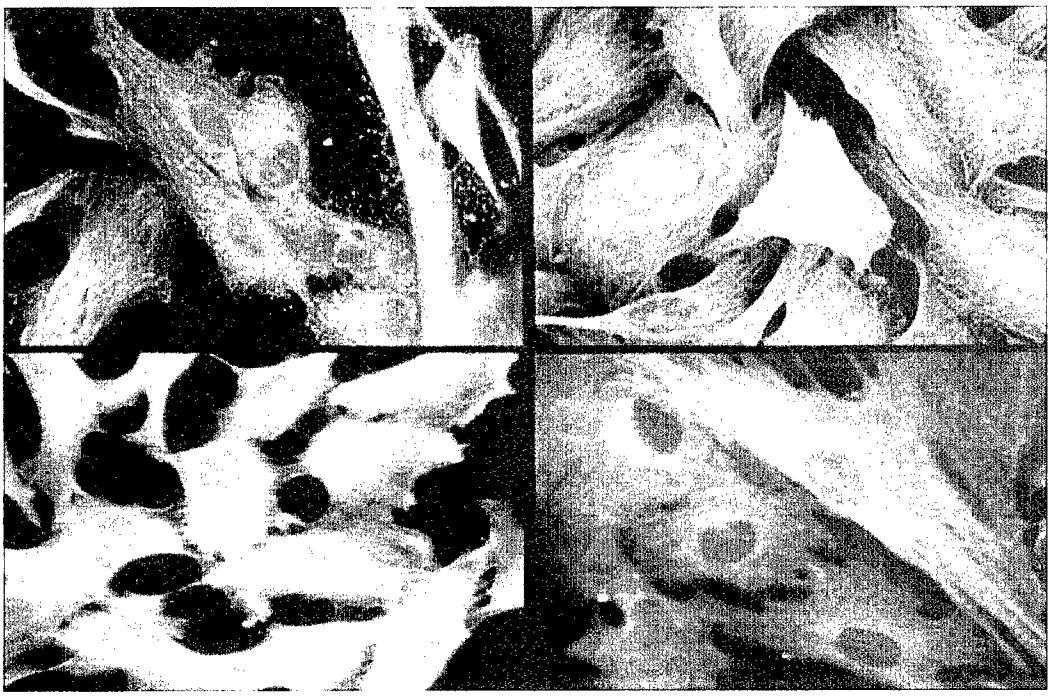

Figure 14

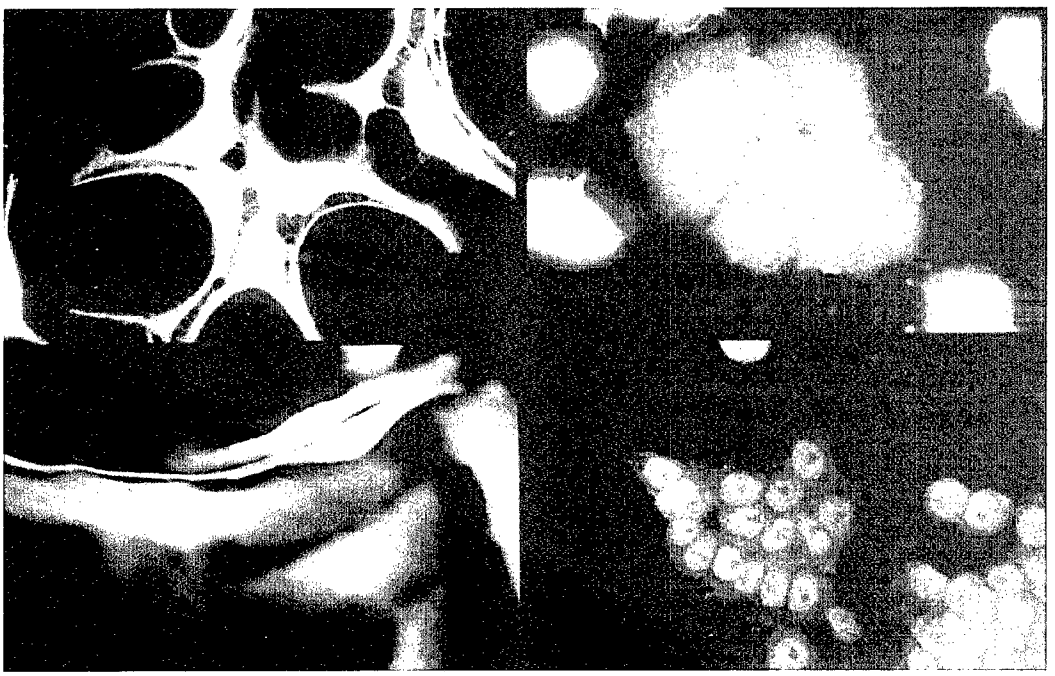

Figure 15

Ductal hyperplasia of the breast, usual type, with cytoplasmic β II tubulin staining.

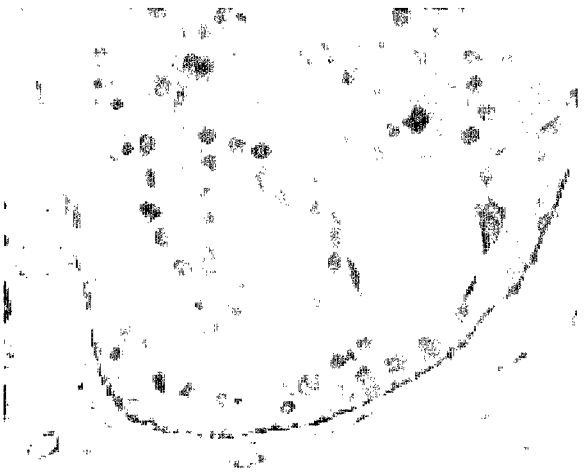

Ductal carcinoma in situ of the breast with nuclear β II tubulin staining.

Colloid carcinoma (invasive) of the breast with nuclear β II tubulin staining.

Figure 16

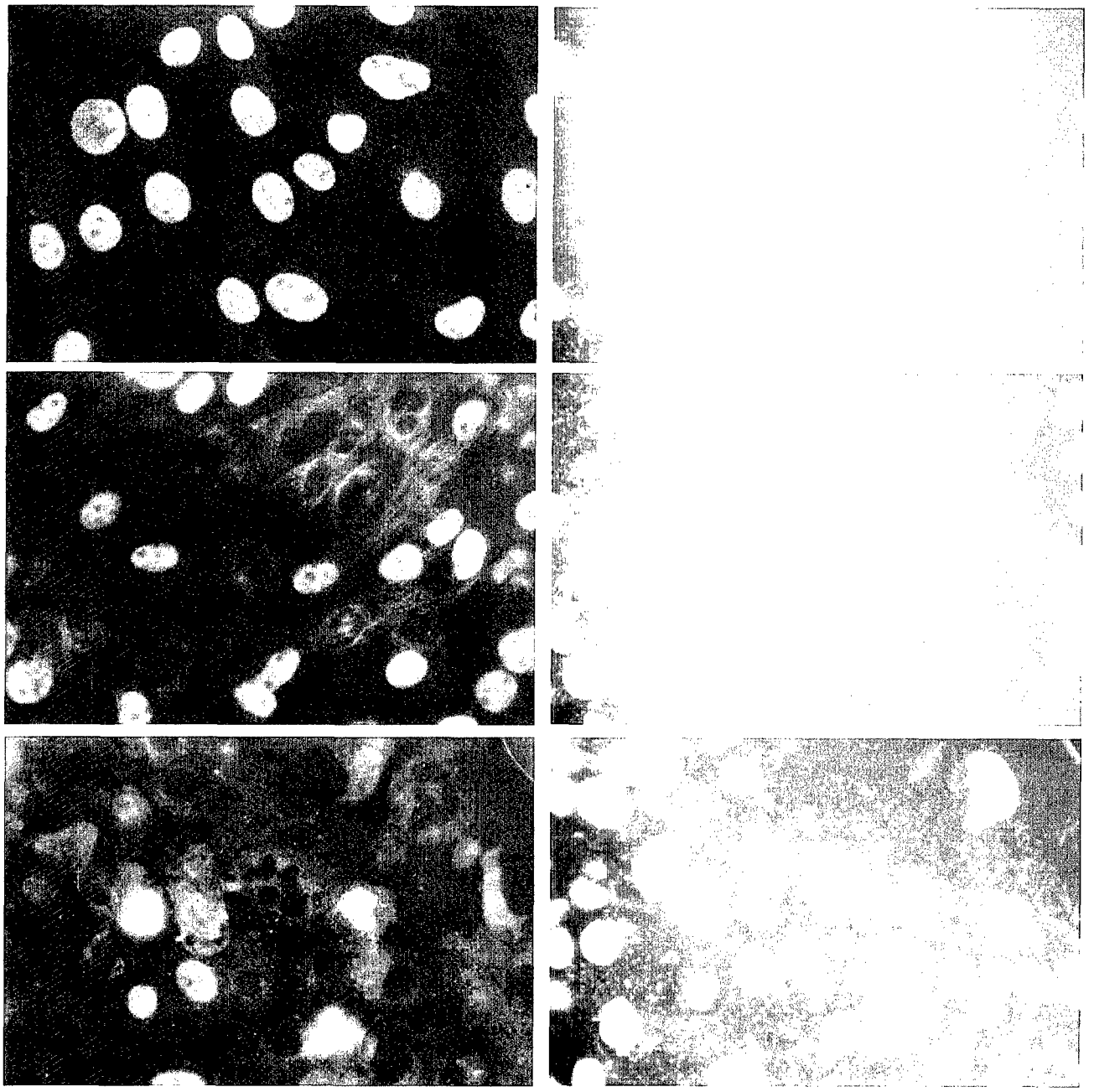

Figure 17

Nuclear βII Depletion Caused by Taxol in MDA Cells

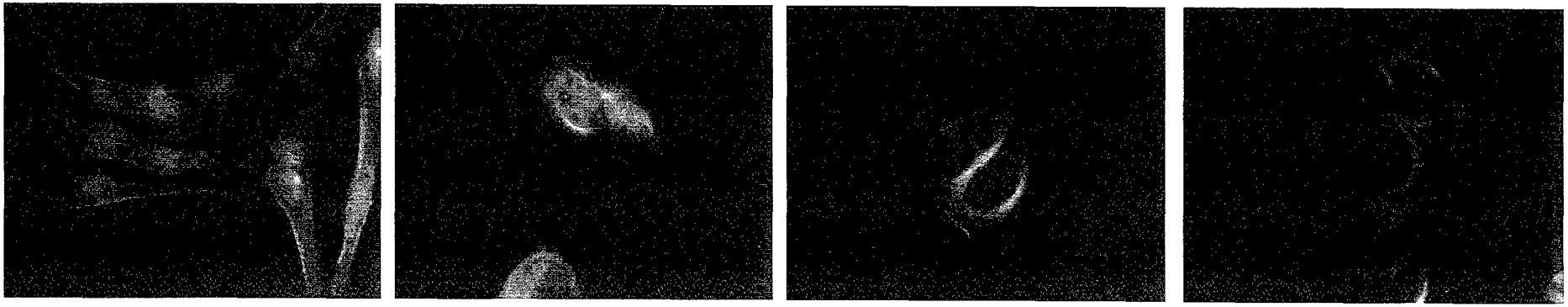

Control (βII) + 30 nM taxol (βII) + 1 μM taxol (βII) + 5 μM taxol (βII)

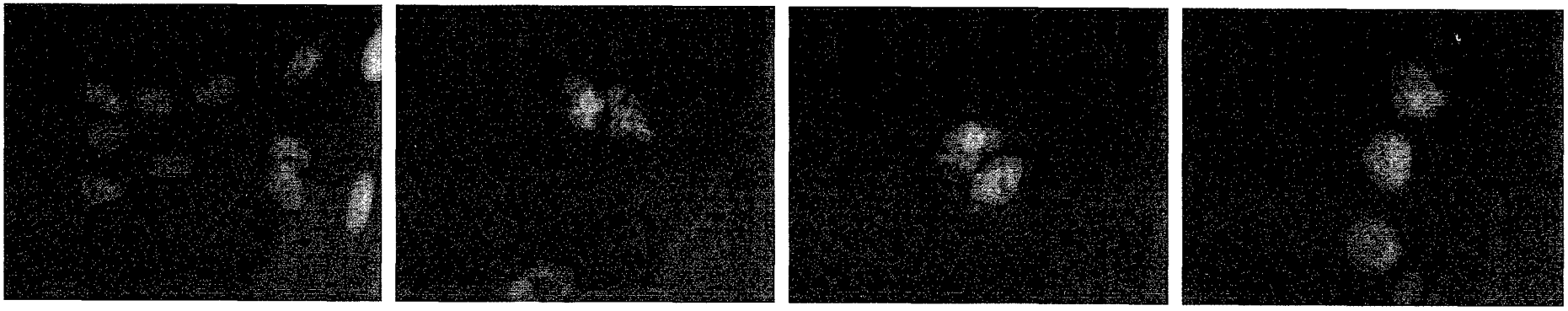

Control (nuclei) + 30 nM taxol (nuclei) + 1 μM taxol (nuclei) + 5 μM taxol (nuclei)

Figure 18

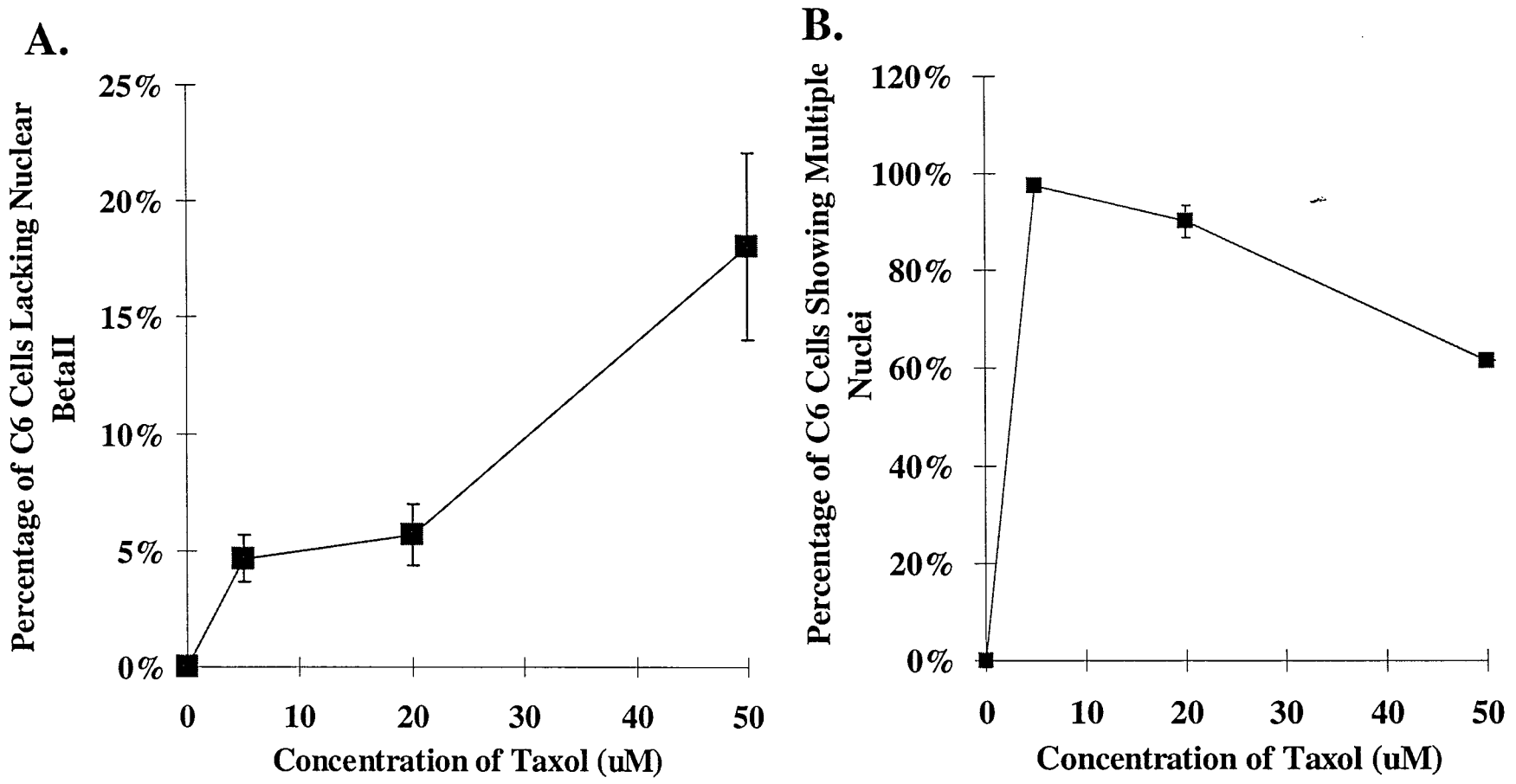
A.
Percentage of C6 Cells Lacking Nuclear BetaII
25%
20%
15%
10%
5%
0%
0
10
20
30
40
50
Concentration of Taxol (uM)
B.
Percentage of C6 Cells Showing Multiple Nuclei
120%
100%
80%
60%
40%
20%
0%
0
10
20
30
40
50
Concentration of Taxol (uM)

Figure 19

Effect of Anti-tubulin Drugs on MDA Cells

Control (βII)

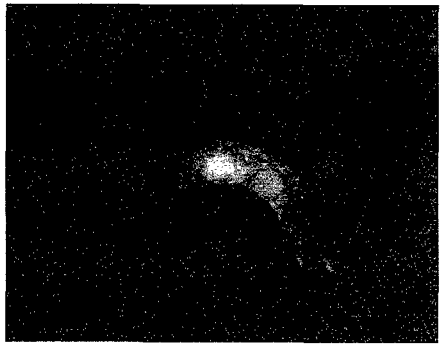

+ 10 μM colchicine (βII)

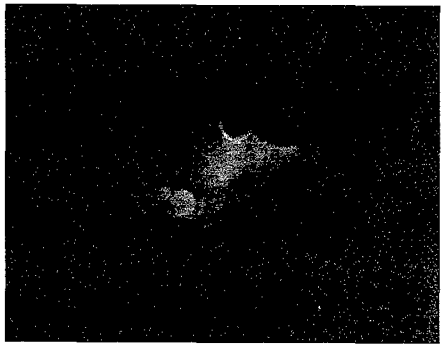

+ 10 μM estramustine (βII)

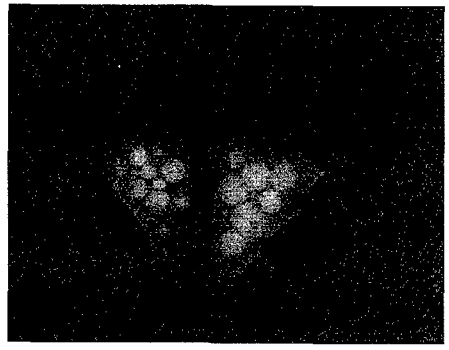

+ 10 μM nocodazole (βII)

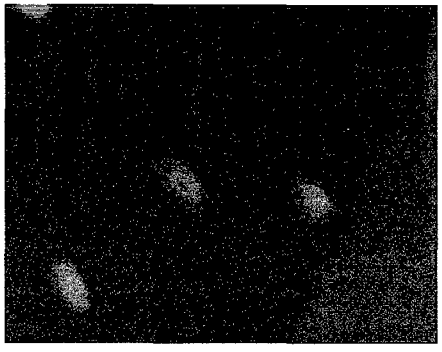

Control (nuclei)

+ 10 μM colchicine (nuclei)

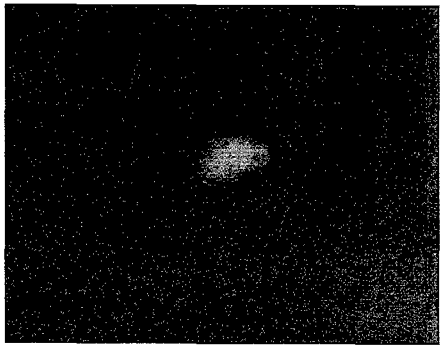

+ 10 μM estramustine (nuclei)

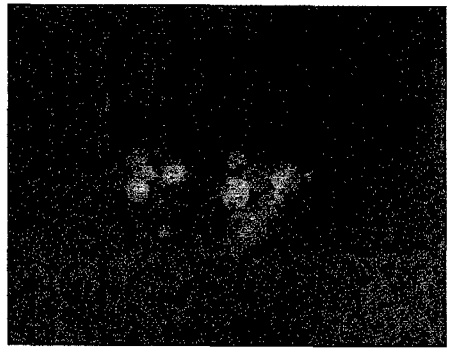

+ 10 μM nocodazole (nuclei)

Figure 20

Effect of Anti-tubulin Drugs on MCF-7 Cells

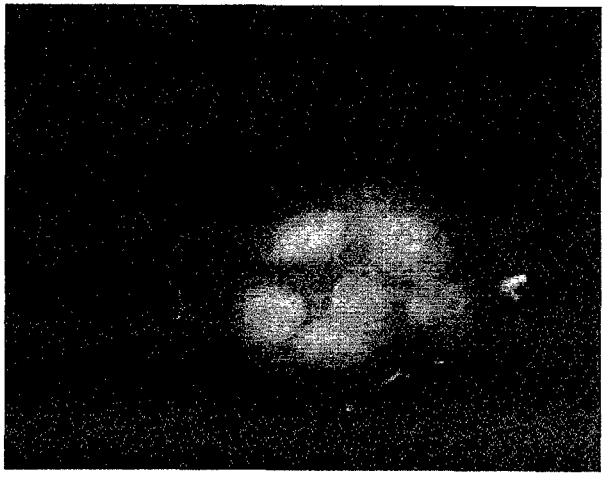

Control (βII)

+ 10 μM colchicine (βII)

+ 10 μM estramustine (βII)

Control (nuclei)

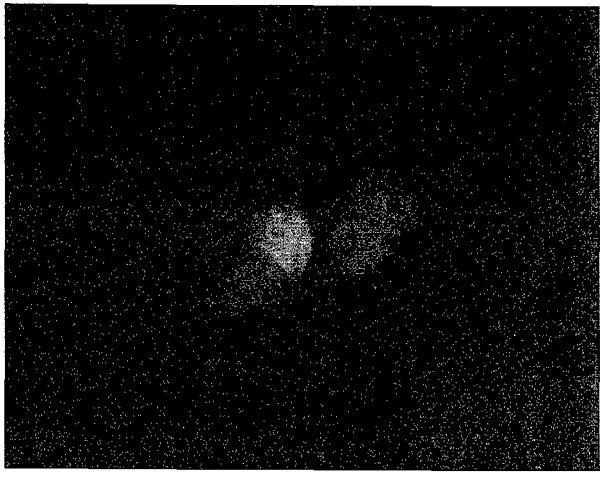

+ 10 μM colchicine (nuclei)

+ 10 μM estramustine (nuclei)

Figure 21

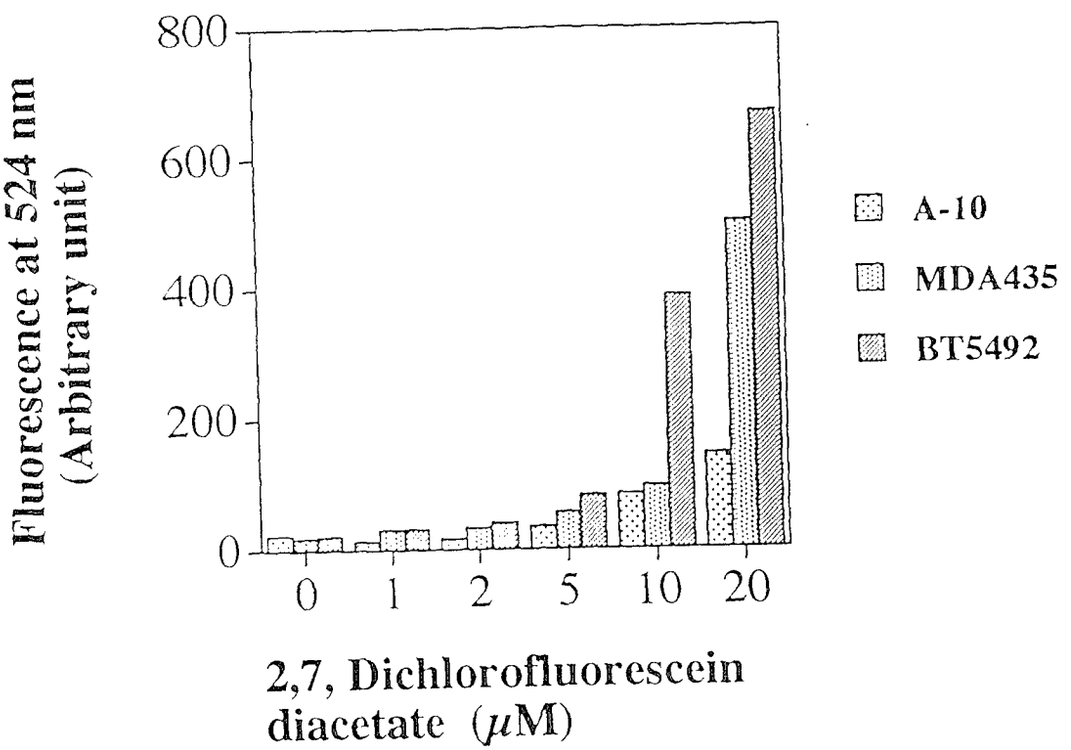
Fluorescence at 524 nm
(Arbitrary unit)
800
600
400
200
0
0
1
2
5
10
20
2,7, Dichlorofluorescein
diacetate (μM)
A-10
MDA435
BT5492

Figure 22

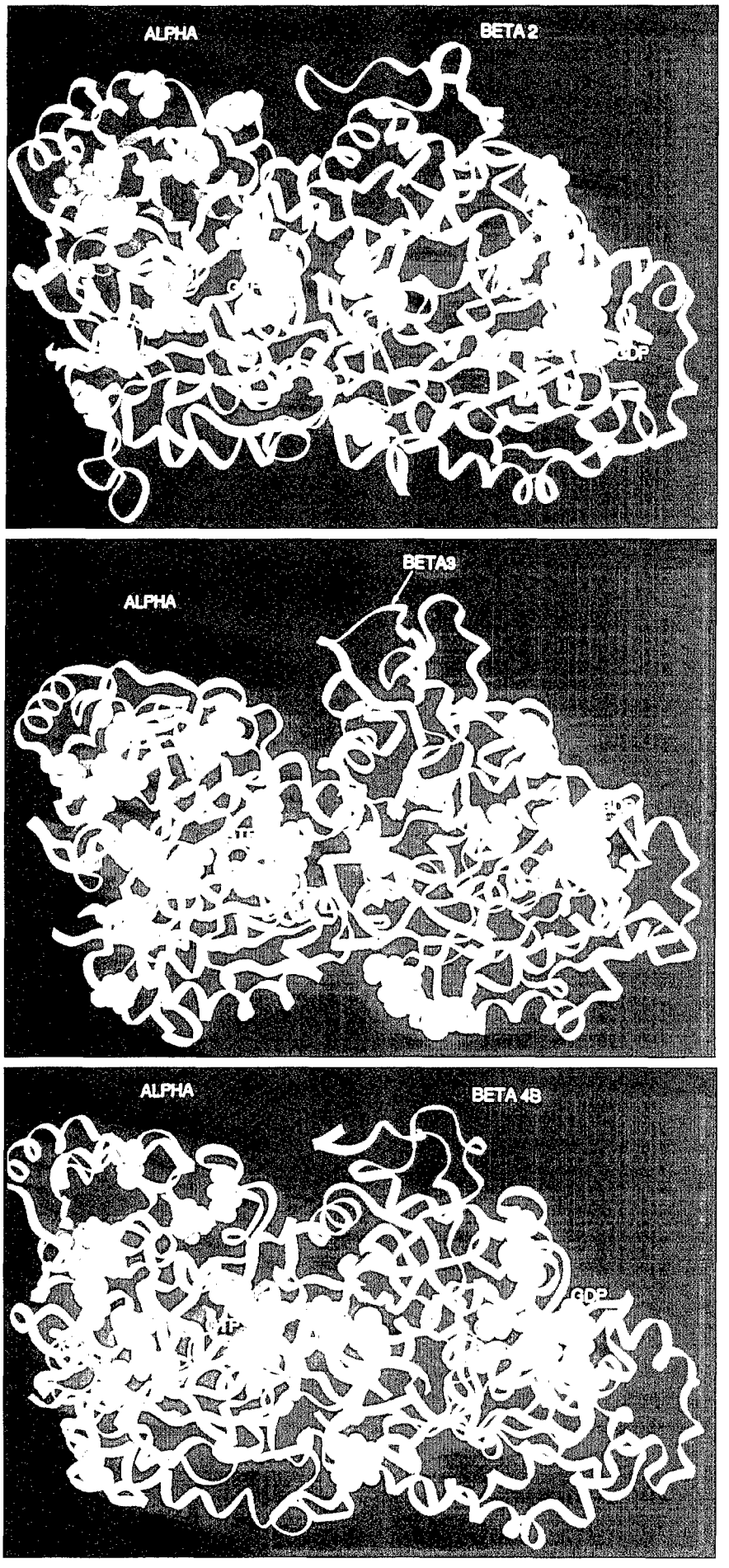

Figure 23

Scheme 1

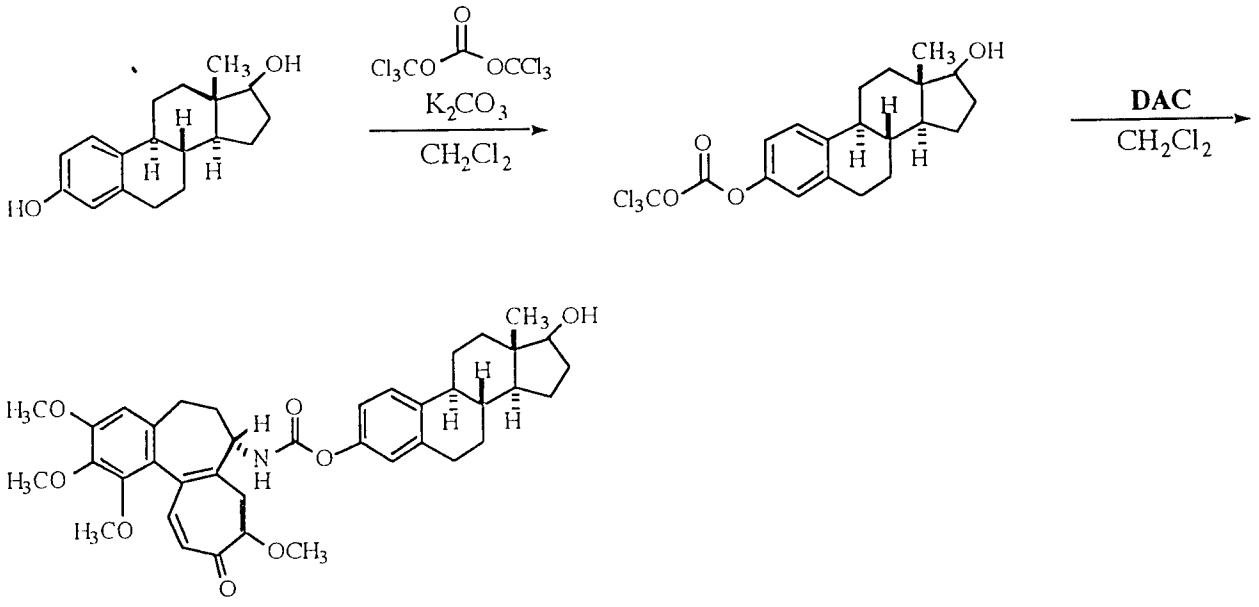

DAC-Estradiol

Scheme 2

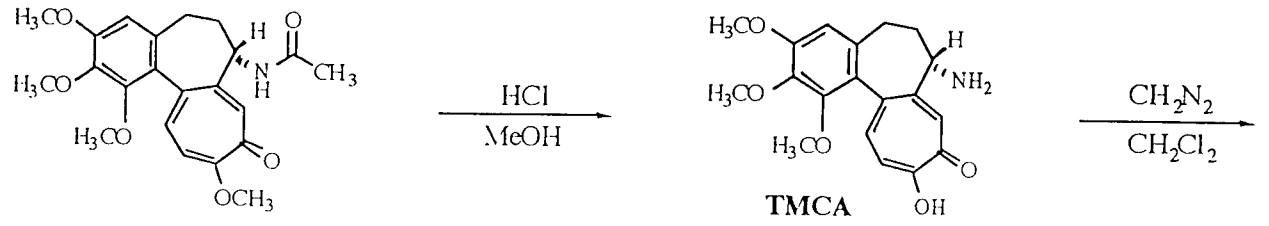

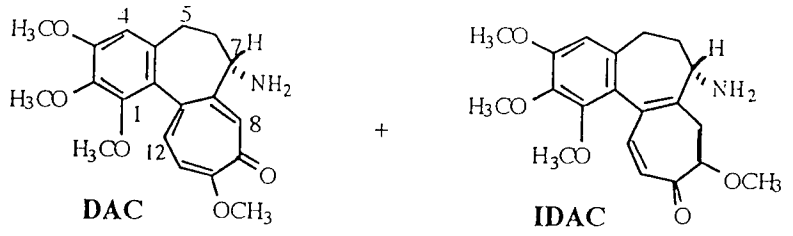

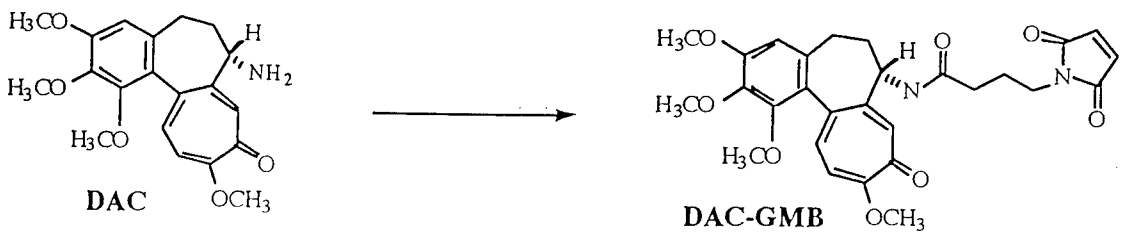

DAC-GMB ----------→ KRPRPCGMNKEARKTKK (DAC: C; Fluor: K)

Peptidyl-colchicine derivative

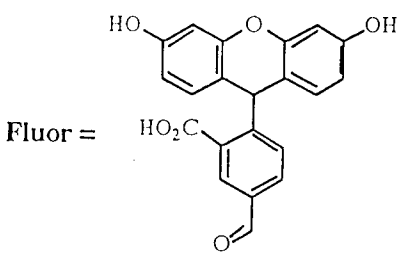

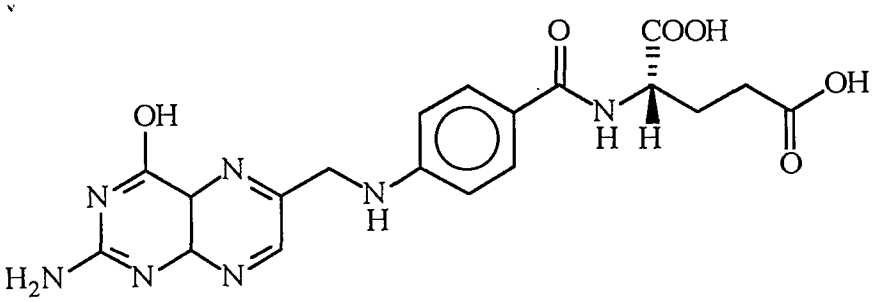

Folic Acid

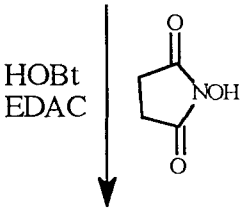

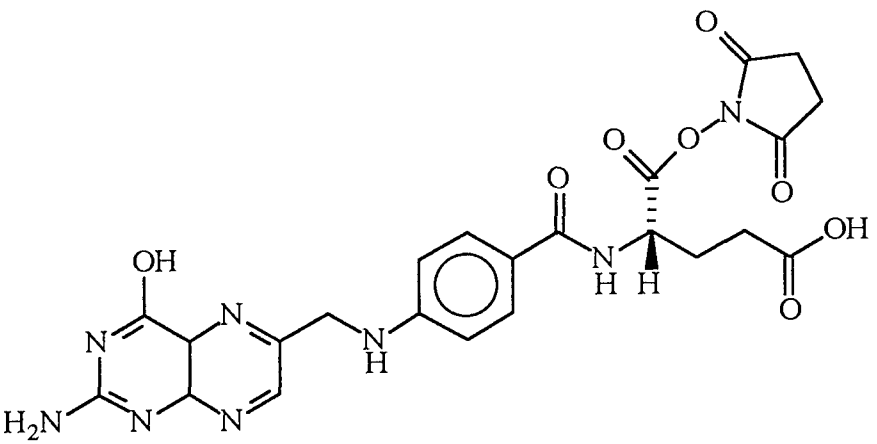

1

+

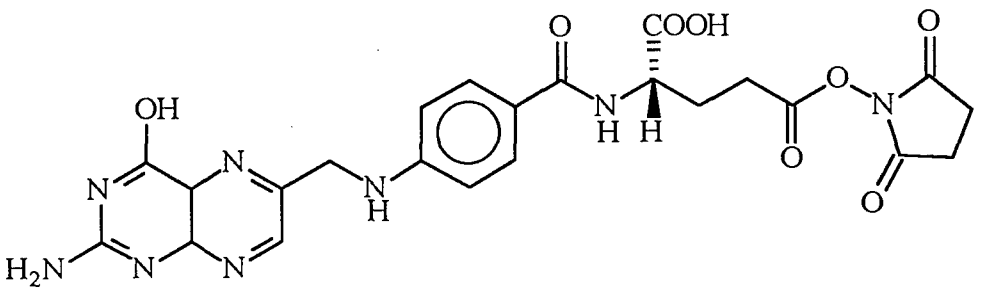

2

Scheme 3

Interaction of the β_{IV}-tubulin Isotype with Actin Stress Fibers in Cultured Rat Kidney Mesangial Cells

Consuelo Walss-Bass*, Veena Prasad*, Jeffrey I. Kreisberg† & Richard F. Ludueña*

*Departments of *Biochemistry and †Surgery, University of Texas Health Science Center, San Antonio, Texas 78284, USA and †The Research and Development Service Department of Veteran Affairs, San Antonio, Texas 78284, USA.*

Send correspondence to:

Dr. Richard F. Ludueña
Department of Biochemistry
University of Texas Health Science Center
San Antonio, TX 78284-7760

Tel: 210-5673732
FAX: 210-5676595
e-mail: luduena@uthscsa.edu

Running Title: β_{IV}-Tubulin Interacts with Actin Stress Fibers

ABSTRACT

Microtubules and actin filaments are two of the major components of the cytoskeleton. There is accumulating evidence for interaction between the two networks. Both the α- and β-subunits of tubulin exist as numerous isotypes, some of which have been highly conserved in evolution. In an effort to better understand the functional significance of tubulin isotypes, we used a double immunofluorescence labeling technique to investigate the interactions between the tubulin β-isotypes and the actin stress fiber network in cultured rat kidney mesangial cells, smooth-muscle-like cells from the renal glomerulus. Removal of the soluble cytoplasmic and nucleoplasmic proteins by detergent extraction caused the microtubule network to disappear while the stress fiber network was still present. In these extracted cells, the β_I- and β_{II}-tubulin isotypes were no longer present in the cytoplasm while the β_{IV}-isotype co-localized with actin stress fibers. Co-localization between β_{IV}-tubulin and actin stress fibers was also observed when the microtubule network was disrupted by the anti-tubulin drug colchicine and also by microinjection of the β_{IV}-tubulin antibody. Our results suggest that the β_{IV} isotype of tubulin may be involved in interactions between microtubules and actin.

Key words: Actin stress-fibers, microtubules, depolymerization, tubulin isotypes

INTRODUCTION

Although it has long been known that actin filaments and microtubules work hand in hand in a variety of cellular processes such as cell division, cell motility and cell trafficking (reviewed in Gavin, 1997), recent findings have suggested that the relationship between these two cytoskeletal systems is more intimate than previously thought. Evidence of direct interactions between actin and microtubules has recently been shown in *Xenopus* egg extracts (Sider *et al.*, 1999; Bement *et al.*, 1997) and a number of actin-microtubule cross-linking proteins have been reported (reviewed in Goode *et al.*, 2000) and connections between the two systems continue to be discovered (Davy *et al.*, 2001). Furthermore, positive feed-back loops have been suggested between the two cytoskeletal systems where assembly of microtubules at the leading edge of cells promotes actin assembly in lamellipodia via activation of Rac1; similarly, disassembly of microtubules in the cell body promotes stress fiber formation and contractility via activation of Rho A (reviewed in Waterman-Storer and Salmon, 1999 and Gunderson and Cook, 1999).

That microtubules can influence the dynamic properties of the actin cytoskeleton has been clearly demonstrated. Early studies showed that when cultured cells are treated with microtubule depolymerizing agents such as colchicine or vinblastine, a rapid increase in cell contractility and actin stress fiber organization is observed (Danowski, 1989). The molecular mechanisms by which this occurs are just now being characterized. Results obtained from several studies have suggested that microtubule depolymerization may activate the RhoA-signaling cascade and promote myosin II based phosphorylation

which induces formation of focal contacts and actin stress fibers (Kolodney and Elson, 1995; Chrzanowska and Burridge, 1996). This has led to the hypothesis that microtubules contain a stress-fiber inducing factor, which is released by depolymerization and activates RhoA (Enomoto, 1996). To date, the identity of this factor remains unknown, although several candidates have been proposed (Gundersen and Cook, 1999).

We have previously examined the distribution of the β_I, β_{II} and β_{IV} isotypes of tubulin in cultured rat kidney mesangial cells (Walss *et al.*, 1999); these are smooth-muscle-like cells from kidney glomeruli that, under certain conditions, are rich in actin stress fibers (Kreisberg et al., 1986). We found that the β_I and β_{IV} isotypes are restricted to the cytoplasm, but that β_{II} is also localized in the nucleus (Walss *et al.*, 1999). We now show that the β_{IV} isotype is associated with actin stress fibers in these cells and that the association becomes apparent when the microtubules are disrupted. This is not seen to occur with either the β_I or β_{II} isotypes. These results may provide new information as to the mechanism by which microtubules influence actin stress fiber assembly.

MATERIALS AND METHODS

Source of cells and antibodies.

Rat kidney mesangial cells were obtained as follows. Glomeruli were isolated from 200 g male Sprague-Dawley rats (Harlan Sprague-Dawley Inc., Indianapolis, IN) using a graded sieve technique and were plated for culture in RPMI 1640 (Gibco BRL, Grand Island, N.Y.) tissue culture medium with 20% FCS plus penicillin, streptomycin and fungizone (E.R. Squibb and Sons) for explant growth of mesangial cells (Ausiello *et al.*, 1980; Kreisberg *et al.*, 1984). One hundred percent of the cells were identified as glomerular mesangial cells. Positive identification was obtained by ultrastructural examination, contractile responsiveness to vasopressin and angiotensin II, and shape change in response to cAMP-elevating agents (Kreisberg *et al.*, 1986; Ausiello *et al.*, 1980; Kreisberg *et al.*, 1984). For the experiments described below, cells were used between the 4th and 40th passage.

The monoclonal antibodies SAP.4G5, JDR.3B8, and ONS.1A6 specific, respectively, for the β_I, β_{II} and β_{IV} isotypes of tubulin were prepared as previously described (Banerjee *et al.*, 1988, 1990, 1992; Roach *et al.*, 1998). The peptide CEAEEEVA, used as immunogen to raise the antibody to β_{IV}-tubulin, was synthesized by the BioSearch Corp., San Rafael CA. Except for the N-terminal cysteine, the sequence of this peptide is identical to the C-terminal sequence of the β_{IV}-tubulin isotype.

Immunofluorescence microscopy.

Rat kidney mesangial cells were grown to near confluency on glass coverslips at 37 °C and 5% CO_2 in RPMI-1640 medium (GibcoBRL, Grand Island, N.Y.) containing 20% fetal calf serum (Atlanta Biologicals, Norcross, GA). Cells were then

washed twice with phosphate-buffered saline (PBS), fixed for 10 min with 3.7 % paraformaldehyde at room temperature and permeabilized for 1 min with 0.5% Triton X-100 in PBS. Cells were then incubated at 4 °C overnight with the respective primary antibody (anti-β_I, 0.05-0.1 mg/ml; anti-β_{II}, 0.03-0.1 mg/ml; anti-β_{IV}, 0.08-0.17 mg/ml) diluted in PBS containing 10% normal goat serum (Jackson Immunoresearch, West Grove, PA). Cells were rinsed in PBS and labeled with Cy3-conjugated goat anti-mouse antibody (1:100, Jackson Immunoresearch, West Grove, PA) for 1 hr at room temperature. Coverslips were mounted on glass slides and examined with a Zeiss epifluorescence photomicroscope using a Plan-Neufluar 63x oil objective. For double labeling experiments using Bodipy phalloidin (Sigma Chemical Co., St. Louis, MO) as a marker for F-actin, cells were treated as described above for regular immunofluorescence experiments and then incubated with Bodipy phalloidin (1:50) for 30 min at room temperature. Cells were then rinsed and fixed for visualization. For immunoblocking experiments, to prove antibody specificity, anti-β_{IV} was incubated with a 200-fold excess of the peptide CEAEEEVA, used as immunogen to raise this antibody, for 30 min at room temperature prior to incubation with fixed and permeabilized cells.

***In situ* cell fractionation.**

Mesangial cells grown to near confluency on glass coverslips were washed twice with ice-cold PBS and incubated on ice for 15 min with cold cytoskeleton buffer (CSK-100, 10 mM Pipes, pH 6.8, 300 mM sucrose, 100 mM NaCl, 3 mM $MgCl_2$, 1 mM EGTA, 1% Triton X-100, 1.2 mM PMSF,0.1% aprotinin, 0.1% pepstatin A), which removes all soluble cytoplasmic proteins, including microtubules (Fey *et al.*, 1984). Intermediate filaments and stress-fibers are not removed. Cells prepared this way were

then fixed with 3.7% paraformaldehyde in CSK 100 buffer and treated as in the regular immunofluorescence procedure.

Experiments using anti-tubulin drugs.

Mesangial cells were plated on glass coverslips and, 24 h after plating, were treated with colchicine (Sigma Chemical Co., St. Louis MO), 10 mg/ml for 30 min at 37 °C. After incubation with drugs, cells were fixed and permeabilized for visualization of microtubules and actin stress-fibers as described above.

Microinjection experiments.

Mesangial cells were plated on glass coverslips fixed at the bottom of 35 mm petri dishes. One day after plating, injection was performed as previously described (Wehland and Willingham, 1983) using a Zeiss microscope. Cells were injected in the cytoplasm with antibodies to β_I, β_{II} and β_{IV} tubulin at concentrations of 14 mg/ml. Approximately 30 cells were injected in every case. Cells were incubated for various periods of time after injection and then fixed with methanol at -20 °C for 15 min. Cells were then labeled with Cy3 conjugated goat anti-mouse antibody to visualize the microtubules of the injected cells and then labeled with Bodipy phalloidin to visualize the actin stress fibers.

RESULTS

We have found that, under conditions of microtubule destabilization, β_{IV}-tubulin is seen to be associated with the actin stress fiber network, whereas β_I and β_{II}, the other isotypes investigated in this study, did not exhibit such an association. Microtubules were depolymerized under three different conditions.

Detergent extraction.

Rat kidney mesangial cells were treated with CSK-100 buffer containing 1% Triton X-100 for 15 min on ice. This procedure removes all soluble cytoplasmic proteins, including microtubules. Only actin stress fibers and intermediate filaments remain. Cells were treated for immunofluorescence before and after detergent extraction. Before extraction, cells treated with anti-β_{IV} revealed that this isotype formed part of the microtubule network; however, the distribution of β_{IV} and actin in these cells appeared to have regions of similarity (Fig. 1A, B). The distribution of β_I, however, was different from that of actin (Fig. 1C); β_I and actin did not appear to co-localize (not shown). As previously reported (Walss *et al.*, 1999), β_I was largely restricted to the nuclei (Fig. 1D). In contrast, after detergent extraction, the β_{IV}-microtubules had disappeared and β_{IV}-tubulin appeared to co-localize with the actin stress fiber network. This was confirmed by the co-localization of anti-β_{IV} stain with that of Bodipy-phalloidin, which binds to actin stress fibers (Fig. 1E, F, G). On the other hand, actin stress fiber staining was not observed with anti-β_I or anti-β_{II} after detergent extraction, suggesting that these isotypes do not associate with actin stress fibers after microtubule disruption caused by detergent extraction (Fig. 1H, I). In order to verify that localization of β_{IV} to actin stress fibers observed after detergent extraction was due to binding of the antibody with β_{IV}-tubulin,

and not because of non-specific interactions, immuno-blocking experiments were performed, as described in Materials and Methods. Pre-incubation of the β_{IV}-antibody with its antigen abolished most of the fluorescence, both before and after detergent extraction; the residual punctate fluorescence is likely to represent non-specific binding (Fig. 1J, K). These results strongly support the specificity of the β_{IV}-antibody and suggest that the actin stress fiber fluorescence seen with anti-β_{IV} after detergent extraction was in fact due to co-localization of β_{IV}-tubulin with the stress fiber network. Also, no reaction was observed when extracted cells were treated with fluorescent secondary antibody in the absence of primary antibody (Fig. 1L), indicating that actin stress fiber staining by β_{IV} was not due to non-specific interactions of the secondary antibody. This was further corroborated by treating an immunoblot of a mesangial cell extract with anti-β_{IV} and finding that the only band that was recognized by the antibody co-migrated with brain β-tubulin (not shown).

Treatment with anti-tubulin drugs.

Rat kidney mesangial cells were treated with colchicine at 10 mg/ml for 30 min at 37 °C. Cells were then fixed and examined by immunofluorescence microscopy. Normal microtubule networks were seen in control cells, as revealed by treatment with anti-β_I and anti-β_{IV} (Fig. 2A, C). In the case of the β_{II} isotype, treatment with anti-β_{II} showed that β_{II} was confined largely to the nuclei, in non-microtubule form (Figure 2B), as we previously showed was the case for these cells (Walss *et al.* 1999). On the other hand, the microtubule network of drug-treated cells had been disrupted. In these cells, treatment with anti-β_I or anti-β_{II} revealed diffuse fluorescence throughout the cytosol, characteristic of cells with depolymerized microtubules (Fig. 2D, E). However, in cells

treated with anti-β_{IV}, staining of actin stress fibers was observed. This staining co-localized with that of Bodipy-phalloidin, which confirmed the association of β_{IV} with actin stress fibers (Fig. 2F, G, H).

Microinjection experiments.

Association of β_{IV}-tubulin with actin stress fibers was also obtained when anti-β_{IV} was microinjected into the cytoplasm of mesangial cells at a concentration of 14 mg/ml. When cells were fixed immediately after injection, β_{IV}-tubulin appeared to form part of a normal microtubule network (Fig. 3A). However, in cells fixed one hour after injection, the microtubule network was depolymerized and the appearance of strap-like fibers, which were reminiscent of actin stress fibers, was observed (Fig. 3B). The staining by anti-β_{IV} in these cells co-localized with that of Bodipy-phalloidin (Fig. 3C, D). Injection of anti-β_{I} or anti-β_{II} into mesangial cells at concentrations of 14 mg/ml revealed a normal microtubule network when cells were fixed both 0 and 1 hr after injection (Fig. 3E-H). No association was seen between these isotypes and actin stress fibers, indicating that such an association is unique to β_{IV}-tubulin.

DISCUSSION

The results shown in this study suggest an association between the β_{IV}-isotype of tubulin and the actin stress fiber network. The association becomes very evident after microtubule disruption (Fig. 1E-G) although it may be in place prior to disruption with the large number of microtubules obscuring the actin-tubulin co-localization (Fig. 1A,B). It is also possible that the β_{IV} released from the disrupted microtubules binds to actin filaments and perhaps even induces their polymerization. If the latter is the case, it is conceivable that β_{IV}-tubulin acts as the stress-fiber-inducing-factor which has been proposed to be released by microtubule depolymerization to activate the Rho A signaling cascade and promote actin stress fiber formation (Enomoto, 1996). If this hypothesis is correct, it suggests a new function for tubulin, one that appears to be non-microtubule related and specific to β_{IV}, since no association was seen between β_{I}- or β_{II}-tubulin and actin stress fibers.

The β_{IV}-actin association, albeit circumstantial, has been reported previously. Inner and outer pillar cells, as well as Deiter cells from the organ of Corti, which express only β_{II}- and β_{IV}-tubulin (Hallworth and Luduena, 2000), appear to exhibit a close association between actin filaments and microtubules (Angelborg and Engstrom, 1972; Slepecky and Chamberlain, 1987; Slepecky and Ulfendahl, 1992). Also, the axonemal microtubules of bovine retinal rod cells, which contain only β_{IV}-tubulin (Renthal *et al.*, 1993), are closely associated with actin (Wolfrum and Schmitt, 2000; Arikawa and Williams, 1989). Our present results suggest a more intimate association between β_{IV}-tubulin and actin, as seen by the almost uninterrupted fluorescent co-localization given by the two protein markers, after microtubule disruption. However, it is likely that this

proposed association is indirect. Many actin-microtubule cross-linking proteins have been reported, including the actin-binding protein caldesmon (Ishikawa *et al.*, 1992), the cytoskeletal linker protein Acf7 (Bernier *et al.*, 2000), microtubule- and actin-based motor proteins (Huang *et al.*, 1999), and the microtubule associated proteins tau, MAP 1, and MAP 2 (Selden and Pollard, 1983; Pedrotti *et al.*, 1994; Arakawa and Frieden, 1984). It has been shown that MAPs, in particular MAP 2, can influence the organization of actin filaments (Sattilaro *et al.*, 1981). The microtubule-associated protein MAP 1 decorates actin stress fibers *in vivo* (Asai *et al.*, 1985). This has also been shown to occur with the motor protein kinesin, which appears to associate with actin stress fibers under conditions of microtubule depolymerization (Okuhara, 1989), just as we now show occurs with β_{IV}-tubulin. Therefore, it is conceivable that kinesin acts as the cross-link between β_{IV} and actin stress fibers in mesangial cells, although it is certainly possible that other proteins are involved. Another motor protein, cytoplasmic dynein, has been proposed to connect microtubules and microfilaments (Waterman-Storer *et al.*, 1998; Karki *et al.*, 1998) and is a good candidate to link β_{IV}-tubulin with actin. Axonemal dynein has been shown to bind to the sequence DATAEE in flagellar β-tubulin, which immediately precedes the sequence EGEFEEE (Audebert *et al.*, 1999). The latter sequence is believed to determine tubulin participation in axonemes (Raff et al., 1997) and, in vertebrates, only β_{IV}-tubulin contains this sequence (Ludueña, 1998). It is possible that cytoplasmic dynein binds to the same sequence as axonemal dynein and if so, it may bind specifically to β_{IV}-tubulin and act as a link between this protein and actin stress-fibers.

In conclusion, we have shown that β_{IV}-tubulin is associated with actin stress fibers after microtubule depolymerization. We hypothesize that cells may use β_{IV} as a signal to promote cross-talk between microtubules and actin microfilaments and in this way coordinate cellular functions such as locomotion. The amino acid sequences of the β_I, β_{II}, β_{III}, β_{IV} and β_V isotypes have been highly conserved in vertebrate evolution (Ludueña, 1998), suggesting that the differences among the isotypes may have functional significance. We have already shown that the β_{IV} isotype is uniquely associated with flagellar and ciliary microtubules (Renthal *et al.*, 1993; Lu *et al.*, 1998). Our results here suggest that β_{IV} may have an additional function, namely, to interact with actin stress fibers.

ACKNOWLEDGMENTS

This work was supported in by grants CA26376 from the National Institutes of Health (R.F.L.), DAMD17-98-1-8246 from the U.S. Army Breast Cancer Research Program (R.F.L.) and AQ-0726 from the Welch Foundation (R.F.L.) and VA Merit Review to J.I.K.

REFERENCES

Angelborg, C. and Engstrom, H. 1972. Supporting elements in the organ of Corti. Fibrillar structures in the supporting cells of the organ of Corti of mammals. Acta Otolaryngol. Suppl. 301:49-60.

Arakawa, T., and Frieden, C. 1984. Interaction of microtubule-associated proteins with actin filaments. J. Biol. Chem. 259:11730-11734.

Arikawa, K., and Williams, D.S. 1989. Organization of actin filaments and immunocolocalization of alpha-actinin in the connecting cilium of rat photoreceptors. J. Comp. Neurol. 288:640-646.

Asai, D.J., Thompson, W.C., Wilson, L., Dresden, C.F., Schulman, H., and Purich D.L. 1985. Microtubule-associated proteins (MAPs): A monoclonal antibody to MAP-1 decorates microtubules *in vitro* but stains stress fibers and not microtubules *in vivo*. Proc. Natl. Acad. Sci. U.S.A. 82:1434-1438.

Audebert, S., White, D., Cosson, J., Huitorel, P., Eddé, B., and Gagnon, C. 1999. The carboxy-terminal sequence Asp427-Glu432 of β-tubulin plays an important function in axonemal motility. Eur. J. Biochem. 261:48-56.

Ausiello, D.A., Kreisberg, J.I., Roy, C., and Karnovsky, M.J. 1980. Contraction of cultured cells of apparent masangial origin after stimulation with angiotensin II and arginine vasopressin. J. Clin. Invest. 65: 754-760.

Banerjee, A., Roach, M. C., Wall, K. A., Lopata, M. A., Cleveland, D. W., and Ludueña, R. F. 1988. A monoclonal antibody against the type II isotype of β-tubulin. Preparation of isotypically altered tubulin. J. Biol. Chem. 263:3019-3034.

Banerjee, A., Roach, M. C., Trcka, P., and Ludueña, R. F. 1990. Increased microtubule

assembly in bovine brain tubulin lacking the type III isotype of β-tubulin. J. Biol. Chem. 265:1794-1799.

Banerjee, A., Roach, M. C., Trcka, P., and Ludueña, R. F. 1992. Preparation of a monoclonal antibody specific for the class IV isotype of β-tubulin. Purification and assembly of $\alpha\beta_{II}$, $\alpha\beta_{III}$, and $\alpha\beta_{IV}$ tubulin dimers from bovine brain. J. Biol.Chem. 267:5625-5630.

Bement, W., Beach, D., Finst, R., Skobel, J., and Sider, J. 1997. MAP and ATP-dependent binding of F-actin to microtubules in Xenopus cell free lysates. Mol. Biol. Cell. 8:273a.

Bernier, G., Pool, M., Kilcup, M., Alfoldi, J., Repentigny, Y. D., and Kothary, R. 2000. Acf7 (MACF) is an actin and microtubule linker protein whose expression predominates in neural, muscle, and lungdevelopment. Develop. Dynam. 219:216-225.

Chrzanowska-Wodnicka, M., and Burridge, K. 1996. Rho-stimulated contractility drives the formation of stress fibers and focal adhesions. J. Cell Biol. 133:1403-1415.

Davy, D. A., Campbell, H. D., Fountain, S., de Jong, D. and Crouch, M. F. 2001. The flightless I protein colocalizes with actin- and microtubule-based structures in motile Swiss 3T3 fibroblasts: evidence for the involvement of PI 3-kinase and Ras-related small GTPases. J. Cell Sci. 114:549-562.

Enomoto, T. 1996. Microtubule disruption induces the formation of actin stress fibers and focal adhesions in cultured cells: possible involvement of the Rho signal cascade. Cell Struct. Funct. 21:317-326.

Fey, E. G., Wan, K. M. and Penman, S. 1984. Epithelial cytoskeletal framework and

nuclear matrix-intermediate filament scaffold: three dimensional organization and protein composition. J. Cell Biol. 98:1973-1984.

Gavin, R.H. 1997. Microtubule-microfilament synergy in the cytoskeleton. Int. Rev. Cytol. 173:207-242.

Goode, B.L., Drubin, D.G., and Barnes, G. 2000. Functional cooperation between the microtubule and actin cytoskeletons. Curr. Op. Cell Biol. 12:63-71.

Gundersen, G.G. and Cook, T.A. 1999. Microtubules and signal transduction. Curr. Op. Cell Biol. 11:81-94.

Hallworth, R. and Ludueña, R.F. 2000. Differential expression of β tubulin isotypes in the adult gerbil cochlea. Hearing Res. 148:161-172.

Huang, J-D., Brady, S.T., Richards, B.W., Stenoien, D., Resau, J.H., Copeland, N.G., and Jenkins,N.A. 1999. Direct interaction of microtubule-and actin-based transport motors. Nature. 397:267-270.

Ishikawa, R., Kagami, O., Hayashi, C., and Kohama, K. 1992. Characterization of smooth muscle caldesmon as a microtubule-associated protein. Cell Motil. Cytosk. 23:244-251.

Karki, S., LaMonte, B., and Holzbaur, E. 1998. Characterization of the p22 subunit of dynactin reveals the localization of cytoplasmic dynein and dynactin to the midbody of living cells. J. Cell. Biol. 142:1023-1034.

Kolodney, M., and Elson, E. 1995. Contraction due to microtubule disruption is associated with increased phosphorylation of myosin regulatory light chain. Proc. Natl. Acad. Sci. U.S.A. 92:10252-10256.

Kreisberg, J.I., Venkatachalam, M.A., and Patel, P.Y. 1984. Cyclic AMP-associated

shape change and its reversal by PGE_2. Kidney Int. 25:874-879.

Kreisberg, J.I., and Venkatachalam, M.A. 1986. Vasoactive agents affect mesangial cell adhesion. Am. J. Physiol. 251:C505-C511.

Lu, Q., Moore, G.D., Walss, C. and Ludueña, R.F. (1998) Structural and functional properties of tubulin isotypes. Adv. Struct. Biol. 5:203-227.

Ludueña, R.F. (1998) The multiple forms of tubulin: different gene products and covalent modifications. Int. Rev. Cytol. 178:207-275.

Okuhara, K., Murofushi, H., and Sakai, H. 1989. Binding of kinesin to stress fibers in fibroblasts under conditions of microtubule depolymerization. Cell Motil. Cytoskeleton.12:71-77.

Pedrotti, B., Colombo, R., and Islam, K. 1994. Microtubule associated protein MAP1A is an actin-binding and crosslinking protein. Cell Motil. Cytoskeleton. 29:110-116.

Raff, E.C., Fackenthal, J.D., Hutchens, J.A., Hoyle, H.D., and Turner, F.R. 1997. Microtubule architecture specified by a β-tubulin isoform. Science 275:70-73.

Renthal, R., Schneider, B. G., Miller, M. M., and Ludueña, R. F. 1993. β_{IV} is the major β-tubulin isotype in bovine cilia. Cell Motil. Cytoskeleton 25:19-29.

Roach, M. C., Boucher, V. L., Walss, C., Ravdin, P., and Ludueña, R. F. 1998. Preparation of a monoclonal antibody specific for the class I isotype of β-tubulin: the β isotypes of tubulin differ in their cellular distributions within human tissues. Cell Motil. Cytoskeleton 39:273-285.

Sattilaro, R.F., Dentler, W.L., and LeCluyse, E.L. 1981. Microtubule-associated

proteins (MAPs) and the organization of actin filaments *in vitro*. J. Cell Biol. 90:467-473.

Selden, S. C., and Pollard, T. D. 1983. Phosphorylation of microtubule-associated proteins regulates their interaction with actin filaments. J. Biol. Chem. 258:7064-7071.

Sider, J.R., Mandato, C.A., Weber, K.L., Zandy, A.J., Beach, D., Finst, R.J., Skoble, J., and Bement, W.M. 1999. Direct observation of microtubule-F-actin interaction in cell free lysates. J. Cell Science. 112:1947-1956.

Slepecky, N., and Chamberlain, S.C. 1987. Tropomyosin co-localizes with actin microfilaments and microtubules within supporting cells of the inner ear. Cell. Tiss. Res. 248:63-66.

Slepecky, N., and Ulfendahl, M. 1992. Actin-binding microtubule associated proteins in the organ of Corti. Hearing Research. 57:201-215.

Walss, C., Kreisberg, J.I. and Ludueña, R.F. (1999) Presence of the β_{II}-isotype of tubulin in the nuclei of cultured rat kidney mesangial cells. Cell Motil. Cytoskeleton 42:274-284.

Waterman-Storer, C.M., and Salmon, E.D. 1999. Positive feedback interactions between microtubules and actin during cell motility. Curr. Op. Cell Biol. 11:61-67.

Waterman-Storer, C.M., Salmon, E.D., and Bement, W.M. 1998. Microtubules modify actin networks in Xenopus egg extracts by dynein-dependent pushing and pulling of actin bundles. Mol. Biol. Cell. 9:54a.

Wehland, J., and Willingham, M.C. 1983. A rat monoclonal antibody reacting

specifically with the tyrosilated form of α-tubulin. II. Effects on cell movement, organization of microtubules and intermediate filaments, and arrangement of golgi elements. J. Cell. Biol. 97:1476-1490.

Wolfrum, U., and Schmitt, A. 2000. Rhodopsin transport in the membrane of the connecting cilium of mammalian photoreceptor cells. Cell Motil. Cytoskeleton 46:95-107.

FIGURE LEGENDS

Fig. 1. Co-localization of β_{IV}-tubulin with the actin stress-fiber network in mesangial cells after detergent extraction. **A:** Control, un-extracted cells treated with anti-β_{IV}. A normal microtubule network is seen. **B:** Same cells as in **A**, stained with Bodipy-phalloidin, a marker for actin stress fibers. Note some places where actin filaments appear to occur in the same pattern as some of the microtubules. **C:** Control, un-extracted cells treated with anti-β_{I}. **D:** Control, un-extracted cells treated with anti-β_{II}. Note the nuclear staining that we have previously reported (Walss *et al.*, 1999). **E:** Detergent-extracted cell treated with anti-β_{IV}. Note the appearance of strap-like fibers. **F:** Same cell as in **E,** stained with bodipy-phalloidin. The actin stress fiber network is observed. **G:** Superimposition of **E** and **F,** shows co-localization of anti-β_{IV} staining with that of bodipy-phalloidin, indicating that the β_{IV}-tubulin isotype co-localizes with actin stress fibers after detergent extraction. (Co-localization is shown in yellow). **H:** Detergent-extracted cells treated with anti-β_{I}. The microtubule network is disrupted; nothing resembling actin stress fibers is observed. **I:** Detergent-extracted cells treated with anti-β_{II}. No cytosolic fluorescence is observed, indicating that this isotype does not interact with actin stress-fibers after detergent extraction. **J:** Control, un-extracted cells treated with anti-β_{IV} that had been pre-incubated with its peptide epitope. Note the absence of cytosolic fluorescence compared to **A**. **K:** Detergent-extracted cells treated with anti-β_{IV} that had been pre-incubated with its peptide epitope. All cytosolic fluorescence, including stress-fiber staining, is completely diminished. **L:** Cells incubated with secondary antibody in the absence of primary antibody.

Fig. 2. Co-localization of β_{IV}-tubulin with the actin stress fiber network in mesangial cells after microtubule de-polymerization by colchicine. **A:** Control, drug-free cells treated with anti-β_I. **B:** Control, drug-free cells treated with anti-β_{II}. Note the nuclear staining. **C:** Control, drug-free cells treated with anti-β_{IV}. Note the microtubule network. **D:** Cells treated with 10 mg/ml colchicine, stained with anti-β_I. **E:** Cells treated with 10 mg/ml colchicine, stained with anti-β_{II}. **F:** Cells treated with 10 mg/ml colchicine, stained with anti-β_{IV}. Note the staining of actin stress fibers. **G:** Same cells as in **F**, stained with bodipy phalloidin to reveal the actin stress fibers. **H:** Superimposition of **G** and **F**, to show co-localization of actin with β_{IV}-tubulin (shown in yellow).

Fig. 3. Co-localization of β_{IV}-tubulin with the actin stress fiber network in mesangial cells after disruption of microtubules by microinjection of β_{IV}-tubulin antibody. **A:** Cells injected with anti-β_{IV} (14 mg/ml), fixed immediately after injection. Note the normal microtubule network. **B:** Cells injected with anti-β_{IV} (14 mg/ml), fixed 1 hr after injection. **C:** Same cells as in **B**, stained with Bodipy-phalloidin, to reveal the actin stress-fibers. **D:** Superimposition of **B** and **C** shows co-localization of anti-β_{IV} staining with that of Bodipy-phalloidin. (Shown in yellow). **E:** Cells injected with anti-β_I (14 mg/ml), fixed immediately after injection. **F:** Cells injected with anti-β_{II} (14 mg/ml), fixed immediately after injection. **G:** Cells injected with anti-β_I (14 mg/ml), fixed 1 hr

after injection. Note the absence of actin stressfiber staining. **H:** Cells injected with anti-β_{II} (14 mg/ml), fixed 1 hr after injection. Note the absence of actin stress fiber staining.

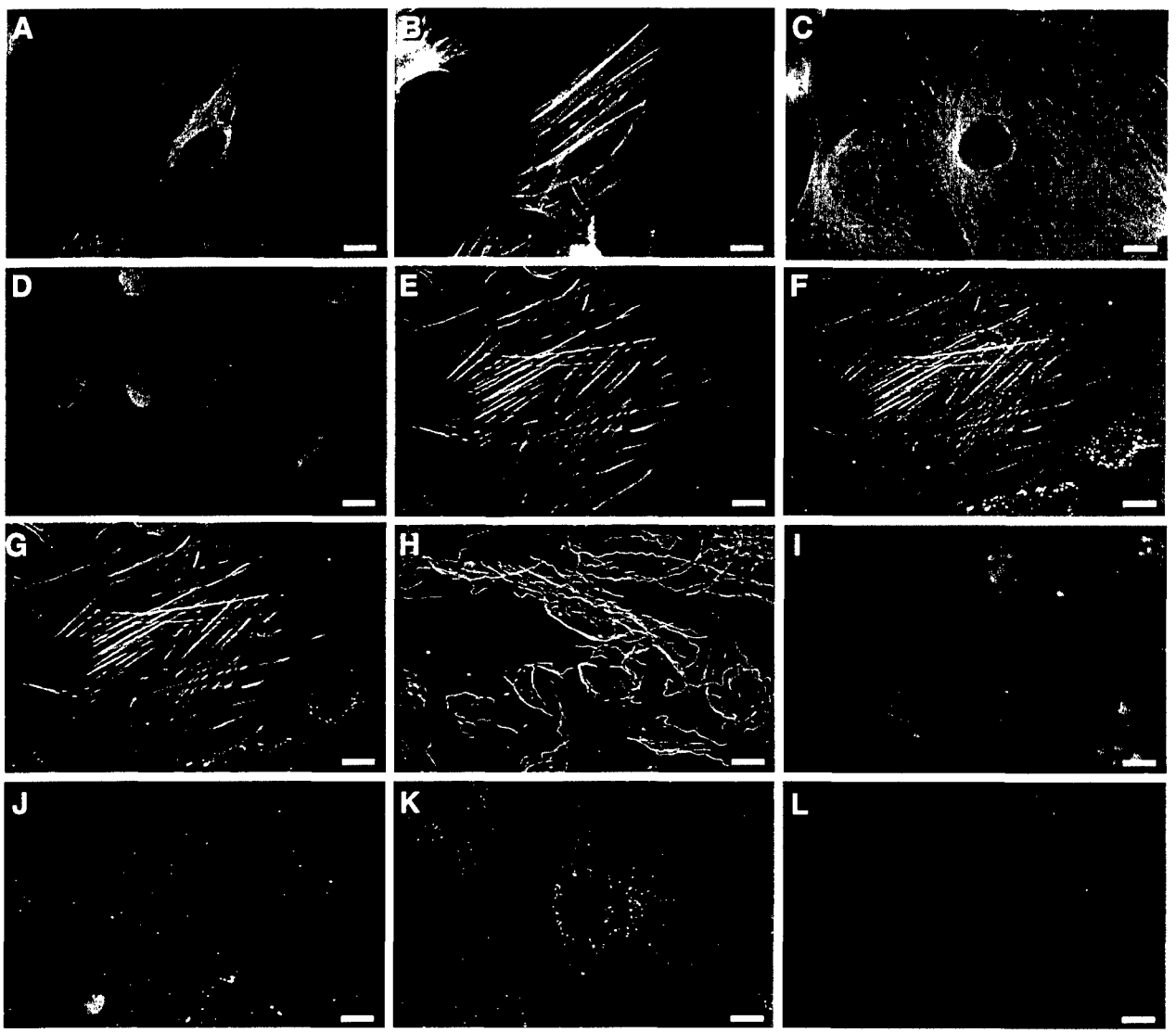

Figure 1

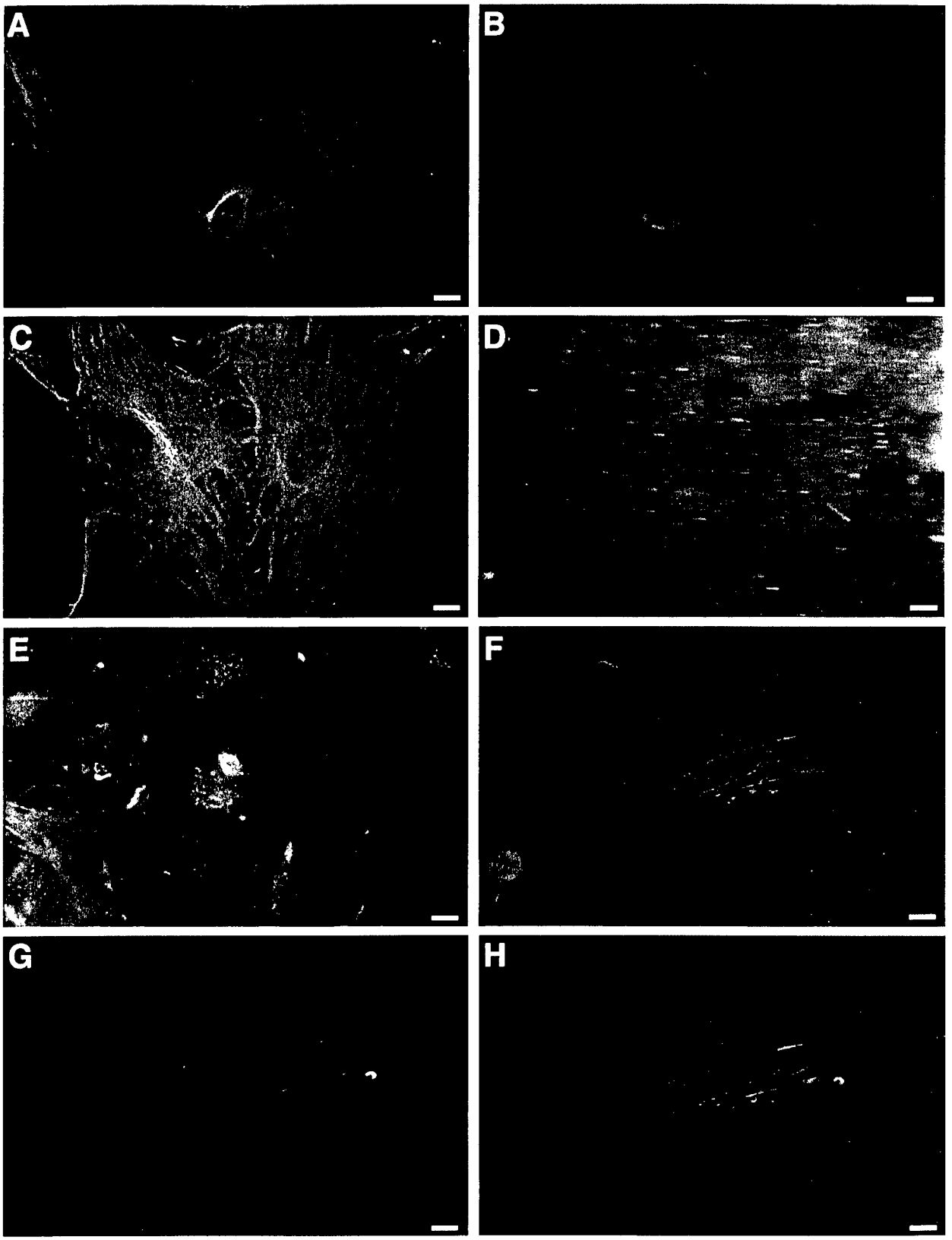

Figure 2

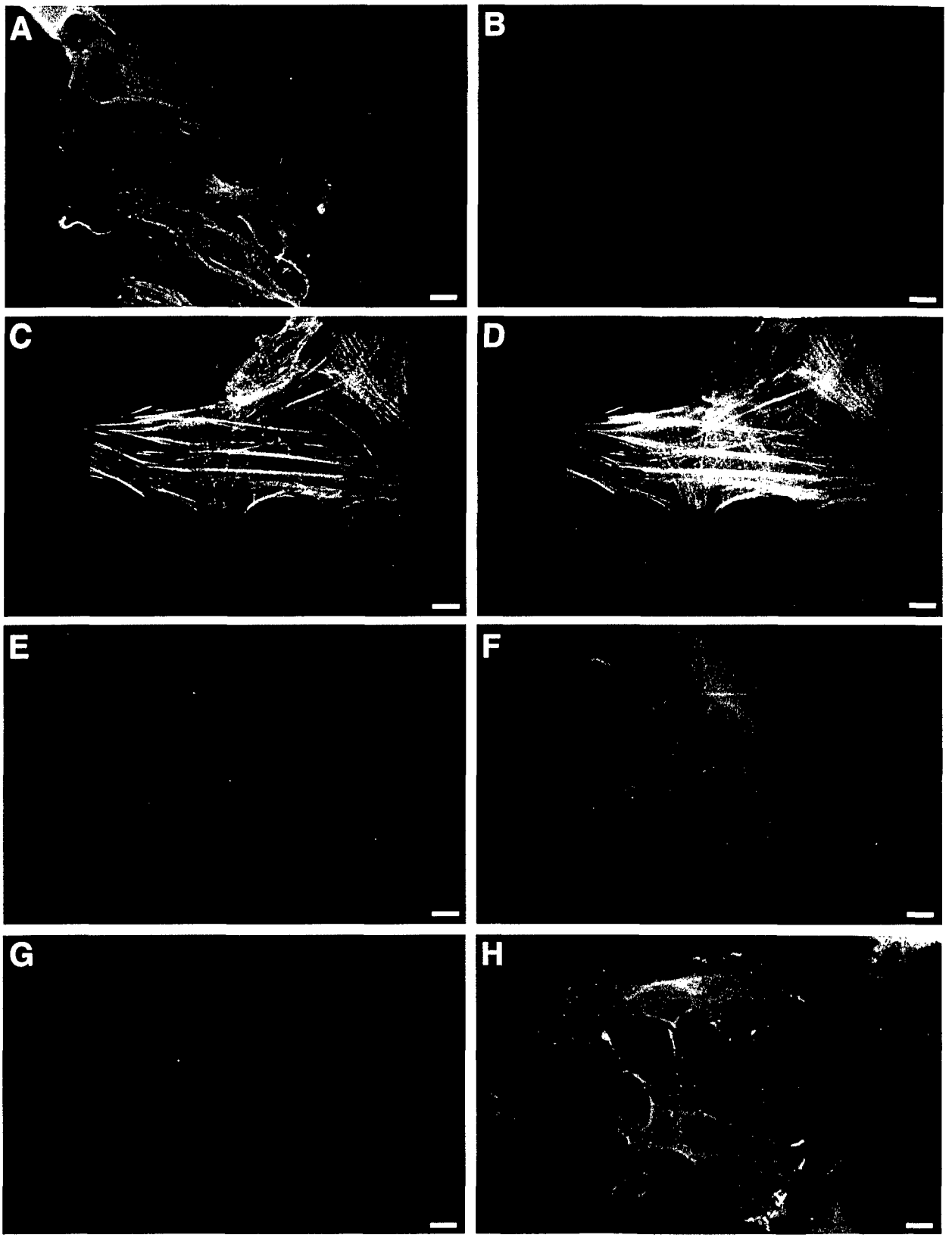

Figure 3

Mechanism of Localization of β_{II}-Tubulin in the Nuclei of Cultured Rat Kidney Mesangial Cells.

Consuelo Walss-Bass*, Jeffrey I. Kreisberg$^{\phi}$, and Richard F. Ludueña*

*Departments of *Biochemistry and $^{\phi}$Pathology, University of Texas Health Science Center, San Antonio, Texas 78229 and $^{\phi}$The Research and Development Service Department of Veteran Affairs, San Antonio, Texas 78229.*

Key words: nuclear loclization, tubulinisotypes, microinjection, nucleolus, mitosis

Number of characters: 21,851

Send correspondence to:

Dr. Richard F. Ludueña

Department of Biochemistry

University of Texas Health Science Center

San Antonio, TX 78229-3900

Tel: 210-5673732

FAX: 210-5676595

E-mail: luduena@uthscsa.edu

Abstract

Tubulin is an αβ heterodimer. Both the α and β polypeptides exist as multiple isotypes. Although tubulin was generally thought to exist only in the cytoplasm, we have previously reported the presence of the β_{II} isotype of tubulin in the nuclei of cultured rat kidney mesangial cells, smooth-muscle-like cells that reside in the glomerular mesangium; nuclear β_{II} exists as an $\alpha\beta_{II}$ dimer, capable of binding to colchicine, but in non-microtubule form (Walss, C., J.I. Kreisberg, and R.F. Ludueña. 1999. *Cell Motil. Cytoskeleton.*42: 274-284). We have now investigated the nature of the process by which $\alpha\beta_{II}$ enters the nuclei of these cells. By micro-injecting fluorescently labeled $\alpha\beta_{II}$ into mesangial cells, we found that $\alpha\beta_{II}$ was present in the nuclei of cells only if they were allowed to go through mitosis. In contrast, there were no circumstances in which microinjected fluorescently labeled $\alpha\beta_{III}$ or $\alpha\beta_{IV}$ dimers entered the nuclei. These findings, together with the absence of any nuclear localization signal in $\alpha\beta_{II}$, strongly favor the model that $\alpha\beta_{II}$, rather than being transported into the intact nucleus, co-assembles with the nucleus at the end of mitosis. Our results also indicate that the nuclear localization mechanism is specific for $\alpha\beta_{II}$. This result raises the possibility that $\alpha\beta_{II}$ may have a specific function that requires its presence in the nuclei of cultured rat kidney mesangial cells.

INTRODUCTION

The finding in recent years of a large number of nuclear proteins that have been shown to possess microtubule-organizing properties and in turn are involved in maintenance of nuclear architecture, has led to the idea that the nucleus and the microtubule cytoskeleton are structurally and functionally interdependent (Baluska *et al.*, 1997). Microtubules have been shown to influence the organization of interphase chromatin in plant cells (Baluska and Barlow, 1993). Conversely, a number of structurally related nuclear proteins have been shown to be essential for proper organization of the mitotic spindle microtubules (reviewed in Baluska *et al.*, 1997). These proteins are known to shuttle between the nucleus during interphase and the mitotic spindle during cell division. Among these proteins are the nuclear matrix associated protein (NuMA, Compton and Cleveland, 1994) and the inner centromere proteins (INCENP's) (Earnshaw and Bernat, 1991). These latter proteins are known as chromosomal passengers, since they are attached to chromosomes during metaphase but dissociate from them during anaphase and, interestingly, become associated with microtubules of the spindle and midbody (Cooke *et al.*, 1987; Earnshaw and Cook, 1991).

We have recently reported the finding of another protein, the β_{II}-isotype of tubulin, which appears to recycle between the nucleus during interphase and the mitotic spindle during cell division in rat kidney mesangial cells (Walss *et al.*, 1999). During interphase, this protein was found to be present in the nuclear matrix, and also in nucleoli, as an $\alpha\beta_{II}$ tubulin dimer.

Typically, a protein must enter the nucleus through the membrane nuclear pores, by use of a "password", known as the nuclear localization signal (NLS) (Kalderon *et al.*, 1984). However, there are many nuclear proteins that do not contain the conventional nuclear localization signal (Dingwall and Laskey, 1991). This suggests that there must be other nuclear targeting signals and/or mechanisms by which proteins can enter the nucleus. Just as the INCENP's and other proteins are chromosomal passengers during mitosis (Earnshaw and Bernat, 1991), the possibility exists that a protein may enter the nucleus as a chromosomal passenger after cell division. We have speculated that this is the case for β_{II}-tubulin, due to its presence in the nucleus during cell division and its role as part of the microtubule spindle during mitosis. It is possible that it remains attached to chromatin after cell division and is then trapped in the nucleus during interphase. If this situation does indeed occur, it would mean that cell division is necessary for β_{II}-tubulin to enter the nucleus.

In efforts to address this question, we have microinjected fluorescently labeled $\alpha\beta_{II}$, $\alpha\beta_{III}$ and $\alpha\beta_{IV}$ tubulin isotypes into rat kidney mesangial cells. We have found that $\alpha\beta_{II}$-tubulin is able to enter the nuclei of mesangial cells under conditions in which cells are able to divide. However, β_{II}-tubulin is unable to enter the nucleus of serum-starved cells, suggesting that cell division is necessary for this protein to enter the nucleus. Neither $\alpha\beta_{III}$ or $\alpha\beta_{IV}$ entered the nuclei, suggesting that the process is specific for $\alpha\beta_{II}$.

MATERIALS AND METHODS

Source of cells and antibodies

Rat kidney mesangial cells were obtained as follows. Glomeruli were isolated from 200 g male Sprague-Dawley rats (Harlan Sprague-Dawley Inc., Indianapolis, IN) using a graded sieve technique and were plated for culture in RPMI 1640 (Gibco BRL, St. Louis, MO) tissue culture medium with 20% FCS plus penicillin, streptomycin and fungizone (E.R. Squibb and Sons) for explant growth of mesangial cells (Ausiello *et al.*, 1980; Kreisberg *et al.*, 1984). One hundred percent of the cells were identified as glomerular mesangial cells. Positive identification was obtained by ultrastructural examination, contractile responsiveness to vasopressin and angiotensin II, and shape change in response to cAMP-elevating agents (Kreisberg *et al.*, 1986; Ausiello *et al.*, 1980; Kreisberg *et al.*, 1984). For the experiments described below, cells were used between the 4th and 40th passage.

The monoclonal antibodies SAP.4G5, JDR.3B8, SDL.3D10 and ONS.1A6, specific, respectively, for the β_I, β_{II}, β_{III} and β_{IV} isotypes of tubulin were prepared as previously described (Banerjee *et al.*, 1988, 1990, 1992; Roach *et al.*,1998).

Preparation of fluorescent protein

The $\alpha\beta_{II}$, $\alpha\beta_{III}$ and $\alpha\beta_{IV}$ tubulin dimers were purified from bovine brain by immunoaffinity chromatography according to Banerjee et al. (1992). The dimers were fluorescently labeled using the procedure described by Wadsworth and Slodoba (1983). The purified tubulin dimers were polymerized in MES buffer (0.1 M Mes, pH 6.4, 1.0 mM EGTA, 0.1 mM EDTA, 1mM GTP) in the presence of 4 M glycerol and 6 mM $MgCl_2$. The assembled protein was mixed for 60 min at 37 °C with 5-(4,6-

dichlorotriazin-2-yl)aminofluorescein (DTAF, Molecular Probes, Eugene, OR.), (50 µl per ml) from a 50 mM solution prepared fresh in DMSO (Sigma Chemical Co., St. Louis, MO). The fluorescent polymer was collected by centrifugation, resuspended in MES buffer, pH 6.4 and depolymerized on ice. The protein was then passed through a Sephadex G-25 column, previously equilibrated with MES buffer, to remove unbound fluorochrome, and the eluted protein was again polymerized. Microtubule assembly was followed by monitoring the absorbance at 350 nm, as previously described (Lu and Ludueña, 1993). In order to visualize the microtubules, an aliquot of the assembled $\alpha\beta_{II}$-DTAF protein was withdrawn for electron microscopy, as previously described. (Banerjee *et al*, 1990). The assembled protein was then collected by centrifugation and depolymerized on ice and stored in liquid nitrogen. The final protein concentrations were determined by the method of Lowry *et al.* (1951). The dye to protein ratios (mol/mol) were determined by measuring the absorbances at 495 and 280 nm respectively and were 0.146, 0.127 and 0.072 for the $\alpha\beta_{II}$, $\alpha\beta_{III}$ and $\alpha\beta_{IV}$ fluorescent protein, respectively.

Fluorescent BSA was prepared by incubation of this protein with DTAF at 37 °C in $NaHCO_3$ buffer, pH 9.0, for 1 hr. The protein was then passed through a Sephadex G-25 column, equilibrated in PBS buffer, to remove unbound fluorochrome.

Microinjection experiments

Mesangial cells were plated on glass coverslips fixed at the bottom of 35 mm petri dishes. One day after plating, cells were synchronized by incubation with 2.5 mM thymidine for 18 h and then incubated with normal media for 5 h. At this time, injection was performed as previously described (Wehland and Willingham, 1983) using am Eppendorf microinjecion system (Kreisberg *et al.*, 1997). The fluorescent tubulin dimers

were injected in the cytoplasm of interphase cells, incubated for 7 and 20 h after injection and then fixed for visualization with methanol at –20 °C for 15 min. The tubulin antibodies were injected into dividing cells, fixed 0 and 5 hrs after injection and then incubated for 1 h with Cy3- conjugated secondary antibody for visualization of microtubules. The cover slips were then mounted on glass slides and examined with an Olympus epifluorescence microscope using a 63x oil objective.

In some experiments, cells previously plated on glass coverslips were incubated in media without serum for 48 hrs prior to injection. At this time, cells were injected with either $\alpha\beta_{II}$-DTAF or BSA-DTAF. After injection, injected cells were either incubated with fresh media for 24 hrs or left in media without serum. Cells were then fixed with methanol for visualization.

RESULTS

Microinjection of fluorescently-labeled tubulin β-isotypes

We microinjected fluorescently-labeled $\alpha\beta_{II}$, $\alpha\beta_{III}$ and $\alpha\beta_{IV}$ tubulin dimers, prepared from bovine brain, as well as fluorescently-labeled BSA, into mesangial cells. Although β_I-tubulin is a major component of the tubulin pool in mesangial cells, it is a minor component in the bovine brain pool (Banerjee *et al.*, 1988) and therefore it was not possible to obtain purified $\alpha\beta_I$-tubulin dimers in quantities large enough to perform microinjection experiments. Also, results from previous studies have shown that mesangial cells do not express β_{III}-tubulin (Walss *et al.*, 1999). Therefore, we have injected this protein, as well as BSA, as a control.

The fluorescently-labeled tubulin protein was assembly-competent at the time of injection. This was evident since the protein was subjected to an assembly process after labeling and the increase in turbidity due to assembly was followed by spectrophotometry at 350 nm (Fig. 1a, b, c). The exponential increase in absorbance is typical of polymerizing tubulin and suggests that the labeled isotypes were able to assemble into normal microtubules. Electron microscopic examination revealed long linear structures (not shown)

The labeled proteins were injected into the cytosol of thymidine-synchronized mesangial cells in two separate experiments. In each case, approximately 30 cells were injected. Of the three β-tubulin isotypes, only β_{II} was able to enter the nucleus (Fig. 2a, b). In the first experiment, cells were fixed 7 hours after injection and nuclear β_{II} was detected in 9 cells. Of the other injected cells, 12 were still in the process of division and 5 cells appeared necrotic. When cells were fixed 20 hours after injection, 16 cells were

counted which appeared to contain β_{II} in their nuclei (Fig. 2c, d) and only a few were still dividing. In some cases the fluorescence was very weak.

As for the β_{III} and β_{IV} isotypes, results from the two separate experiments showed that these isotypes do not enter the nucleus (Fig. 2e, f). Each isotype was injected into approximately 30 cells, but fluorescence was only seen in the cytoplasm of the injected cells. The fluorescence of the β_{IV}-isotype was extremely weak. This is most likely due to the weaker affinity of the β_{IV}-isotype for DTAF, as can be seen from the fluorescence ratios (see Materials and Methods).

In order to determine if cell division is necessary for β_{II}-tubulin to enter the nucleus, fluorescent $\alpha\beta_{II}$-tubulin was injected into the cytosol of cells made quiescent by by serum deprivation for 48 hours. Immediately after injection, some of the injected cells were incubated in fresh media containing 20% fetal calf-serum. The remaining injected cells were kept quiescent by incubating in media without serum. Cells were then fixed after 24 h. It was found that $\alpha\beta_{II}$ tubulin was able to enter the nucleus in cells that were incubated with serum after injection (Fig. 3a, b). Nuclear fluorescence was seen in 20 out of the 30 injected cells. On the other hand, no nuclear fluorescence was seen in the 30 injected cells that were kept quiescent; instead, the fluorescent protein seemed to accumulate around the nucleus in each of the injected cells (Fig. 3c, d). This suggests that β_{II}-tubulin was only able to enter the nucleus in cells that were allowed to divide. The same experiments were performed with fluorescent BSA-protein. It was found that BSA was not able to enter the nuclei of either quiescent or non-quiescent cells, but remained in the cytoplasm and accumulated around the nucleus in what appeared like a halo (Fig. 3e, f).

Microinjection of β-tubulin antibodies

Antibodies to the β_I, β_{II} and β_{IV}-tubulin isotypes were microinjected into mesangial cells at concentrations around 14 mg/ml. Approximately 30 cells were injected in each case. Cells were injected during the process of division and fixed 0 and 5 h after injection. Cells were then labeled with a fluorescent secondary antibody for visualization of the injected cells. All three antibodies were seen to label the mitotic spindle when fixed 0 hrs after injection (Fig. 4a, b, c). In contrast, cells fixed 7 h after injection had apparently completed division. Nuclear fluorescence was observed in all the cells that had been injected with anti-β_{II} during division (Fig. 4e). It appeared, therefore, that this antibody appeared in the nucleus after the division process was complete. On the other hand, cells that were injected with anti-β_I or anti-β_{IV} during division did not appear to contain antibody in their nuclei after division, as these antibodies were seen to label only the cytoplasmic microtubules (Fig. 4d, f). These results confirm that β_{II} is the only isotype present in the nucleus of mesangial cells and that this protein enters the nucleus after cell division.

DISCUSSION

We have recently reported that the β_{II} isotype of tubulin is present in the interphase nuclei of cultured rat kidney mesangial cells (Walss *et al.*, 1999). Since these cells have relatively little β_{II} in the cytoplasm, the nuclear β_{II} is quite striking. The work described here addresses the question of how β_{II} comes to be localized in the nuclei. Our results suggest that 1) the process does not take place in quiescent cells and may require that the cell go through a cycle of mitosis and 2) the process is specific for the $\alpha\beta_{II}$ dimer, not occurring with the $\alpha\beta_{I}$, $\alpha\beta_{III}$ or $\alpha\beta_{IV}$ dimers. It is likely that a full understanding of the mechanism by which nuclear localization of β_{II} occurs would be closely connected to an understanding of its functional significance.

In principle, one can imagine several mechanisms by which β_{II} can enter the nucleus. The first mechanism is one in which β_{II} never enters the intact nucleus but instead requires that the nucleus disintegrate during mitosis and then the β_{II} would end up inside the nucleus as the nucleus re-forms at the end of mitosis. In other words, in this process the nucleus would, in a sense, re-form around β_{II}, thus trapping β_{II} inside. In our experiments, we find no evidence that β_{II} enters a quiescent nucleus but rather that no nuclear localization occurs until the cell has been stimulated to go through mitosis. We find, first, that β_{II} microinjected during interphase does not enter the nucleus until mitosis has occurred in that cell. We also find that the monoclonal antibody specific for β_{II} enters the nucleus when injected during mitosis. The antibody does not enter the nucleus of quiescent cells. The fact that the antibodies specific for β_{I} and β_{IV} do not enter the nucleus indicates that antibody localization to the nucleus follows the same specificity and mechanisms as does β_{II} localization, namely, that it occurs when the nucleus re-forms

around the antibody. The mechanism of the nucleus re-forming around β_{II} is consistent with our previous findings. We found that β_{II}-tubulin is present in the nucleus during interphase, forms part of the mitotic spindle and the midbody during mitosis and cytokinesis, and then re-enters the nucleus after cell division is over (Walss et al., 1999).

In order for such a mechanism to occur, it is likely that β_{II} binds to some component of the nucleus that is incorporated into the re-forming nucleus. One such possibility is chromatin itself. Tubulin has been reported to interact with chromatin *in vitro* (Mithieux et al., 1986) raising the possibility that it could interact *in vivo* as well. Nevertheless, it is certainly possible that β_{II} interacts with some other component of the nucleus. Our data suggest, however, that such a component binds specifically to β_{II} and not to the other isotypes.

A second possible mechanism by which β_{II} could enter the nucleus is through the pores in the nuclear envelope. It is possible that serum addition not only induces mitosis but also activates transport through the nuclear pores. This model does not preclude the previous model. In other words, β_{II} could enter the nucleus via nuclear pores during interphase but also have the nucleus re-form around it at the end of mitosis. The model that β_{II} enters through the nuclear pores, but not in quiescent cells, is consistent with the work of Feldherr and Akin (1991) who found that nuclear transport was greatly reduced in such cells. Nevertheless, our results do not completely rule out the possibility that β_{II} can enter the nuclei of quiescent cells; they do indicate, however, that the bulk of it enters the nucleus only after cells are activated by addition of serum.

The model that β_{II} enters the nucleus through the nuclear pores has certain constraints and implications. First, β_{II} appears to lack a nuclear localization sequence

that is very common among proteins that are transported into the nuclei via the nuclear pores (Komeili and O'Shea, 2000). In our studies, we have used purified β_{II}-tubulin from bovine brain, which has not been sequenced. However, computer analysis using PROSITE and PSORT of the known β_{II} protein sequences from chicken (Sullivan *et al.*, 1985) and mouse (Lewis *et al.*, 1985) has revealed that β_{II} does not contain a nuclear localization signal. Hence, it may "hitchhike" on another protein that does contain such a signal.

An intriguing aspect of the possibility that β_{II} is transported into the nucleus via the pores is connected with the role of Ran. Ran is a protein playing several important roles in a variety of eukaryotic cells, including mammalian cells. One role of Ran is to mediate transport of proteins into and out of the nuclei, by interacting with both export receptors and with import receptors such as importin-β (Quimby et al, 2000; Azuma and Dasso, 2000). Ran need not bind directly to the cargo but rather to one of the receptors. Perhaps more significantly, Ran also plays a major role in mitosis. When a cell enters mitosis, Ran (bound to GTP) is released from the nucleus in large amounts and stimulates nucleation of microtubules around the centrosome (Wilde and Zheng, 1999; Carazo-Salas et al., 2001). The mechanism of this stimulation is that Ran-GTP induces release from importin-β of proteins that stimulate microtubule assembly, including NuMA and TPX2 (Wiese et al., 2001; Nachury et al, 2001; Gruss et al., 2001). This has been most closely studied in the case of TPX2 (Gruss et al., 2001); TPX2 is a microtubule-associated protein that stimulates microtubule assembly. During interphase it is localized to the nucleus and kept inactive by being bound to importin-α, an "adapter" protein that is in turn bound to importin-β. When mitosis begins, Ran-GTP binds to the importin complex

and causes the release of TPX2 that then stimulates microtubule assembly. Since Ran mediates a mechanism to sequester microtubule-binding proteins in the nucleus, it is not too unreasonable to speculate that tubulin itself may also be sequestered in the nucleus under certain circumstances, perhaps by the same mechanism. Since the proteins that interact directly with the importins apparently contain nuclear localization sequences, which are not present in β_{II}, one must postulate that β_{II} is a hitchhiker that binds to another protein containing such a sequence. TPX2 could be one such protein. However, the binding is likely to be specific for β_{II}. In this model, and in any model for nuclear β_{II} localization, it is necessary to postulate that isotype specificity may involve either binding to a specific sequence present only in β_{II} or else recognizing a conformation present in the $\alpha\beta_{II}$ dimers but absent from the $\alpha\beta_{I}$, $\alpha\beta_{III}$ and $\alpha\beta_{IV}$ dimers.

In terms of the connection between Ran and tubulin, it is worth mentioning that Ran has a strong effect on microtubule dynamics, perhaps through activation of a motor protein (Wilde et al, 2001) and that hydrolysis of Ran-bound GTP is required for nuclear envelope re-assembly after mitosis (Hetzer et al., 2000). Thus, Ran may be involved in the re-formation of the nucleus around β_{II} as postulated in the first model for β_{II} localization in the nucleus.

A third possible model for the entry of β_{II} into nuclei involves the pores, but not Ran. There appear to be transport mechanisms through the pores in which Ran is not involved (Ryan and Wente, 2000). It is certainly conceivable that β_{II} could enter nuclei through a Ran-free mechanism, but in view of the many connections between Ran and the microtubule system, such a model is unlikely.

A fourth model to consider is based on the fact that there exist eukaryotic cells with nuclear tubulin in which this tubulin plays a major role. These are yeast cells---*Saccharomyces cerevisiae* and *Schizosaccharomyces pombe*---whose nuclei not only contain tubulin, but a significant portion of the mitotic spindle as well (Byers and Goetsch, 1975; Baum et al., 1978). The yeast mitotic spindle is formed from the spindle pole body that enters the nuclear envelope and proceeds to nucleate the spindle (Sobel, 1997; Knop et al., 1999). It is intriguing that spindle pole body localization in yeast is yet another process in which Ran is thought to play a role (Quimby et al., 2000). The precise mechanism appears to involve a localized disintegration of the nuclear envelope to form a sizable gap called a "fenestra" (McIntosh and O'Toole, 1999). The fenestra are large enough to permit entry of an organelle bound to several microtubules; they would certainly be large enough to allow entry of free tubulin dimers. Could such a mechanism explain β_{II} localization in the nuclei of rat kidney mesangial cells? Alternatively, could the localization of β_{II} in the nuclei be a residual phenomenon from a possibly once widespread mechanism that is found today only in yeast cells? These are both unlikely to be true, for the following reasons. First, no evidence of such fenestra has been seen in higher eukaryotic cells. Second, fenestra are sufficiently large that it is hard to imagine that they would only permit entry of $\alpha\beta_{II}$ dimers and not of either the $\alpha\beta_{I}$, $\alpha\beta_{III}$ or $\alpha\beta_{IV}$ dimers. Third, yeast nuclear tubulin forms a mitotic spindle inside the nucleus; in contrast, nuclear β_{II}, together with the other isotypes, forms a spindle, but only after the nucleus disintegrates (Walss et al., 1999). Fourth, in yeast the spindle pole body is on the opposite side of the nucleus from the nucleolus, implying that the nucleolus has no connection to either tubulin or microtubules (Yang et al., 1989); in contrast, we find that

nuclear β_{II} is actually concentrated in the nucleoli (Walss et al., 1999). Finally, a residual connection between nuclear β_{II} and yeast nuclear tubulin would imply that yeast β-tubulin resembles mammalian β_{II} more than it does the other isotypes. A BLAST search of protein sequences indicates that this is not the case. Of the human β isotypes, for example, the one that most closely resembles the yeast β-tubulins is β_{IVb} (77 % identity for *S. cerevisiae* and 78 % identity for *S. pombe*). The stronger resemblance to β_{IVb} is consistent with the possibility that this tubulin may be more highly conserved in evolution as a result of the fact that it is the isotype that forms the highly organized axonemal microtubules of cilia and flagella (Renthal et al., 1993; Roach et al., 1998; Lu et al., 1998). Identity to human β_{II} is 74 % and 77 %, respectively, for β-tubulins from *S. cerevisiae* and *S. pombe*. For all these reasons, therefore, it is very unlikely that the yeast model explains nuclear β_{II} localization in mesangial cells.

Finally, it is conceivable that β_{II} enters the nucleus by penetrating the nuclear envelope but at some site other than the pores. Such a possibility may be acknowledged, but there is no evidence for the existence of such a mechanism. One could postulate that nuclear pores may have arisen precisely because other transport mechanisms for crossing the nuclear envelope do not exist.

The various models advanced above bear upon the question of the physiological role of nuclear β_{II}. In principle, one could imagine that there are three explanations, none of them mutually exclusive, for the functional significance of nuclear β_{II}. First, it may play some role within the nuclei, perhaps being involved in intra-nuclear transport or compartmentalization within the nucleus. At present, there is no evidence to support this possibility. Second, nuclear β_{II} could be a passenger protein, one that is sequestered

within the nucleus until mitosis, at which point it is released by the nucleus to play a specific role in mitosis. This has been proposed to be the pattern with other proteins such as mitosin, NuMA and the mitotic apparatus protein p62, (Zhu et al., 1997; Saredi *et al.*, 1996; Warner and Sloboda, 1999). These proteins are released from the nucleus during prophase, play important roles in microtubule organization during cell division and reorganize into the nucleus at the start of a new cell cycle. There is great similarity between the cycles of these proteins and the one that we find to occur for β_{II}-tubulin. There are a variety of other observations that are consistent with this hypothesis. For one, β_{II} is most concentrated in the nucleoli, organelles that are thought to play a role in sequestering proteins involved in cell cycle regulation, releasing them during mitosis (Visintin and Amon, 2000). Also, Ran-GTP is present in the interphase nucleus, being released when mitosis begins, at which point it is thought that a cloud of Ran-GTP around the centrosomes stimulates microtubule assembly there (Carazo-Salas et al., 2001; Gruss et al., 2001). The mechanism involves Ran-induced release of microtubule-associated proteins (Gruss et al., 2001). There is a certain symmetry in the hypothesis that $\alpha\beta_{II}$-tubulin may also be released from the nucleus and cluster around the centrosomes ready to be assembled by a Ran-initiated mechanism. Such a model would imply that β_{II} has a particular role in mitosis, one different from those of the other isotypes; this is a fact that has yet to be demonstrated, however. A third possibility is that β_{II} is sequestered in the nucleus during interphase to keep it from affecting a function carried out in the cytoplasm by some other isotype, for example, β_I or β_{IV}. This is certainly consistent with the observation that proteins such as TPX2 are kept inactivated during interphase by being sequestered in the nucleus (Gruss et al., 2001). Although such

a model would be conceivable for β_{II} in the context of mesangial cells, that have very little cytoplasmic β_{II}, it is not consistent with our observation that many other cultured cell types have both nuclear and cytoplasmic β_{II} (Luduena et al, 2001).

A final possibility to be considered is that nuclear β_{II} has no functional significance at all, that it is some freak of abnormal development in cultured mesangial cells. However, we have seen nuclear β_{II} in a large variety of cultured cells, both transformed and non-transformed. These include human aortic and venous endothelial cells as well as breast, ovarian, prostate, colon and other cancer cells (Walss et al., 2000; Luduena et al., 2001; Luduena, Mittal, Sprague, Centonze and Xu, unpublished observations). The fact that nuclear β_{II} is a widespread phenomenon implies that it is likely to have some functional significance, although its nature is presently unclear.

ACKNOWLEDGMENTS

This research was supported by grants GM23476 and CA26376 from the National Institutes of Health (R.F.L), AQ-0726 from the Welch Foundation (R.F.L.), DAMD17-98-1-8246 from the U.S. Army Medical Research Program (R.F.L.) and VA Merit Review (J.I.K.).

REFERENCES

Ausiello DA, Kreisberg JI, Roy C, Karnovsky MJ. 1980. Contraction of cultured cells of apparent mesangial origin after stimulation with angiotensin II and arginine vasopressin. J Clin Invest 65:754-760.

Azuma Y, Dasso M. 2000. The role of Ran in nuclear function. Curr Op Cell Biol 12:302-307.

Baluska F, Barlow PW. 1993. The role of microtubular cytoskeleton in determining nuclear chromatin structure and passage of maize root cells through the cell cycle. Eur J Cell Biol 61:160-167.

Baluska F, Volkmann D, Barlow PW. 1997. Nuclear components with microtubule-organizing properties in multicellular eukaryotes: functional and evolutionary considerations. Int Rev Cyt 175:91-135.

Banerjee A, Roach MC, Wall KA, Lopata MA, Cleveland DW, Ludueña R F. 1988. A monoclonal antibody against the type II isotype of β-tubulin. Preparation of isotypically altered tubulin. J Biol Chem 263:3019-3034.

Banerjee A, Roach MC, Trcka P, Ludueña RF. 1990. Increased microtubule assembly in bovine brain tubulin lacking the type III isotype of β-tubulin. J Biol Chem 265: 1794-1799.

Banerjee A, Roach MC, Trcka P, Ludueña RF. 1992. Preparation of a monoclonal antibody specific for the class IV isotype of β-tubulin. Purification and assembly of $\alpha\beta_{II}$, $\alpha\beta_{III}$, and $\alpha\beta_{IV}$ tubulin dimers from bovine brain. J BiolChem 267:5625-5630.

Baum P, Thorner J, Honig L. 1978. Identification of tubulin from the yeast

Saccharomyces cerevisiae. Proc Nat Acad Sci USA 75:4962-4966.

Byers B, Goetsch L. 1975. Behavior of the spindle plaques in the cell cycle and conjugation of *Saccharomyces cerevisiae*. J Bacteriol 124:511-523.

Carazo-Salas RE, Gruss OJ, Mattaj IW, Karsenti E. 2001. Ran-GTP coordinates regulation of microtubule nucleation and dynamics during mitotic-spindle assembly. Nature Cell Biol 3:228-234.

Compton DA, Cleveland DW. 1994. NuMA, a nuclear protein involved in mitosis and nuclear reformation. Curr Opin Cell Biol 6:343-346.

Cooke CA, Heck MMS, Earnshaw WC. 1987. The INCENP antigens: movement from the inner centromere to the midbody during mitosis. J Cell Biol 105:2053-2067.

Dingwall C, Laskey RA. 1991. Nuclear targeting sequences: a consensus? TIBS 16:478-481.

Earnshaw WC, Bernat RL. 1991. Chromosomal passengers: Toward an integrated view of mitosis. Chromosoma 100:139-146.

Earnshaw WC, Cooke CA. 1991. Analysis of the distribution of the INCENP's through out mitosis reveals the existence of a pathway of structural changes in the chromosome during metaphase and early events in cleavage furrow formation. J Cell Sci 98: 443-461.

Feldherr CM, Akin D. 1991. Signal-mediated nuclear transport in proliferating and growth-arrested BALB/c 3T3 cells. J Cell Biol 115:933-939.

Gruss OJ, Carazo-Salas RE, Schatz CA, Guarguaglini G, Kast J, Wilm M, Le Bot N, Vernos I, Karsenti E, Mattaj IW. 2001. Ran induces spindle assembly by reversing the inhibitory effect of importin α on TPX2 activity. Cell 104, 83-93.

Hetzer M, Bilbao-Cortes D, Walther TC, Gruss OJ, Mattaj IW. 2000. GTP hydrolysis by Ran is required for nuclear envelope assembly. Mol Cell 5:1013-1024.

Kalderon D, Roberts BL, Richardson WD, Smith AE. 1984. A short amino acid sequence able to specify nuclear location. Cell 39:499-509.

Knop M, Pereira G, Schiebel E. 1999. Microtubule organization by the budding yeast spindle pole body. Biol Cell 91:291-304.

Komeili A, O'Shea EK. 2000. Nuclear transport and transcription. Curr Op Cell Biol 2:355-360.

Kreisberg JI, Venkatachalam MA. 1986. Vasoactive agents affect mesangial cell adhesion. Am J Physiol 251:C505-C511.

Kreisberg JI, Venkatachalam MA, Patel PY. 1984. Cyclic AMP-associated shape change and its reversal by PGE_2. Kidney Int 25:874-879.

Kreisberg JI, Ghosh-Choudhury N, Radnik RA, Schwartz MA. 1997. Role of Rho and myosin phosphorylation in actin stress fiber assembly in mesangial cells. Am J Physiol 273:F283-F288.

Lewis S A, Lee MG, Cowan NL. 1985. Five mouse tubulin isotypes and their regulated expression during development. J Cell Biol 101:852-861.

Lowry OH, Rosebrough NJ, Farr AL, Randal RJ. 1951. Protein measurement with folin phenol reagent. J Biol Chem 193:265-275.

Lu Q, Ludueña RF. 1993. Removal of β_{III} isotype enhances taxol induced microtubule assembly. Cell Struct Funct 18:173-182.

Lu Q, Moore GD, Walss C, Ludueña RF. 1998. Structural and functional properties of tubulin isotypes. Adv Struct Biol 5:203-227.

Luduena RF, Banerjee M, Centonze V, Yeh IT, Pressley O. 2001. Occurrence of the βII isotype of tubulin in the nuclei of ovarian cancer cells. Proc AACR 42:404.

McIntosh JR, O'Toole ET. 1999. Life cycles of yeast spindle pole bodies: getting microtubules into a closed nucleus. Biol Cell 91:305-312.

Mithieux G, Roux B, Rousset B. 1986. Tubulin-chromatin interactions: evidence for tubulin-binding sites on chromatin and isolated oligonucleosomes. Biochim Biophys Acta 888:49-61.

Nachury MV, Maresca TJ, Salmon WC, Waterman-Storer CM, Heald R, Weis K. 2001. Importin β is a mitotic target of the small GTPase Ran in spindle assembly. Cell 104:95-106.

Quimby BB, Wilson CA, Corbett AH. 2000. The interaction between Ran and NTF2 is required for cell cycle progression. Mol Biol Cell 11:2617-2629.

Renthal R, Schneider BG, Miller MM, Ludueña RF. 1993. β_{IV} is the major β-tubulin isotype in bovine cilia. Cell Motil Cytoskeleton 25:19-29.

Roach MC, Boucher VL, Walss C, Ravdin P, Ludueña RF. 1998. Preparation of a monoclonal antibody specific for the class I isotype of β-tubulin: the β isotypes of tubulin differ in their cellular distributions within human tissues. Cell Motil Cytoskeleton 39:273-285.

Ryan KJ, Wente SR. 2000. The nuclear pore complex: a protein machine bridging the nucleus and cytoplasm. Curr Op Cell Biol 12:361-371.

Saredi A, Howard L, Compton DA. 1996. NuMA assembles into an extensive filamentous structure when expressed in the cell cytoplasm. J Cell Sci 109:619-630.

Sobel SG. 1997. Mini review: mitosis and the spindle pole body in *Saccharomyces cerevisiae*. J. Exptl Zool 277:120-138.

Sullivan KF, Lau JTY, Cleveland DW. 1985. Apparent gene conversion between β-tubulin genes yields multiple regulatory pathways for a single β-tubulin polypeptide isotype. Mol Cell Biol 5:2454-2465.

Visintin R, Amon A. 2000. The nucleolus: the magician's hat for cell cycle tricks. Curr Op Cell Biol 12:372-377.

Wadsworth P, Slodoba RD. 1983. Microinjection of fluorescent tubulin into dividing sea urchin cells. J Cell Biol 97:1249-1254.

Walss C, Kreisberg JI, Ludueña RF. 1999. Presence of the β_{II} isotype of tubulin in the nuclei of cultured mesangial cells from rat kidney. Cell Motil Cytoskeleton 42:274-284.

Walss C, Barbier P, Banerjee M, Bissery MC, Luduena RF, Fellous A. 2000. Nuclear tubulin as a possible marker for breast cancer cells. Proc AACR 41:553.

Warner AK, Sloboda RD. 1999. C-terminal domain of the mitotic apparatus protein p62 targets the protein to the nucleolus during interphase. Cell Motil Cytoskeleton 44:68-80.

Wehland J, Willingham MC. 1983. A rat monoclonal antibody reacting specifically with the tyrosilated form of α-tubulin. II. Effects on cell movement, organization of microtubules and intermediate filaments, and arrangement of golgi elements. J Cell Biol 97:1476-1490.

Wiese C, Wilde A, Moore MS, Adam SA, Merdes A, Zheng Y. 2001. Role of importin-β in coupling Ran to downstream targets in microtubule assembly. Science

291:653-656.

Wilde A, Zheng Y. 1999. Stimulation of microtubule aster formation and spindle assembly by the small GTPase Ran. Science 284:1359-1362.

Wilde A, Lizarraga SB, Zhang L, Wiese C, Gliksman NR, Walczak CE, Zheng Y. 2001. Ran stimulates spindle assembly by altering microtubule dyamics and the balance of motor activities. Nature Cell Biol 3:221-227.

Yang CH, Lambie EJ, Hardin J, Craft J, Snyder M. 1989. Higher order structure is present in the yeast nucleus: autoantibody probes demonstrate that the nucleolus lies opposite the spindle pole body. Chromosoma 98:123-128.

Zhu,X, Ding L, Pei G. 1997. Carboxyl-terminus of mitosin is sufficient to confer spindle pole localization. J Cell Biochem 66:441-449.

FIGURE LEGENDS

Figure 1. Effect of tubulin fluorescence-labeling on microtubule assembly. Fluorescein-labeled tubulin isotypes were assembled at 37 °C for 1 h in the presence of 1 mM GTP and 6 mM $MgCl_2$. The increase in turbidity, as shown by an increase in absorbance at 350 nm, indicates that all tubulin isotypes were able to polymerize after fluorescent labeling. **a,** Fluorescent $\alpha\beta_{II}$-tubulin. **b,** Fluorescent $\alpha\beta_{III}$-tubulin. **c,** Fluorescent $\alpha\beta_{IV}$-tubulin.

Figure 2. Microinjection of fluorescein-labeled β-isotypes into rat kidney mesangial cells. **a,** Cells injected in the cytoplasm during interphase with $\alpha\beta_{II}$-DTAF (3.5 mg/ml), fixed 7 h after injection. Notice accumulation of fluorescence in the nuclei and nucleoli. **b,** Phase contrast of same cells as in **a**, showing position of the nuclei and nucleoli. **c,** Cells injected in the cytoplasm during interphase with $\alpha\beta_{II}$-DTAF (3.5 mg/ml), fixed 20 h after injection. Notice accumulation of fluorescence in the nucleus. **d,** Phase contrast of same cells as in **c**, showing position of the nuclei. **e,** Cells injected in the cytoplasm during interphase with $\alpha\beta_{III}$-DTAF (4.9 mg/ml) fixed 20 hrs after injection. **f,** Cells injected in the cytoplasm during interphase with $\alpha\beta_{IV}$-DTAF (2.35 mg/ml), fixed 20 hrs after injection. Notice accumulation of fluorescence in the cytoplasm in **e** and **f**. **a-d,f,** Bar = 28 μ. **e,** Bar = 19 μ.

Figure 3. Microinjection of fluorescein-labeled β_{II}-tubulin into the cytosol of quiescent mesangial cells. **a,** Cell injected in the cytosol with $\alpha\beta_{II}$-DTAF (4.7 mg/ml) and incubated in media with serum for 24 h. Notice accumulation of β_{II}-tubulin in the

nucleus and nucleolus. **b,** Phase contrast of same cell as in **a,** showing position of the nucleus and nucleolus. **c,** Cells injected in the cytosol with $\alpha\beta_{II}$-DTAF (4.7 mg/ml) and incubated in media without serum for 24 h. Notice accumulation of fluorescence around the nucleus. **d,** Phase contrast of same cells as in **c**. **e,** Cell injected in the cytosol with BSA-DTAF (3.9 mg/ml) and incubated in media with serum for 24 h. **f,** Cells injected in the cytosol with BSA-DTAF (3.9 mg/ml) and incubated in media without serum for 24 h. Bar = 28 μ.

Figure 4. Microinjection of β-tubulin antibodies into rat kidney mesangial cells during cell division. **a, d,** Cells injected with anti-β_I. **b, e,** Cells injected with anti-β_{II}. **c, f:** Cells injected with anti-β_{IV}. **a, b, c,** Cells injected during division, fixed immediately after injection. Notice labeling of mitotic spindles with all three antibodies. **d, e, f,** Cells injected during division, fixed 7 h after injection, to allow cells to complete division. Notice accumulation of β_{II} antibody in the nucleus in **e**. Bar = 28 μ.

A

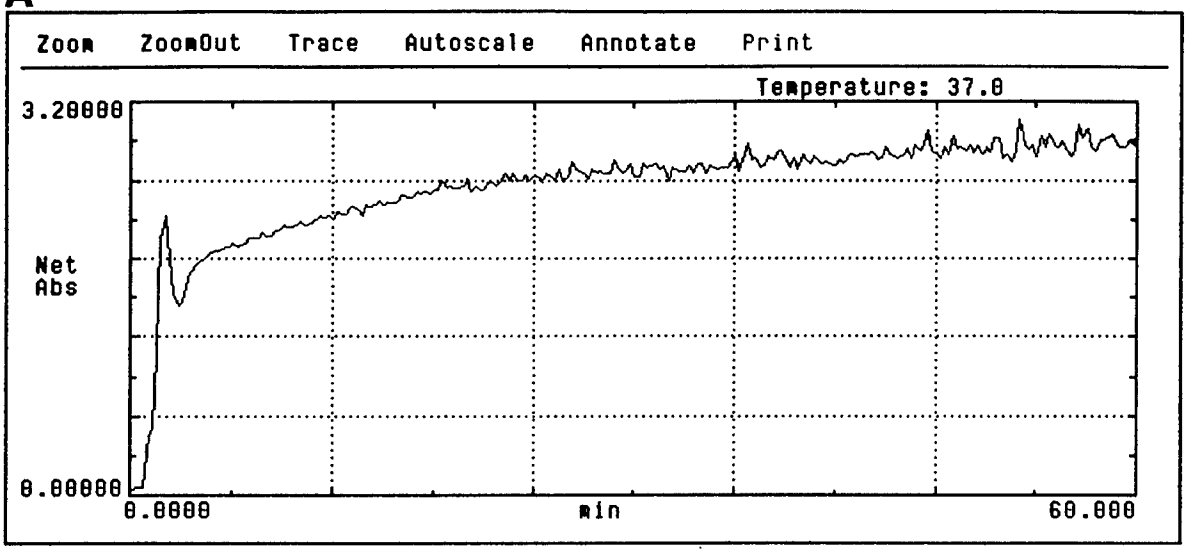
Zoom
ZoomOut
Trace
Autoscale
Annotate
Print
Temperature: 37.0
3.20000
Net
Abs
0.00000
0.0000
Min
60.000

B

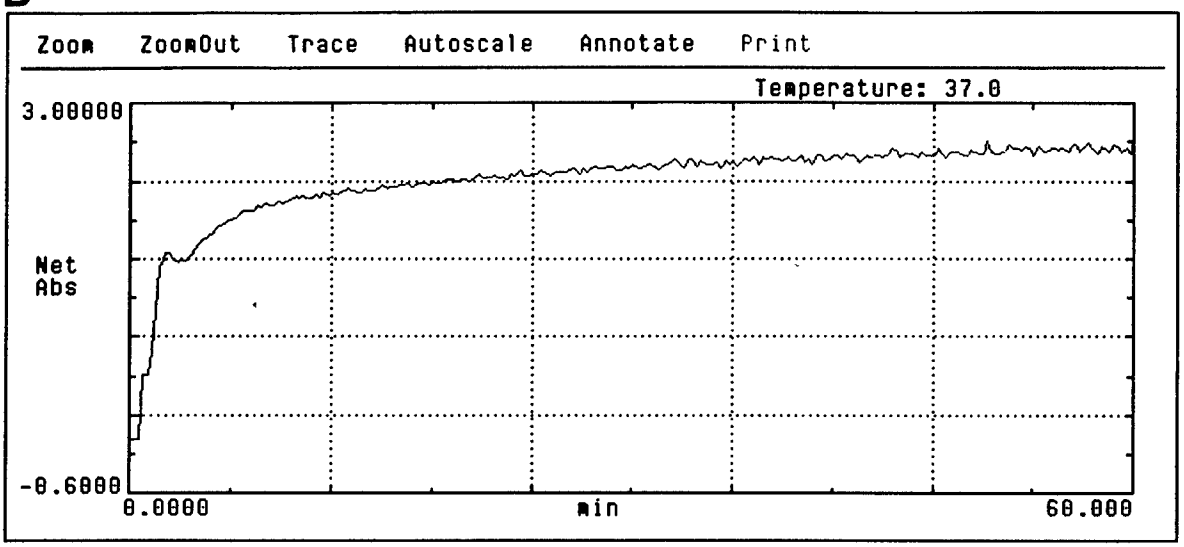
Zoom
ZoomOut
Trace
Autoscale
Annotate
Print
Temperature: 37.0
3.00000
Net
Abs
-0.6000
0.0000
Min
60.000

C

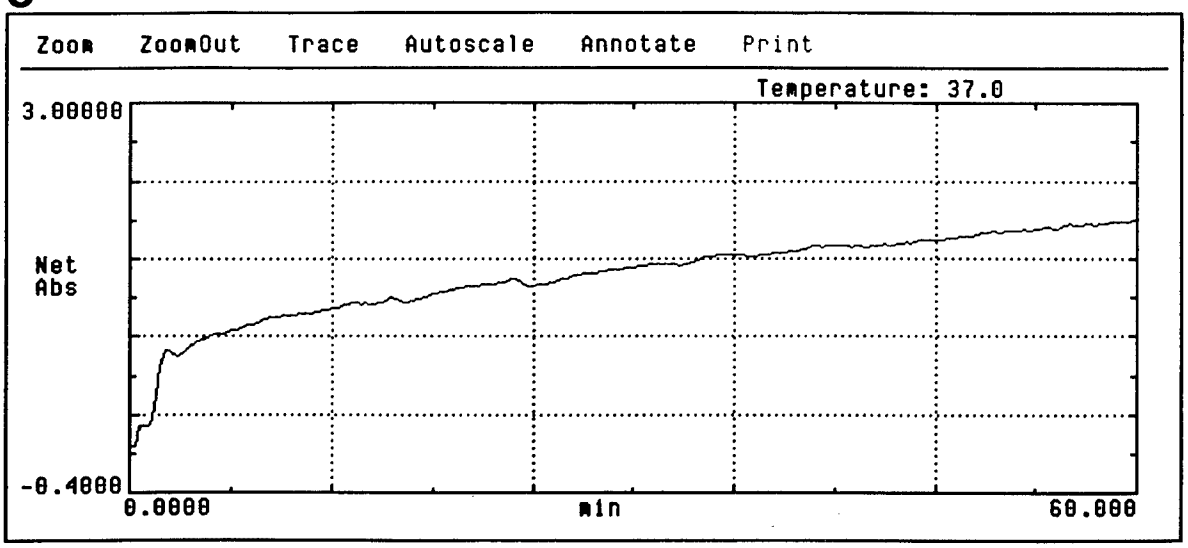
Zoom
ZoomOut
Trace
Autoscale
Annotate
Print
Temperature: 37.0
3.00000
Net
Abs
-0.4000
0.0000
Min
60.000

Figure 1

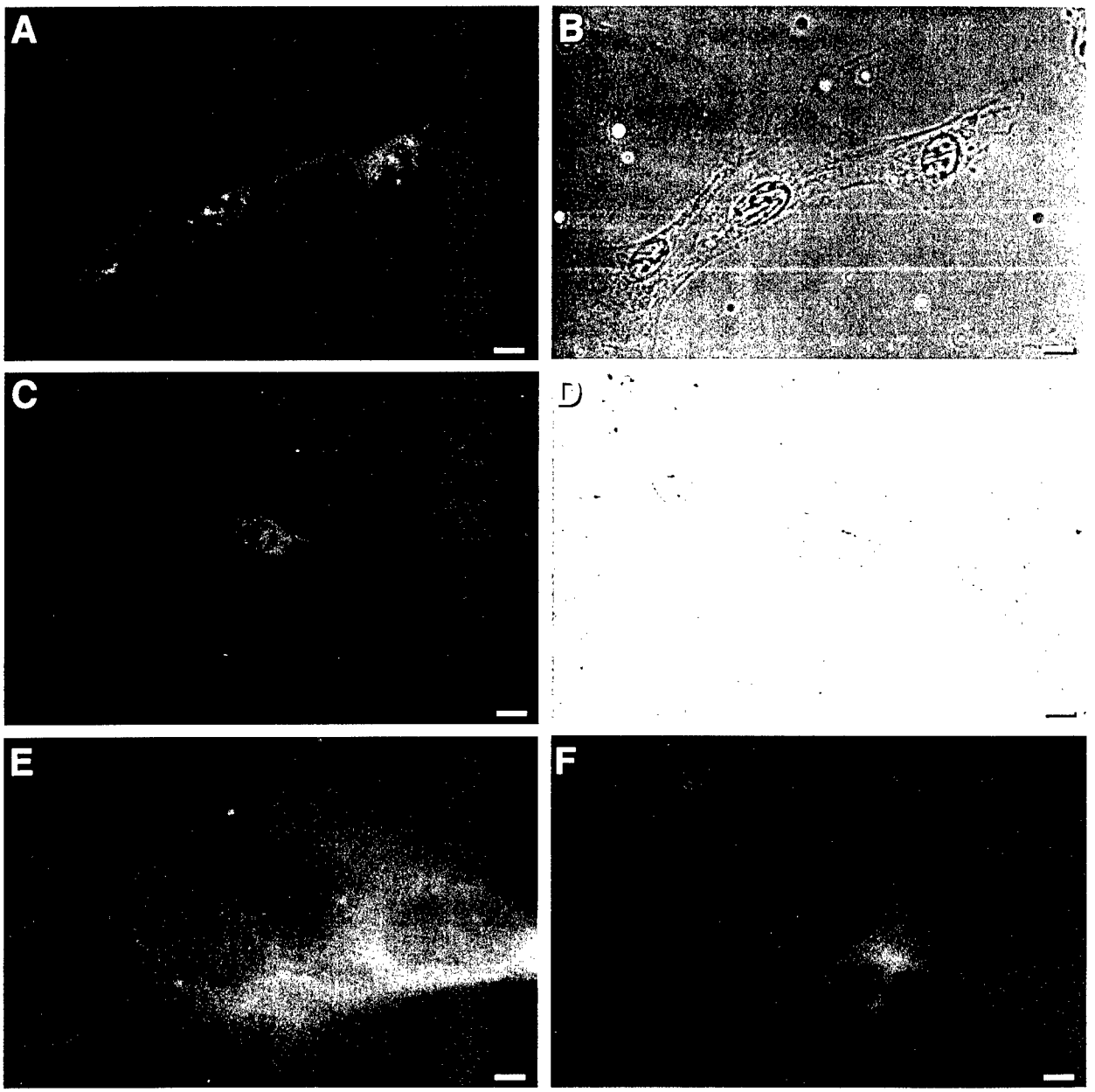

Figure 2

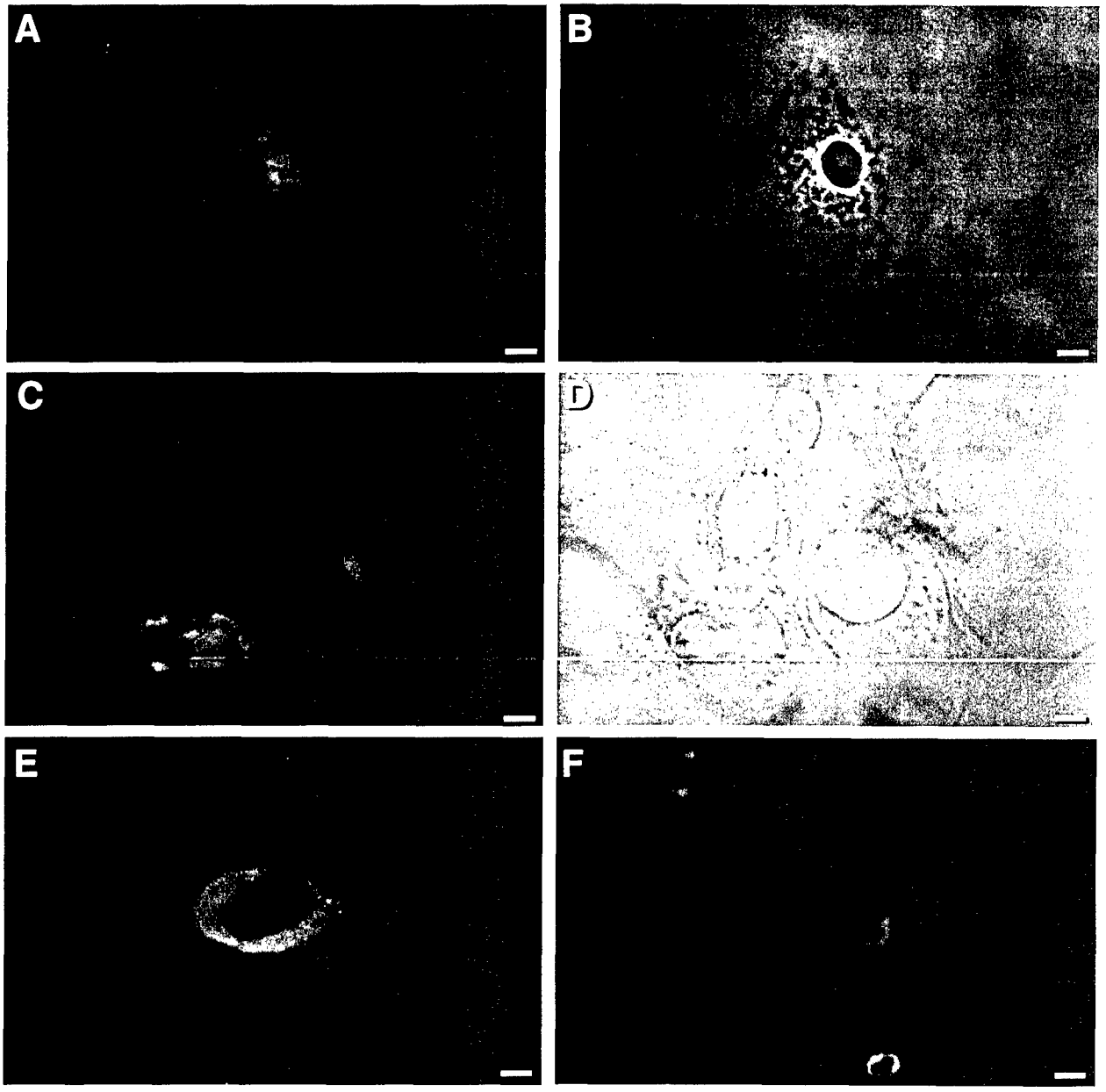

Figure 3

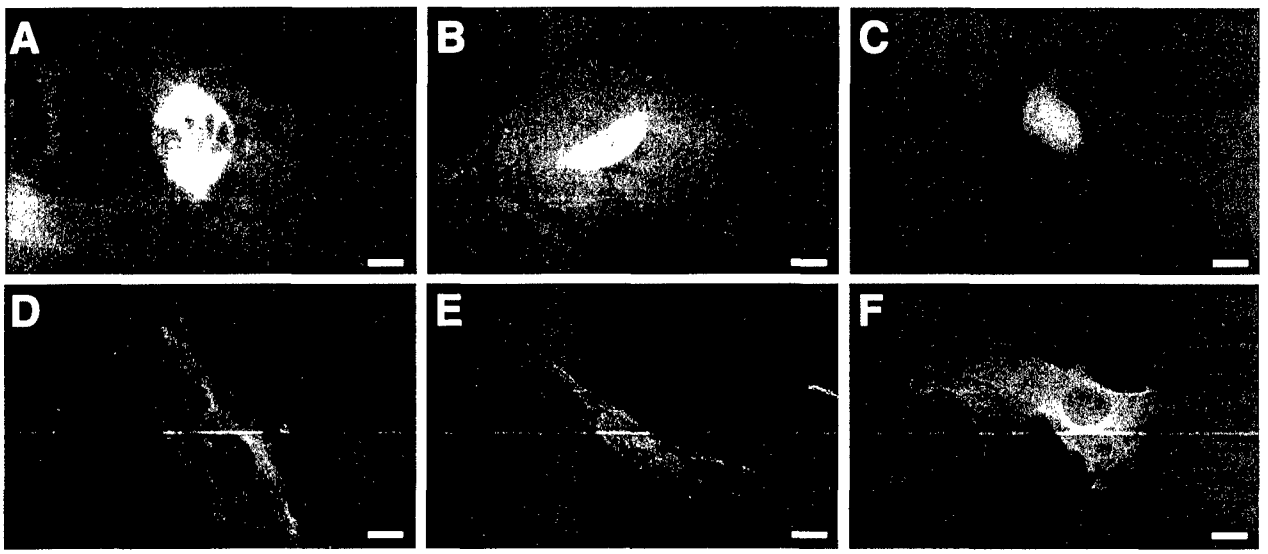

Figure 4

Over-expression of βI Tubulin in MDCK Cells and Incorporation of Exogenous βI Tubulin into Microtubules Interferes with Adhesion and Spreading.

R. Lezama[1], A. Castillo[1], R.F. Luduena[3], and I. Meza[2]

[1] *Departamentos de Biología Celular and* [2] *Biomedicina Molecular, CINVESTAV del IPN, México, D. F.*
[3]*Department of Biochemistry, U. of Texas, San Antonio*

Correspondence to:
Dr. I. Meza
Depto. de Biomedicina Molecular
CINVESTAV del IPN
Apartado 14-740
México D:F. 07360
México Tel (525) 747-3800 ext 5001
Fax (525) 747 71 34
e-mail imeza@cell.cinvestav.mx

Running Title: βI Tubulin Over-expression

ABSTRACT

Little is known about the presence and distribution of tubulin isotypes in MDCK cells although essential epithelial functions in these monolayers are regulated by dynamic changes in the microtubule architecture. Using specific antibodies we show here that the βI, βII and βIV isotypes are differentially distributed in the microtubules of these cells. Microtubules in subconfluent cells radiating from the perinuclear region contain βI and βII tubulins, while those extending to the cell edges are enriched in βII. In contrast, confluent cells contain βI and βII along the entire microtubule length. βIV is the less abundant isotype and shows a similar distribution to βII. The effect of modifying tubulin isotype ratios in the microtubules that could affect their dynamics and function was analyzed by stably expressing in MDCK cells βI tubulin from CHO cells. Three recombinant clones expressing different levels of the exogenous βI tubulin were selected and subcloned. Clone 17-2 showed the highest expression of CHO β1 tubulin. Total βI tubulin levels (MDCK+CHO) in the clones were approximately 1.8 to 1.1-fold higher than in control cells transfected with the empty vector only expressing MDCK β1 tubulin. In all these cells βII tubulin levels remained unchanged. The cells expressing CHO β1 tubulin showed defective attachment, spreading and delayed formation of adhesion sites at short times after plating, whereas control cells attached and spread normally. Analysis of cytoskeletal fractions from clone 17-2 showed a MDCK βI/CHO βI ratio of 1.89 at 2 h that gradually decreased to 1.0 by 24 h. The ratio of the two isotypes in the soluble fraction remained unchanged, although with higher values than those found for the polymerized βI tubulin. By 24 h the transfected cells had regained normal spreading and formed a confluent monolayer. Our results show that excess levels of total βI tubulin, resulting from the expression of the exogenous β1 isotype and incorporation of it into microtubules, affect normal adhesion and spreading of the cells. As the levels return to normal the cells recover their normal phenotype. Regulation of βI

tubulin levels implies the release of the MDCK βI isotype from the microtubules into the soluble fraction where it would be degraded.

Key words: Tubulin isotypes ratio; epithelial cell functions

INTRODUCTION

Microtubules are one of the main components of the cytoskeleton and their dynamic behavior is fundamental for normal function and viability of eukaryotic cells. Microtubules are formed by tubulin dimmers, called α and β. Both tubulins consist of several isotypes, encoded by different genes, that contain diverse post-transcriptional modifications. The carboxyl-terminal end is quite variable among isotypes, making it an isotype discriminatory region. In mammals, seven genes are known for α tubulin and seven for β-tubulin (Sullivan , 1988, Stanchi et al., 2000). Studies done on β tubulin isotypes have shown that they can be differentially distributed within microtubules of the same cell, and that different isotypes can constitute microtubules in different cellular types and tissues. (Sullivan and Cleveland, 1986; Raff et al. , 1997; Roach et al., 1998). These results suggest an isotype-function relationship that might modulate the dynamics of microtubule polymerization which determines specific functions in different cells and sometimes in the same cell (Arai et al., 1988; Ludueña, 1993, 1998; Hyams and Lloyd, 1994). In support of this hypothesis, it has been observed that over-expression of some β tubulin isotypes and their incorporation into microtubules alters their stability (Haber et al., 1995; Ranganathan et al., 1996, 1998; Carles et al., 1999), and that over-expression of the βI and βII tubulin isotypes induces an increase in the density of the microtubule network (Narishige et al., 1999). Other experiments, in

which βI, βII or βIVb tubulins were independently over-expressed indicated that microtubules became resistant to antimitotic drugs when the βI tubulin isotype was mutated (Blade, et al., 1999). In addition, it has been shown that microtubules made from αβIII dimers are more dynamic *in vitro* than those made from either αβII or αβIV dimers (Panda et al., 1994).

Microtubules play a role in cell migration by regulation of cell adhesion and retraction (Bershadsky et al., 1991, 1996; Small et al., 1999; Ballestrem et al., 2000). When cells are treated with microtubule depolymerizing drugs, cellular adhesion and spreading are significantly reduced (Domnina et al., 1985; Evans et al., 1997). Recent evidence suggests that microtubules regulate adhesive or protrusive events through pathways involving the small GTPases Rho and Rac (Nobes et al., 1999; Waterman-Storer and Salmon, 1999). Activation of these events requires combined cycles of polymerization-depolymerization of microtubules and organization of actin filaments (Bershadsky, et al.,1996; Mandato et al., 2000). Waterman-Storer and Salmon proposed in 1999 a model of positive feedback interactions between microtubules and actin in which microtubule disassembly in the cell body activates Rho A, with the consequent formation of focal contacts and contraction of the cell. In contrast, microtubule assembly at the leading edge results in Rac activation and lamellipodium formation. Other studies have shown that microtubule positive ends are found in the boundaries of cell-cell and cell-substrate contact sites suggesting that microtubules use motor proteins to transport factors that modulate the formation of contact sites by regulating acto-myosin-dependent contraction (Kaverina et al., 1998, 1999).

It is well established that in MDCK cells microtubules are essential for cellular polarity participating in protein transport to the apical region via motor proteins such as kinesin and dynein (Marja et al., 1990; Ojakian and Schwimmer, 1992; Kreitzer et al., 2000), and that microtubule architecture is different in subconfluent and confluent cells. (Bacallao et al., 1989). However, as tubulin isotypes in these cells have not yet been identified and their distribution within the microtubules is not established, it is also unknown how the dynamic changes of the microtubular organization could regulate the formation of a polarized monolayer.

We identified in this work three isotypes of β tubulin in MDCK cells and explored whether variation in the expression of a determined isotype could modify the intrinsic organization and functions of the microtubules. For this purpose, βI tubulin from CHO cells was stably expressed in MDCK cells. Three recombinant clones were selected which expressed CHO βI tubulin in different proportion . In all the cells the distribution of the exogenous βI tubulin was similar to that of the endogenous βI isotype. However, adhesion and extension were impaired in the transfected cells at early times after plating. Such alterations apparently resulted from an excess of total βI tubulin (MDCK+CHO) and the incorporation of exogenous βI tubulin into microtubules. Once the ratio of polymerized βI tubulin, (βI endogenous/ βI exogenous) decreased to normal levels, the cells recovered their normal phenotype, indicating that MDCK cells can regulate the levels of βI tubulin incorporated into microtubules by preferentially releasing the endogenous isotype. As the levels of total soluble βI remain constant all the time, the soluble endogenous βI released from microtubules would also be preferentially degraded.

MATERIALS AND METHODS

Materials

All reagents, unless otherwise indicated, were analytical grade and purchased from Sigma Chemical Co. (St. Louis, MO.) Cell culture reagents were obtained from GIBCO-Life Technologies (Gaithersburg, MD).

Cell culture

The MDCK (NBL-2) cell line was obtained from the American Type Culture Collection, and maintained in Eagle-Dulbecco-Vögt modified medium (DMEM, GIBCO cat No. 12100-061) supplemented with 10% fetal calf serum, 100 U /ml penicillin, 100 $\mu g\ ml^{-1}$ streptomycin and 0.8 U ml^{-1} insulin.

Antibodies

Monoclonal antibodies specific for the βI (SAP.4G5) and βIV (ONS.1A6) tubulin isotypes were obtained as indicated (Roach et al., 1998; Banerjee et al., 1992). Although mammals have two forms of βIV, designated βIVa and βIVb, the monoclonal antibody ONS.1A6 is unable to discriminate between them. The polyclonal antibody specific for the βII tubulin isotype, Ab 196, was kindly donated by Dr. R. Armas-Portela at the University of Madrid, Spain (Armas-Portela et al., 1999). The monoclonal antibody against HA tag (Clone 12CA5) was purchased from Boehringer Mannheim, Germany (Cat. No. 1 583 816). The monoclonal antibody against total β tubulin was purchased from ICN Biomedicals, Costa Mesa, CA (Cat. No. 63781). The monoclonal antibody against actin was prepared using rat brain actin as indicated in a previous work (Manning-Cela et al., 1994).

Immunofluorescense and confocal microscopy

Cells were grown on glass coverslips in complete medium, rinsed in PBS, and then fixed with 3.0% formaldehyde (ultrapure grade, Tousimis Research Co., Rockville, MD) at room temperature for 20 min. Cells were permeabilized by 3 min treatment with 0.5% Triton X-100 and then blocked with 0.5% bovine serum albumin in PBS (PBS/BSA) for 30 min. After rinsing with PBS, cells were incubated with the first antibody diluted 1:50 or 1:100 in PBS/BSA for 60 min at 37°C. For simultaneous localization of β tubulin isotypes cells were incubated with monoclonal and polyclonal antibodies at the same time. After incubation, cells were rinsed with PBS and the secondary antibodies goat anti-mouse IgG tagged with FITC and goat anti-rabbit IgG tagged with rhodamine (1:50 dilution with PBS/BSA) were added for 60 min at room temperature. After rinsing with PBS, the coverslips were mounted on glass slides containing 50 ul of a 9:1 PBS/ glycerol mixture pH 8.5, for epifluorescence observation, or in α-quenching medium (Vecta Shield H-100, Vector Laboratories Inc. Burlingame, CA) for observation in a confocal laser microscope (Bio Rad MRC-600, Watford, UK). Double-immunofluorescence preparations were protographed in each of the corresponding fluorescence excitation filters and then each image was independently analyzed using the program Confocal Assistant from Bio Rad.

Electrophoretic Procedures

Cells grown on Petri dishes were lysed with ice cold buffer, containing 20 mM Tris-HCL, pH 7.5, 1% sodium dodecyl sulphate, 2 mM EGTA and Complete proteinase inhibitor cocktail tables (used as indicated by the manufacturer, Amersham, Pharmacia

Biotech Inc. Piscataway, NJ) and sonicated by 30 sec cycles. Protein concentration was determined by Lowry before polyacrylamide gel electrophoresis (PAGE) carried out in 7.5% SDS-discontinuous gels. Proteins were electrotransferred to nitrocellulose membranes, which were stained with Ponceau S to verify the amount of protein transferred in each lane. The nitrocellulose paper was blocked with 5% skim milk in PBS, and incubated in a 1: 1000 dilution of the antibody against HA tag, 1: 5000 dilution for βI or 1:10000 dilution of the βII antibody, overnight at 4°C. In this primary incubation the monoclonal antibody specific for actin (1:250 dilution) was also added to act as internal standard for the amount of protein loaded in each lane. The blots were then washed 3 times (20 min each) in PBS and incubated for 1 h in a 1:5000 dilution of peroxidase-conjugated goat antimouse IgG. Positive bands were visualized with the Amersham enhanced chemiluminiscence ECL kit.

Expression Vector

MDCK cells were transfected with the expression vector pRc/HA-β1 which was a generous gift from Drs. M. Gonzalez-Garay and F. Cabral at the University of Texas, Houston. This vector contains the entire coding sequence for βI tubulin of CHO cells, and was modified to encode a 9 amino acid hemagglutinin antigen (HA) epitope tag from the influenza virus at the C-terminus of the βI tubulin sequence (González-Garay and Cabral, 1995).

Isolation of stable transfected cells

MDCK cells were transfected with plasmid DNA by the calcium phosphate coprecipitacion technique, including a 10% glycerol shock step (Chen and Okayama, 1987). Forty-eight hours after transfection, cells were subcultured in complete medium

containing 0.6 mg of G418 (selection medium). The G418 resistant colonies, were picked and expanded in selection medium. Recombinant clones were selected by immunofluorescence using the anti-HA antibody to detect the CHO tubulin and then subcloned by limited dilution to obtain a homogeneous population, as assessed by the levels of expression of the transfected protein. Increased expression of the transfected gene was induced adding 2 mM sodium butyrate overnight to the cell culture medium (Barlow et al., 1994)

Cytoskeleton and soluble fraction preparation

Cells grown on Petri dishes were rinsed several times with PBS. Lysis buffer containing 0.5% Triton X-100, 10 mM Tris-HC1 pH 7.7, 25 mM KC1, 120 mM NaCl, 2 mM EGTA, 4 ug/ml taxol and Complete proteinase inhibitor was added to the cells and gently detached with a rubber policeman. The cell suspension maintained at 4°C was sonicated and then centrifuged at 12 000 x g for 10 min at 4°C. Supernatans containing the soluble fraction were carefully separated from pellets containing the membrane cytoskeleton protein and placed in separated tubes. The pellets were resuspended in 10 mM tris-HCl pH 7.5, 0.05% SDS and Complete. Both fractions were precipitated with acetone for 10 min at 4°C and then centrifuged at 10 000 x g 10 min at 4°C. The pellets were resuspended in 10 mM Tris-HCl pH 7.5, 0.05% SDS and Complete. Protein concentration was determined before immunoblots were carried out.

Cell adhesion assays

Cells were seeded in 24-well cell culture dishes for the times required in the experiments, rinsed three times with PBS to wash away non-adhered cells and fixed with 3% formaldehyde for 20 min at room temperature. After rinsing with PBS, attached

cells were stained with 0.1% methylene blue dissolved in borate buffer pH 8.7 (0.2 M boric acid, 0.5M sodium borate) for 30 min at room temperature. After rinsing with borate buffer pH 8.7, cells were lysed with 0.1 N HCl for 30 min at room temperature. The absorbance of the released dye was measured at 630 nm in an ELISA plate reader. Cell adhesion values were expressed as percentage considering the adhesion of mock cells as 100%.

Densitometric measurements

Quantification of the immunoblot reactive bands was done by scanning the fluorographies obtained in at least three independent experiments of the same type, followed by integration of the areas under the curves using the gel analysis software, Sigma gel version 1.0.

Morphometric measurements

They were made collecting a number of optical slices (1.0 μm step) of rhodamine-stained cells at different times of culture. The longest axis and the projection of the area of the cells were analyzed with the program included for morphometry in the confocal microscope.

RESULTS

Presence and Distribution of β-Tubulin Isotypes in MDCK Cells

The identity and expression of tubulin isotypes in MDCK cells was determined using antibodies that could discriminate between βI, βII and βIV tubulins. As none of these antibodies can be used for immunoprecipitation, the quantification of the reactive bands in the immunotransference assays was done normalizing the protein

concentration measured in each band to the concentration value obtained with an actin monoclonal antibody, used as an internal protein standard, in densitometric measurements (Fig. 1). Two bands were positive in all cases; one of approximately 50 kDa corresponding to the molecular weight reported for tubulin monomers and one of 43 kDa corresponding to actin. These results showed that MDCK cells express the βI, βII and βIV isotypes of tubulin. The distributions of the βI and βII isotypes were determined by indirect immunofluorescence (IIF) using the antibodies coupled to two different fluorescent markers (Fig. 2). In subconfluent cells, the βI isotype was localized in the microtubule network radiating from the perinuclear region but was not present in the region where the microtubules reached the cell edges (Fig. 2a). This distribution was not modified at higher concentrations of the antibody. The βII isotype was also localized in the microtubules forming the perinuclear network but it was particularly enriched in the microtubules extending to the cellular borders (Fig. 2b). This zonal distribution was confirmed in superimposed images (Fig. 2c) and in cross sections of the same images (Fig. 2d). In confluent cells βI and βII isotypes co-localized along the complete length of the microtubules (Figs. 2e, f, g). A less dense microtubule network following the same pattern as βII tubulin was observed with the βIV antibody (data not shown). Our results with IIF not only corroborated previous results showing changes of the microtubule organization in subconfluent and confluent MDCK cells, but showed that the changes imply rearrangements in the distribution of βI tubulin isotypes during the formation of a confluent polarized monolayer.

Expression of the exogenous βI-Tubulin in MDCK Cells

Variation in the expression of βI tubulin was induced by expression of a βI tubulin cDNA sequence from CHO cells in the MDCK cells. This sequence has been cloned in plasmid pRc/HA-βI which also contains a sequence encoding nine amino acids of the influenza virus (HA) in its carboxyl-end, and a sequence to confer resistance to G418. (González-Garay and Cabral , 1995). Three stable recombinant clones with different levels of expression of the exogenous protein, initially assessed by IIF using an anti-HA antibody, were selected and subcloned to have a homogeneous population. As a control, cells transfected with the same plasmid lacking the βI tubulin gene were also cloned (mock cells). The levels of expression of exogenous βI-tubulin in transfected cells were measured in western blots of total cell extracts from the three clones and from mock cells using the anti-HA antibody. An anti-actin antibody was added as an internal standard. Figure 3 (lanes 2, 3 and 4) shows a representative fluorograph in which the bands corresponding to CHO β1 tubulin and actin can be seen. Densitometric analyses indicated that cells from the clone 17–2 expressed the highest levels of exogenous βI-tubulin. This value was taken as 100%. Cells from clone 39–7 expressed 25% less than clone 17-2 and cells from clone 2-26 expressed 90-95 % less. Lane 5 is an overexposure of lane 4 to facilitate the visualization of the exogenous protein band. Cell extracts from mock cells (lane 1) only showed the band corresponding to actin.

Incorporation of exogenous βI-tubulin into microtubules was monitored by IIF also using the anti-HA labeling. In all the transfected cells the exogenous βI tubulin showed the same distribution as that observed in control cells. Figure 4 shows the distribution in confluent control cells (Fig. 4a), confluent cells of clone 17-2 (Fig. 4b), and the similar but less intense labeling of microtubules in the 39-7 (Fig. 4c) and 2-26 cells (Fig. 4d).

These observations agree with the results obtained by immunotransference, indicating that the 3 subclones differentially expressed the CHO cell βI tubulin.

βI-Tubulin levels in control and transfected cells.

MDCK cells plated on culture dishes adhere almost immediately but require nearly 2 h to extend, form ruffles and lamellae. After 6–8 h, most of the cells are completely extended and have made cell-cell contacts. By 24 h the cells have formed a confluent monolayer, where transepithelial resistance can be registered indicating closure of the tight junctions and establishment of cell polarity (for review see, Cereijido et al., 2000). βI-tubulin levels (both exogenous and endogenous) were quantified in subcellular fractions from control cells (mock) and transfected cells plated for 2, 6, and 24 h. These times were chosen as adhesion, changes in cell shape, formation of cell-cell contacts and confluency could be clearly monitored. Discrimination between the 2 types of βI tubulin being expressed in the cells was possible because antibody SAP.4G5 exclusively recognized the endogenous βI-tubulin, and the exogenous βI-tubulin was specifically labeled by anti-HA. Non-polymerized tubulin was quantified in the Triton X-100 soluble fraction (sol), whereas polymerized tubulin (pol), remained in the cytoskeleton or Triton X -100 resistant fraction . The Western blot in Figure 5A shows the reactive bands in the two fractions from mock and clone 17–2 cells labeled with three different antibodies. A band of approximately 50 KDa corresponded to the endogenous (end) βI tubulin, a band of slightly lower relative mobility corresponded to the exogenous (exo) βI tubulin, and a 43 kDa band corresponded to actin. Lanes 1 and 2 at the different times show the soluble and polymerized fractions from clone 17-2 cells. Lanes 3 and 4 show the same fractions from mock cells in which the band

corresponding to exogenous βI tubulin was not present. The band corresponding to endogenous βI tubulin in the soluble fraction of 17-2 cells (lane 1) remained unchanged while the same tubulin band in the polymerized fraction decreased with time of culture (lane 2). The exogenous βI tubulin also remained constant during culture time (lane 1) in the soluble fraction. In the polymerized fraction from 2 to 6 h there was no significant change, but a large decrease was observed at 24 h (lane 2). In mock cells a change in the levels of βI tubulin (endogenous) was not detected in the soluble nor in the polymerized fractions (lanes 3 and 4).

Densitometric analyses shown in Figure 5B, were performed in equivalent blots from 3 independent experiments. Results showed that total levels of βI tubulin (end+exo) in the cells from clone 17-2 reached values 80, 60, and 45% above the values measured in mock cells which only contain endogenous βI tubulin at 2, 6 and 24 h. The densitometric analyses of the polymerized fraction in the blots from mock and 17-2 clone cells are shown in figure 5C. After 2h of culture, endogenous βI tubulin levels from mock cells (pol mock) and those of the same type of βI tubulin in cells from clone 17–2 (end pol) were not significantly different. At 6 and 24h the levels of endogenous polymerized βI tubulin in the cells of clone 17–2 significantly decreased in comparison to the levels present in mock cell during the same times of culture (pol mock and end pol). In the 17-2 clone the incorporation into microtubules of significant levels of exogenous βI could be detected at all times of culture (exo pol). These levels were not significantly different at 6h but then decreased considerably by 24h . Figure 5D shows the levels of soluble βI tubulin in the 17–2 cells, both endogenous and exogenous (end

sol and exo sol), remained unchanged during culture, in the same way as the levels of soluble βI tubulin did not change in the mock cells (sol mock).

From the densitometric values in the fractions from cells 17-2 the end/exo ratios of polymerized βI tubulin were calculated. Values of 1.8, 1.19, and 1.0 were obtained at 2, 6, and 24 h of culture, respectively. The reduction in this ratio in these cells was due to the decrease of endogenous βI tubulin (end pol in Fig. 5C at all the culture times) as exogenous polymerized βI tubulin (exo pol) significantly decreased only in the period between 6 and 24 h of culture. On the other hand, analysis of βII-tubulin expression using the anti-βII tubulin antibody in both soluble and cytoskeleton fractions in cells from the 17–2 clone or mock cells at 2, 6, and 24 hours, showed no significant variation (data not shown). These results indicate that the levels of endogenous βI tubulin are regulated in the mock and also in the transfected cells expressing CHO βI tubulin.

Effect of βI Tubulin Over-expression in Cellular Adhesion

The above results indicated that at short times after plating, the microtubules being organized in the cells have not only incorporated the exogenous βI isotype but also increased the proportion of total βI. When adhesion of cells expressing different levels of the exogenous βI tubulin was analyzed, it was found that mock cells had completely adhered by 30 min (Fig. 6, 100 % value). At this time whole the cells from clone 17-2 showed an adhesion of only 60 % whereas the cells from clone 39-7 showed 75 % adhesion compared to mock cells and cells those from clone 2-26 showed an adhesion of 90 %. However, adhesion in the three clones increased gradually, reaching by 6 h close values to those of mock cells but with a slower kinetics. These results suggest that the defective adhesion showed by the transfected cells expressing different levels

of CHO βI tubulin and thus containing higher levels of total βI , colud result from the higher proportion of this isotype incorporated in the microtubules (Fig. 5C). The results obtained with the different clones rule out the possibility that plasmid integration into the MDCK cell DNA had occurred into regulatory or codifying regions that could cause the adhesion defect, as this is overcome during longer culture times.

Effect of βI-Tubulin Over-expression in Cellular Spreading

The above results showing defective adhesion of the transfected cells suggested that cellular spreading, also depending on microtubule and actin organization could be altered in these cells. Therefore, the distribution and organization of microtubules and actin filaments was analyzed by immuno-localization using the total βI tubulin antibody and rhodamine-labeled phalloidin.

During the first 2 h of culture, cells from clone 17–2 that could make contact with the substrate remained completely rounded, microtubules were localized as dense rings around the nucleus, and actin filaments displayed a tight cortical distribution (Figs. 7 a, d). During the same period, mock cells were already extended, have developed lamellae and the microtubules radiating from the perinuclear region showed an incipient network organization (Fig. 7 a'). Actin filaments in these cells formed stress fibers along the cellular margins (Figs. 7 d'). In contrast, the 17–2 cells began spreading only after 6 h when few ruffles and scarce stress fibers were visible (Figs. 7 b, e). Mock cells were already extended and even made several several cell-cell contacts and both microtubules and microfilaments were organized (Figs. 7b', e'). By 24 h microtubules and microfilaments in the 17–2 and mock cells showed a similar organization with a

microtubule network radiating from the perinuclear region and actin filaments forming the cortical ring typical of epithelial cells (Figs. 7 c, f, c', f').

Morphometric analyses were performed to corroborate the observed morphological changes. The area and the longest axis of mock and clone 17-2 cells were measured in 100 cells found in different fields at 2, 6 and 24 h of culture (Table I). Mock cells did not show rounded cells at any culture time, whereas the fields containing clone 17-2 cells showed mostly rounded cells after 2 h (Area = 926 ± 81 μm^2 vs 313 ± 34 μm^2 and longest axis = 41 ± 2 μm vs 20 ± 1 μm) . By 6 h spreading cells (60%) of clone 17-2 were seen. The longest axis and the area in these cells were approximately one half of those in mock cells (44 ± 5 μm and 1625 ± 170 μm^2 vs 76.5 ± 5 μm and 3405 ± 172 μm^2). At 24 h these parameters were very similar in both types of cells (117 ± 17 μm and 6823 ± 420 μm^2 vs 115 ± 14 μm and 7014 ± 393 μm^2). These results indicate that transfected cells expressing high levels of the β1 tubulin isotype have impaired spreading at early times of culture and, as in the case of adhesion, this defect could be overcome after 6 h in culture.

Delayed formation of adhesion sites in transfected cells.

Microtubules and actin microfilaments are known to participate in the establishment and maintenance of adhesion sites. (Kaverina et al., 1998, 1999). The rounded shape, the defective adhesion, as well as the delayed spreading shown at early culture times by the cells overexpressing β1 tubulin, in particular the cells from clone 17-2, could be related with inadequate establishment of adhesion sites. To explore this possibility adhesion sites in the mock and transfected cells were visualized using an antibody against vinculin, tagged with FITC. Figure 8 shows mock and clone 17-2 cells at 2, 6

and 24 h of culture. Focal adhesions were absent in the 17-2 cells (Figs. 8 a, b) whereas in the mock cells clearly formed adhesion sites were seen at 2 h (Fig. 8 a') with an important increase in number of adhesion sites by 6 h of culture (Fig, 8 b'). However, after 24 h in culture, organized focal adhesions were observed in both control and transfected cells. (Figs. 8 c, c'). These results suggest that over-expression of βI tubulin and incorporation of CHO βI tubulin into microtubules could retard the formation of focal adhesion sites at early times of culture and contribute to the defective adhesion and spreading of the transfected cells.

DISCUSSION

Expression of β Tubulin Isotypes in MDCK Cells

The monolayers of MDCK cells form *in vitro* a polarized epithelium allowing vectorial transport, which includes absorption, secretion, and bi-directional transcytosis. It has been established that a dynamic microtubular system plays an important role in maintaining the monolayer functions. (Rodríguez-Boulan and Nelson, 1989; Meads and Schroer, 1995; Fanning et al., 1999; Cereijido et al., 2000). In spite of this evidence, few studies with these cells have addressed their microtubule intrinsic organization.

This work reports for the first time the presence of at least 3 isotypes of β tubulin in MDCK cells, how they distribute within microtubules, and the effects of isotype overexpression in microtubular functions. The expression of different β tubulin isotypes and their integration into microtubules has been reported as having a specific tissue pattern probably related to the function of the cells. βI, βII and βIV tubulins are

considered to be constitutive, βI being perhaps the most widespread. (Sullivan and Cleveland, 1986; Sullivan, 1988).

The microtubular distribution of βI and βII was found to differ in subconfluent and confluent cells. In isolated cells the βI isotype was localized in microtubules forming the network radiating from the perinuclear region in the zone closest to the nucleus, while βII, although present in the same microtubules, was very much enriched in microtubules reaching the cellular borders. In confluent cells, the βI and βII-isotypes colocalized all along the microtubules. The distribution of βIV was found to be similar to that of β II and did not change at the different growth stages. These observations suggested dynamic changes in the architecture of the isotypes during the formation of a confluent functional monolayer. It has been reported that in subconfluent MDCK cells and PtK1 cells, microtubules do not use centrosomes as the sole nucleation site and the majority of them do not originate by centrosomal growth (Meads and Schroer, 1995; Keating et al., 1997). The half-life of these microtubules has been calculated as approximately 30 min with an exchange of heterodimers every 9 min. In confluent or polarized cells, the half-life of the microtubules was calculated as 2 h, and the exchange of heterodimers occurs every 30 min. These microtubules are more resistant to depolymerization by drugs than more dynamic microtubules as those present in subconfluent cells. Furthermore, when growth of the plus ends of the microtubules was measured, a growth of 11.1 μm/min was registered in subconfluent cells and in confluent cells microtubules grew 2.7 μm/min (Bré et al., 1987, 1990; Bacallao et al., 1989; Pepperkok et al., 1990; Meads and Schroer, 1995; Wadsworth and Bottaro, 1996).

Our present observations indicate that microtubules containing a higher proportion of βI than of βII or containing only βI are concentrated at the perinuclear region while microtubules mostly containing βII reach the cell edges. Furthermore, those microtubules found in zones where cellular extension is occurring consist largely of βII. These microtubules presumably participate in formation of adhesion sites involved in cellular extension, as shown in other cell systems (Kaverina et al., 1998, 1999). This raises the possibility that βII is involved in adhesion. One can further hypothesize that once the cells make contact with each other and cellular extension can no longer take place, the distinct zonal distributions of the β tubulin isotypes within the microtubules are lost and the microtubules acquire a more stable architecture. Although we are tentatively proposing βII as being involved in adhesion, it is certainly possible that βIV also plays a role here because microtubules in these zones also contain some βIV. Furthermore, there is also the βV isotype whose distribution in mammals is as yet unknown and for which no monoclonal antibody is available. The microtubules involved in adhesion could easily contain βV and we would not be able to tell. However, the most likely hypothesis that arises from these data is that the βI isotype is not directly involved in adhesion.

Effects of Over-expression of βI-Tubulin in MDCK Cells

To test this hypothesis, we studied the effect of tubulin isotype ratio modification on particular cell functions, transfecting MDCK cells with a plasmid that contained the sequences of βI tubulin from CHO cells to induce over-expression of the βI isotype. Over-expression of βI tubulin and incorporation of the CHO isotype into microtubules rendered cells defective in adhesion, spreading and development of focal adhesion

sites. Cell adhesion to a substrate or to extracellular matrix is particularly important for the organization of the monolayer and the apicobasal axis of polarity in MDCK cells (Yeman, et al., 1999). It has been proposed that microtubules and actin interact at cell adhesion sites to the substrate and that the number of microtubule ends at these sites is proportional to the strength of binding by directing cellular extension and modulating the contraction of acto-myosin complexes (Vasiliev, 1991; Kaverina et al., 1998, 1999). The defect in adhesion and extension observed in the transfected cells was proportional to the levels of βI and could be due to the corresponding higher incorporation of this isotype (both endogenous and exogenous) into microtubules during the first hours of culture. This could modify microtubule stability and affinity for proteins related with the assembly of adhesion sites and extending cell edges. However, these defects were overcome when the cells adjusted the excess of βI tubulin levels and the ratio of endogenous/exogenous βI tubulin in microtubules, which in our experiments occurred at approximately 6h of culture. At this time, cells started to recover a normal phenotype to finally acquire a confluent-cell cytoskeleton architecture. These results are consistent with the zonal distribution and changes of the βI and βII isotypes observed by immunofluorescence in control cells and suggest that although βI tubulin could not directly participate in adhesion and spreading, the modification of total βI levels has a deleterious effect on the dynamics of the microtubules containing abnormal ratios of βI/βII that could then impair these processes.

Regulation of βI Tubulin levels in MDCK Cells

The model of negative autoregulation of tubulin proposes that stability of the union between ribosomes and β tubulin mRNA regulates tubulin levels in the cells (Yen et al.,

1988). In the case of an excess of β tubulin, a putative factor will bind to the first four amino acids in the nascent tubulin peptide emerging from the ribosome. This union activates a ribonuclease or freezes the ribosome, resulting in the degradation of the mRNA and the consequent decrease of the levels of the protein being translated.

Sisodia et al., (1990) over-expressed chicken βIV tubulin in CHO cells and observed that in stable transfections, chicken βIV tubulin was rapidly degraded, while in transient transfections endogenous βIV tubulin decreased gradually. At the same time, no change in the endogenous synthesis of βI tubulin was observed. These authors concluded that in vivo, β tubulin isotypes can be biochemically distinguished and that the stability of the βI and βIV isotypes is established in part by specific interactions with other cellular factors.

In 1995, González-Garay and Cabral over-expressed βI tubulin in CHO cells and found a reduction in endogenous tubulin expression and an increase in α-tubulin synthesis. Later , these same authors (1996) reported a reduction in endogenous α tubulin synthesis while overexpressing α tubulin but found no effect on β tubulin synthesis nor decrease of its mRNA levels. They proposed a mechanism of regulation in which both α and β tubulins are involved, as equimolar concentrations of both are required to form the heterodimers. When the synthesis of one of the two isotypes increases, a limiting quantity of the other isotype is necessary thus, the monomer in excess is degraded. Additionally, they proposed that synthesis of the transfected protein was not regulated since regions of repression in the 5' and 3' UTR regions could be necessary and were not present in the transfected gene.

The results obtained in the present work with MDCK cells indicate that cells that co-expressed a heterologous isotype of βI tubulin preferentially regulate the endogenous isotype by significantly decreasing the levels of the polymerized endogenous tubulin, while polymerized exogenous βI tubulin only decreased at later times of culture. At the same time as the ratio of total soluble βI (endogenous + exogenous) is maintained constant, the endogenous βI in the soluble fraction has to be degraded. These observations could partially agree with the negative autoregulation model, since regulation was observed for the endogenous βI isotype. However, if both endogenous and exogenous βI tubulin genes contain the sequences required for negative autoregulation, the exogenous βI tubulin should be regulated at all times and this did not happen at early times of culture. Furthermore, as expression of βII tubulin did not change in the transfected cells, the preferential regulation of the endogenous βI tubulin points to an isotype-specific regulation, as suggested by Sisodia et al., (1990). On the other hand, our results could be interpreted by the model of González-Garay and Cabral, (1996) in which equimolar concentrations of α and β monomers are necessary and if a monomer is in excess, it is degraded. Furthermore, as the levels of endogenous βI in the microtubules are always slightly higher than the levels of exogenous βI in the transfected cells, it seems that MDCK cells preferentially incorporate their own tubulin into microtubules, discriminating between the exogenous and endogenous forms of βI. This could be the reason why a better regulation of the endogenous βI tubulin is achieved, although we still do not know which mechanism operates in these cells. Experiments are underway to explore these aspects.

ACKNOWLEDGMENTS

We are very grateful to Drs. G. Contreras, R. Manning-Cela and N. Villegas for their critical evaluation of this work, to J. Luna for expert assistance with the confocal microscope and to D. Moreno for secretarial help. R. L. was a predoctoral fellow from CONACYT, México and TELMEX Foundation. R. F. L. was supported by grants CA26376, AQ-0726 and DAMD 17-98-1-8246 from the National Institutes of Health, the Welch Foundation, and the USA Army Medical Research Program, respectively.

REFERENCES

Arai T, Matsumoto G. 1988. Subcellular localization of functionally differentiated microtubules in squid neurons: Regional distribution of microtubule-associated proteins and β-tubulin isotypes. J Neurochem 51:1825-1838.

Armas-Portela R, Parrales M A, Albar J P, Martinez-A C, Avila J. 1999. Distribution and characteristics of βII tubulin-enriched microtubules in interphase cells. Exp Cell Res 248: 372-380.

Bacallao R, Anthony C, Dotti C, Karsenti E, Stelzer E H K, Simons K. 1989. The subcellular organization of Madin-Darby canine kidney cells during the formation of a polarized epithelium. J Cell Biol 109:2817-2832.

Ballestrem C, Wehrle-Haller B, Hinz B, Imhof BA. 2000. Actin-dependent lamellipodia formation and microtubule-dependent tail retraction control-directed cell migration. Mol Biol Cell 11:2999-3012.

Banerjee A, Roach M A, Trcka P, Ludueña R F. 1992. Preparation of a monoclonal antibody specific for the class IV isotype of β tubulin. J Biol Chem 267:5625-5630.

Barlow S, Gonzalez-Garay M L, West R R, Olmsted J B, Cabral F. 1994. Stable expression of heterologous microtubule-associated proteins (MAPS) in Chinese

Hamster Ovary cells: Evidence for differing roles of MAPs in microtubule organization. J Cell Biol 126:1017-1029.

Bershadsky A, Vaisberg EA, Vasiliev JM. 1991. Pseudopodial activity at the active edge of migrating fibroblasts is decreased after drug-induced microtubule depolymerization. Cell Motil Cytoskeleton 19:152-158.

Bershadsky A, Chausovsky A, Becker E, Lyubimova A, Geiger B. 1996. Involvement of microtubules in the control of adhesion-dependent signal transduction. Curr Biol 6:1279-1289.

Blade K, Menick D R, Cabral F. 1999. Overexpression of class I, II or IVb β-tubulin isotypes in CHO cells is insufficient to confer resistance to paclitaxel. J Cell Sci 112:2213-2221.

Bré MH, Kreis TE, Karsenti E. 1987. Control of microtubule nucleation and stability in Madin-Darby canine kidney cells: The occurrence of noncentrosomal, stable detyrosinated microtubules. J Cell Biol 105:1283-1296.

Bré MH, Pepperkok R, Hill AM, Levilliers N, Ansorge W, Stelzer E H K, Karsenti E. 1990. Regulation of microtubule dynamics and nucleation during polarization in MDCK II cells. J Cell Biol 111:3013-3021.

Carles G, Braguer D, Dumontet C, Bourgarel V, Goncalves A, Sarrazin M, Rognoni J B, Briand C. 1999. Differentiation of human colon cancer cells changes the expression of β-tubulin isotypes and MAPS. Brit. J. Cancer. 80: 1162-1168.

Cereijido M, Shoshani L, Contreras R G. 2000. Molecular physiology and pathophysiology of tight junctions. I. Biogenesis of tight junctions and epithelial polarity. Am J Physiol Gastrointest Liver Physiol 279:G477-G482.

Chen C, Okayama H. 1987. High-efficiency transformation of mammalian cells by plasmid DNA. Mol Cell Bio 7:2745-2752.

Domnina LV, Rovensky JA, Vasiliev JM, Gelfand I M. 1985. Effect of microtubule-destroying drugs on the spreading and shape of cultured epithelial cells. J Cell Sci 74:267-282.

Evans DM, Steele JG. 1997. Multiple attachment mechanisms of corneal epithelial cells to a polymer-cells can attach in the absence of exogenous adhesion proteins through a mechanism that requires microtubules. Exp Cell Res 233:88-98.

Fanning A.S, Mitic L L, Anderson J M. 1999. Transmembrane proteins in the tight junction barrier. J Am Soc Nephrol 10: 1337-1345.

González-Garay ML., Cabral F. 1995. Overexpression of an epitope-tagged β-tubulin in Chinese Hamster Ovary Cells causes an increase in endogenous α-tubulin synthesis. Cell Motil Cytoskeleton 31:259-272.

González-Garay ML, Cabral F. 1996. α tubulin limits its own synthesis: Evidence for a mechanism involving translational repression. J Cell Biol 135:1525-1534.

Haber M, Burkharts CA, Regl DL, Madafiglio J, Norris MD, Horwitz SB. 1995. Altered expression of Mβ2, the class II β-tubulin isotype, in a murine J774.2 cell line with a high level of taxol resistance. J Biol Chem 270: 31269-31275.

Hyams JS, Lloyd CW. 1994. The role of multiple tubulin isoforms in celular microtubule function. In: Raff E editor Microtubules. New York: John Wiley & Sons p 85-109.

Kaverina I, Rottner K, Small J V. 1998. Targeting, capture, and stabilization of microtubules at early focal adhesions. J Cell Biol 142:181-190.

Kaverina I, Krylyshkina O, Small J V. 1999. Microtubule targeting of substrate contacts promotes their relaxation and dissociation. J Cell Biol 146:1033-1043.

Keating T J, Peloquin J G, Rodionov V I, Momcilovic D, Borisy G G. 1997. Microtubule release from the centrosome. Proc Natl Acad Sci USA. 94: 5078-5083.

Kreitzer,G, Marmorstein A, Okamoto P, Vallee R, Rodriguez-Boulan E. 2000. Kinesin and Dynamin are required for post-golgi transport of plasma-membrane protein. Nature Cell Biol 02:125-127.

Ludueña R F. 1993. Are tubulin isotypes functionally significant. Mol Biol Cell 4: 445-457.

Ludueña R F. 1998. Multiple forms of tubulin: Different gene products and covalents modifications. Int Rev Cytol 178:207-273.

Mandato CA, Benink H A, Bement W M. 2000. Microtubule-actomyosin interactions in cortical flow and cytokinesis. Cell Motil Cytoskeleton 45:87-92.

Manning-Cela R, Meraz M A, Hernandez M, Meza I. 1994. Actin mRNA levels and actin synthesis during the encystation of *Entamoeba invadens*. J Euk Microbiol 41:360-365.

Marja J A H, Van-Zeijl, V, Matlin K S. 1990. Microtubule perturbation inhibits intracellular transport of apical membrane glycoprotein in a substrate-dependent manner in polarized Madin-Darby canine kidney epithelial cells. Cell Regul 1: 921-936.

Meads T, Schroer T A. 1995. Polarity and nucleation of microtubules in polarized epithelial cells. Cell Motil Cytoskeleton 32: 273-288.

Narishige T, Blade K L, Ishibashi Y, Nagai T, Hamawaki M, Menick D R, Kuppuswamy D, Cooper IV G. 1999. Cardiac hypertrophic and developmental regulation of the β-tubulin multigene family. J Biol Chem 274: 9692-9697.

Nobes C D, Hall A. 1999. Rho GTPases control polarity, protusion and adhesion during cell movement. J Cell Biol 144:1235-1244.

Ojakian G K, Schwimmer R. 1992. Antimicrotubule drugs inhibit the polarized insertion of an intracellular glycoprotein pool into the apical membrane of Madin-Darby canine kidney (MDCK) cells. J Cell Sci 103:677-687.

Panda D, Miller H P, Banerjee A, Ludueña R F, Wilson L. 1994. Microtubule dynamics *in vitro* are regulated by the tubulin isotype composition. Proc Natl Acad. Sci USA 91:11358-11362.

Pepperkok R, Bré M H, Davoust J, Kreis T E. 1990. Microtubules are stabilized in confluent epithelial cells but not in fibroblasts. J Cell Biol 111:3003-3012.

Raff E C, Fackenthal J D, Hutchens J A, Hoyle H D, Turner FR. 1997. Microtubule architecture specified by a β-tubulin isoform. Science 275:70-73.

Ranganathan S, Dexter D W, Benetatos C A, Chapman A E, Tew K D, Hudes G R. 1996. Increase of β III and βIVa tubulin isotypes in human prostate carcinoma cells as result of estramustine resistance. Cancer Res 56:2584-2589.

Ranganathan S, Benetatos C A, Colarusso P J, Dexter D W, Hudes G R. 1998. Altered β-tubulin isotype expression in paclitaxel-resistant human prostate carcinoma cells. Brit J Cancer 77:562-566.

Roach M C, Boucher V L, Walls C, Ravdin P M, Ludueña R F. 1998. Preparation of monoclonal antibody specific for the class I isotype of β tubulin: The β isotypes of tubulin differ in their cellular distributions within human tissues. Cell Motil Cytoskeleton 39:273-285.

Rodriguez-Boulan E, Nelson W J. 1989. Morphogenesis of the polarized epithelial cell phenotype. Science. 245:718-725.

Sisodia S S, Gay D A, Cleveland D W. 1990. *In vivo* discrimination among β-tubulin isotypes: selective degradation of a type IV β-tubulin isotype following overexpression in cultured animal cells. New Biologist 2:66-76.

Small J V, Kaverina I, Krylyshkina O, Rottner K. 1999. Cytoskeleton cross-talk during cell motility. FEBS letters 452:96-99.

Stanchi F, Corso V, Scannapieco P, Levolella C, Negrisolo E, Tiso N, Lanfranchi G, Valle G. 2000. TUBA 8: a new tissue-specific isoform of α-tubulin that is highly conserved in human and mouse. Biochem Biophys Res Comm 270: 1111-1118.

Sullivan K F, Cleveland D W. 1986. Identification of conserved isotype-defining variable region sequences for four vertebrate β tubulin polypeptide classes. Proc Natl Acad Sci USA 83: 4327-4331.

Sullivan K F. 1988. Structure and utilization of tubulin isotypes. Ann Rev Cell Biol 4:687-716.

Vasiliev J M. 1991. Polarization of pseudopodial activities: cytoskeletal mechanisms. J Cell Sci 98:1-4.

Wadsworth P, Bottaro D P. 1996. Microtubule dynamic turnover is suppressed during polarization and stimulated in hepatocyte growth factor scattered Madin-Darby canine kidney epithelial cells. Cell Motil Cytoskeleton 35:225-236.

Waterman-Storer CM, Salmon E D. 1999. Positive feedback interactions between microtubules and actin dynamics during cell motility. Curr Opin Cell Biol 11: 61-67.

Yeman C, Grindstaff KK, Nelson WJ. 1999. New prespectives on mechanisms involved in generating epithelial cell polarity. Physiol Rev 79:73-98.

Yen T J, Gay D A, Pachter J S, Cleveland D W. 1988. Autoregulated changes in stability of polyribosome-bound β-tubulin mRNAs are specified by the first 13 translated nucleotides. Mol Cell Biol 8:1224-1235.

FIGURE LEGENDS

Fig 1. Expression of tubulin isotypes βI, βII, βIV in MDCK cells. Fluorograph of an immunoblot using specific antibodies against tubulin isotypes: βI (lane 1), βII (lane 2) and βIV (lane 3). Anti-actin antibody was used as an internal standard to normalize protein concentration in each lane.

Fig 2. Distribution of tubulin isotypes in isolated and confluent MDCK cells as seen by confocal microscopy. βI was stained with the FITC-labeled antibody and β II with the corresponding rhodamine-tagged antibody. Distribution of βI (a) and βII in an isolated cell (b). Merge of images a and b (c), lateral view (d). Distribution of βI (e) and βII (f) in confluent cells. Merge of images e and f (g). Bar = 20 μm.

Fig 3. Expression of CHO βI tubulin in transfected MDCK cells. Fluorograph of a representative immunoblot using the anti-HA antibody and anti-actin for protein normalization . Cell extracts were prepared from mock cells and the three different clones. Mock (lane1), clone 39-7 (lane 2), clone 17-2 (lane 3), clone 2-26 (lane 4). Lane 5 is an overexposure of lane 4 to see the band corresponding to the exogenous βI tubulin being expressed in clone 2-26.

Fig 4. Distribution of the exogenous βI tubulin in cells from the different clones. Immunofluorescence with anti-HA tagged with FITC, observed by confocal microscopy, mock (a), clone 17-2 (b), 39-7 (c), 2-26 (d) Bar = 10 μm

Fig 5. Levels of polymerized and soluble βI tubulin (endogenous and exogenous) in clone 17-2 and mock cells. A) Fluorographies of immunoblots using anti-HA antibody to detect exogenous βI tubulin, anti βI tubulin antibody to detect endogenous βI tubulin and

anti-actin as protein internal standard. Cells were cultivated for 2, 6 and 24 h. Clone 17-2 (lanes 1-2), mock cells (lanes 3-4). Soluble fraction (1,3), polymerized fraction (2,4). B) Over-expression of total βI tubulin in clone 17-2, in which the total βI tubulin (endogenous and exogenous) from cells in clone 17-2 were compared with polymerized and soluble tubulin in mock cells at different times of culture. C) Levels of polymerized βI tubulin in clone 17-2 and mock cells. D) Levels of soluble βI tubulin in clone 17-2 and mock cells. Densitometric values represent the values from 3 different experiments. The levels of protein are expressed in arbitrary optical density units (ODU). * Statistical significant difference $p<0.001$.

Fig 6. Adhesion rates of transfected and mock cells. The percentage of adhesion of cells from the different clones was measured at different times of culture. Cells were plated in 24-well culture dishes, fixed at the indicated times and stained with methylene blue. The dye was removed with 300 ul of HCL and quantified in an ELISA plate reader at 630 nm. Values represent 3 different experiments done by triplicate.

Fig 7. Spreading of transfected and mock cells. Plated cells were analyzed for the presence of lamellae and microtubular networks using anti-total β tubulin tagged with FITC to visualize microtubules and rhodamine-phalloidin to visualize actin filaments. Clone 17-2 (a-f), mock cells (a'-f') observed at 2 h (a, d, a', d'), 6 h (b, e, b', e') and 24h of culture (c, f, c', f'). Bar = 20 μm

Fig 8. Focal adhesion sites of transfected and mock cells. Adhesion sites were visualized with an antibody against vinculin tagged with FITC. Clone 17-2 (a-c), mock cells (a-c'). 2h (a, a'), 6h (b, b') and 24h of culture (c, c'). Arrowheads point to the adhesion sites. Bar = 20μm

Table I. Morphometric measurements of mock and 17-2 cells at different culture times

Culture time	2h		6h		24h	
	L. axis μm	Area μm²	L. axis μm	Area μm²	L. axisμm	Area μm²
mock	41 ± 2	926 ± 81	76 ± 5	3405 ± 172	115 ± 14	7014 ± 393
17-2	20 ± 1	313 ± 34	44 ± 5	1625 ± 170	117 ± 17	6823 ± 420

L. axis = Longest axis

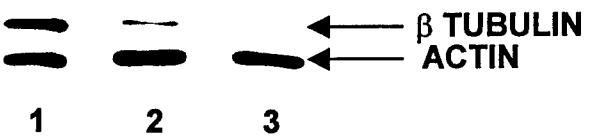

Figure 1

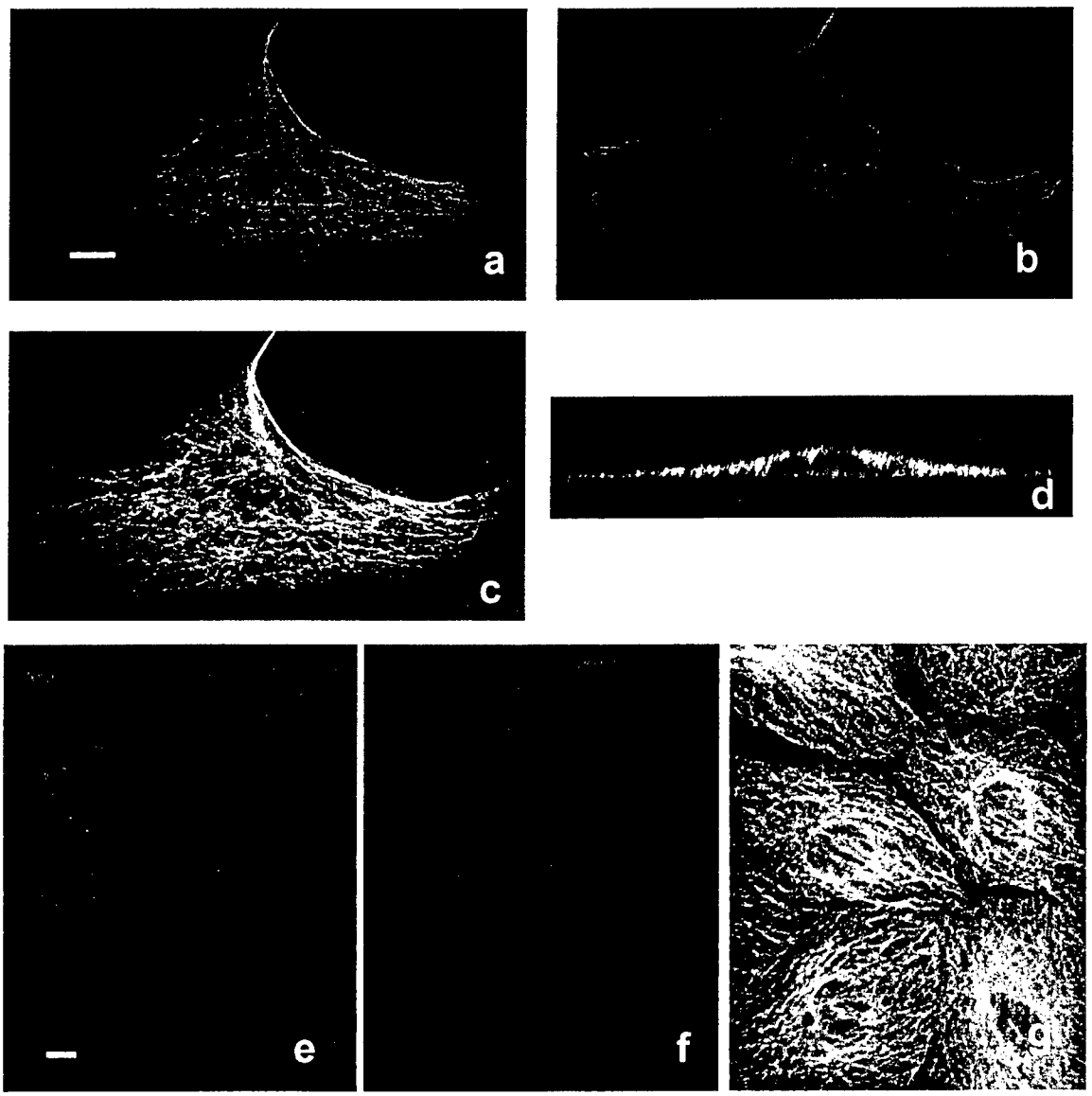

Figure 2

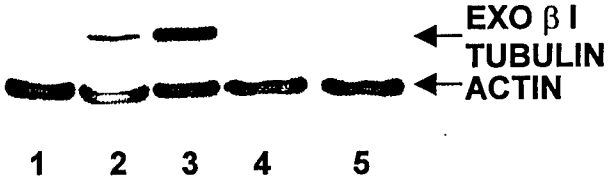

Figure 3

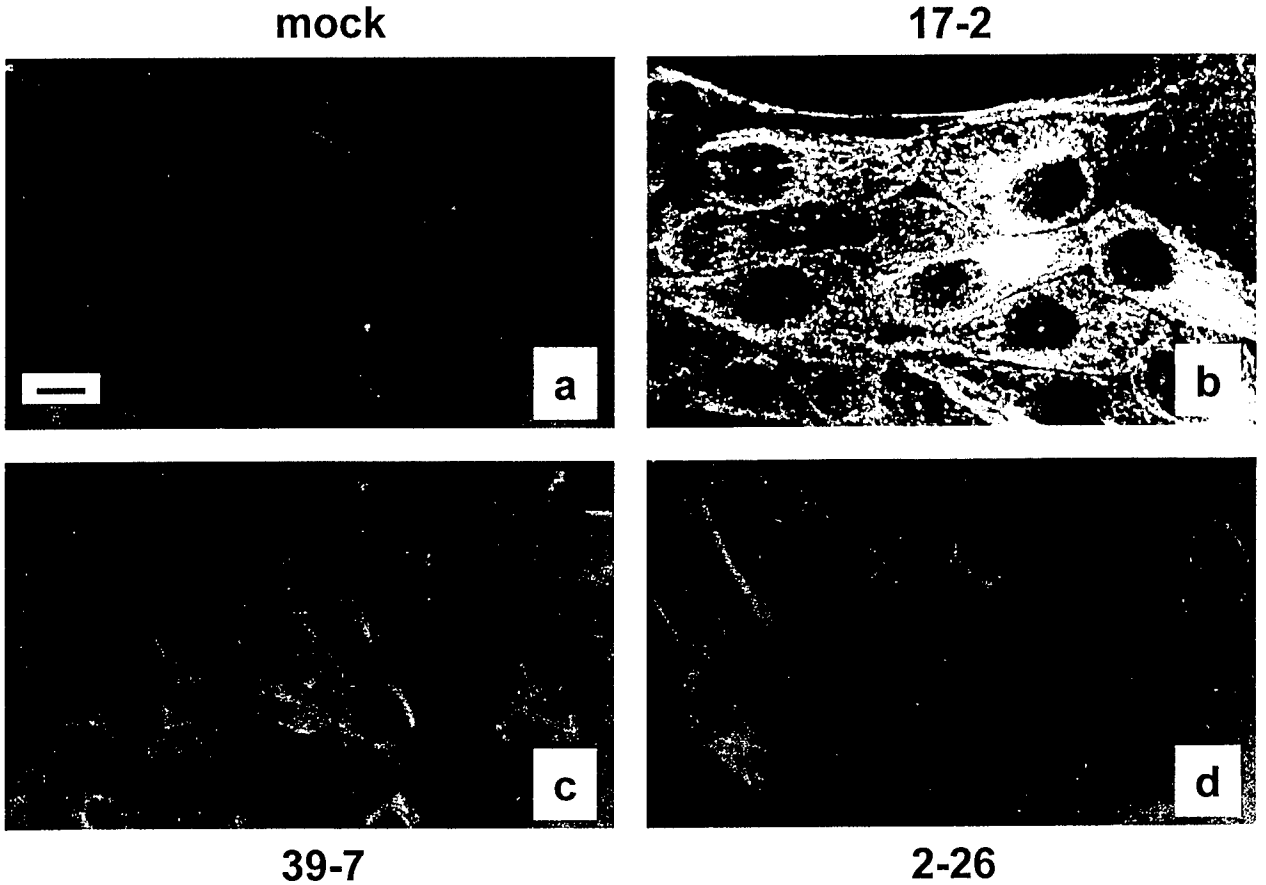

Figure 4

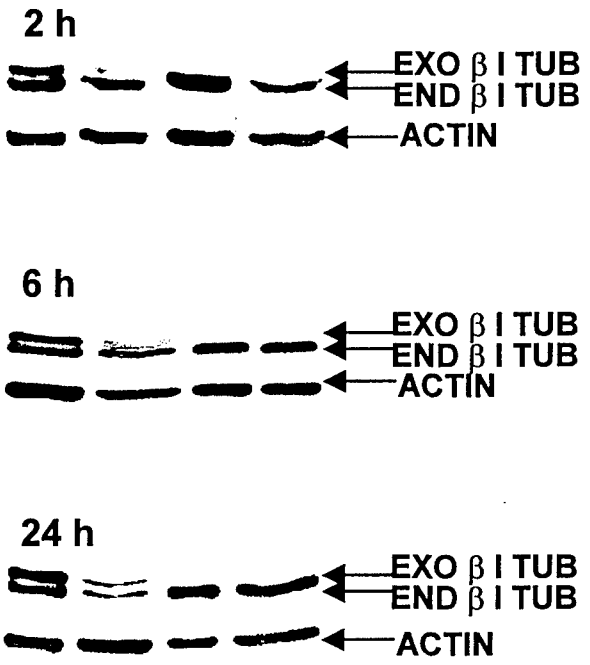
2 h
EXO β I TUB
END β I TUB
ACTIN
6 h
EXO β I TUB
END β I TUB
ACTIN
24 h
EXO β I TUB
END β I TUB
ACTIN
1 2 3 4
sol pol sol pol
clone 17- 2 mock

Figure 5A

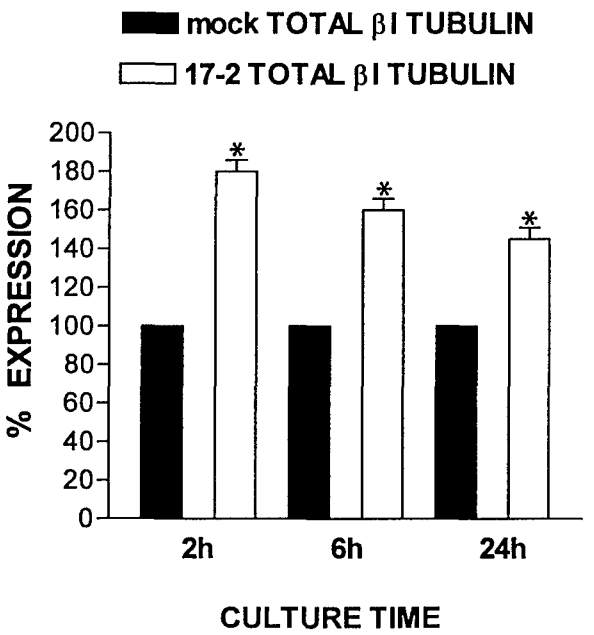
mock TOTAL βI TUBULIN
17-2 TOTAL βI TUBULIN
% EXPRESSION
200
180
160
140
120
100
80
60
40
20
0
*
*
*
2h
6h
24h
CULTURE TIME

Figure 5B

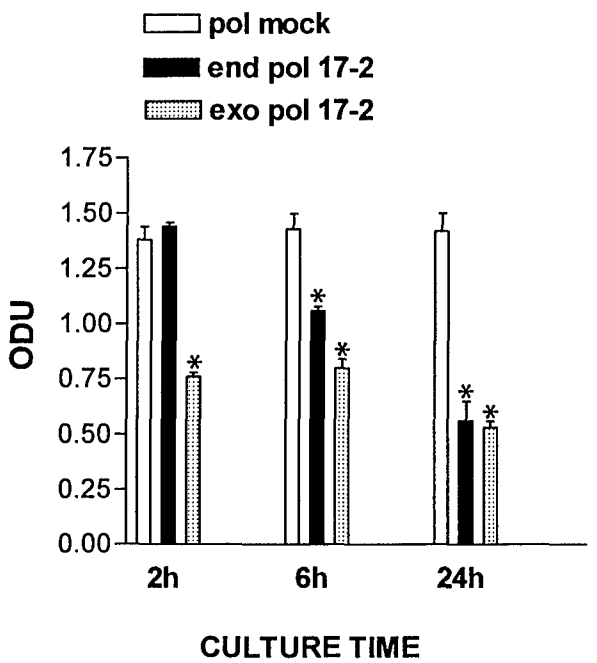

Figure 5C Lezama et al.

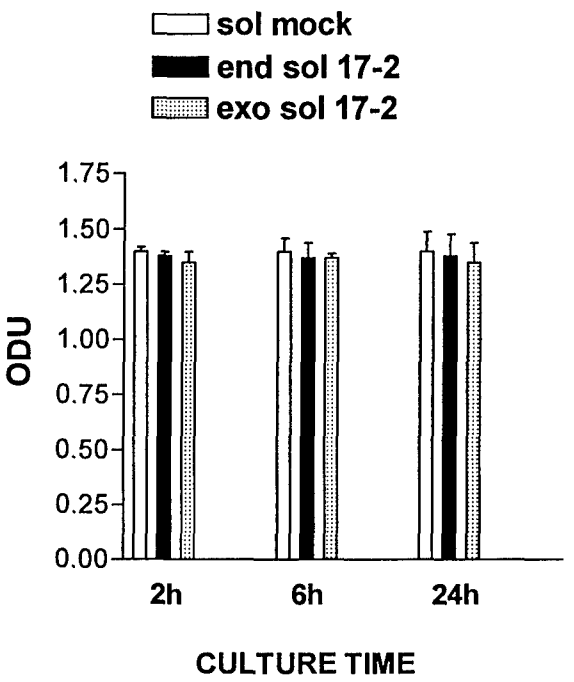
sol mock
end sol 17-2
exo sol 17-2
1.75
1.50
1.25
1.00
0.75
0.50
0.25
0.00
ODU
2h
6h
24h
CULTURE TIME

Figure 5D

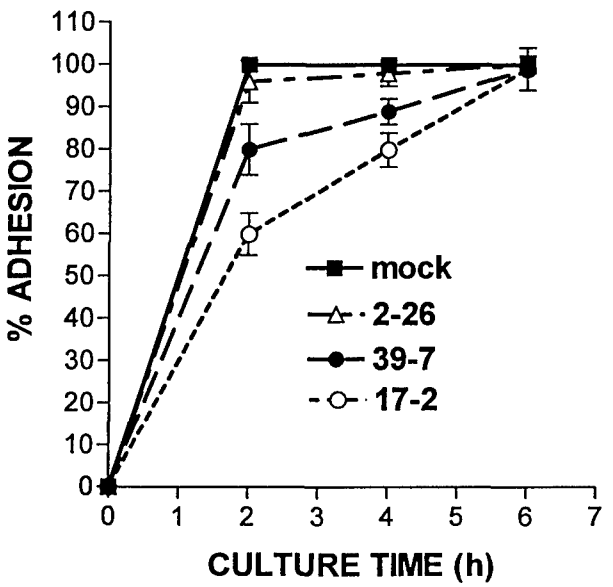
% ADHESION
110
100
90
80
70
60
50
40
30
20
10
0
0
1
2
3
4
5
6
7
CULTURE TIME (h)
mock
2-26
39-7
17-2

Figure 6

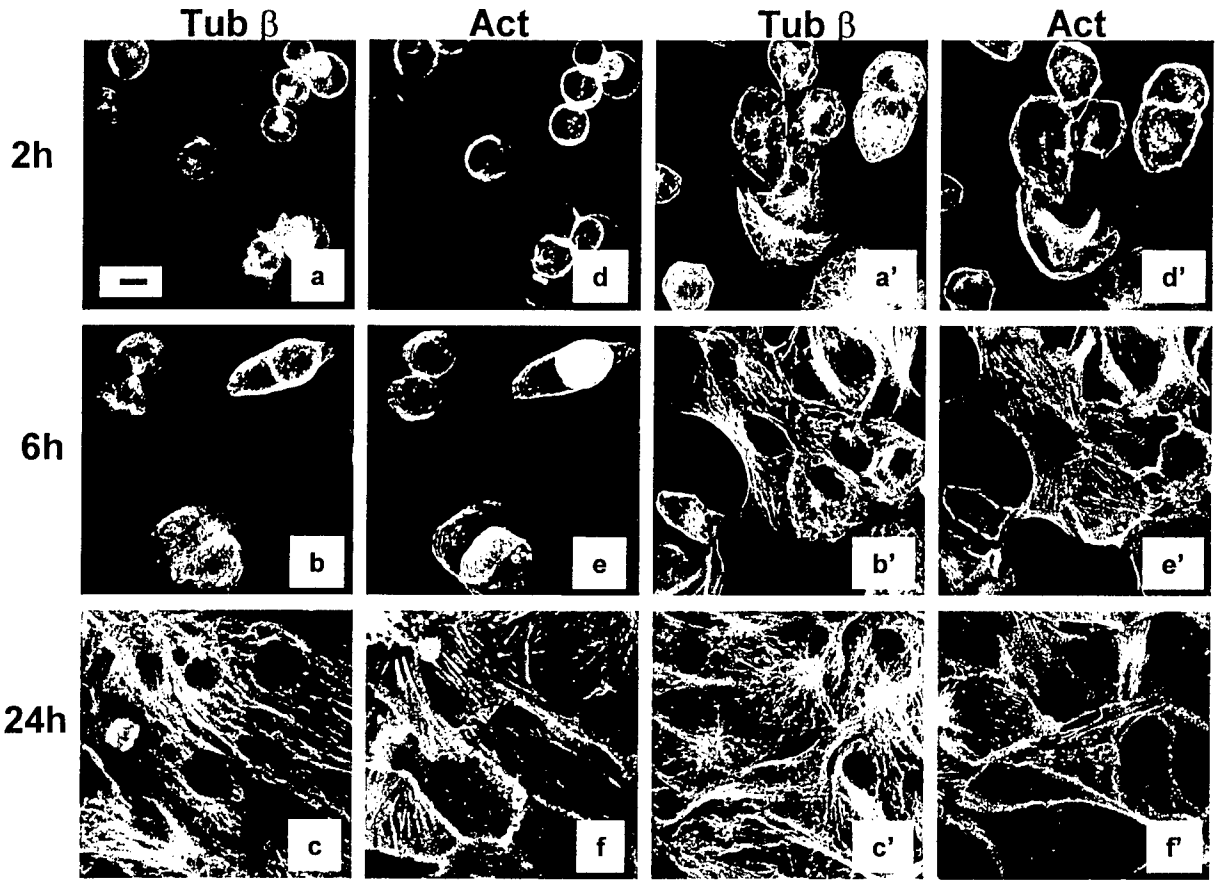

Figure 7

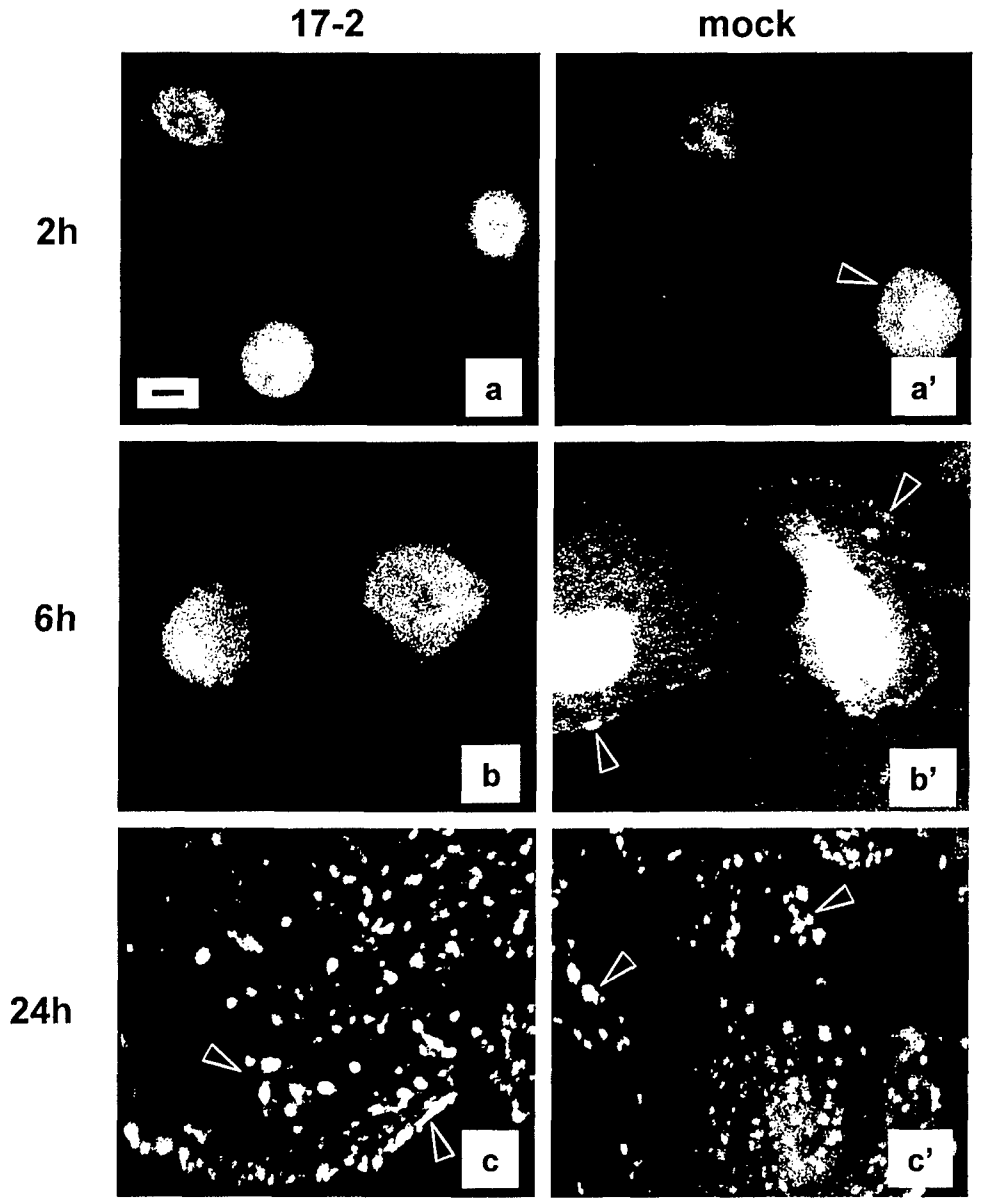

Figure 8

DIFFERENT EFFECTS OF VINBLASTINE ON THE POLYMERIZATION OF ISOTYPICALLY PURIFIED TUBULINS FROM BOVINE BRAIN[†]

Israr A. Khan[‡] and Richard F. Ludueña*

Department of Biochemistry, University of Texas Health Science Center at San Antonio, TX 78229-3900.

[†]Supported by grants CA26376 and HL07446 from the National Institutes of Health, DAMD17-98-1-8246 from the U.S. Army Medical Research and Materiel Command and AQ-0726 from the Welch Foundation.

Keywords: Tubulin/ Tubulin Isotypes/ Microtubules/ Vinblastine

Running title: Interaction of tubulin isotypes with vinblastine.

**Address for Correspondence:*

Dr. Richard F. Ludueña

Department of Biochemistry: Mail Code 7760

U.T. Health Science Center

7703 Floyd Curl Drive

San Antonio, TX 78229-3900

Phone: (210) 567-3732 Fax: (210) 567-6595 E-mail: luduena@UTHSCSA.edu

Present address: Alpha Diagnostics International, 5415 Lost Lane, San Antonio, TX 78238

[1]Abbreviations used are: EDTA, Ethylenediminetetraacetic acid; EGTA, ethylene glycol-bis(βaminoethyl ether)-N',N',N',N'-tetraacetic acid; GTP, guanosine 5'-triphosphate; MES, 2-(N-morpholino) ethanesulfonic acid; PBS, phosphate-buffered saline (0.01 M Na phosphate, pH 7.0, 0.15 M NaCl, 0.01 M EDTA); MAP2, microtubule associated protein-2.

ABSTRACT

Vinblastine, a highly successful anti-tumor drug, targets the tubulin molecule. Tubulin, the subunit protein of microtubules, consists of an α- and a β-subunit. Both α and β consist of numerous isotypes, encoded by different genes. We have purified three isotypes of bovine brain tubulin namely, $\alpha\beta_{II}$, $\alpha\beta_{III}$, and $\alpha\beta_{IV}$. Microtubule Associated Protein-2 (MAP2) and Tau-induced assembly of these isotypes were compared in the presence and absence of the vinblastine. MAP2-induced assembly of unfractionated tubulin and all the isotypes except $\alpha\beta_{II}$ tubulin was resistant to 1 μM vinblastine. Vinblastine at low concentrations (<10 μM) progressively inhibited the assembly of $\alpha\beta_{II}$, $\alpha\beta_{III}$ and $\alpha\beta_{IV}$ isotypes but the vinblastine concentration required for inhibition of MAP2 assembly varied from one isotype to another, being minimal for $\alpha\beta_{II}$. Moreover, the assembly of $\alpha\beta_{III}$ but not of $\alpha\beta_{II}$ or $\alpha\beta_{IV}$ could be completely inhibited by low concentrations of vinblastine before any detectable vinblastine-induced aggregation of the tubulin-MAP2 complex was evident. The tau-induced assembly of unfractionated and $\alpha\beta_{III}$ were equally sensitive to 1 μM vinblastine whereas $\alpha\beta_{II}$ and $\alpha\beta_{IV}$ were much more sensitive to vinblastine. The microtubules obtained in the presence of tau from unfractionated tubulin, $\alpha\beta_{II}$, and $\alpha\beta_{IV}$ could be easily aggregated by 20 μM vinblastine whereas such an aggregation of microtubules obtained from $\alpha\beta_{III}$ and tau required approximately 40 μM vinblastine. Electron microscopy of steady state polymers obtained from unfractionated, $\alpha\beta_{II}$, $\alpha\beta_{III}$ and $\alpha\beta_{IV}$ tubulins revealed that at low vinblastine concentrations microtubules were formed when the assembly was induced by MAP2, however, polymers formed from $\alpha\beta_{II}$ also included bundles of protofilaments. In the case of tau-induced assembly polymers obtained from unfractionated, $\alpha\beta_{II}$ and $\alpha\beta_{IV}$ included microtubules and spirals whereas $\alpha\beta_{III}$ produced clusters

of protofilaments. Our results indicate that among the tubulin isotypes, $\alpha\beta_{II}$ is the most sensitive to vinblastine while $\alpha\beta_{III}$ is the most resistant and this intrinsic resistance of $\alpha\beta_{III}$ dimers persists in the polymeric form of $\alpha\beta_{III}$ tubulin as well.

INTRODUCTION

Microtubules are long cylindrical organelles playing critical roles in a variety of processes such as mitosis, axonal transport and axonemal motility (1). The major constituent of microtubules is the 100 kDa protein tubulin, which is a heterodimer consisting of two polypeptide chains designated α and β (1,2). Both α- and β-tubulins exist in several isotypic forms (3). *In vitro* characterization of these dimers has indicated that properties of microtubules are strongly influenced by the isotypic composition of the constituent β-tubulin. For example, the intrinsic dynamicity of microtubules that is a critical regulator of their function both *in vivo* and *in vitro* (4,5) has been shown to be affected dramatically by the isotypic composition of tubulin (6). Our previous studies have clearly demonstrated that shortening rates of microtubules composed of purified β–tubulin isotypes are less sensitive to taxol than the microtubules assembled from unfractionated tubulin (7). The fact that different isotypes assemble into microtubules at different rates (8,9) could be one of the factors affecting the dynamic behavior of microtubules. However, it is not known how the dynamicity and the relative stability of microtubules composed of segregated isotypes are related *in vivo* but the stability of different microtubules is often reflected in their *in vitro* sensitivity to various tubulin/microtubule binding drugs (7,10-13). Recently (10), we have demonstrated that the antimitotic compound IKP-104 inhibits the assembly of $\alpha\beta_{II}$ dimers more than that of $\alpha\beta_{III}$ and $\alpha\beta_{IV}$ dimers and that high concentrations of IKP-104 induce formation of spiral aggregates from $\alpha\beta_{II}$ and $\alpha\beta_{III}$ but not from $\alpha\beta_{IV}$. On the other hand, the $\alpha\beta_{III}$ dimer interacts much less strongly with colchicine, and taxol than do the $\alpha\beta_{II}$ and $\alpha\beta_{IV}$ dimers (7,14). Also, the incorporation of estramustine into the $\alpha\beta_{III}$ isotype of tubulin occurs with a reduced efficiency compared to that of the other isotypes (12).

Among various anti-tubulin agents, vinblastine, a dimeric indole alkaloid derived from *Catharanthus (Vinca) roseus*, is of special interest because of its widespread use as an antimitotic drug in cancer therapy. It is thought that vinblastine exerts its antimitotic activity by disrupting the functions of microtubules. The vinblastine-induced inhibition of microtubule-function requires a direct interaction of the drug with tubulin and/or the microtubules. At low concentrations (0.2-1 μM), vinblastine acts as a suppresser of microtubule dynamic instability by binding at both ends of microtubules and thus increasing the time spent in the attenuated state (15,16). At intermediate concentrations, vinblastine acts as an inhibitor of microtubule assembly or promoter of disassembly both *in vitro* and in cells. At concentrations >1 μM it depolymerizes the microtubules by inducing the splaying and peeling of their protofilaments, presumably by interacting with low affinity sites along the microtubule surface (17,18). At higher concentrations (>5-10 μM) vinblastine induces formation of paracrystals and other aggregates composed of tubulin complexed with vinblastine (19-25). In previous studies the effect of vinblastine was tested on unfractionated tubulin which is a complex mixture of a number of isotypes. In the present study we have investigated the interaction of 1 to 20 μM vinblastine with isotypically pure tubulins, namely $\alpha\beta_{II}$, $\alpha\beta_{III}$ and $\alpha\beta_{IV}$. Furthermore we have used two different microtubule associated proteins (MAPs), namely, MAP2 and tau, to dissect the responses of different isotypes to vinblastine in the presence of MAPs. Our results suggest that, of the various tubulin dimers, polymerization of $\alpha\beta_{II}$ is the most sensitive and that of $\alpha\beta_{III}$ the least sensitive to vinblastine.

MATERIALS AND METHODS

Purification of tubulin isotypes. Microtubules, MAP2 and tau were prepared from bovine cerebra and tubulin purified from the microtubules by phosphocellulose chromatography following the procedure of Fellous *et al.* (26). The isotypically purified $\alpha\beta_{II}$, $\alpha\beta_{III}$ and $\alpha\beta_{IV}$ tubulin dimers were prepared as described previously (27). All isotypically purified tubulins were stored at -80 °C until ready for use. The MAP2- or tau-induced assembly and electron microscopy of the polymers obtained were studied using the same batch of the tubulin isotypes. The sedimentation and turbidimetric measurements on assembly of isotypically pure tubulins were performed by using two different batches of tubulin isotypes. At a fixed tubulin concentration, the net amount of polymers obtained from several different batches of untreated isotypes varied from 0 to 20%.

Tubulin polymerization. Tubulin was thawed on ice water and spun at 18,000 x *g* for 6 minutes at 4 °C to remove any insoluble tubulin aggregates from the sample. Tubulin present in the supernatant was quantitated by the method of Lowry *et al.* (28) and mixed with vinblastine and MAP2 or tau in Mes buffer (0.1 M 2-(*N*-morpholino)ethanesulfonic acid, 1 mM GTP, 0.5 mM $MgCl_2$, 0.1 mM EDTA, 1 mM EGTA, 1 mM β-mercaptoethanol, pH 6.4) at 4 °C. Unless otherwise mentioned, the final concentrations of tubulin, MAP2 and tau were 1.5, 0.3 and 0.15 mg/mL, respectively. The temperature of the samples was raised from 4 to 37 °C and the tubulin polymerization was followed by either of the following two methods (27). (A) *Sedimentation.* Aliquots (100 µl) were withdrawn at various time intervals and centrifuged for 4 minutes in the Beckman airfuge at 175,000 x *g*. The polymer concentration in the pellets was measured by first solubilizing the pellet in a final volume of 100 µl of 0.05 N NaOH and then quantitating the total

protein in the sample by the method of Lowry et al. (28). (B) *Turbidimetry*. The polymerization of tubulin was followed by measuring the change in turbidity at 350 nm on either a Beckman DU7400 or Gilford 250 spectrophotometer. The assembly profiles presented in this study are one of at least two representative experiments performed under identical conditions.

Electron microscopy. The mixtures of tubulin, MAP2 or tau were incubated for at least 30 minutes at 37 °C in the presence or absence of the indicated amount of vinblastine sulfate (Sigma Chemical Co., St. Louis, MO). 50 µl aliquots were withdrawn and treated with 1 % glutaraldehyde for 30 seconds, and then layered on 400-mesh carbon over formavar-coated copper grids. After 1 minute the grids were washed with 4 drops of water and stained with 1% uranyl acetate for 1 minute. Excess stain was removed and, after air-drying, grids were examined in a Phillips 300 electron microscope with an operating voltage of 60 kV (10).

RESULTS

Effect of vinblastine on the polymerization of tubulin isotypes in the presence of MAP2. The turbidimetric measurements on the MAP2-induced assembly of unfractionated tubulin and $\alpha\beta_{II}$ are shown in Figures 1A and B. Compared to unfractionated tubulin, which appeared to be insensitive to 1 μM vinblastine, $\alpha\beta_{II}$ tubulin lost almost one third of its ability to polymerize into microtubules. However, the polymerization of $\alpha\beta_{III}$ and $\alpha\beta_{IV}$ was not affected by 1 μM vinblastine. In fact, a slight increase of approximately 3% was observed in the case of unfractionated tubulin and $\alpha\beta_{IV}$ (Figures 1A and 1D). The morphology of the polymers obtained from various forms of tubulin in the presence and absence of 1 μM vinblastine is shown in Figs 2A-D. In the presence of 1 μM vinblastine, microtubules of apparently normal appearance were obtained from unfractionated tubulin and isotypically pure dimers (Figs. 2A2, 2B2 bottom, 2C2 and 2D2); however, in the case of $\alpha\beta_{II}$, polymers also included bundles of protofilaments (Fig. 2B2 top).

The addition of 20 μM of vinblastine to the assembly mixture prior to the initiation of assembly caused a gradual increase in the turbidity of the sample (Figs. 1A-D). Similarly, addition of 20 μM vinblastine to preformed microtubules resulted in the depolymerization of microtubules as reflected in a decrease in absorbance at 350 nm (Figures 1A-D). This greatly exceeded the decrease expected from the 6.7 % dilution of the sample. The turbidity obtained in the presence of vinblastine reflected formation of spirals in the case of unfractionated tubulin (Fig. 2A3) and $\alpha\beta_{IV}$ (Fig. 2D3); for $\alpha\beta_{II}$, addition of vinblastine led to formation of a protofilamentous structure resembling a spiral (Fig. 2B3). In the case of $\alpha\beta_{III}$, bundles of protofilaments were the dominant structures (Fig. 2C3).

It is evident from the above data that vinblastine at substoichiometric concentrations (1 μM) caused incomplete inhibition of microtubule assembly whereas at high concentrations (20 μM) it caused depolymerization of microtubules and complete inhibition of microtubule assembly. We considered it important to measure the effect of intermediate concentrations of vinblastine on the polymerization of various tubulin dimers and the results of this experiment are shown in Figures 3A-D. The effect of vinblastine on microtubule assembly could be dissected into two parts. First, at lower concentrations (<10 μM), vinblastine inhibited the MAP-induced formation of microtubules from unfractionated and isotypically pure tubulins. This effect of the drug accounts for almost complete inhibition of the polymerization of $\alpha\beta_{III}$ tubulin by 5 μM vinblastine. Second, at higher concentrations of the drug, the depolymerization of microtubules (if any) and the aggregation of tubulin takes place. It should be noted that in the absence of vinblastine and irrespective of the method used to study the polymerization of tubulin, the extent of MAP-induced polymerization of unfractionated tubulin and the isotypes varied from each other. For example, the concentration of polymer mass, as measured by sedimentation, for $\alpha\beta_{II}$, unfractionated tubulin, $\alpha\beta_{III}$ and $\alpha\beta_{IV}$ were 0.41, 0.21, 0.19 and 0.11 mg/mL, respectively (Figures 3A-D). Similarly, the approximate absorbance values, obtained by turbidimetry, for the steady state microtubules obtained from for $\alpha\beta_{II}$, unfractionated tubulin, $\alpha\beta_{III}$ and $\alpha\beta_{IV}$ were 0.23, 0.15, 0;19 and 0.16, respectively (Figures 1A-D). From the above results, it is evident that polymerization of tubulin is more extensive in the case of $\alpha\beta_{II}$ than in either unfractionated tubulin or the other isotypes. It is therefore not surprising that in comparison to unfractionated tubulin or the other isotypes, $\alpha\beta_{II}$ is more sensitive to vinblastine. It is interesting to note that the concentration of vinblastine required for half-maximal inhibition of MAP2-induced assembly

was lowest for $\alpha\beta_{II}$ and highest for unfractionated tubulin (Table 1); this is consistent with the data obtained by turbidimetry (Figures 1A-D). The maximal yield of polymer obtained in the presence of high concentrations of vinblastine varied greatly depending on the isotype composition of the tubulin. $\alpha\beta_{II}$ gave the highest yield (0.74 mg/mL) followed by unfractionated tubulin (0.38 mg/mL), $\alpha\beta_{III}$ (0.33 mg/mL) and $\alpha\beta_{IV}$ (0.22 mg/mL), indicating that the aggregation is more extensive in the case of $\alpha\beta_{II}$ than in unfractionated tubulin or other isotypes. The apparent drug-induced aggregation of tubulin started in the range of vinblastine concentration where the drug caused maximum inhibition of tubulin polymerization (lowest point the curves shown in Figures 3A-D. At 20 μM, vinblastine formed approximately 0, 65, 25 and 52 % of the total aggregates of $\alpha\beta_{II}$, unfractionated tubulin, $\alpha\beta_{III}$ and $\alpha\beta_{IV}$, respectively (Figures 3A-D). This result supports the data of Figure 1 that in comparison to unfractionated tubulin, $\alpha\beta_{III}$ and $\alpha\beta_{IV}$, $\alpha\beta_{II}$ is more sensitive to vinblastine. This conclusion is also supported by the apparent IC_{50} values for aggregation of unfractionated tubulin, $\alpha\beta_{II}$, $\alpha\beta_{III}$ and $\alpha\beta_{IV}$ (Table 1).

Effect of vinblastine on the polymerization of tubulin isotypes in the presence of tau. In contrast to MAP2-induced assembly of unfractionated tubulin, which was resistant to 1μM vinblastine, tau-induced assembly was inhibited by almost 32% (Figure 4A). The isotypically pure tubulins were more sensitive to 1μM vinblastine than was unfractionated tubulin, and, among the isotypes, the polymerization of $\alpha\beta_{II}$ tubulin was most sensitive to 1 μM vinblastine (Figures 4A-D and Table 1). Addition of 20 μM vinblastine to microtubules preformed from unfractionated tubulin, $\alpha\beta_{II}$ and $\alpha\beta_{IV}$ resulted in depolymerization of microtubules initially; followed by rapid aggregation (Figures 4A, 4B and 4D). This phenomenon of rapid aggregation was not observed with either unfractionated or isotypically pure tubulins when the assembly was

induced by MAP2 (Figures 2A-D). The most striking difference among the isotypes was that $\alpha\beta_{III}$ did not aggregate even in the presence of 20 μM vinblastine (Figure 4C). However, aggregates of tau- induced microtubules appeared once the vinblastine concentration was raised to 40 μM or above (Figure 5). A tremendous aggregation was observed when 20 μM vinblastine was included in the assembly mixture prior to initiation of the tau-induced polymerization of unfractionated tubulin, $\alpha\beta_{II}$ and $\alpha\beta_{IV}$ (Figures 4A, 4B and 4D). Again in contrast, in the case of $\alpha\beta_{III}$, there was very little aggregation and the amount of aggregates was only 4% of the one produced in the presence of 50 μM vinblastine (Figures 4C and 5). Similar results were obtained when assembly was measured by sedimentation (Figure 7)..

The morphology of the tau-induced polymers obtained from tubulin in the presence and absence of vinblastine are shown in Figure 6. The polymers of tubulin obtained in the presence of 1 μM vinblastine included microtubules combined with other protofilamentous structures in the cases of unfractionated tubulin (Fig.6A2), $\alpha\beta_{II}$ (Fig.6B2) and $\alpha\beta_{IV}$ (Fig.6D2, *top* and *bottom*). In contrast, in the case of $\alpha\beta_{III}$ only bundles of protofilaments were observed (Fig. 6C2, *top* and *bottom*). The inclusion of higher amounts of the drug, e.g., 20 μM vinblastine, in the assembly mixture led to formation of only protofilamentous spirals in $\alpha\beta_{IV}$ (Fig.6D3), linear bundles in unfractionated tubulin (Fig. 6A3) and $\alpha\beta_{II}$ (Fig. 6B3, *top*) or other aggregates perhaps resembling spirals in $\alpha\beta_{II}$ (Fig. 6B3, *bottom*) and $\alpha\beta_{III}$ (Fig. 6C3). As shown in Figs. 4 and 5, irrespective of the presence of vinblastine in the polymerization mixture, the resultant tau-induced polymers could be depolymerized by 20-40 μM vinblastine.

As seen in Figure 7, the inhibition of tau-induced polymerization of unfractionated and isotypically pure tubulins was observed in the lower concentration range of vinblastine.

However, this range of vinblastine concentration for unfractionated tubulin, $\alpha\beta_{II}$ and $\alpha\beta_{IV}$ (1-5 μM vinblastine) was considerably lower than that required for $\alpha\beta_{III}$ (1-20 μM vinblastine). It is also interesting to note that, in the presence of 1 μM vinblastine, unfractionated tubulin, $\alpha\beta_{II}$, $\alpha\beta_{III}$ and $\alpha\beta_{IV}$ lost approximately 50%, 81%, 32% and 67%, respectively, of their ability to polymerize into microtubules (Figures 7A-D). This is consistent with the pattern of data obtained by turbidimetry (Table 1). Higher concentrations of vinblastine reveal a striking difference between $\alpha\beta_{III}$ on the one hand and $\alpha\beta_{II}$, $\alpha\beta_{IV}$ and unfractionated tubulin, on the other hand. For the latter three, the least polymer was obtained at 5 μM vinblastine, whereas for $\alpha\beta_{III}$, this occurred at 20 μM vinblastine. For the latter three, formation of non-microtubule aggregate in the presence of 20 μM vinblastine was much greater than microtubule assembly in the absence of vinblastine. In contrast, for $\alpha\beta_{III}$, this required 40 μM vinblastine. In conjunction with the fact that MAP2-induced assembly of $\alpha\beta_{II}$ isotype is most sensitive to 1 μM vinblastine (Table 1), the data of Figures 2 and 7 suggest that sensitivity of polymerization of tubulin to vinblastine-induced inhibition is influenced by the type of the tubulin as well as the nature of microtubule associated proteins.

The concentration of vinblastine required for half maximal inhibition of MAP2-induced assembly was lowest for $\alpha\beta_{II}$ tubulin and highest for unfractionated tubulin (Table I). However, $\alpha\beta_{IV}$ whose assembly appeared to have less sensitivity to vinblastine than did that of $\alpha\beta_{II}$ when MAP2 was used, exhibited a sensitivity to vinblastine similar to that of $\alpha\beta_{II}$ when tau was used (Table 1).

DISCUSSION

In the present study we found that vinblastine, at low concentrations, inhibited polymerization of tubulin and its isotypically pure forms into microtubules. At higher concentrations, the drug depolymerized microtubules and induced formation and aggregation of spirals. These observations are in agreement with the consensus on the presence of two types of vinblastine binding sites on tubulin. The first binding site is specific and strong, involving residues 175-213 on β-tubulin (29) and is probably responsible for the substoichiometric inhibition of microtubule assembly (30). There are two additional vinblastine-binding sites on tubulin that are weak, nonspecific and responsible for aggregation (29,31). Since MAPs are present *in vivo*, we considered it important to study the effect of vinblastine on tubulin in the presence of MAPs.

Our results indicate that the type of MAP used to induce tubulin polymerization affected the inhibition of this process by vinblastine. The inhibitory effect of vinblastine on MAP-induced assembly of tubulin may arise from a drug-induced conformational change in either tubulin itself or at the sites where the MAPs bind. Evidence for a structural change induced in tubulin by the drug has come from quenching of tubulin fluorescence, from changes in sulfhydryl reactivity and crosslinking, from altered proteolytic susceptibility, and from immunological reactivity (32-35). A direct interaction between vinblastine and MAPs has not been documented. Since the sites of interaction of vinblastine and MAP(s) on the tubulin molecule are distinct, it is likely that the drug-induced conformational change in tubulin itself is responsible for the substoichiometric inhibition of assembly (31). Since the binding of MAPs to the carboxyl terminal of tubulin influences and regulates both lateral and longitudinal interactions between

subunits in tubulin polymers, the drug-induced conformational change in tubulin can be influenced by the nature of the MAPs present in the assembly mixture. It is not surprising, therefore, that at substoichiometric concentrations of vinblastine, unfractionated tubulin was resistant to the drug when assembly was induced by MAP2. On the contrary, a 32% inhibition of the assembly was observed when its assembly was induced by tau instead of MAP2. This result is supported by previous findings that, in the presence of vinblastine, tau and MAP2 interact differently with tubulin (36). This would imply that the regions in the tubulin dimer where the majority of the vinblastine-induced changes occur might alter the subunit-subunit interactions and that the latter is propagated differently to the site(s) within the tubulin molecule where MAP2 and tau bind. By this interpretation, the substoichiometric inhibition of tubulin polymerization by vinblastine should not vary among the isotypes of tubulin, provided the conformations of all the forms of tubulin are identical. As discussed below, however, our results from the experiments with isotypically pure tubulin dimers differ significantly from these expectations.

Vinblastine, at low concentrations, had a very strong inhibitory effect on MAP2-induced assembly of $\alpha\beta_{II}$ whereas the assembly of the other isotypes was affected much less. This suggests that tubulin isotypes are structurally different from each other and therefore that the magnitude and the propagation of vinblastine-induced conformational change differs among the isotypes. A tubulin isotype with a relatively rigid conformation would be expected to be more resistant to vinblastine-induced inhibition of assembly. This conclusion is also supported by our observation that among the isotypes, $\alpha\beta_{II}$ dimers were found to be most sensitive to vinblastine when assembly was induced by either tau or MAP2. It is worth emphasizing that $\alpha\beta_{III}$, which

has a more rigid conformation than those of the other isotypes (37,38) was the least sensitive to low concentrations of vinblastine when assembly was induced by tau.

If the structural rigidity of tubulin isotypes is assumed to be directly related to their relative sensitivity to low concentrations of vinblastine, then polymers formed from a rigid isotype are likely to be most resistant to depolymerization and subsequent aggregation by high concentrations of the drug. As expected, in contrast to unfractionated tubulin, $\alpha\beta_{II}$ and $\alpha\beta_{IV}$, the polymers obtained from $\alpha\beta_{III}$ could not be aggregated by 20 μM vinblastine indicating that $\alpha\beta_{III}$, both in its dimeric and polymeric forms, is most resistant to vinblastine. A much higher concentration of vinblastine (~40-50 μM) was required to induce depolymerization and subsequent aggregation. This further supports our earlier conclusion that conformational stability and thus relative sensitivity of tubulin varies among the isotypes.

Both MAP2 and tau stimulated the vinblastine-induced aggregation of unfractionated, $\alpha\beta_{II}$ and $\alpha\beta_{IV}$ tubulins, but the aggregation was more evident in the case of tau. Similar enhancement of aggregation has been reported after the removal of the carboxyl terminals of tubulin (31). In the case of $\alpha\beta_{III}$, however, aggregation of tubulin dimers stimulated by tau in the presence of 20 μM vinblastine did not occur. This finding further substantiated our conclusion that among the isotypes, $\alpha\beta_{III}$ is most resistant to vinblastine.

Among all the forms of tubulin tested, only $\alpha\beta_{II}$ exhibited a significant loss in its ability to polymerize into microtubules when the assembly was stimulated by MAP2 in the presence of 1 μM vinblastine. The relatively higher sensitivity of $\alpha\beta_{II}$ was also evident from electron microscopy data. The polymers formed from $\alpha\beta_{II}$ included microtubules as well as a large population of other protofilament-based non-microtubule structures. In contrast, at this

concentration of vinblastine, only microtubules were seen with unfractionated tubulin, $\alpha\beta_{III}$ or $\alpha\beta_{IV}$. Similar abnormal structures were obtained in the case of $\alpha\beta_{III}$ but higher (20 μM) vinblastine concentrations were required. At these concentrations, however, other forms of tubulin generated spirals and aggregates. Since the aggregation is induced by binding of vinblastine to weak and nonspecific sites on tubulin, it appears that the affinity of these sites also varies among the isotypes. As described below, our results also provide evidence that isotypically pure tubulins are more sensitive to vinblastine than is unfractionated tubulin but at the same time are less prone to vinblastine-induced aggregation.

From the analysis of the morphology of the tau-induced polymers obtained in the presence of substoichiometric concentration of vinblastine it is clear that in the case of $\alpha\beta_{II}$ and $\alpha\beta_{IV}$, polymers include microtubules and other aggregates as well as spirals. In contrast, polymers obtained from $\alpha\beta_{III}$ include aggregates and bundles of protofilaments but not spirals. In the case of $\alpha\beta_{III}$ a small proportion of polymers included aggregates and spirals, but only at high (20 μM) concentrations of the drug, at which vinblastine interacts nonspecifically with weaker sites on the tubulin molecule.

Our results would appear to contradict those of Lobert *et al.* (11,39) who found no difference in the binding of vinblastine to the $\alpha\beta_{II}$ or $\alpha\beta_{III}$ dimers. They also observed that vinblastine promoted self-association of $\alpha\beta_{II}$ and $\alpha\beta_{III}$ to the same extent (11). Interestingly, they also found that vincristine, which is structurally very similar to vinblastine, enhanced self-association of $\alpha\beta_{II}$ better than it did that of $\alpha\beta_{III}$ (11). A major difference between the experiments of Lobert *et al.* (11,40) and ours, however, is that the self-association experiments described here were done in the presence of either MAP2 or tau while those of Lobert *et al.*

(11,39) were performed in the absence of MAPs. It is quite reasonable to postulate that the real difference among the isotypes involves only the regions on the tubulin molecule which transduce conformational effects between the vinblastine and the MAP binding sites. We already know that this region is exquisitely sensitive to temperature, as well as to the nature and integrity of the MAP (37,40,41).

In summary, our results indicate that $\alpha\beta_{II}$ is the most sensitive to vinblastine and that $\alpha\beta_{III}$ is the least sensitive. Since vinblastine is a major anti-tumor drug, our results raise the possibility that sensitivity and resistance of tumors to this drug can be modulated by the tubulin isotype composition of the microtubules in the tumor cell, as was previously postulated by Lobert *et al.* (11) to be the case for vincristine and as is apparently the case with taxol and estramustine (42-44). In the case of taxol, we have measured its effect on the dynamic behavior of microtubules formed from isotypically purified tubulin (7). To choose one parameter, the shortening rate of microtubules made from $\alpha\beta_{II}$ is 4.6-4.7 times more sensitive to taxol than is the case for microtubules made from $\alpha\beta_{III}$ or $\alpha\beta_{IV}$ (7). Consistent with this finding, tumors treated with taxol often respond by increasing their expression of $\alpha\beta_{III}$ and $\alpha\beta_{IV}$ (42,45). Future investigation may reveal whether a similar pattern occurs in tumors treated with vinblastine.

Acknowledgments: We are grateful to Drs. Asok Banerjee and Asish R. Chaudhury for their valuable suggestions. We thank Veena Prasad, Mohua Banerjee, Pat Schwarz and Alka Mittal for their help during the preparation of microtubules from bovine cerebra.

REFERENCES

1. Dustin, P. Microtubules, 2nd Ed., Berlin: Springer-Verlag, 1984.

2. Ludueña, R.F., Shooter, E.M., and Wilson, L. Structure of the tubulin dimer. J. Biol. Chem., *252*: 7006-7014, 1977.

3. Ludueña, R.F. Multiple forms of tubulin: different gene products and covalent modifications.

Int. Rev. Cytol., *178*: 207-275, 1998.

4. Wilson, L., and Jordan, M.A. *In*: J. S. Hyams, and C.W. Lloyd (eds.), Microtubules, pp. 59-83. New York: Wiley-Liss, 1994.

5. Wordeman, L., and Mitchison, T. *In*: J. S. Hyams, and C.W. Lloyd (eds.), Microtubules, pp. 287-301, New York: Wiley-Liss, 1994.

6. Panda, D., Miller, H.P., Banerjee, A., Ludueña, R.F. and Wilson, L. Microtubule dynamics *in vitro* are regulated by the tubulin isotype composition. Proc. Natl. Acad. Sci. USA, *91*: 11358-11362, 1994.

7. Derry, W.B., Wilson, L., Khan, I. A., Ludueña, R.F., and Jordan, M. A. Taxol differentially modulates the dynamics of microtubules assembled from unfractionated and purified β-tubulin isotypes. Biochemistry, *36*: 3554-3562, 1997.

8. Banerjee, A., Roach, M.C., Trcka, P. and Ludueña, R.F. Increased microtubule assembly in bovine brain tubulin lacking the type III isotype of β-tubulin. J. Biol. Chem,. *265*: 1794-1799, 1990.

9. Banerjee, A., Roach, M.C., Trcka, P., and Ludueña, R.F. Preparation of a monoclonal antibody specific for the class IV isotype of β-tubulin. Purification and assembly of $\alpha\beta_{II}$,

$\alpha\beta_{III}$, and $\alpha\beta_{IV}$ tubulin dimers from bovine brain. J. Biol. Chem., *267*: 5625-5630, 1992.

10. Khan, I. A., Tomita, I., Mizuhashi, F., and Ludueña, R.F. Differential interaction of tubulin isotypes with the antimitotic compound IKP-104. Biochemistry, *39*: 9001-9009, 2000.
11. Lobert, S., Frankfurter, A., and Correia, J. J. Energetics of Vinca alkaloid interactions with tubulin isotypes: implications for drug efficiency. Cell Motil. Cytoskeleton, *39*: 107-121, 1998.
12. Laing, N., Dahllöf, B., Hartley-Asp, B., Ranganathan, S., and Tew, K.D. Interaction of estramustine with tubulin isotypes. Biochemistry, *36*: 871-878, 1997.
13. Banerjee, A., and Ludueña, R.F. Distinct colchicine binding kinetics of bovine brain tubulin lacking the type III isotype of β-tubulin. J. Biol. Chem., *266*: 1689-1691, 1991.
14. Banerjee, A., and Ludueña, R. F. Kinetics of colchicine binding to purified β-tubulin isotypes from bovine brain. J. Biol. Chem., *267*: 13335-13339, 1992.
15. Toso, R.J., Jordan, M.A., Farrell, K.W., Matsumoto, B. & Wilson, L. Kinetic stabilization of microtubule dynamic instability *in vitro* by vinblastine. Biochemistry, *32*: 1285-1293, 1993.
16. Dhamodharan, P., Jordan, M. A., Thrower, D., Wilson, L., and Wadsworth, P. Vinblastine suppresses dynamics of individual microtubules in living interphase cells. Mol. Biol. Cell, *6*: 1215-1229, 1995.
17. Jordan, M.A., Margolis, R.L., Himes, R.H., and Wilson, L. Identification of a distinct class of vinblastine binding sites on microtubules. J. Mol. Biol., *187*: 61-73, 1986.

18. Singer, W.D., Jordan, M.A., Wilson, L., and Himes, R.H. Binding of vinblastine to stabilized

microtubules. Mol. Pharmacol,. *36*: 366-370, 1989.

19. Wilson, L., Jordan, M.A., Morse, A., and Margolis, R.L. Interaction of vinblastine with steady-state microtubules *in vitro*. J. Mol. Biol,. *159*: 125-149, 1982.

20. Hamel, E. Interactions of tubulin with small ligands. *In*: J. Avila, (ed.), Microtubule Proteins,

pp. 89-191, Boca Raton: CRC Press, 1990.

21. Bensch, K.G. and Malawista, S.E. Microtubular crystals in mammalian cells. J. Cell Biol., *40*: 95-107, 1969.

22. Warfield, R. K. N. and Bouck, G. B. Microtubule-macrotubule transition: intermediates after exposure to the mitotic inhibitor vinblastine. Science, *186*: 1219-1220, 1974.

23. Himes, R. H. Interaction of the catharanthus (*Vinca*) alkaloids with tubulin and microtubules.

Pharmac. Ther., *51*: 257-267,1991.

24. Schochet, S. S., Jr., Lambert, P.W., and Earle, K. M. Neuronal changes induced by intrathecal vincristine sulfate. J. Neuropathol. Exp. Neurol., *27*: 645-658, 1968.

25. Wilson, L., Morse, A. N. C., and Bryan, J. Characterization of *acetyl*-^{3}H-labeled vinblastine binding to vinblastine-tubulin crystals. J. Mol. Biol., *121*: 255-268, 1978.

26. Fellous, A., Francon, J., Lennon, A.-M., and Nunez, J. Microtubule assembly *in vitro*. Purification of assembly-promoting factor. Eur. J. Biochem., *78*: 167-174, 1977.

27. Khan, I.A., and Ludueña, R.F. Phosphorylation of β_{III}-tubulin. Biochemistry, *35*: 3704-3711,

1996.

28. Lowry, O.H., Rosebrough, N.H., Farr, A.L., and Randall, R.J. Protein measurement with the Folin phenol reagent. J. Biol. Chem., *193*: 265-275, 1951.

29. Rai, S.S. and Wolff, J. Localization of the vinblastine-binding site on β-tubulin. J. Biol. Chem., *271*: 14707-14711, 1996.

30. Timasheff, S.N., Andreu, J.M., and Na, G.C. Physical and spectroscopic methods for the evaluation of the interaction of antimitotic agents with tubulin. Pharmac. Ther., *52*: 191-210,

1991.

31. Correia J. J. Effects of antimitotic agents on tubulin-nucleotide interactions. Pharmac. Ther., *52*: 127-147, 1991.

32. Ludueña, R.F. and Roach, M.C. Tubulin sulfhydryl groups as probes and targets for antimitotic and antimicrotubule agents. Pharmac. Ther., *49*: 13-152, 1991.

33. Morgan, J.L. and Spooner, B.S. Immunological detection of microtubule poison-induced conformational changes in tubulin. J. Biol. Chem., *258*: 13127-13133, 1983.

34. Prakash, V., and Timasheff, S.N. The interaction of vincristine with calf brain tubulin. J. Biol. Chem., *258*: 1689-1697, 1983.

35. Lee, J.C., Harrison, D., and Timasheff, S. N. Interaction of vinblastine with calf brain microtubule protein. J. Biol. Chem., 250: 9276-9282, 1975.

36. Ludueña, R.F., Fellous, A., McManus, L., Jordan, M.A., and Nunez, J. Contrasting roles of tau and microtubule-associated protein 2 in the vinblastine-induced aggregation of brain tubulin. *J. Biol. Chem., 259*: 12890-12898, 1984.

37. Schwarz, P.M., Liggins, J.R. and Ludueña, R.F. β-Tubulin isotypes purified from bovine brain have different relative stabilities. Biochemistry, *37*: 4687-4692, 1998.

38. Banerjee, A., and Ludueña, R.F. Kinetics of colchicine binding to purified β-tubulin isotypes from bovine brain. J. Biol. Chem., *267*: 13335-13339, 1992.

39. Lobert, S., Frankfurter, A., and Correia, J.J. Binding of vinblastine to phosphocellulose-purified and αβ-class III tubulin: the role of nucleotides and β-tubulin isotypes. Biochemistry, *34*: 8050-8060, 1995.

40. Prasad, V., Jordan, M.A. and Ludueña, R.F. Temperature sensitivity of vinblastine-induced tubulin polymerization in the presence of microtubule-associated proteins. J. Prot. Chem., *11*:

509-515, 1992.

41. Fellous, A., Prasad, V., Ohayon, R., Jordan, M.A. and Ludueña, R.F. Removal of the projection domain of microtubule-associated protein 2 alters its interaction with tubulin. J. Prot. Chem., *13*: 381-391, 1994.

42. Ranganathan, S., Dexter, D.W., Benetatos, C.A., Chapman, A.E., Tew, K.D. and Hudes, G.R. Increase of β_{III} - and β_{IVa}-tubulin isotypes in human prostate carcinoma cells as a result of estramustine resistance. Cancer Res., *56*: 2584-2589, 1996.

43. Haber, M., Burkhart, C.A., Regl, D.L., Madafiglio, J., Norris, M.D., and Horwitz, S.B. Altered expression of Mβ2, the class II β-tubulin isotype, in a murine J774.2 cell line with a high level of taxol resistance. J. Biol. Chem., *270*: 31269-31275, 1995.

44. Dumontet, C., Duran, G.E., Steger, K.A., Beketic-Oreskòvic, L., and Sikic, B. I. Resistance mechanisms in human sarcoma mutants derived by single-step exposure to paclitaxel (taxol).

Cancer Res., *56*: 1091-1097, 1996.

45. Jaffrézou, J.P., Dumontet, C., Derry, W.B., Durán, G., Chen, G., Tsuchiya, E., Wilson, L., Jordan, M.A., and Sikic, B.I. Novel mechanism of resistance to paclitaxel (taxol) in human K562 leukemia cells by combined selection with PSC833. Oncol. Res., *7*: 517-527, 1995.

Table 1. Effect of vinblastine on the assembly of tubulin isotypes.

Tubulin	% Inhibition[a]		IC_{50}[b]		IC_{50}[c]
	Tau	MAP2	Tau	MAP2	MAP2
Unfractionated	32	(3)	1	3.8	52
$\alpha\beta_{II}$	89	29	0.6	0.5	17
$\alpha\beta_{III}$	31	3	2.1	1.8	33
$\alpha\beta_{IV}$	69	(3)	0.6	2	48

[a]Assembly was followed by measuring the turbidity of the samples at 350 nm. Inhibition of tau and MAP2-induced microtubule assembly of tubulins by vinblastine was calculated from the data in Figures 1 and 4. The figures in parenthesis represent increase in the assembly.

[b]Assembly of tubulin was induced by either MAP2 (Figures 1 and 3) or tau (Figures 4 and 7) in the presence of 0 to 200 μM vinblastine. Assembly was followed by sedimentation and the vinblastine concentration required for half-maximal inhibition was calculated from the plot of polymer concentration *vs.* vinblastine concentration. [c]The assembly of tubulin was induced by MAP2 in the presence of 0-200 μM vinblastine (Figures 3A-D). The polymer concentration at the onset of aggregation of unfractionated tubulin, $\alpha\beta_{II}$, $\alpha\beta_{III}$ and $\alpha\beta_{IV}$ were 0.17, 0.2, 0.025 and 0.075 mg/mL, respectively (Figures 3A-D). These values together with those for the maximum yield of polymer for unfractionated tubulin (0.38 mg/mL), $\alpha\beta_{II}$ (0.74 mg/mL), $\alpha\beta_{III}$ (0.33 mg/mL) and $\alpha\beta_{IV}$ (0.22 mg/mL) (Figures 3A-D) were used to calculate the IC50 for the vinblastine-induced aggregation.

FIGURE LEGENDS

Fig. 1. Effect of vinblastine on MAP2-induced assembly of unfractionated and isotypically purified tubulin isotypes. In each sample, tubulin (1.5 mg/mL) was incubated with MAP 2 (0.3 mg/mL) in the absence (●) or in the presence of vinblastine concentrations of either 1 μM (○) or 20 μM (▲). Assembly was followed by turbidimetry. The arrows represent addition of vinblastine (final concentration 20 μM) to the assembly mixture. Conditions were as described in "Materials and Methods". Samples were as follows: unfractionated tubulin (A), $\alpha\beta_{II}$ (B), $\alpha\beta_{III}$ (C) and $\alpha\beta_{IV}$ (D).

Figure 2. Effect of vinblastine on the morphology of the tubulin polymers. The assembly mixtures containing MAP2 and unfractionated tubulin (A), $\alpha\beta_{II}$ (B), $\alpha\beta_{III}$ (C) or $\alpha\beta_{IV}$ (D) were mixed with the indicated amount of vinblastine at 0 °C (panels 1-3 in Figures A-D). Assembly was initiated by warming the samples to 37 °C and the polymers formed were processed for electron microscopy. The magnifications of electron micrographs were as follows: **2A (1),** 132000; **2A (2)**, 264000; **2A (3),** 400000; **2B (1)**, 132000; **2B (2)** *top*, 264000; **2B (2)** *bottom*, 200000; **2B (3),** 400000; **2C (1)**, 400000; **2C (2),** 180180; **2C (3),** 132000; **2D (1)**, 132000; **2D (2)**, 264000; **2D (3)**, 200000.

Figure 3. Effect of 0-200 μM vinblastine on MAP2-induced assembly of unfractionated and isotypically pure tubulins. Assembly was followed by sedimentation. The arrows represent addition of vinblastine (final concentration 20 μM) to the assembly mixture. Samples were as follows: unfractionated tubulin (A), $\alpha\beta_{II}$ (B), $\alpha\beta_{III}$ (C) and $\alpha\beta_{IV}$ (D) tubulin.

Figure 4. Effect of vinblastine on tau-induced assembly of unfractionated and isotypically purified tubulins. In each sample, tubulin (1.5 mg/mL) was incubated with tau (0.15 mg/mL) in the absence (●) or in the presence of vinblastine concentrations of either 1 μM (○) or 20 μM (▲). Assembly was followed by turbidimetry. Samples were as follows: unfractionated tubulin (A), $\alpha\beta_{II}$ (B), $\alpha\beta_{III}$ (C) and $\alpha\beta_{IV}$ (D).

Figure 5. Effect of 40-50 μM vinblastine on the polymerization of $\alpha\beta_{III}$. Assembly was followed by turbidimetry and the depolymerization of microtubules at the steady state was induced by addition of vinblastine to a final concentration of either 40 μM (○) or 50 μM (●) (indicated by the arrows).

Figure 6. Effect of vinblastine on the morphology of tubulin polymers. The assembly mixtures containing tau and either unfractionated tubulin (A), $\alpha\beta_{II}$ (B), $\alpha\beta_{III}$ (C) or $\alpha\beta_{IV}$ (D) were mixed with indicated amount of vinblastine at 0 °C (panels 1-3 in Figures A-D). Assembly was initiated by warming the samples to 37 °C and the polymers formed were processed for electron microscopy. The magnifications of electron micrographs were as follows: **6A (1)**, 132000; **6A (2)**, 264000; **6A (3),** 132000; **6B (1)**, 132000; **6B (2)**, 132000; **6B (3),** 132000; **6C (1)**, 132000; **6C (2)**, *top* 520000; **6C (2)**, *bottom*, 264000; **6C (3),** 520000; **6D (1)**, 99000; **6D (2)**, *top* 200000; **6D (2)**, *bottom*, 400000; **6D (3)**, 132000.

Figure 7. Effect of vinblastine on tau-induced assembly of unfractionated and isotypically

purified tubulins. Samples of tubulin (1.5 mg/mL) were incubated at 37 °C in the presence of tau (0.15 mg/mL) with the indicated concentrations of vinblastine. Samples were as follows: unfractionated tubulin (A), $\alpha\beta_{II}$ (B), $\alpha\beta_{III}$ (C) and $\alpha\beta_{IV}$ (D). Assembly was followed by sedimentation.

(1988) *J. Biol. Chem.* 263, 3029-3034.

Alexander, J.E., Hunt, D.F., Lee, M.K., Shabanowitz, J., Michel. H., Berlin, S.C., Macdonald, T.L., Swedberg, R. J., Rebhun, L.I., and Frankfurter, A. (1991) *Proc. Nat. Acad. Sci. U.S.A* 88, 4685-4689.

Banerjee, A., Roach, M.C., Wall, K.A., Lopata, M.A., Cleveland, D.W., and Ludueña, R.F.

Bhattacharyya, B., and Wolff, J. (1974) *Biochemistry* 13, 2364-2369.

Boucher, D., Larcher, J-C., Gross, F., and Denoulet, P. (1994) *Biochemistry* 33, 12471- 12477.

Burns, R.G., and Surridge, C. (1990) *FEBS Lett.* 271, 1-8.

Bylund, D.B., and Krebs, E.G. (1975) *J. Biol. Chem.* 250, 6355-6361.

Edd?, B., Rossier, J., Le Caer, J.-P., Desbruy res, E., Gros, F., and Denoulet, P. (1990) *Science* 247, 83-85.

Gard, D.L., and Kirschner, M.W. (1985) *J. Cell Biol.* 100, 764-774.

Gaskin, F., Cantor, C.R., and Shelanski, M.L.(1974) *J. Mol. Biol.* 89, 737-758.

Hsiao, H-J., Sandberg, A.R., and Li, H.C. (1978) *J. Biol. Chem.* 253, 6901-6907.

Khan, I. A., and Ludueña, R. F. (1994) *Mol. Biol. Cell* **5**, 284a

Khan, I. A., and Ludueña, R. F. (1995) *Mol. Biol. Cell* **6**, 30a

Khan, I.A., and Ludueña, R.F. (1990) *J. Cell Biol.* 111, 174a.

Khan, I.A., and Ludueña, R.F. (1991a) *J. Cell Biol.* 115, 383a.

Khan, I.A., and Ludueña, R.F. (1991b) *Biochim. Biophys. Acta* 1076, 289-297.

Khan, I.A., and Ludueña, R.F. (1992) *Molecular Biology of the Cell* 3, 49a

Kirschner, M.W., Suter, M., Weingarten, M., and Littman, D. (1975) *Ann. N.Y. Acad. Sci. U.S.A.* 253, 90-106.

Kotani, S., Kawai, G., Yokoyama, S., Murofushi, H. (1990) *Biochemistry* 29, 10049-10054.

Laemmli, U.K. (1970) *Nature (London)* 227, 680-685.

Little, M., and Seehaus, T. (1988) *Comp. Biochem. Physiol.* 90B, 655-670.

Lopata, M.A., and Cleveland, D.W. (1987) *J. Cell Biol.* 105, 1707-1720.

Ludueña, R.F., Roach, M.C., Trcka, P.P., Little, M., Palanivelu, P., Binkley, P., and Prasad, V. (1982) *Biochemistry* 21, 4787-4794.

Ludueña, R.F., Zimmermann, H.-P., and Little, M. (1988) *FEBS Lett.* 230, 142-146.

Raybin, D., and Flavin, M. (1977) *Biochemistry* 16, 2189-2194.

Reddington, M., and Lagnado, J.R. (1973) *FEBS Lett.* 30, 188-194.

Redeker, V., Melki, R., Prom?, D., Le Caer, J-P., and Rossier, J. (1992) *FEBS Lett.* 313, 185-192.

Roach, M.C., Trcka, P.P., Banerjee, A., and Ludueña, R.F. (1988) *J. Cell Biol.* 107, 22a.

Schwarz, P., Liggins, J. R., and Ludueña, R.F (1998) *Biochemistry* 37, 4687-4692.

Stephens, R.E. (1975) in *Molecules and Cell Movement* (Inoue, S., and Stephens, R. E., Eds.), pp 181-204, Raven Press, New York.

Suganuma, M., Fujiki, H., Okabes, S., Nishiwaki, S., Brautigan, D., Ingebritsen, T., and Rosner, M.R. (1992) *Toxicon.* 30, 873-878.

Sullivan, K.F. (1988) *Ann. Rev. Cell Biol.* 4, 687-716.

Sullivan, K.F., and Cleveland, D.W. (1986) *Proc. Nat. Acad. Sci. U.S.A.* 83, 4327-4331.

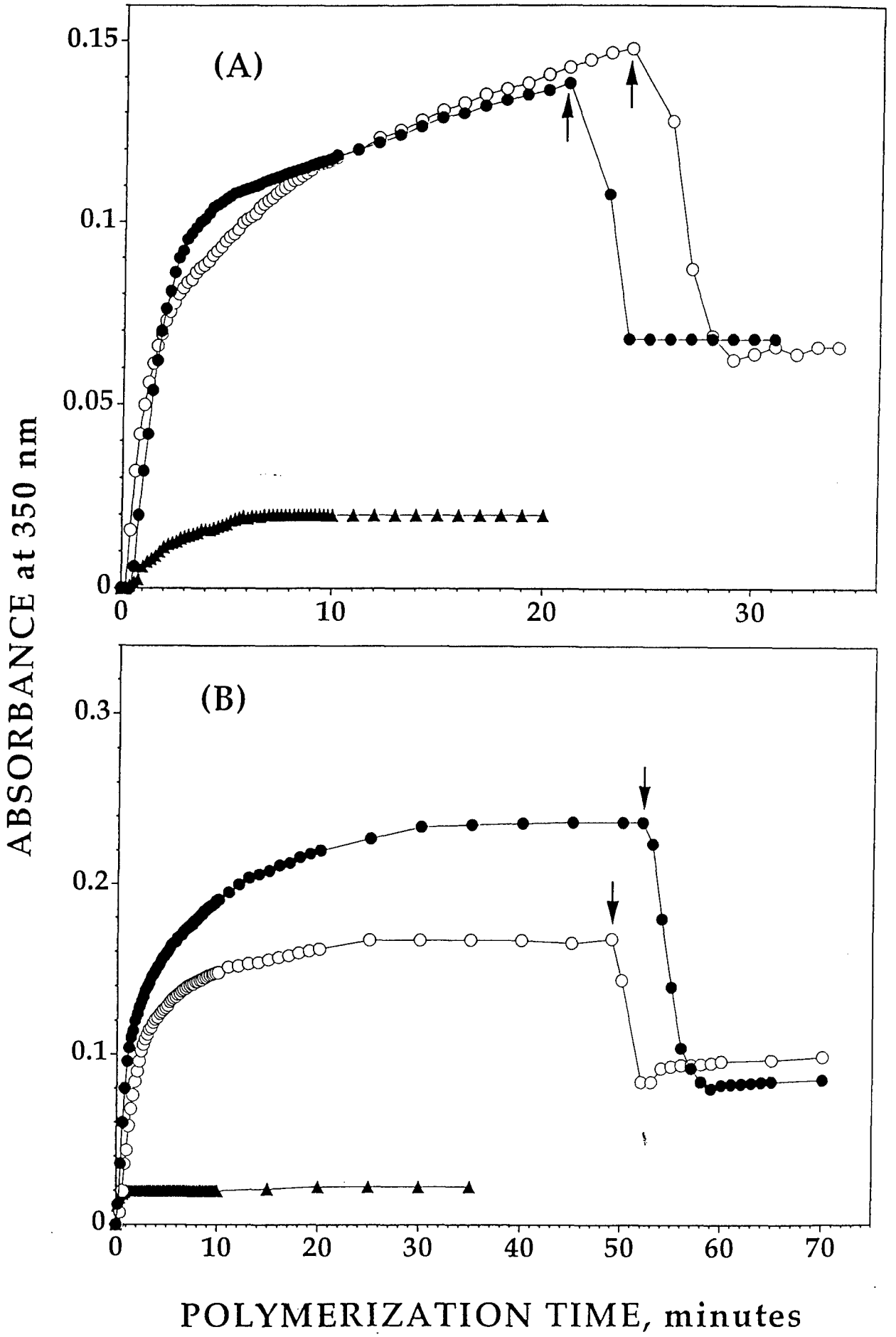

Figures 1A and 1B

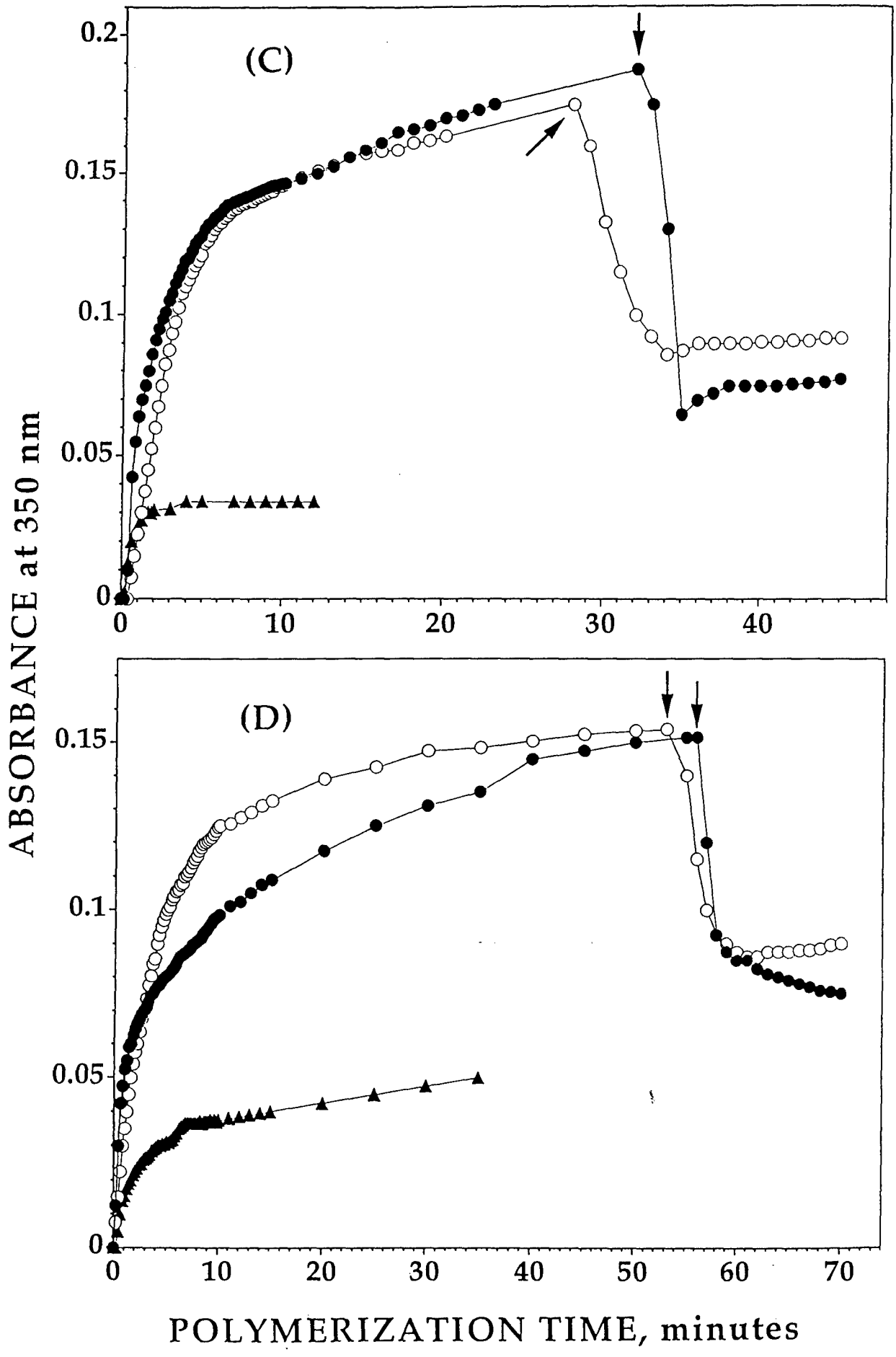

Figures 1C and 1D

(1). (PCT + 0 μM VBL + MAP2)

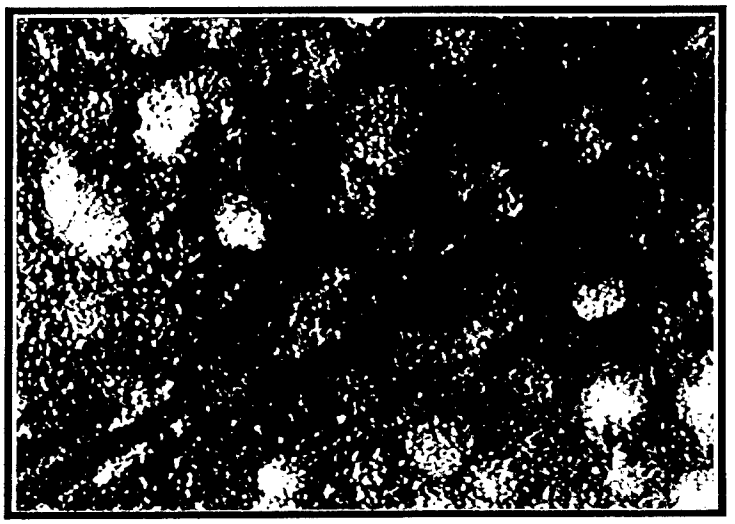

(2). (PCT + 1 μM VBL + MAP2)

(3). (PCT + 20 μM VBL + MAP2)

Figure 2A

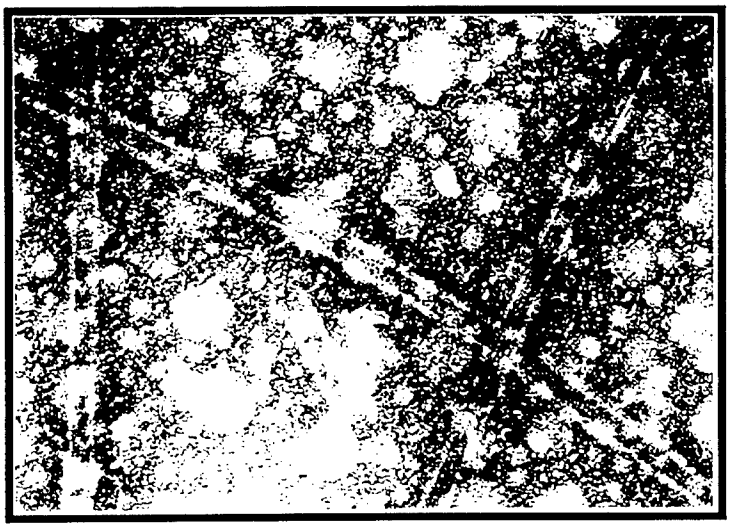

(1). ($\alpha\beta_{II}$ + 0 μM VBL + MAP2)

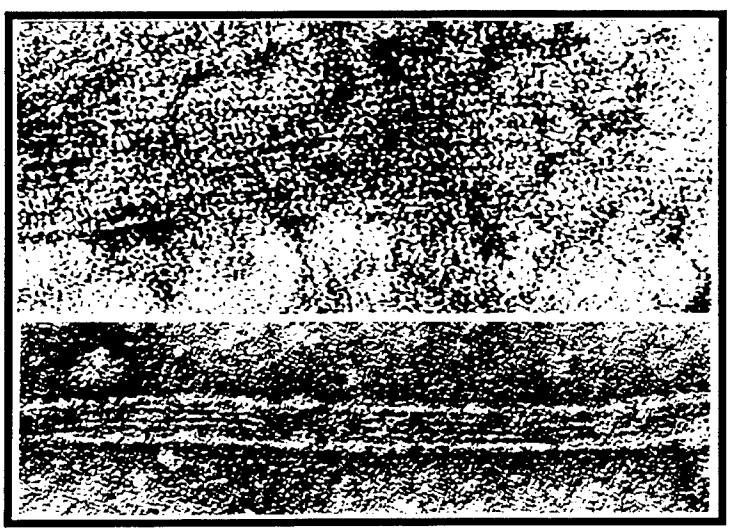

(2). ($\alpha\beta_{II}$ + 1 μM VBL + MAP2)

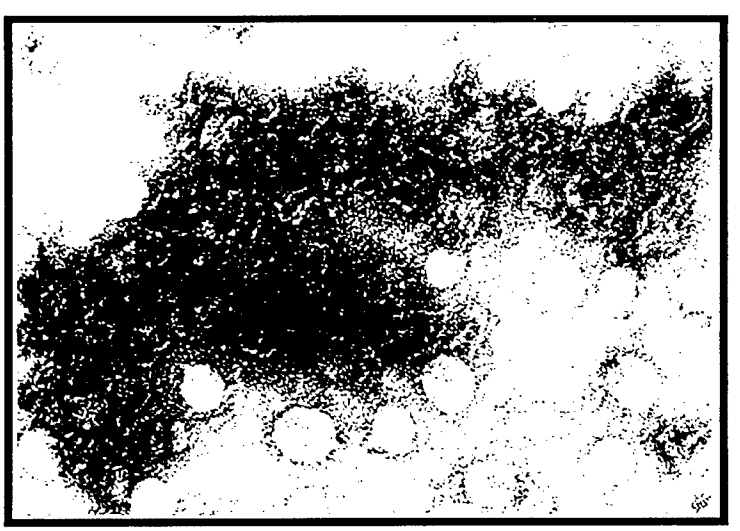

(3). ($\alpha\beta_{II}$ + 20 μM VBL + MAP2)

Figure 2B

(1). ($\alpha\beta_{III}$ + 0 μM VBL + MAP2)

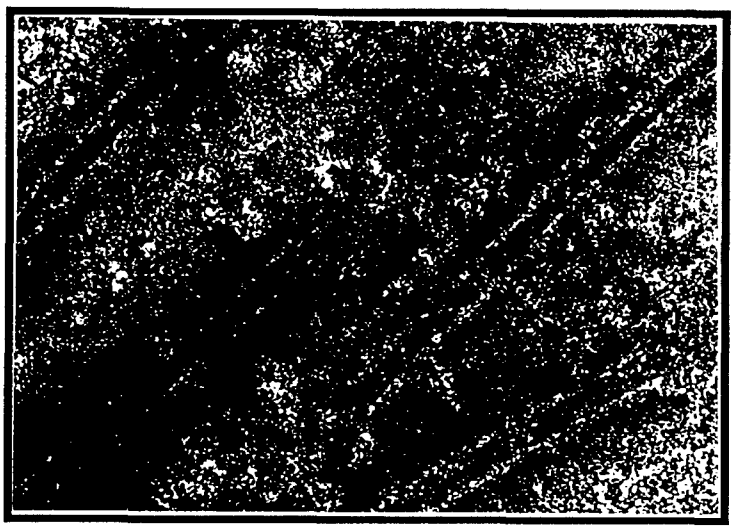

(2). ($\alpha\beta_{III}$ + 1 μM VBL + MAP2)

(3). ($\alpha\beta_{III}$ + 20 μM VBL + MAP2)

Figure 2C

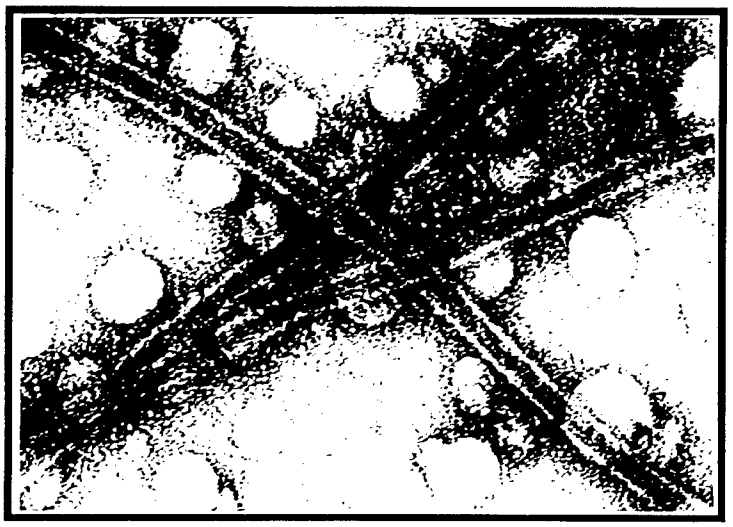

(1). ($\alpha\beta_{IV}$ + 0 μM VBL + MAP2)

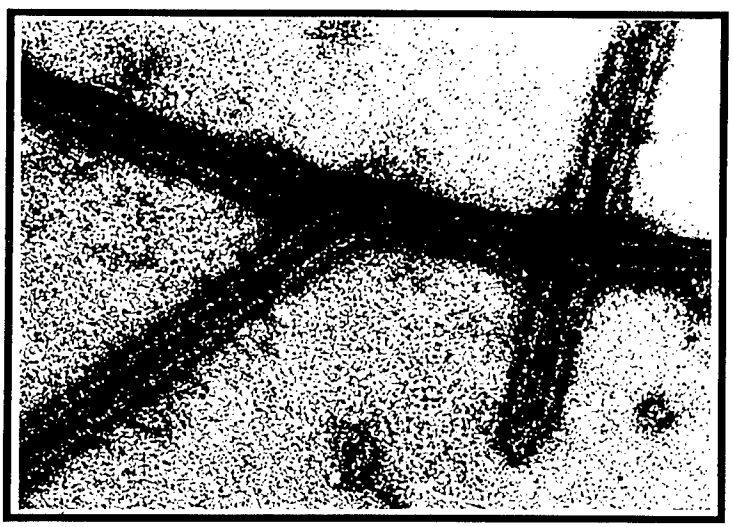

(2). ($\alpha\beta_{IV}$ + 1 μM VBL + MAP2)

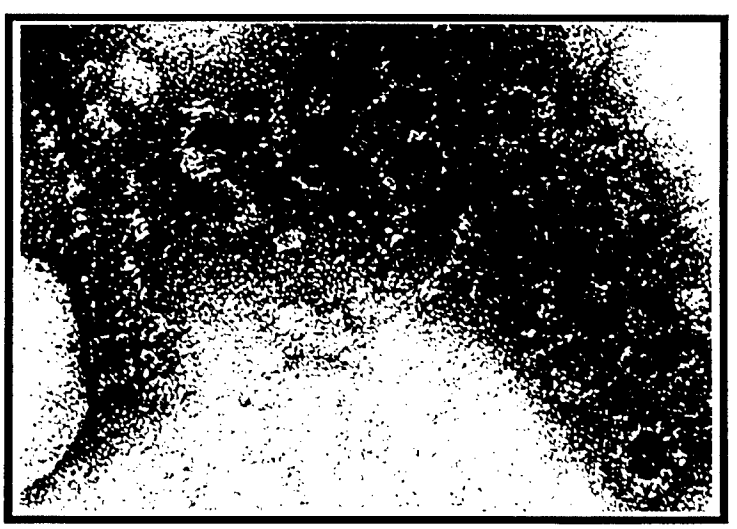

(3). ($\alpha\beta_{IV}$ + 20 μM VBL + MAP2)

Figure 2D

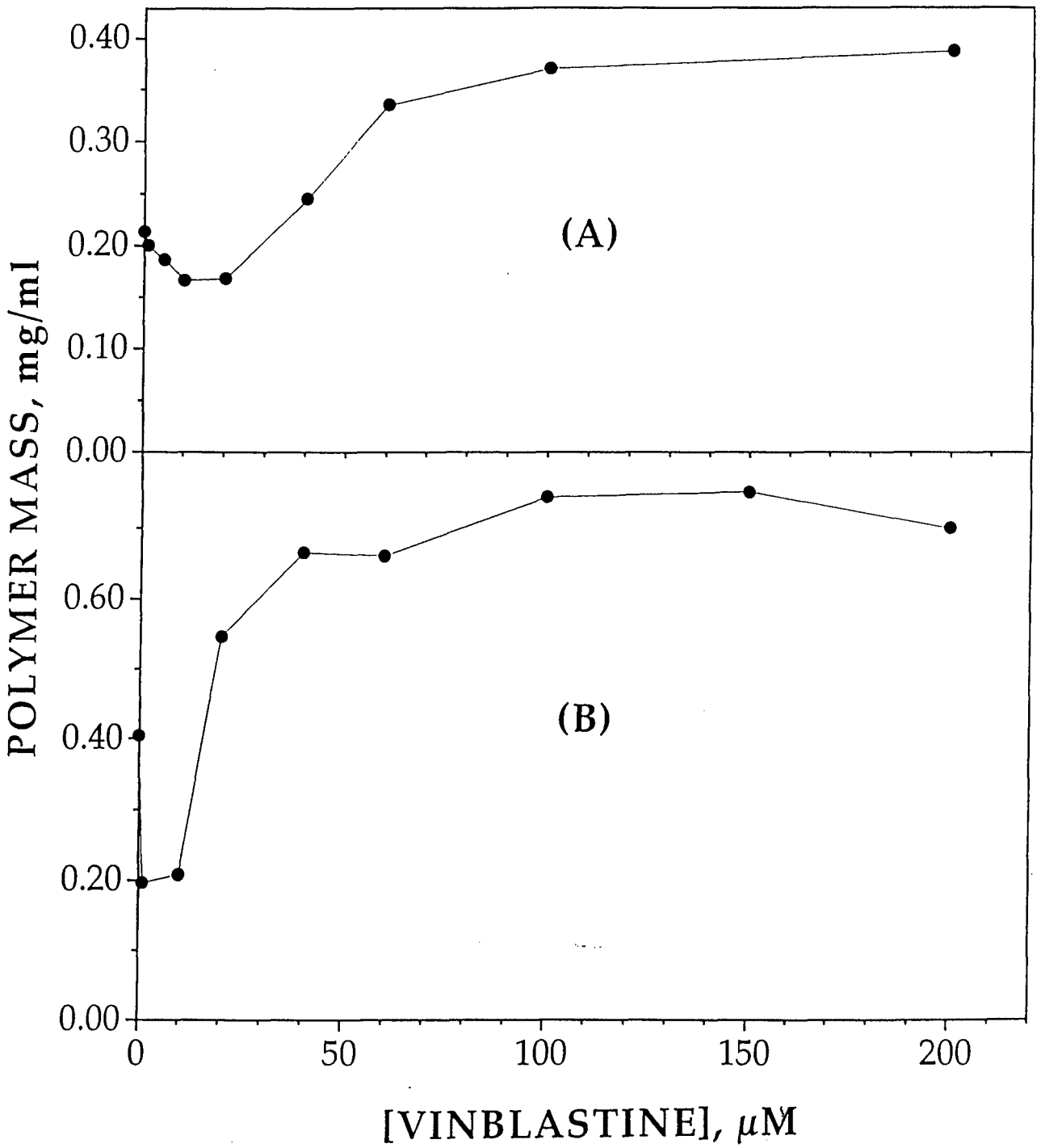

Figures 3A and 3B

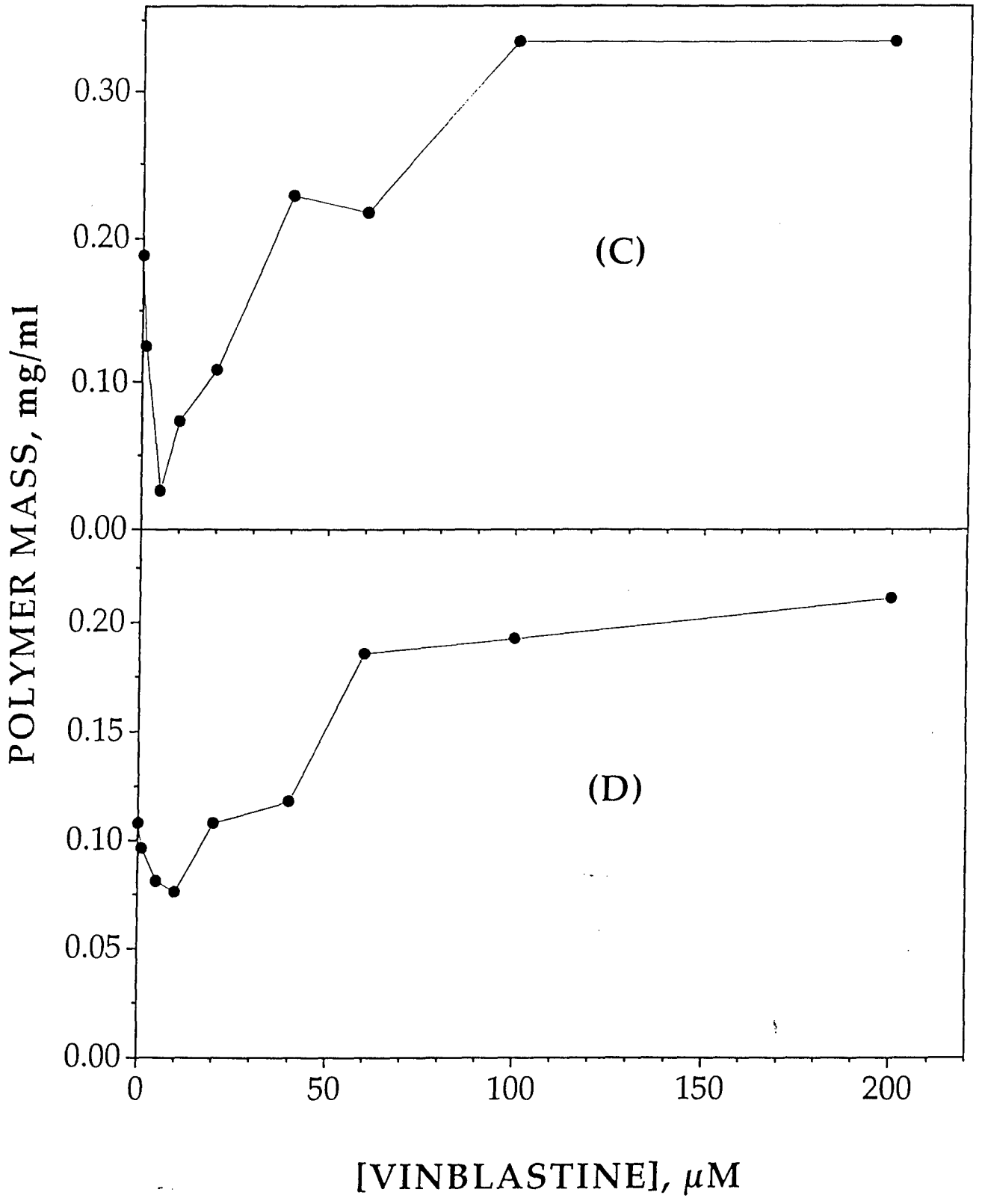

Figures 3C and 3D

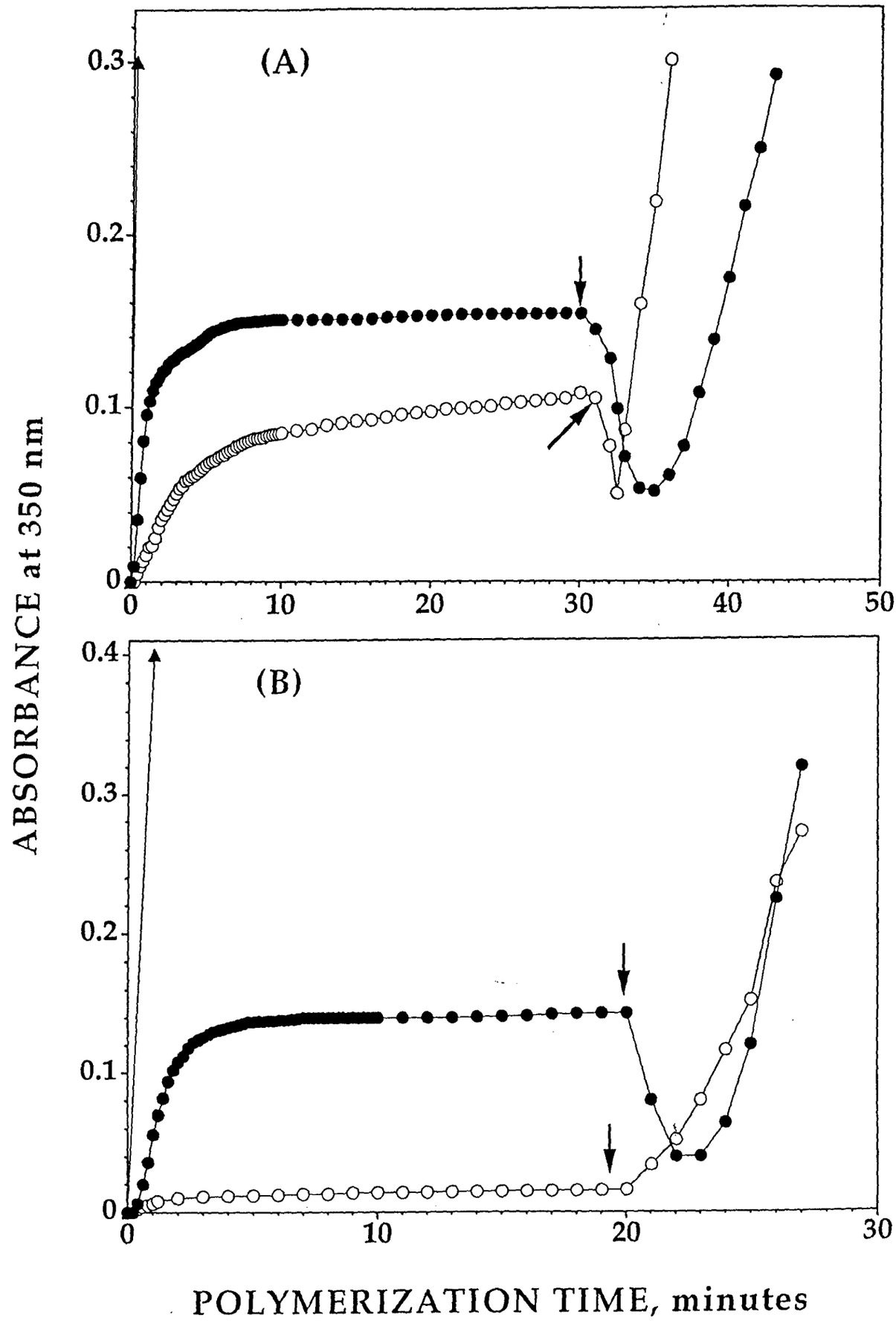

Figures 4A and 4B

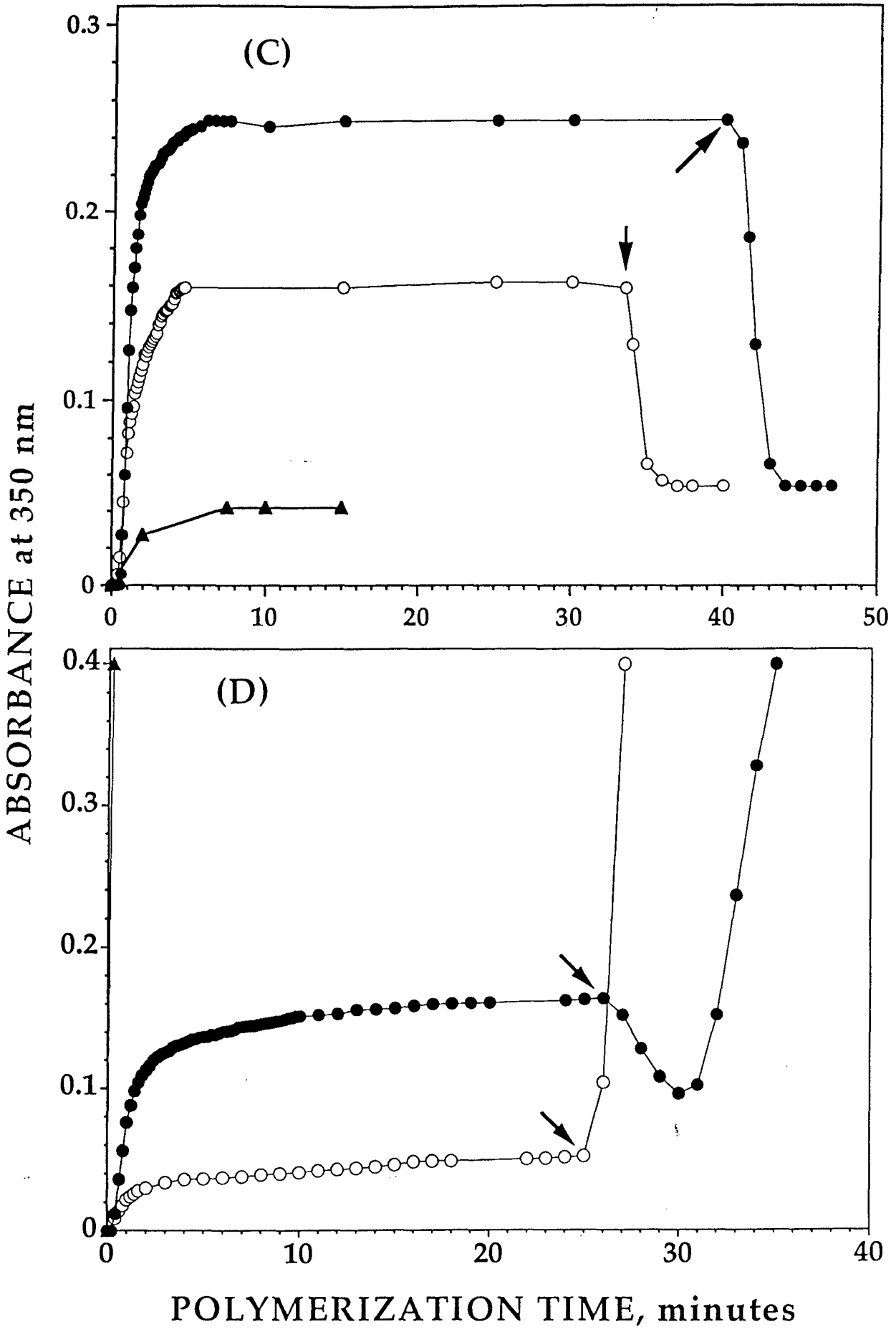

Figures 4C and 4D

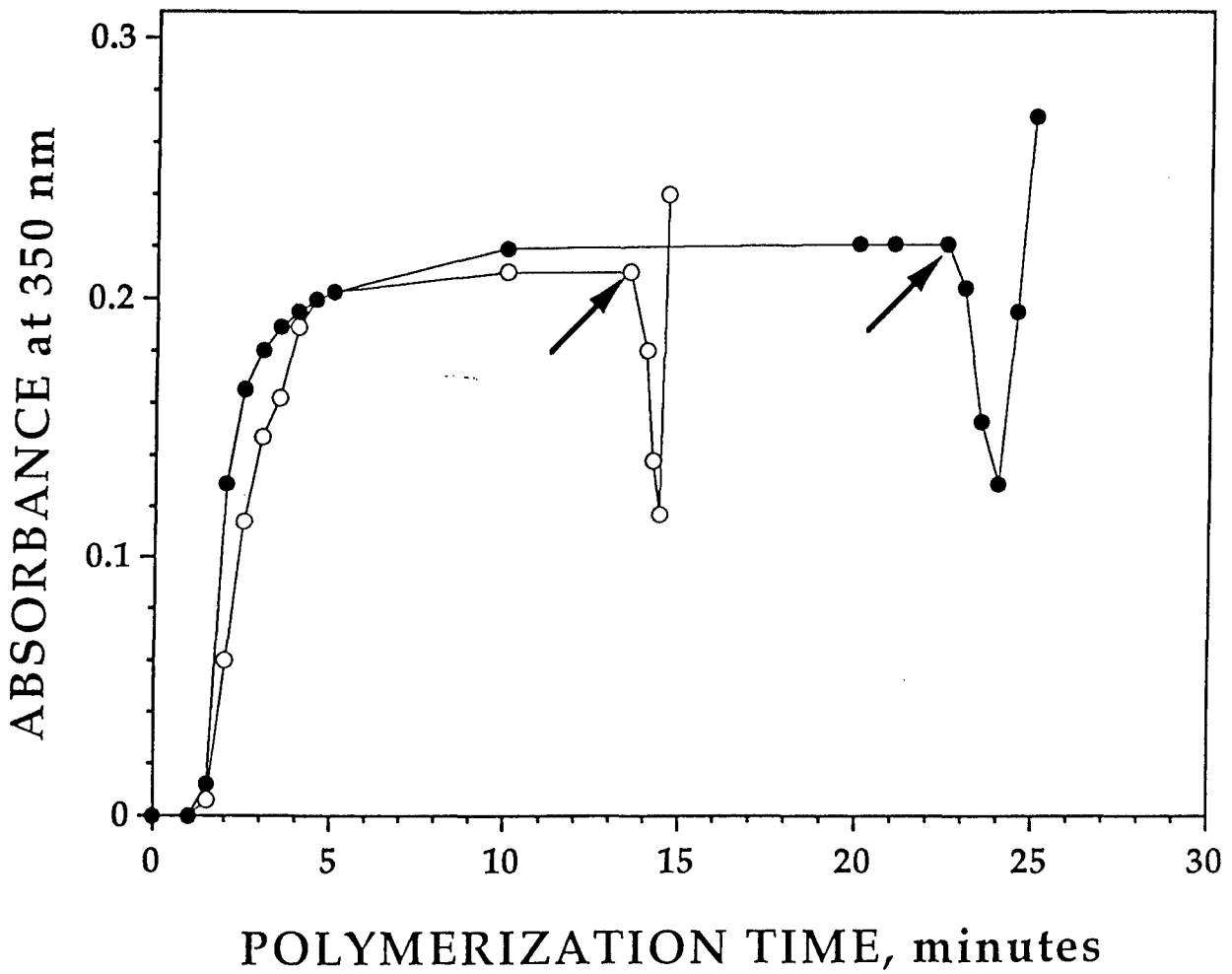
ABSORBANCE at 350 nm
0.3
0.2
0.1
0
0
5
10
15
20
25
30
POLYMERIZATION TIME, minutes

Figure 5

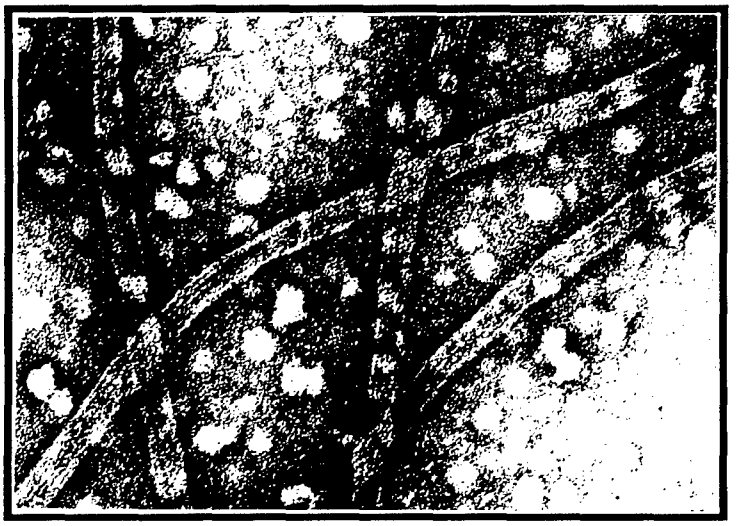

(1). (PCT + 0 μM VBL + Tau)

(2). (PCT + 1 μM VBL + Tau)

(3). (PCT + 20 μM VBL + Tau)

Figure 6A

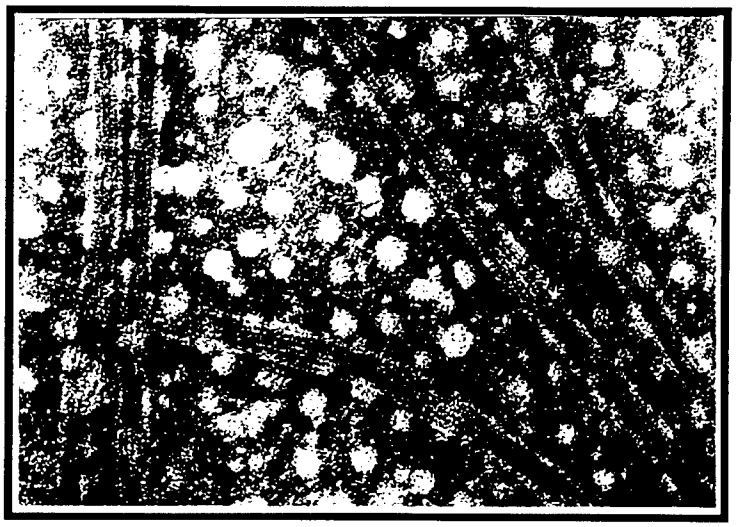

(1). ($\alpha\beta_{II}$ + 0 μM VBL + Tau)

(2). ($\alpha\beta_{II}$ + 1 μM VBL + Tau)

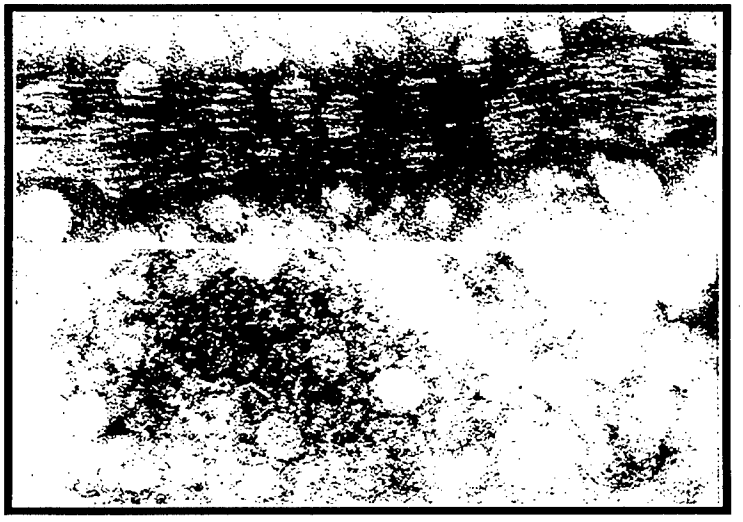

(3). ($\alpha\beta_{II}$ + 20 μM VBL + Tau)

Figure 6B

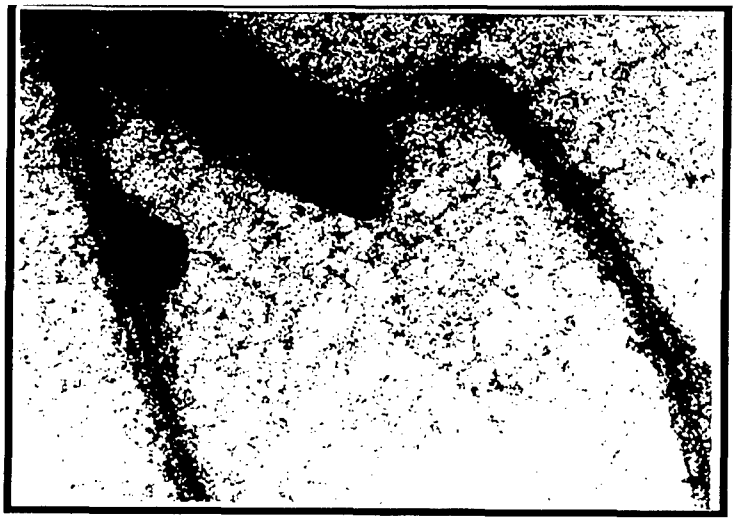

(1). ($\alpha\beta_{III}$ + 0 μM VBL + Tau)

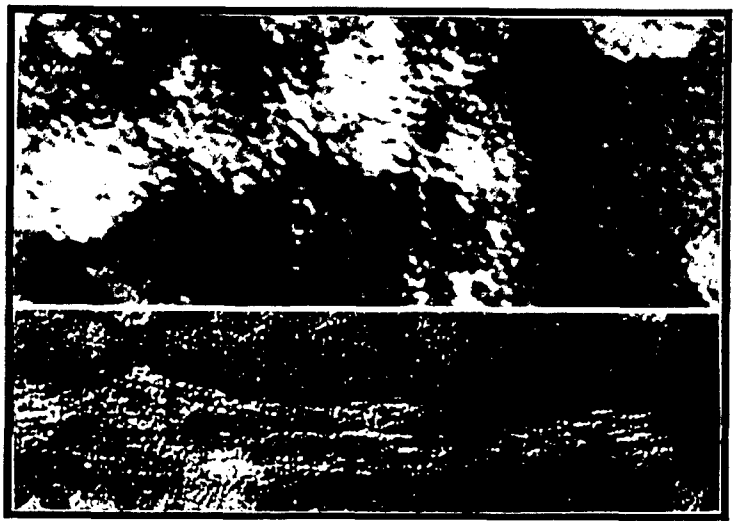

(2). ($\alpha\beta_{III}$ + 1 μM VBL + Tau)

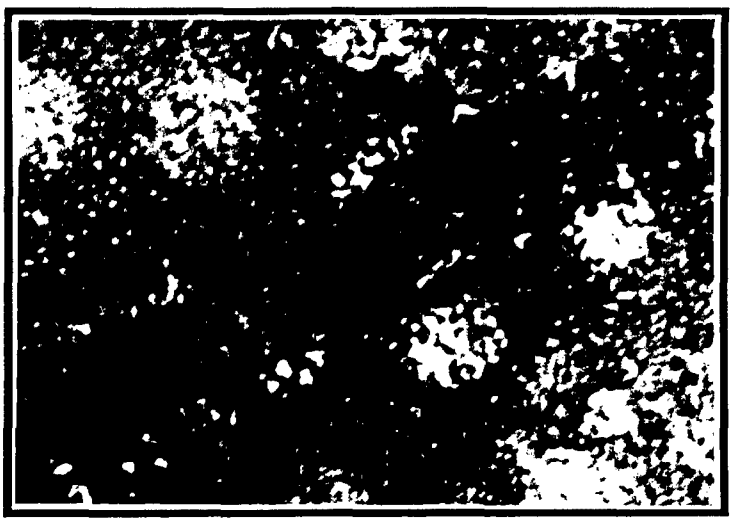

(3). ($\alpha\beta_{III}$ + 20 μM VBL + Tau)

Figure 6C

(1). ($\alpha\beta_{IV}$ + 0 μM VBL + Tau)

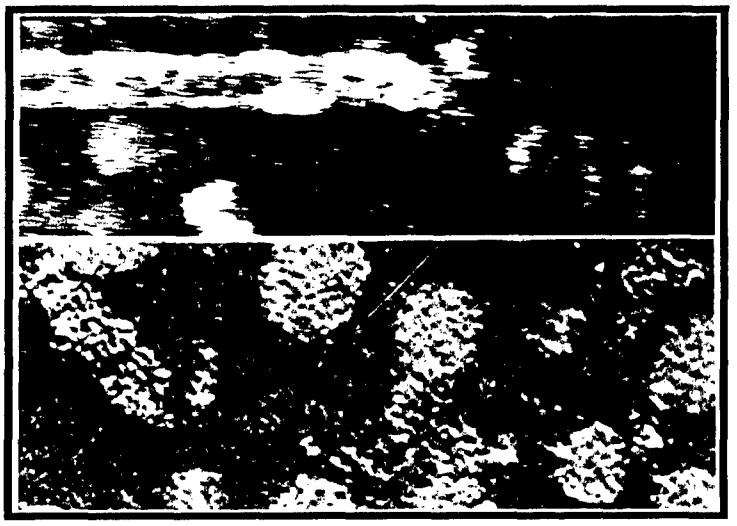

(2). ($\alpha\beta_{IV}$ + 1 μM VBL + Tau)

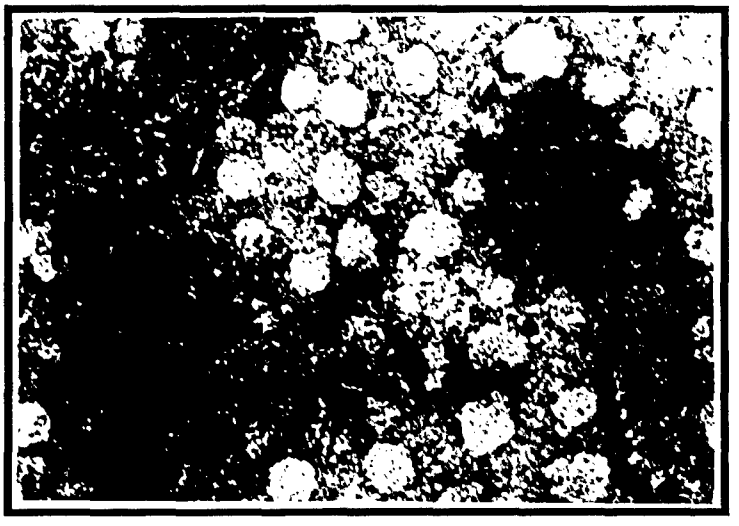

(3). ($\alpha\beta_{IV}$ + 20 μM VBL + Tau)

Figure 6D

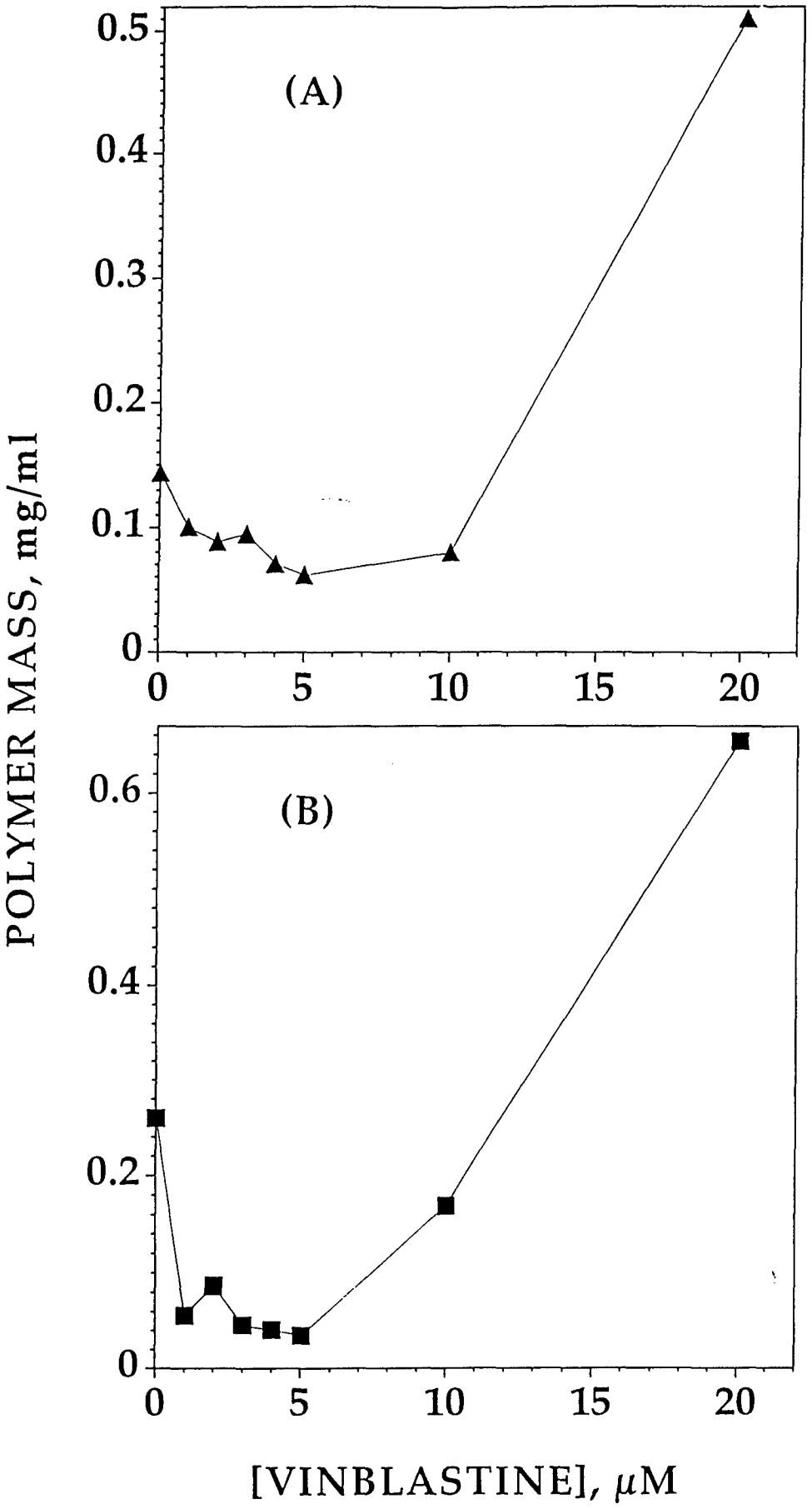

Figures 7A and 7B

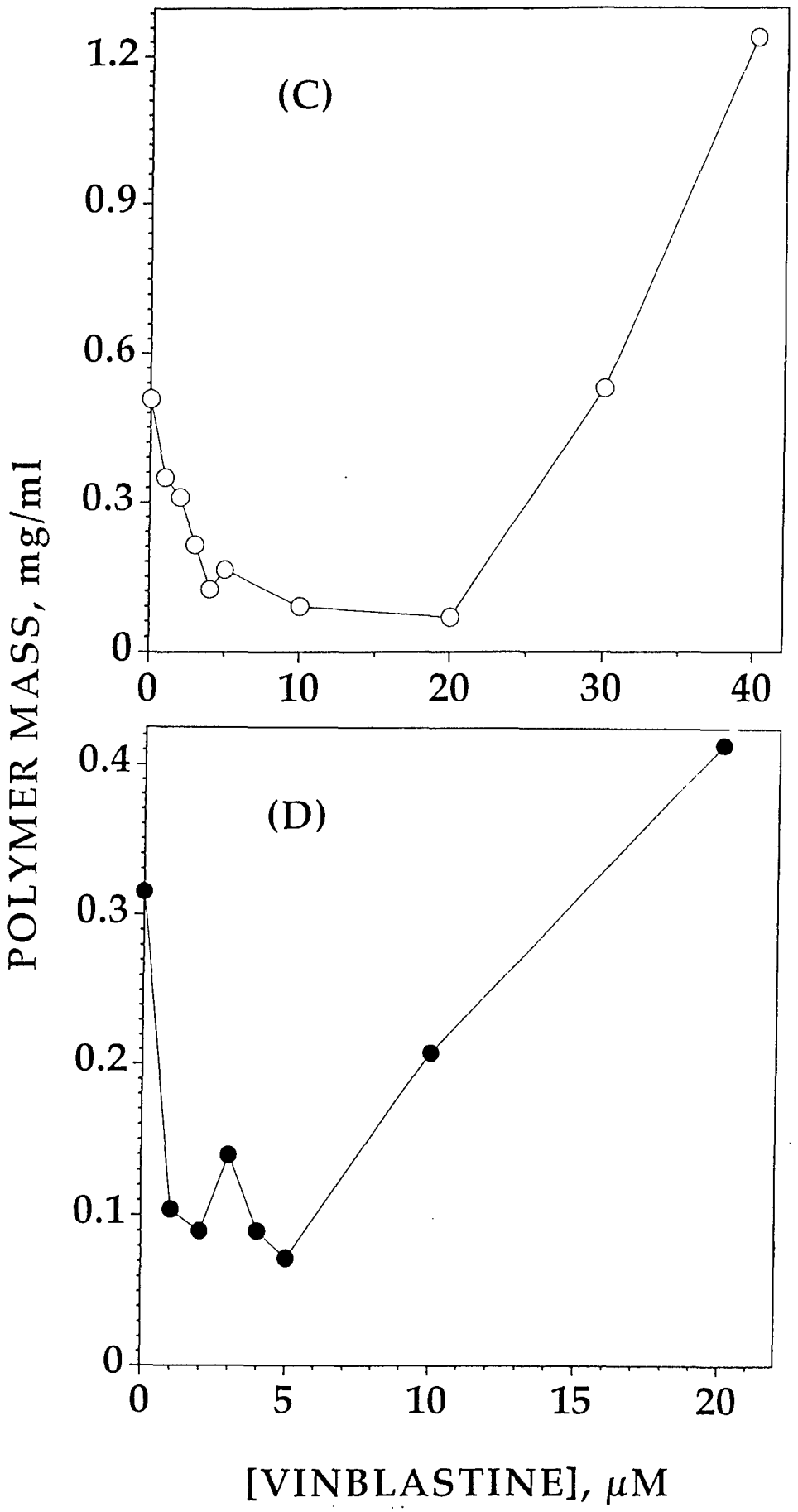

Figures 7C and 7D

Effect of the Anti-Tumor Drug Vinblastine on Nuclear β_{II}-Tubulin in Cultured Rat Kidney Mesangial Cells[1]

Consuelo Walss-Bass*, Jeffrey I. Kreisberg† & Richard F. Ludueña*[2]

Departments of Biochemistry and Surgery, University of Texas Health Science Center, San Antonio, Texas 78284, USA and the †The Research and Development Service Department of Veteran Affairs, San Antonio, Texas 78284, USA.

Key words: tubulin isotypes, microtubules, vinblastine, nuclear localization, DNA fragmentation.

Footnotes:

[1] This research was supported by grants CA26376 from the National Institutes of Health (R.F.L.), AQ-0726 from the Welch Foundation (R.F.L.), DAMD17-98-1-8246 from the U.S. Army Medical Research Program (R.F.L.) and VA Merit Review to J.I.K.

[2] Send correspondence to: Dr. Richard F. Ludueña, Department of Biochemistry, University of Texas Health Science Center, San Antonio, TX 78282-7760. Tel: 210-5673732; FAX: 210-5676595; e-mail: luduena@uthscsa.edu

[3]The abbreviations used are: *DAPI*, 4',6-diamidino-2-phenylindole, dihydrochloride, *PBS*, phosphate-buffered NaCl solution.

[4]Submitted for publication, this journal: Walss-Bass, C., and Ludueña, R.F. Nuclear β_{II}-tubulin as a marker for rapid cell proliferation.

ABSTRACT

Tubulin, the main component of microtubules, is a major target for anti-tumor drugs, such as vinblastine. We have recently discovered that the β_{II} isotype of tubulin is present in the nuclei of cultured rat kidney mesangial cells, smooth muscle-like cells present in the renal glomerular mesangium (Walss, C., Kreisberg, J.I., and Ludueña, R.F. Cell Motil. Cytoskeleton, 42: 274-284, 1999). Here, we have investigated the effect of vinblastine on nuclear β_{II}-tubulin in these cells. We have found that, at concentrations of 15 nM and higher, vinblastine caused a reversible loss of β_{II}-tubulin from the nucleus. Our results raise the possibility that nuclear β_{II}-tubulin constitutes a population of tubulin that could be a novel target for anti-tumor drugs such as vinblastine.

INTRODUCTION

Because of their crucial role in chromosome segregation during cell division, microtubules have long been a target for anti-tumor drugs (1). These drugs inhibit microtubule dynamics by binding to tubulin, the building block of microtubules (2). Vinblastine, a member of the *Vinca* alkaloid family, is an anti-tubulin drug widely used in chemotherapy (3). By binding to the β-subunit of tubulin, vinblastine inhibits microtubule dynamics (2). At high concentrations, vinblastine causes microtubule depolymerization (4) and the formation of tubulin para-crystals (5). Therefore, this drug is known as a microtubule destabilizing agent. At low, clinically relevant concentrations, vinblastine is known to arrest cells in mitosis by suppressing the dynamics of spindle microtubules, without significantly changing the amount of polymerized tubulin (6). The end result of this drug at low concentrations is to impede cell division and ultimately cause cell death.

We have previously reported the presence of a specific isotype of tubulin, β_{II}, in the nuclei of rat kidney mesangial cells (7). Nuclear β_{II}-tubulin exists as an $\alpha\beta_{II}$ tubulin dimer and appears to be in non-microtubule form and, as such, it constitutes a novel population of cellular tubulin. Recently, we have found that β_{II} is present in the nuclei of a variety of human cancer cells, but seems to be absent from the nuclei of most normal human cells[4]. Since tubulin is a major target of certain anti-tumor drugs, it is of interest to examine the effects of these drugs on nuclear tubulin. Therefore, we have now investigated the effect of vinblastine on nuclear β_{II}-tubulin in rat kidney mesangial cells, smooth-muscle-like cells from the renal mesangium. We have found that, at concentrations higher than clinically relevant, these drugs appear to cause β_{II} tubulin to

exit the nucleus. Loss of nuclear tubulin occurs after microtubule depolymerization caused by vinblastine. Removal of the drug allows β_{II} to re-enter the nucleus. Treatment of cells with anti-tumor drugs has been shown to induce apoptosis. The mechanism by which this occurs remains unclear (8). Our results raise the possibility that vinblastine may act by binding to nuclear β_{II}-tubulin and preventing it from executing its as yet unknown function.

MATERIALS AND METHODS

Source of cells and antibodies. Rat kidney mesangial cells were obtained as follows. Glomeruli were isolated from 200 g male Sprague-Dawley rats (Harlan Sprague-Dawley, Inc, Indianapolis, IN) using a graded sieve technique and were plated for culture in RPMI 1640 (Gibco BRL, Grand Island, N.Y.) tissue culture medium with 20% FCS plus penicillin, streptomycin and fungizone (E.R. Squibb and Sons) for explant growth of mesangial cells (9, 10). One hundred percent of the cells were identified as glomerular mesangial cells. Positive identification was obtained by ultrastructural examination, contractile responsiveness to vasopressin and angiotensin II, and shape change in response to cAMP-elevating agents (9, 10, 11). For the experiments described below, cells were used between the 4th and 40th passage.

The monoclonal antibodies SAP.4G5 and JDR.3B8 specific for the β_I and β_{II} isotypes of tubulin, were prepared as previously described (12, 13).

Immunofluorescence microscopy. Rat kidney mesangial cells were plated on glass coverslips in RPMI-1640 medium (Gibco BRL, Grand Island, N.Y.) containing 20% fetal calf serum (Atlanta Biologicals, Nrocross, GA). After 24 h, cells were treated with various concentrations of vinblastine (Sigma Chemical Co., St. Louis. MO.), from a 1 mM stock solution prepared fresh in H_2O. After various periods of time, cells were washed twice with PBS[3] (0.15M NaCl, 0.0027 M KCl, 0.00147M KH_2PO_4, 0.01M $NaHPO_4$, pH 7.2), fixed for 15 min with 3.7 % paraformaldehyde at room temperature and permeabilized for 1 min with 0.5% Triton X-100 in PBS. Cells were then incubated at 4 °C overnight with the respective isotype-specific monoclonal IgG mouse antibody (anti-β_I, 0.05-0.1 mg/ml; anti-β_{II}), diluted in PBS containing 10% normal goat serum

(Jackson Immunoresearch, West Grove, PA). After rinsing in PBS, coverslips were stained with a Cy3-conjugated goat anti-mouse antibody (1:100, Jackson Immunoresearch) for 1 hr at room temperature. For DNA detection, cells were stained with DAPI[3] (Molecular Probes, Eugene, OR.) (2 μl/ml in PBS) during the last wash with PBS after incubation with the secondary antibody. Coverslips were mounted on glass slides and examined with an Olympus epifluorescence photomicroscope using a Plan-Neufluar 100x oil objective. For drug reversibility experiments, cells were incubated with vinblastine at various concentrations for 24 h, after which the drug was removed and cells were incubated in fresh media for 24 h. Cells were then fixed and treated as described above.

RESULTS

Because we were not interested in blocking cells in mitosis, we chose to use vinblastine concentrations higher than those clinically relevant. Therefore, rat kidney mesangial cells were incubated with vinblastine at concentrations of 15 to 50 nM for 1 to 6 h. Cells were then fixed and stained with monoclonal antibodies to β_I- and β_{II}-tubulin. The β_{II}-tubulin antibody has been reported previously to detect nuclear β_{II}-tubulin (7). The β_I-tubulin antibody was used to observe the effect of vinblastine on cytosolic microtubules, since this isotype is present only in the cytosol (7). Cells treated with anti-β_I in the absence of drug revealed a normal microtubule network in the cytosol (Fig. 1*A*). However, 1hr treatment with 15 nM vinblastine, the lowest drug concentration used, was enough to completely depolymerize the microtubules (Fig. 1*B*). No difference in the cytosolic fluorescence pattern was observed when cells were treated longer or with higher drug concentrations.

Staining of control, drug-free cells, with anti-β_{II} tubulin revealed that all cells contained β_{II}-tubulin in the nucleus, as had been previously reported (7) (Fig. 1*C*). Very little fluorescence was observed in the cytosol. After treatment with 15 nM vinblastine for 1 h, 3 out of 10 cells seemed to have lost their nuclear tubulin, as they contained no nuclear fluorescence (Fig. 1*D*). The nuclei of these cells appeared unaffected, as seen by DAPI staining (Fig. 1*E*). After 3 h of treatment with 15 nM vinblastine, 8 out of 10 cells had lost their nuclear tubulin (Fig. 1*F*) and, as before, DAPI staining revealed that the nuclei of these cells appeared intact (not shown). By increasing the vinblastine concentration to 30 nM, 1 h of treatment was enough to cause the loss of nuclear tubulin in 7 out of 10 cells (Fig. 1*G*). At this drug concentration, micro-nucleation, or DNA

fragmentation, was seen by DAPI staining in 3 out of 10 cells, indicating that these cells were probably undergoing apoptosis (Fig. 1*H*). Micro-nucleation appeared to occur regardless of whether β_{II}-tubulin was present in the nucleus or not. Furthermore, the nuclei of cells that had lost their nuclear tubulin, but had not entered apoptosis, appeared to be normal, as indicated by DAPI staining (Fig. 1*H*). After 3 h of treatment with 30 nM vinblastine, nuclear tubulin was absent in 9 out of 10 cells (Fig. 1*I*, *J*). Treatment of cells with concentrations of 40 to 60 nm for 1 h caused the total disappearance of nuclear tubulin (Fig. 1*K*, *L*).

In order to determine if the effect of vinblastine on nuclear tubulin was reversible, cells were incubated with vinblastine at concentrations from 15 to 50 nM for 24 h and then incubated in media without drug for 24 h. Treatment of these cells with anti-β_{II} revealed that cells were able to recover form the effect of the drug, even at the higher concentrations used. Cells appeared nearly confluent, indicating that they were able to proliferate, and very few apoptotic cells were observed. Furthermore, β_{II}-tubulin was able to re-enter the nucleus of the cells, as appearance of nuclear fluorescence was seen in nearly all cells examined (Fig. 2).

DISCUSSION

The results shown here revealed that the anti-tumor drug vinblastine, when used at high concentrations, causes β_{II}-tubulin to exit the nucleus. The exit of β_{II}-tubulin from the nucleus may be due to vinblastine binding directly to nuclear tubulin, or, it may be an indirect result of the effect of this drug on cytoplasmic microtubules. It is possible that, in an effort to counteract the effect of vinblastine on microtubules, cells may translocate β_{II}-tubulin into the cytosol, where it may be needed more. However, our studies did not reveal an increase in cytosolic β_{II}-tubulin after treatment with vinblastine. This is most likely due to the fact that vinblastine causes microtubule depolymerization. In fact, vinblastine has been shown to inhibit the assembly of $\alpha\beta_{II}$ microtubules more than it does the assembly of $\alpha\beta_{III}$ and $\alpha\beta_{IV}$ microtubules (14).

The effect of vinblastine on nuclear tubulin was found to be reversible, since β_{II}-tubulin appeared to re-enter the nucleus after the drug was removed and cells were able to recover. This is consistent with the findings by Jordan *et al.* (15), who reported that vinblastine is effluxed from cells after the drug is removed from the media. The mechanism by which vinblastine, and other anti-tumor drugs, trigger apoptosis remains unknown (16). It is tempting to speculate that the effect of these drugs on nuclear tubulin may somehow be related to activation of the programmed cell death pathway. However, in our present studies we have found that vinblastine causes cells to enter apoptosis regardless of whether they contain nuclear β_{II}-tubulin or not. This suggests that activation of the apoptotic pathway is independent of the presence of β_{II}-tubulin in the nucleus.

Our studies on nuclear tubulin have revealed that β_{II}-tubulin is present in the nuclei of a wide variety of human cancer cells, while it is absent from the nuclei of normal human cells[4]. Although the rat kidney mesangial cells used in the present experiments are considered normal, they grow extremely fast in culture (17) and in this sense resemble cancerous cells. These findings have led us to believe that β_{II}-tubulin may be somehow involved in assisting rapid cell proliferation. By blocking microtubule dynamics, the anti-tubulin drug vinblastine inhibits cell proliferation (6). Therefore, it is possible that the function of β_{II}-tubulin in the nucleus is inhibited by this drug. Vinblastine has been shown to affect cellular processes such as DNA and RNA synthesis (18, 19). The finding of β_{II}-tubulin in the nucleus, and the fact that vinblastine appears to cause this isotype to exit the nucleus, could explain the effect of this drug on these seemingly non-tubulin related functions. Further studies are necessary to determine whether nuclear β_{II}-tubulin is in fact involved in DNA and RNA synthesis.

In conclusion, our present studies on the effect of vinblastine on nuclear β_{II}-tubulin have revealed that anti-tubulin drugs may be useful tools to determine the exact role of β_{II}-tubulin in the nucleus. They also raise the possibility that these drugs may exert their anti-tumor activity through an interaction with nuclear tubulin.

REFERENCES

1. Dustin, P. (ed.), Microtubules, 2nd Ed., Berlin: Springer-Verlag, 1984.
2. Wilson, L., and Jordan, M.A. Pharmacological probes of microtubule function. *In*: J. S. Hyams and C.W. Lloyd (eds.), Microtubules, pp. 59-83. New York: Wiley-Liss, 1994.
3. Gerzon, K. Dimeric catharanthus alkaloids. *In*: J.M. Cassady and J.D. Douros (eds.), Anticancer agents based on natural product models, pp271-317. New York: Academic Press, 1980.
4. Owellen, R.J., Hartke, C.A., Dickerson, R.M., and Haines, F.O. Inhibition of tubulin-microtubule polymerization by drugs of the *Vinca* alkaloid class. Cancer Res., *36*: 3798-3802, 1976.
5. Na, G.C., and Timasheff, S.N. In vitro vinblastine-induced tubulin paracrystals. J. Biol. Chem., *257*: 10387-10391, 1982.
6. Jordan, M.A., Thrower, D., and Wilson, L. Mechanism of inhibition of cell proliferation by *Vinca* alkaloids. Cancer Res., *51*: 2212-2222, 1991.
7. Walss, C., Kreisberg, J.I., and Ludueña, R.F. Presence of the β_{II} isotype of tubulin in the nuclei of cultured mesangial cells from rat kidney. Cell Motil. Cytoskeleton, *42*: 274-284, 1999.
8. Tsukidate, K., Yamamoto, K., Snyder, J.W., and Farber, J.L. Microtubule antagonists activate programmed cell death (apoptosis) in cultured rat hepatocytes. Am J. Pathol., *143*: 918-925, 1993.

9. Ausiello, D.A., Kreisberg, J.I., Roy, C., and Karnovsky, M.J. Contraction of cultured cells of apparent mesangial origin after stimulation with angiotensin II and arginine vasopressin. J. Clin. Invest., *65*: 754-760, 1980.

10. Kreisberg, J.I., Venkatachalam, M.A., and Patel, P.Y. Cyclic AMP-associated shape change and its reversal by PGE_2. Kidney Int., *25*: 874-879, 1984.

11. Kreisberg, J.I., and Venkatachalam, M.A. Vasoactive agents affect mesangial cell adhesion. Am. J. Physiol., *251*: C505-C511, 1986.

12. Banerjee, A., Roach, M. C., Wall, K. A., Lopata, M. A., Cleveland, D. W., and Ludueña, R. F. A monoclonal antibody against the type II isotype of β-tubulin. Preparation of isotypically altered tubulin. J. Biol. Chem., *263*: 3019-3034, 1988.

13. Roach, M. C., Boucher, V. L., Walss, C., Ravdin, P., and Ludueña, R. F. Preparation of a monoclonal antibody specific for the class I isotype of β-tubulin: the β isotypes of tubulin differ in their cellular distributions within human tissues. Cell Motil. Cytoskeleton, *39*: 273-285, 1998.

14. Khan, I.A., and Ludueña, R.F. Effect of vinblastine on the assembly of isotypically pure tubulins from bovine brain. Mol. Biol. Cell, *6*: 30a, 1995.

15. Jordan, M.A., Wendell, K., Gardiner, D., Derry, W.B., Copp, H., and Wilson, L. Mitotic block induced in HeLa cells by low concentrations of paclitaxel (taxol) results in abnormal mitotic exit and apoptotic cell death. Cancer Res., *56*: 816-825, 1996.

16. Sorger, P. K., Dobles, M., Tournebize, R., and Hyman, A.A. Coupling cell division and cell death to microtubule dynamics. Curr. Opin. Cell Biol., *9*: 807-814, 1997.

17. Floege, J., Topley, N., Hoppe, J., Barrett, T.B., and Resch, K. Mitogenic effect of

platelet-derived growth factor in human glomerular mesangial cells: modulation and/or suppression by inflammatory cytokines. Clin. Exp. Immunol., *86*: 334-341, 1991.

18.Creasey, W.A. Modifications in biochemical pathways produced by the *Vinca* alkaloids. Cancer. Chemother. Res., *52*: 501-507, 1968.

19.Bernstam, V.A., Gray, R.H., and Bernstein, I.A. Effect of microtubule-disrupting drugs on protein and RNA synthesis in *Physarum polycephalum* Amoebae. Arch. Microbiol., *128*: 34-40, 1980.

FIGURE LEGENDS

Fig. 1. Effect of vinblastine on nuclear tubulin in mesangial cells. (*A*), Control, drug-free cells, stained with anti-β_I. (*B*), Cells treated with 15 nM vinblastine for 1 h, stained with anti-β_I. Notice depolymerization of microtubules. (*C*), Control, drug-free cells stained with anti-β_{II}. Notice the strong nuclear fluorescence. (*D*), Cells treated with 15 nM vinblastine for 1 h, stained with anti-β_{II}. (*E*), Same cells as in *D*, stained with DAPI to reveal the nuclei. (*F*), Cells treated with 15 nM vinblastine for 3 h, stained with anti-β_{II}. (*G*), Cells treated with 30 nM vinblastine for 1 h, stained with anti-β_{II}. (*H*), same cells as in *G*, stained with DAPI to reveal the nuclei. (*I*), Cells treated with 30 nM vinblastine for 3 h, stained with anti-β_{II}. (*J*), Same cells as in *I*, stained with DAPI to reveal the nuclei. (*K*), Cells treated with 50 nM vinblastine for 1 h, stained with anti-β_{II}. (*L*), Same cells as in *K*, stained with DAPI, to reveal the nuclei. Arrows indicate micronucleation.

Fig. 2. The effect of vinblastine on nuclear tubulin is reversible. (*A*, *C*, *E*), Cells stained with anti-β_{II}. (*B*, *D*, *F*), Cells stained with DAPI. (*A*, *B*), Cells treated with 15 nM vinblastine for 6 h, then incubated in media without drug for 24 h. (*C*, *D*), Cells treated with 30 nM vinblastine for 6 h, then incubated in media without drug for 24 h. (*E*, *F*), Cells treated with 50 nM vinblastine for 6 h, then incubated in media without drug for 24 h.

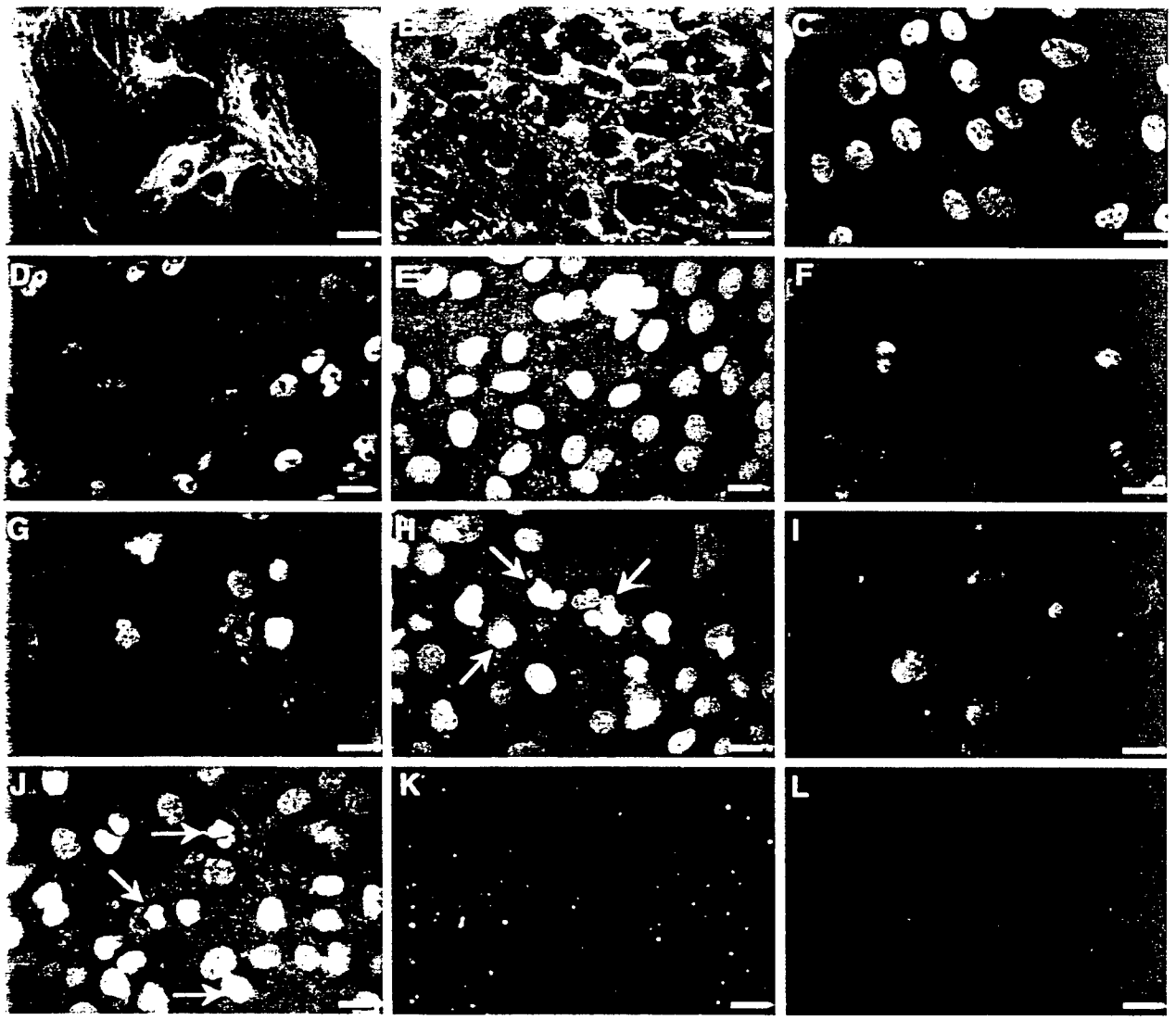

Figure 1

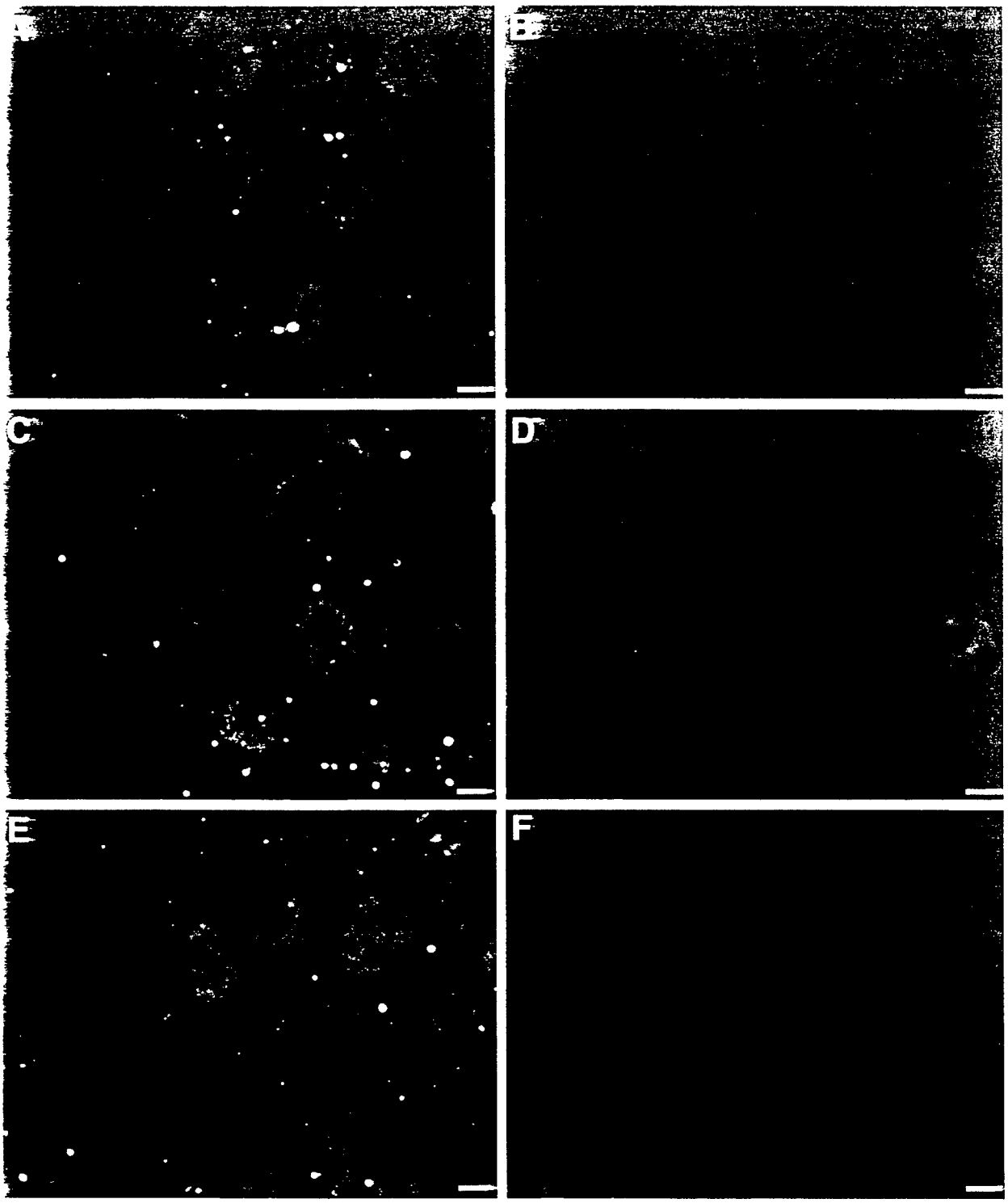

Figure 2

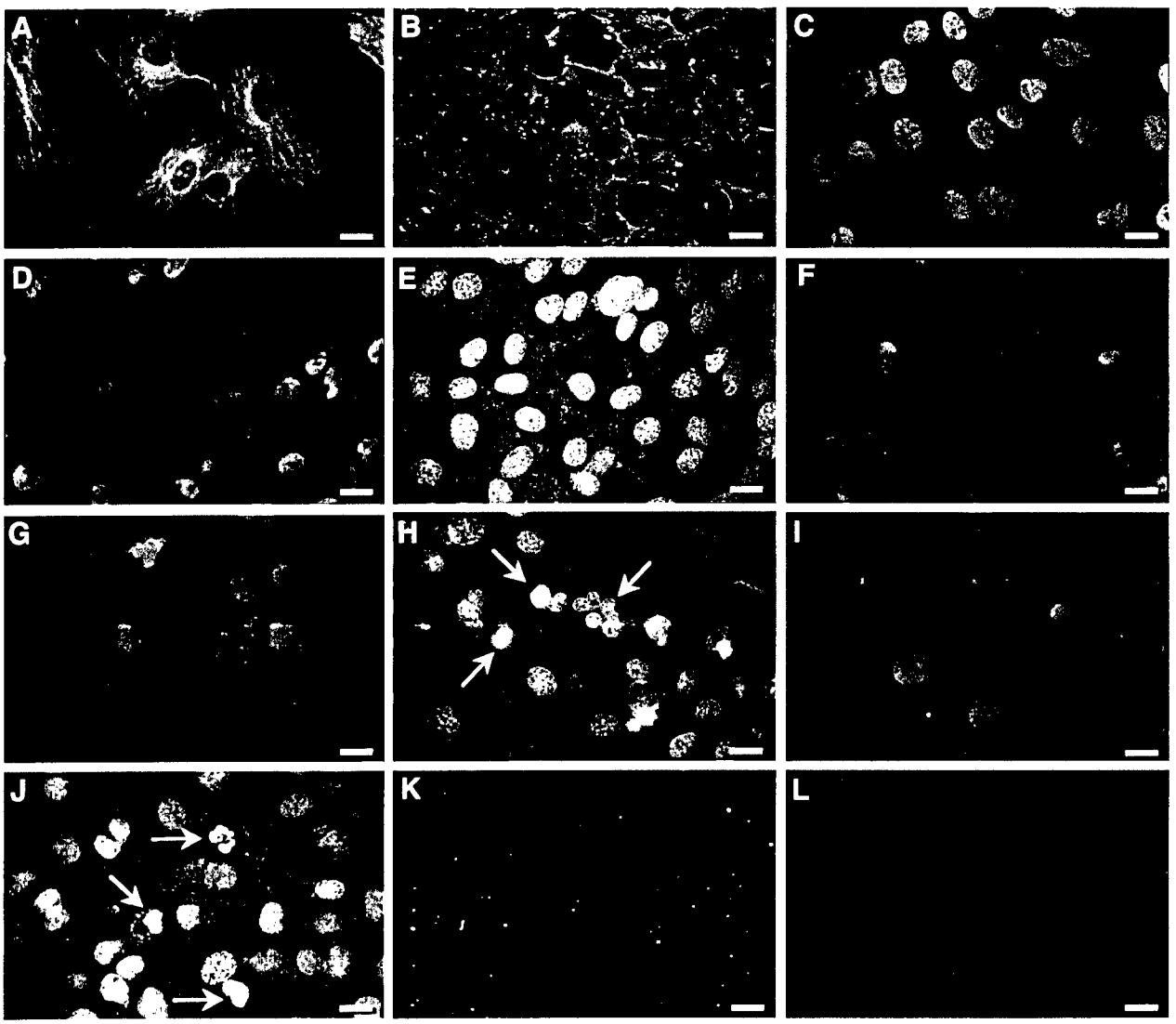

Figure 1

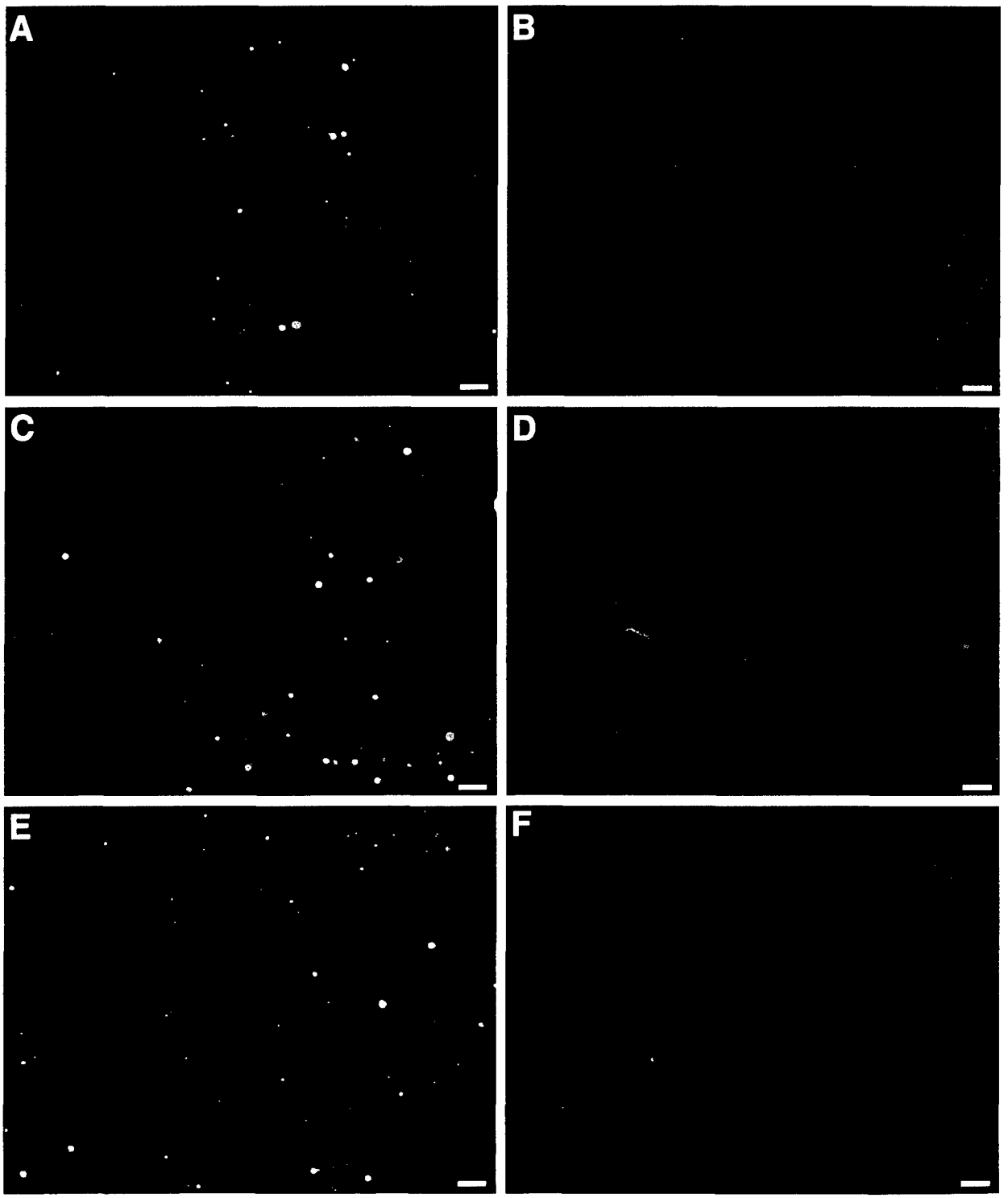

Figure 2

Nuclear β_{II}-Tubulin as a Marker for Rapid Cell Proliferation[1]

Consuelo Walss-Bass and Richard F. Ludueña[2]

Department of Biochemistry, University of Texas Health Science Center, San Antonio, Texas 78284, USA.

Key words: tubulin, nuclear tubulin, tubulin isotypes, cell proliferation, immunofluorescence

Footnotes:

[1]This research has been supported by grants CA26376 from the National Institutes of Health, AQ-0726 from the Welch Foundation, and DAMD17-98-1-8246 from the U.S. Army Breast Cancer Research Program to R.F.L.

[2]Send correspondence to: Dr. Richard F. Ludueña, Department of Biochemistry, University of Texas Health Science Center San Antonio, Texas 78284-7760. Tel: 210-5673732, FAX: 210-5676595; e-mail: luduena@uthscsa.edu

[3]The abbreviations used are: PBS, phosphate-buffered NaCl solution; DAPI, 4',6-diamidino-2-phenylindole, dihydrochloride; LNCaP, lymph node carcinoma of the prostate; EGTA, ethyleneglycol-bis-(β-aminoethylether)*N,N,N,N'*-tetraacetic acid; PIPES, piperazine-*N,N'*-bis(2-ethanesulfonic acid); PMSF, phenylmethyl sulfonyl fluoride; PDGF, platelet-derived growth factor; IL-1, interleukin-1.

ABSTRACT

Microtubules are cylindrical organelles that play critical roles in cell division. Their subunit protein, tubulin, is a target for various anti-tumor drugs. Tubulin exists as various forms, known as isotypes. In most normal cells, tubulin occurs only in the cytosol and not in the nucleus. However, we have recently reported the finding of the β_{II} isotype of tubulin in the nuclei of cultured rat kidney mesangial cells (Walss, C., Kresiberg, J.I. and Ludueña, R.F. Cell Motil. Cytoskeleton. *42*: 274-284, 1999). Mesangial cells, unlike most normal cell lines, have the ability to proliferate rapidly in culture. In efforts to determine if nuclear β_{II}-tubulin occurred in other cell lines, we examined the distribution of the β_{I}, β_{II} and β_{IV} mammalian tubulin isotypes in a variety of normal and cancer human cell lines by immunofluorescence microscopy. We have found that, in the normal cell lines, all three isotypes are present in the cytosol. However, the β_{II} isotype of tubulin is located in the nuclei of LNCaP prostate carcinoma, MCF-7, MDA and Calc18 breast carcinoma cell lines. In contrast, the β_{I} and β_{IV}-isotypes, which are also expressed in these cancer cells, are not localized to the nucleus but are restricted to the cytoplasm. These results suggest that transformation may lead to localization of β_{II}-tubulin in cell nuclei, serving an as yet unknown function, and that nuclear β_{II} may be a useful marker for detection of tumor cells.

INTRODUCTION

A fundamental fact about cancer is that cancer cells are our own cells misbehaving. They are not really alien cells. Most anti-cancer drugs target cell division, a process that is faster in cancer cells than in most normal cells. The problem, however, is that certain normal cells, such as those of the bone marrow, also divide fairly rapidly. Hence, the agents of chemotherapy have serious side effects, which limit their use. Therefore, the challenge for cancer chemotherapy is to find a drug that attacks cancer cells but not normal cells.

Microtubules, made of the protein tubulin, are organelles that play a critical role in mitosis; they attach to chromosomes as they line up in metaphase and help move them into the daughter cells (1). For this reason, the protein tubulin is a major target for anti-tumor drugs such as vinblastine and taxol (2). Nevertheless, these drugs do not discriminate between normal and cancer cells, both of which contain tubulin, and therefore have serious side effects and limitations.

The tubulin protein is made of two subunits, α and β (1). These subunits exist as numerous isotypes, which differ in their tissue and subcellular localization, as well as in their interaction with anti-tumor drugs (3). We have previously found that the β_{II} isotype of tubulin is present in the nuclei of rat kidney mesangial cells (4). In order to determine whether this unexpected finding was an isolated incident, or occurred in other cell types, we have now examined the intracellular distribution of the vertebrate β-tubulin isotypes β_I, β_{II} and β_{IV} in several cultured human cell lines, both normal and cancerous. We have found that the β_{II}-isotype of tubulin is present in all the cancer cells investigated, but is

absent from the nuclei of most of the normal cells. These results suggest that transformation may lead to localization of β_{II} in cell nuclei, serving an as yet unknown function. Furthermore, nuclear β_{II} may be a useful marker for detection of tumor cells and may serve as a target for anti-tumor drugs, such as taxol and vinblastine, to selectively attack cancer cells.

MATERIALS AND METHODS

Source of cells and antibodies. The HDF human dermal fibroblasts were a kind gift from Dr. Eugene Sprague. (UTHSCSA, San Antonio, Tx). The 506 smooth muscle cells from human colon and the HSK fibroblasts from baby foreskin were a kind gift from Dr. Mary Pat Moyer. (UTHSCSA San Antonio, TX). The osteoblasts were a kind gift from Dr. John Lee (UTHSCSA, San Antonio, TX). The MCF-10F breast epithelial cells, the LNCaP prostate carcinoma cells, as well as the MCF-7, and MDA breast carcinoma cells were a kind gift from Dr. Nandini Chaudhuri (UTHSCSA, San Antonio, TX). The Calc 18 breast carcinoma cell line was a kind gift from Dr. Arlette Fellous (INSERM, Paris, France).

The monoclonal antibodies SAP.4G5, JDR.3B8, and ONS.1A6 specific, respectively, for the β_I, β_{II}, and β_{IV} isotypes of tubulin were prepared as previously described (5, 6, 7).

Immunofluorescence microscopy. All cells were grown to near confluency on glass coverslips at 37 °C and 5% CO_2. Cells were then washed twice with PBS[3] (0.15M NaCl, 0.0027 M KCl, 0.00147M KH_2PO_4, 0.01M $NaHPO_4$, pH 7.2), fixed for 15 min with 3.7 % paraformaldehyde at room temperature and permeabilized for 1 min with 0.5% Triton X-100 in PBS. Cells were then incubated at 4 °C overnight with the respective isotype-specific monoclonal IgG mouse antibody (anti-β_I, 0.05 mg/ml; anti-β_{II}, 0.03 mg/ml; anti-β_{IV}, 0.08) diluted in PBS containing 10% normal goat serum (Jackson Immunoresearch, West Grove, PA). Cells were rinsed in PBS and labeled with Cy3-conjugated goat anti-mouse antibody (1:100, Jackson Immunoresearch) for 1 hr at room temperature. Cells were then rinsed three times with PBS. For DNA detection, cells were stained with

DAPI[3], (Molecular Probes, Eugene OR.), (2 μl/ml in PBS) during the last wash with PBS after incubation with the secondary antibody. Coverslips were mounted on glass slides and examined with a Zeiss epifluorescence photomicroscope using a Plan-Neufluar 63x oil objective.

***In situ* cell fractionation.** LNCaP[3] cells, grown on glass coverslips, were washed twice with ice-cold PBS and incubated on ice for 5 min with cold cytoskeleton buffer (10 mM PIPES[3], pH 6.8, 300 mM sucrose, 100 mM NaCl, 3 mM $MgCl_2$, 1 mM EGTA[3], 1% Triton X-100, 1.2 mM PMSF[3], 0.1% aprotinin, 0.1% pepstatin A, 1% vanadyl ribonucleoside complex). This procedure removes all soluble cytoplasmic and nucleoplasmic proteins. This was followed by 5 min incubation on ice with double detergent buffer (10 mM Tris-HCl, pH 7.4, 10 mM NaCl, 3 mM $MgCl_2$, 0.5% deoxycholate, 1% Tween-40, 1.2 mM PMSF, 0.1% aprotinin, 0.1% pepstatin A, 1% vanadyl ribonucleoside complex), which removes all cytoskeletal proteins, except the intermediate filaments that remain tightly associated with the nucleus. Cells prepared this way are the cytosol-extracted cells. For nuclear matrix preparations, these cells were further incubated at room temperature for 1 hr in cytoskeleton-50 buffer (same as above except with 50 mM NaCl instead of 100 mM) containing 100 μg/ml of DNAse I (Sigma Chemical Co., St. Louis, MO.). The chromatin was then removed by adding 2M $(NH_4)_2SO_4$ dropwise to a final concentration of 0.25 M. What is left behind is the nuclear matrix structure and the intermediate filaments (8). Cells were then fixed with 3.7% paraformaldehyde in cytoskeleton buffer and treated as in the regular immunofluorescence procedure. For DNA detection, cells were stained with DAPI, (2 μl/ml in PBS) during the last wash with PBS after incubation with the secondary

antibody. Removal of chromatin in the nuclear matrix preparations was monitored in this way. For blocking experiments, primary antibodies were incubated with a 200-fold excess of the respective peptide for 30 min at room temperature, prior to incubation with fixed and permeabilized cells.

RESULTS

We have examined the intracellular distribution of the β_I, β_{II} and β_{IV} tubulin isotypes by indirect immunofluorescence on 5 different cultured normal human cell lines: HDF human dermal fibroblasts, HSK fibroblasts from baby foreskin, MCF-10F breast endothelial cells, osteoblasts, and 506 smooth muscle cells. In each case, the β_I- and β_{IV} -tubulin isotypes were found in the cytosol, as part of the microtubule network (Fig. 1*A*, *D*, *G*, *J*, *M* for β_I and *C*, *F*, *I*, *L*, *O* for β_{IV}). The same was seen for β_{II}-tubulin in these cell lines (Fig. 1*B*, *E*, *H*, *K*, *N*). In addition, in the smooth muscle cells, β_{II}-tubulin appeared to be expressed in the centrosomes (Fig. 1*N*). In no case were any of the isotypes, including β_{II}, found to be expressed in the nuclei, as no nuclear fluorescence was observed in any of the cell lines investigated.

The presence of β_{II}-tubulin in the nuclei was detected by labeling with anti-β_{II} in all the cancer cell lines investigated. These include LNCaP prostate carcinoma and three types of breast carcinoma: MCF-7, MDA and Calc 18 cell lines (Fig. 2*B*, *E*, *H*, *J*). In the LNCaP, MCF-7 and MDA cells, the nucleus was almost indistinguishable from the cytosol; the whole cell appeared to be stained equally with anti-β_{II} (Fig. 2*B*, *E*, *H*). Comparison of the nuclear staining by anti-β_{II} in these cells with that of DAPI, which shows the position of the nuclei, reveals that anti-β_{II} does in fact stain the nucleus in LNCaP, MCF-7 and MDA cells (not shown). In contrast, in the Calc 18 cells, the cytosol was labeled only weakly by anti-β_{II}, while the nuclear labeling was very strong (Fig. 2 *J*). The intra-nuclear distribution of β_{II}-tubulin appeared to be the same in all the cancer cells. The pattern of nuclear fluorescence was homogenous within the nucleus, except for the Calc 18 cells, in which there appeared to be no β_{II} staining in the nucleoli (Figure 2*J*).

The β_I- and β_{IV} -isotypes were found only in the cytosol, as part of the interphase microtubule network, of each of the cancer cells investigated (Fig. 2*A*, *D*, *G* for β_I and *C*, *F*, *I* for β_{IV}).

To determine the sub-nuclear localization of β_{II}-tubulin, *in situ* cell fractionation was performed in LNCaP cells. Removal of the soluble cytoplasmic and nucleoplasmic proteins by detergent extraction did not cause the nuclear fluorescence, obtained by staining with anti-β_{II}, to disappear (Fig. 3*A*). Furthermore, nuclear fluorescence was still detected after chromatin and chromatin-associated proteins were removed by DNAse digestion (Fig. 3*C*). In these cells, β_{II} appeared to accumulate in the nucleolar remnants. These results suggest that β_{II}-tubulin is part of the nuclear matrix in LNCaP cells. Pre-incubation of anti-β_{II} with its peptide epitope inhibited the nuclear fluorescence in both the cytosol-extracted, and the nuclear matrix preparations, indicating that nuclear fluorescence obtained in these cells was due to specific binding of the antibody to β_{II}-tubulin (Fig. 3*E*, *G*).

DISCUSSION

The results presented here raise the possibility that localization of tubulin in the nucleus may be a phenomenon that occurs in cancer cells. We have found β_{II}-tubulin to be present in the nuclei of LNCaP prostate carcinoma as well as in the breast carcinoma cell lines MCF-7, MDA and Calc-18, but not in the nuclei of normal cells. Similarly, Ranganathan *et al.* (9), have found β_{II}-tubulin in the nuclei of prostate carcinoma but not in benign prostate hypertrophy. Our initial discovery of nuclear β_{II}-tubulin was in rat kidney mesangial cells, obtained from a non-transformed primary cell line. Although these cells are not cancerous, they grow very fast in culture. Mesangial cells are known to maintain a basal proliferation rate *in vitro*, even in the absence of exogenous mitogens (10). This is most likely due to the fact that these cells self-produce growth factors such as PDGF[3], (11), and IL-1[3], (12), and in this way undergo autocrine-mediated proliferation *in vitro* (13). Furthermore, cultured mesangial cells are commonly maintained in the presence of 20% fetal calf serum, of which PDGF is the principal mitogen (14). PDGF is known to be the most potent mitogen for cultured mesangial cells, as it has been shown to increase the thymidine incorporation rate in these cells by 10-15 fold (14). This explains the rapid proliferation of mesangial cells *in vitro*, in contrast to normal mesangial cells *in vivo*, which are almost non-proliferative (15), and have been shown to proliferate rapidly only in cases of renal glomerular injury or disease (16). Considering these facts, together with our present finding of β_{II}-tubulin in the nuclei of cultured cancer cells, we hypothesize that nuclear β_{II}-tubulin may play a role in assisting rapid cell proliferation. This would explain the finding of β_{II} inside the nuclei of cancer cells but not normal cells.

It is possible that other normal cells that proliferate rapidly may also contain β_{II} in their nuclei.

The β_{II} isotype of tubulin has been found to be part of the nuclear matrix in mesangial cells and also has been shown to accumulate in the nucleolus. We know show that this is also the case for β_{II}-tubulin in LNCaP cells; nuclear fluorescence due to anti-β_{II} staining was detected in the nuclear matrix and the nucleolar remnants after chromatin digestion. The fact that tubulin has been reported to interact with chromatin *in vitro* (17) could be related to the functions of β_{II} in the nucleolus and the nuclear matrix. In the former case, β_{II} could be binding to the DNA regions, which contain the ribosomal RNA genes, whereas in the latter situation it could be functioning as a chromosomal scaffold. Interestingly, it is known that the anti-tubulin drug vinblastine affects biochemical processes that are seemingly unrelated to tubulin, such as DNA and RNA synthesis (18, 19). It is possible that its effects on these processes could occur through an interaction with nuclear β_{II}- tubulin.

We have shown that β_{II}-tubulin accumulates preferentially in the nuclei of cancer cells. Perhaps its role in the nucleus is to accelerate DNA and RNA synthesis and therefore facilitate proliferation. Alternatively, nuclear β_{II} may have no specific nuclear function, but rather a unique and as yet unknown function in the mitotic spindle; its location in the nucleus, therefore, may allow it to act quickly when mitosis begins. If either hypothesis were correct, it makes sense that nuclear β_{II} would be needed more in cancer cells, to assist rapid cell proliferation. In conclusion, one may speculate that nuclear β_{II} may become an interesting and novel target for cancer chemotherapy; a tubulin-specific drug whose major effects are on cancer cells would be very exciting.

ACKNOWLEDGMENTS

We thank Dr. Eugene Sprague for providing the human dermal fibroblasts, Dr. Mary Pat Moyer for providing the 506 smooth muscle cells and the HSK fibroblasts, Dr. John Lee for providing the osteoblasts, Dr. Nandini Chaudhuri for providing the LNCaP and the MCF-7 asnd MDA cells, and Dr. Arlette Fellous for providing the Calc 18 cells.

REFERENCES

1. Hyams, J.S., and Lloyd, C.W., (eds.), Microtubules, New York: Wiley-Liss, 1994.
2. Wilson, L., and Jordan, M.A. Pharmacological probes of microtubule function. *In*: J. S. Hyams and C. W. Lloyd (eds.), Microtubules, pp. 59-83. New York: Wiley-Liss, 1994.
3. Ludueña, R. F. Multiple forms of tubulin: different gene products and covalent modifications. Int. Rev. Cytol., *178*: 207-275, 1998.
4. Walss, C., Kreisberg, J.I., and Ludueña, R.F. Presence of the β_{II} isotype of tubulin in the nuclei of cultured mesangial cells from rat kidney. Cell Motil. Cytoskeleton, *42*: 274-284, 1999.
5. Banerjee, A., Roach, M. C., Wall, K. A., Lopata, M. A., Cleveland, D. W., and Ludueña, R. F. A monoclonal antibody against the type II isotype of β-tubulin. Preparation of isotypically altered tubulin. J. Biol. Chem., *263*: 3019-3034, 1988.
6. Banerjee, A., Roach, M. C., Trcka, P., and Ludueña, R. F. Preparation of a monoclonal antibody specific for the class IV isotype of β-tubulin. Purification and assembly of $\alpha\beta_{II}$, $\alpha\beta_{III}$, and $\alpha\beta_{IV}$ tubulin dimers from bovine brain. J. Biol.Chem., *267*: 5625-5630, 1992.
7. Roach, M. C., Boucher, V. L., Walss, C., Ravdin, P., and Ludueña, R. F. Preparation of a monoclonal antibody specific for the class I isotype of β-tubulin: the β isotypes of tubulin differ in their cellular distributions within human tissues. Cell Motil. Cytoskeleton, *39*: 273-285, 1998.

8. Fey, E. G., Wan, K. M. and Penman, S. Epithelial cytoskeletal framework and nuclear matrix-intermediate filament scaffold: three dimensional organization and protein composition. J. Cell Biol., *98*: 1973-1984, 1984.

9. Ranganathan, S., Salazar, H., Benetatos, C. A., and Hudes, G. R. Immunohistochemical analysis of β-tubulin isotypes in human prostate carcinoma and benign prostate hypertrophy. Prostate, *30*: 263-268, 1997.

10. Floege, J., Topley, N., Wessel, K., Kaever, V., Radeke, H.H., Hoppe, J., Kishimoto, T., and Resch, K. Monokines and platelet-derived growth factor modulate prostanoid production in growth arrested human mesangial cells. Kidney Int., *37*: 859-869, 1990.

11. Abboud, H.E., Poptic, E., and Dicorleto, P.E. Production of platelet–derived growth factor-like protein by rat mesangial cells in culture. J. Clin. Invest., *80*: 675-683, 1987.

12. Mene, P., Simonson, M.S., and Dunn, M.J. Physiology of the mesangial cell. Physiol. Rev., 69: 1347-1424, 1989.

13. Floege, J., Topley, N., and Resch, K. Regulation of mesangial cell proliferation. Am. J. Kidney Diseases., *17*: 673-676, 1991a.

14. Floege, J., Topley, N., Hoppe, J., Barrett, T.B., and Resch, K. Mitogenic effect of platelet-derived growth factor in human glomerular mesangial cells: modulation and/or suppression by inflammatory cytokines. Clin. Exp. Immunol., *86*: 334-341, 1991b.

15. Pabst, R., and Sterzel, R.B. Cell renewal of glomerular cell types in normal rats. An autoradiographic study. Kidney Int., *24*: 626-631., 1983.

16. Schocklmann, H.O., Lang, S., and Sterzel, R.B. Regulation of mesangial cell proliferation. Kidney Int., *56*: 1199-1207, 1999.

17. Mithieux, G., Roux, B., and Rousset, B. Tubulin-chromatin interactions: evidence for tubulin-binding sites on chromatin and isolated oligonucleosomes. Biochim. Biophys. Acta, *888*: 49-61, 1986.

18. Creasey, W.A. Modifications in biochemical pathways produced by the *Vinca* alkaloids. Cancer. Chemother. Res., *52*: 501-507, 1968.

19. Bernstam, V.A., Gray, R.H., and Bernstein, I.A. Effect of microtubule-disrupting drugs on protein and RNA synthesis in *Physarum polycephalum* Amoebae. Arch. Microbiol., *128*: 34-40, 1980.

FIGURE LEGENDS

Fig. 1. Detection of the tubulin β-isotypes, β_I, β_{II} and β_{IV} in cultured normal human cells. (*A, D, G, J, M*), Cells treated with anti-β_I by indirect immunfluorescence. (*B, E, H, K, N*), Cells treated with anti-β_{II} by indirect immunofluorescence. (*C, F, I, L, O*), Cells treated with anti-β_{IV} by indirect immunfluorescence. (*A-C*), Human dermal fibroblasts. (*D-F*), HSK fibroblasts. (*G-I*), MCF-10F breast endothelial cells. (*J-L*), Osteoblasts. (*M-O*), 506 smooth muscle cells.

Fig.2. Occurrence of β_{II}-tubulin in the nuclei of cultured human cancer cells. (*A, D, G*), Cells treated with anti-β_I by indirect immunfluorescence. (*B, E, H, J*), Cells treated with anti-β_{II} by indirect immunofluorescence. (*C, F, I*), Cells treated with anti-β_{IV} by indirect immunofluorescence. (*A-C*), LNCaP prostate carcinoma cells. (*D-F*), MCF-7 breast carcinoma cells. (*G-I*), MDA breast carcinoma cells. (*J*), Calc 18 breast carcinoma cells.

Fig. 3. Subcellular localization of β_{II}-tubulin in LNCaP cells. (*A*), Cytosol-extracted cells treated with anti-β_{II}. (*B*), Same cells as in A, stained with DAPI. (*C*), Cytosol- and chromatin-extracted cells treated with anti-β_{II}. (*D*), Same cells as in C, stained with DAPI. The almost complete absence of fluorescence indicates that most of the chromatin was successfully removed. (*E*), Cytosol-extracted cells treated with anti-β_{II} that had been blocked with its peptide epitope. (*F*), Same cells as in E, stained with DAPI to show position of nuclei. (*G*), Cytosol- and chromatin-extracted cells treated with anti-β_{II} that had been previously blocked with its peptide epitope. Note the absence of fluorescence.

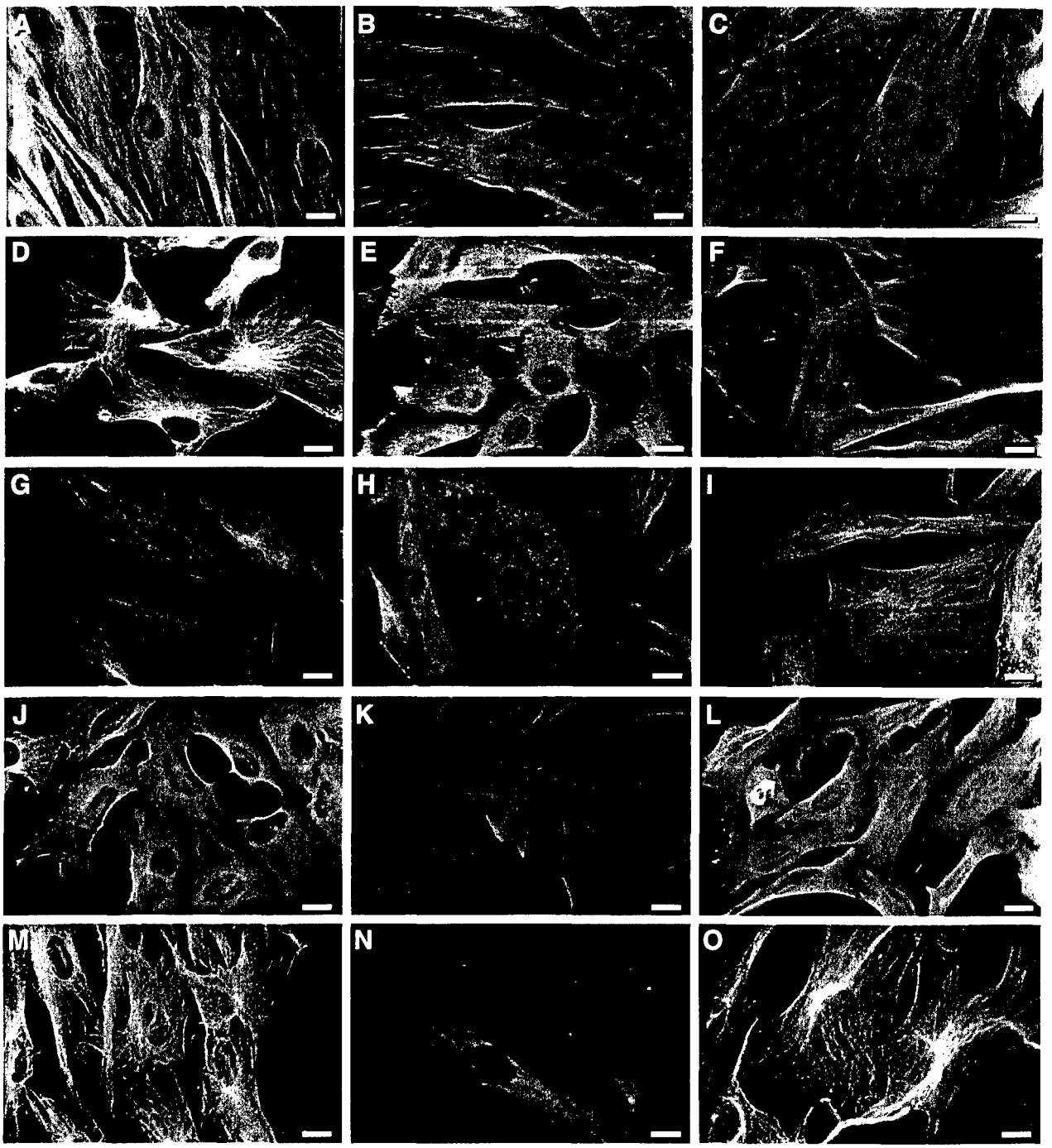

Figure 1

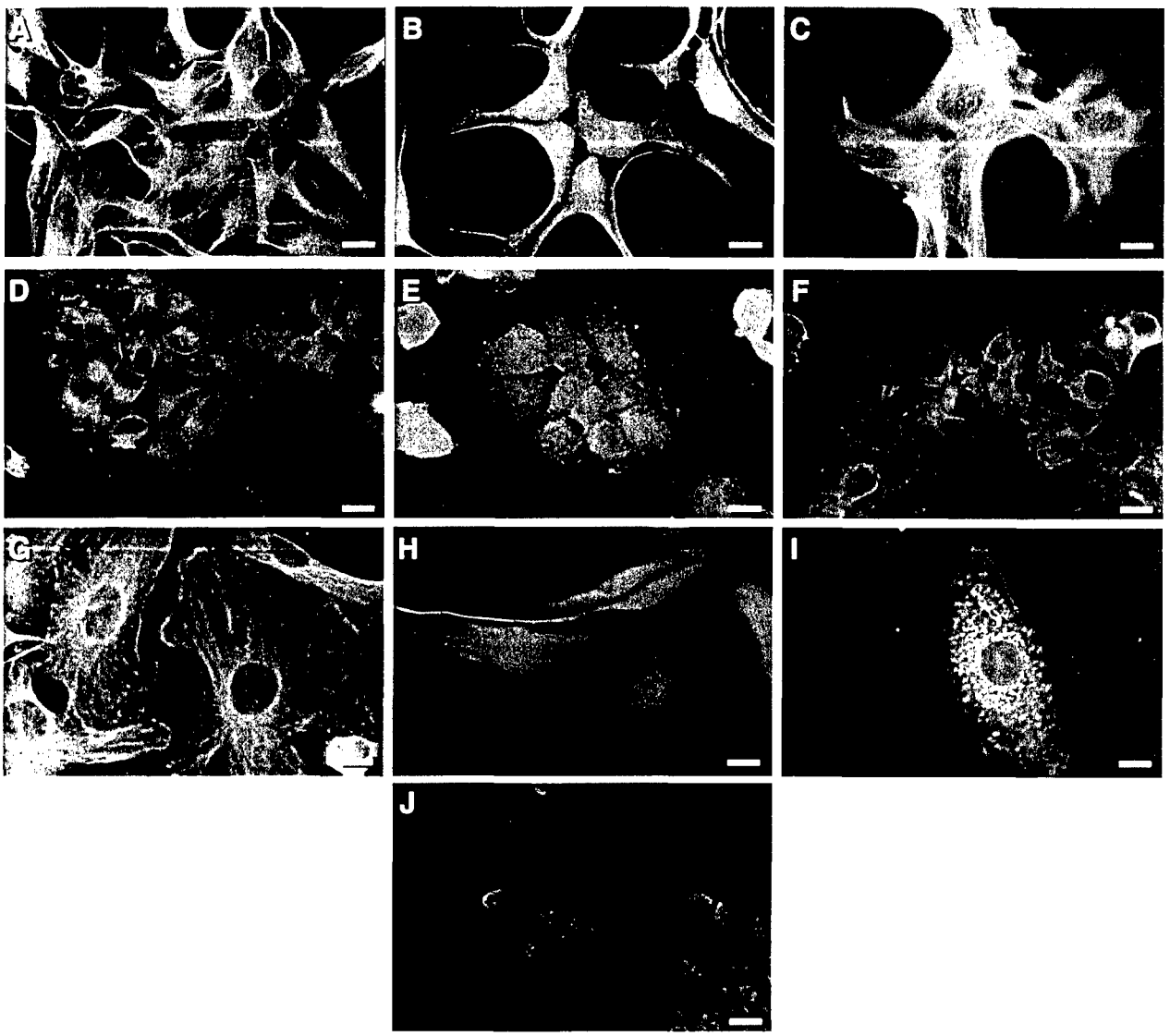

Figure 2

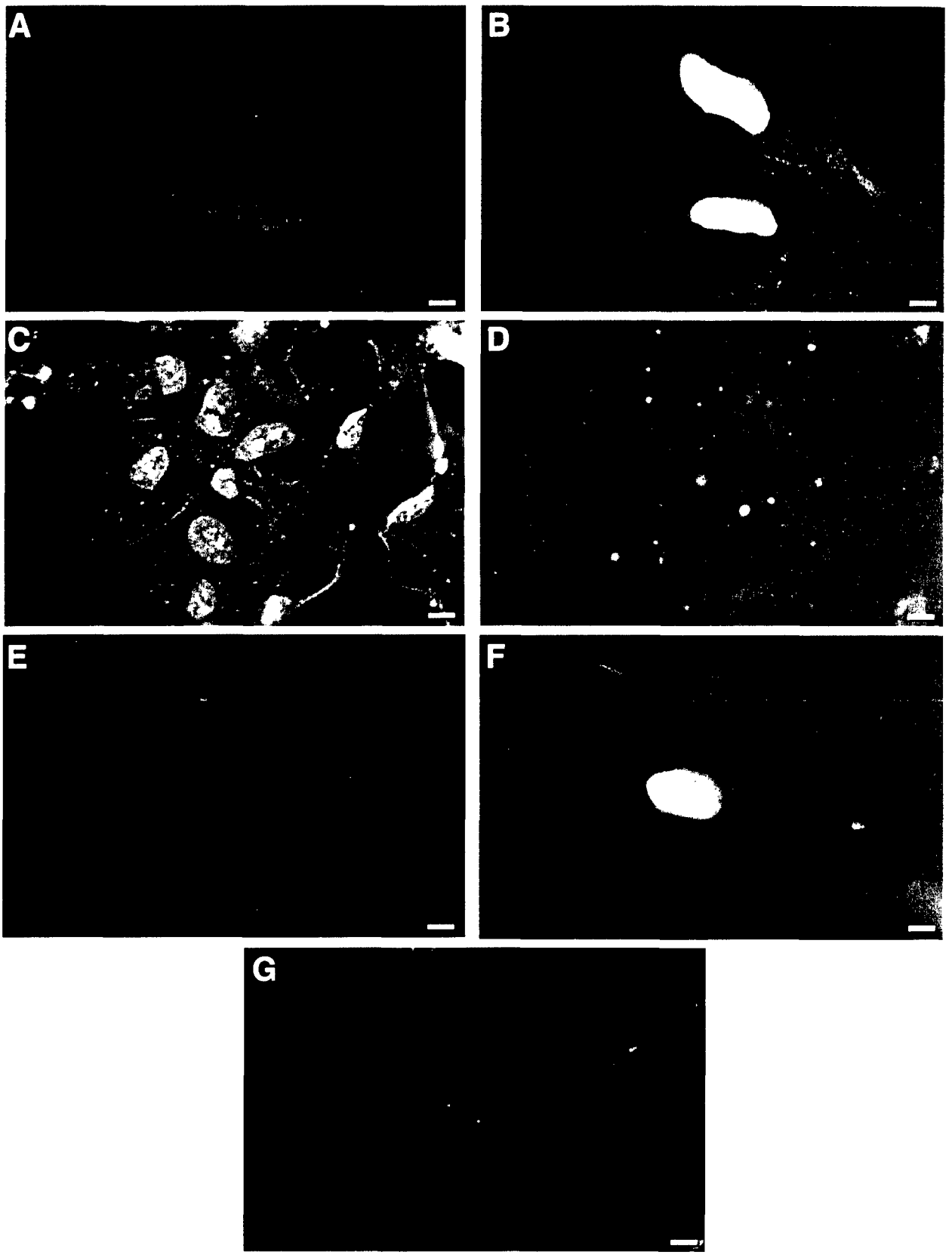

Figure 3

Appendix 8

Differential Expression of β Tubulin Isotypes in Gerbil Nasal Epithelia

KAREN WOO[1], RICHARD F. LUDUEÑA[2], AND RICHARD HALLWORTH[3]

[1]The Medical School, [2]Department of Biochemistry, and [3]Department of Otolaryngology-Head and Neck Surgery, The University of Texas Health Science Center at San Antonio, San Antonio, Texas 78229-3900

Running Head: Beta Tubulin in the Nose
Target Journal: Cell and Tissue Research
Corresponding Author:
Richard Hallworth
Department of Biomedical Sciences
Creighton University
2500 California Plaza
Omaha, NE 68179
Ph: (402) 280-3057
FAX: (402) 280-2690
Email: hallw@creighton.edu

Summary

The mammalian β isoform of tubulin, the major protein of microtubules, is known to exist in seven isotypes with remarkably similar amino acid sequences, and evidence for separate functions for the isotypes has been lacking. If β tubulin isotypes have separate functions, this should be reflected in patterns of isotype expression that differ by cell type, or even by sorting of isotypes to pools within the cell. Olfactory epithelia offer two cell types, the sensory neurons and the respiratory epithelial cells, that bear microtubule-containing organelles called kinocilia. Comparison of microtubules in these kinocilia, with those elsewhere in the cells, offers the opportunity to look for sorting of isotypes to within-cell pools. To characterize the expression of β tubulin isotypes in olfactory and respiratory epithelium, gerbil nasal epithelium was examined using specific antibodies to four β tubulin isotypes (β_I, β_{II}, β_{III}, and β_{IV}). Three of the isotypes (β_I, β_{II}, and β_{III}) were expressed in the dendrites, soma and axons of olfactory neurons, and in basal cells, but olfactory sensory kinocilia instead contained β_I, β_{III} and β_{IV}. The kinocilia of respiratory epithelial cells contained only β_I and β_{IV}, suggesting that, even in kinocilia, functional differences may be reflected in differences in isotype expression. Our results therefore providing strong corroborative evidence for the hypothesis that β tubulin isotypes have specific functions.

Key Words: *Tubulin isotypes, β tubulin, olfactory neuron, respiratory epithelium, kinocilium*

Introduction

Microtubules perform a variety of functions in the eukaryotic cell, ranging from providing cell strength and rigidity to controlling movement within the cell. Microtubules consist of heterodimers of α and β tubulin, both of which exist as numerous isotypes. Seven isotypes of mammalian β tubulin have been shown to exist, termed β_I, β_{II}, β_{III}, β_{IVa}, β_{IVb}, β_V and β_{VI} (Ludueña 1998). However, little is known about the significance of the existence of these seven isotypes, except that the β_{IVb} isotype appears to be associated with axonemal microtubules (Renthal et al. 1993; Lu et al. 1998; Roach et al. 1998). The β-tubulin isotypes are among the most highly conserved proteins known (Ludueña 1998). Yet, it has been found that different cell types express different isotypes in the same tissue (Roach et al., 1998; Hallworth and Ludueña, 2000).

The multi-tubulin hypothesis (Fulton and Simpson 1976) proposes that the different tubulin isotypes have specific functional roles. A consequence of this hypothesis is that β tubulin isotypes should be differentially expressed in different cell types or even be sequestered to different compartments in the same cell. Preliminary evidence suggests that β-tubulin isotypes are segregated to different pools within vestibular hair cells (Perry et al., 2001). Specifically, the body of the hair cell contains the β_I, β_{III} and β_{IV} isotypes, but the kinocilium, an axoneme-like structure, contains only β_{IV}.

In olfactory epithelia, microtubules exist in discreet populations within sensory neurons (Burton, 1992). Olfactory kinocilia, which extend from the dendritic bulb at the external surface, contain the 9+2 arrangement of microtubules typical of an axoneme, but are not motile. Within the neural dendrites, microtubules are longitudinally arranged (Graziadei, 1973). The soma of the olfactory neuron represents a distinct compartment for microtubules and the axons may contain yet another population of microtubules. In addition, bordering the olfactory sensory epithelia is respiratory epithelium, whose cells contain a population of motile kinocilia.

The variety of microtubule populations in olfactory and respiratory epithelia therefore offers a rich opportunity to investigate the multi-tubulin hypothesis. This study was designed to determine if any of the potential pools of microtubules in nasal epithelia contain different β tubulin isotypes. The distribution of β tubulin isotypes in the gerbil nasal epithelium has therefore been examined using isotype-specific antibodies and indirect immunofluorescence. While some overlap in tubulin isotype expression was found, other isotypes were selectively expressed in different cell types. In sensory neurons, the isotypes found in kinocilia are different ~~to~~ from those elsewhere in the cell, thus demonstrating sorting of isotypes in olfactory neurons. Further, the isotypes in sensory kinocilia are different ~~to~~ from those in respiratory kinocilia. Our results are therefore consistent with and reinforce the multi-tubulin hypothesis.

Portions of this study have been presented elsewhere in abstract form (Woo et al., 2001).

Materials and Methods

The expression of β tubulin isotypes was examined in gerbil nasal epithelium using indirect immunofluorescence in sections of sensory and respiratory epithelium. Adult gerbils (22 days old or older) were anesthetized with Nembutal and cardiac-perfused with 4% paraformaldehyde in phosphate buffered saline (PBS). Nasal epithelium was then dissected away from the septum. The epithelium was then rinsed in PBS and immersed in solutions of sucrose as a cryoprotectant (30 minutes with agitation at room temperature at concentrations of, successively, 10% sucrose; 2:1 10%:30% sucrose; 1:1 10%:30% sucrose; 1:2 10%:30% sucrose; and 30% sucrose). Transepithelial frozen sections, 10 μm thick, were cut after freezing in O.C.T (Tissue-Tek, Miles Laboratories). Sections were blocked and permeabilized in PBS containing 1% bovine serum albumin (BSA), 0.25% Triton-X100 and 1% normal goat serum for 3 hours at room temperature and then rinsed in PBS plus 0.1% BSA. Sections were then labeled with primary antibodies specific for β tubulin isotypes, raised in mouse, for 3 hours at room temperature, rinsed in PBS plus 0.1% BSA, and labeled with secondary antibody (goat anti mouse IgG coupled to F.I.T.C, Sigma), for 3 hours at room temperature. Sections were rinsed in PBS plus 0.1% BSA and then sealed under cover slips on glass slides in 50% PBS:50% glycerol containing 1% *n*-propylgallate. Sections were examined under a Zeiss Axioskop II microscope equipped for epifluorescence with 40x and 100x oil-immersion objectives. Images were acquired digitally using a Spot RT cooled digital camera.

The monoclonal antibodies used to localize the different tubulin isotypes had the following specificities: β_I (SAP.4G5), β_{II} (JDR.3B8), β_{III} (SDL.3D10), and β_{IV} (ONS.1A6). The antibodies were prepared and tested as previously described (Banerjee et al., 1988, 1990, 1992; Roach et al., 1998). Each antibody was prepared to an epitope unique to the C-terminus of that isotype. Since the C-termini

of β_{IVa} and β_{IVb} are virtually identical, the anti-β_{IV} antibody was unable to discriminate between them. Negative controls were performed by omitting the primary antibody.

Animal care and handling was performed in conformance with approved protocols of the U.T.H.S.C.S.A. Institutional Animal Care and Use Committee.

Results

The sensory epithelium of the nose consists of a pseudo-stratified layer of round cell bodies. The lowest layer of cell bodies consists of basal cells, which are embryonic olfactory neurons, and the middle layer is the somas of the mature sensory neurons. Each neuron sends a dendritic process to the epithelial surface, and an axonal process away from the epithelium to the olfactory bulb. The long sensory kinocilia arise from a small swelling at the apical surface of the dendrite, termed the dendritic bulb. Above the neuronal somata are the cell bodies of supporting cells whose processes span the epithelium and intercalate between neurons. The respiratory epithelium consists of a thin uniform layer of epithelial cells bearing multiple short kinocilia.

β_I

In the sensory portion of the nasal epithelium, label for β_I tubulin was found in the olfactory neurons and basal cells (Figure 1A). The label consisted of, first, a bright, slightly irregular strip along the free surface of the olfactory epithelium, likely representing the receptor kinocilia (*kc*). Fine strands of label were also seen to be running perpendicular to the kinocilia layer, apparently representing the dendrites of the sensory neurons. Deeper in the epithelium, labeling was evident in the somas of the olfactory neurons (*sn*) and basal cells (*b*). The nuclei of supporting cells (*s*) were unlabeled. Irregularly shaped bundles of bright label, likely representing the axons of olfactory neurons, were present in scattered locations deep in the epithelium (*ax*).

In the respiratory portion of the epithelium (Figure 1B), labeling for β_I was ~~limited to~~ mainly the kinocilia layer (*kc*), similar to the labeling present in the olfactory portion. ~~Little or no~~ significantly less label was seen elsewhere in the respiratory epithelium (*re*).

COMMENT #1

{insert Figure 1 near here}

β_{II}

Inspection of the labeling pattern for β_{II} in the olfactory sensory epithelium (Figure 2A) failed to reveal ~~any revealed~~ any label at the epithelial surface, ~~which suggested~~ suggesting that β_{II} was not present in olfactory kinocilia. Fine strands of dendritic labeling (*d*) ran from the superficial aspect of the epithelium to the deeper layers and terminated in the neuronal soma layer (*sn*), similar to the pattern of β_I tubulin. Deeper in the epithelium, label in the basal cells (*b*) also resembled that observed with β_I. As with β_I, no label was observed in the nuclei of the supporting cells (*s*). Beneath the epithelium, bright labeling in the axon bundles was found (*ax*).

In the respiratory epithelium (Figure 2B), ~~no~~ almost no labeling with antibodies to β_{II} tubulin was detected. The figure illustrates the abrupt transition from the label present in the thicker sensory epithelium (*se*) to the relative absence of label in the thinner respiratory epithelium (*re*).

{insert Figure 2 near here}

β_{III}

In the olfactory sensory epithelium (Figure 3A), β_{III} tubulin was found in the receptor kinocilia layer (*kc*). The somas (*sn*) and dendrites (*d*) of the sensory neurons, and the basal cells (*bc*), were labeled in a pattern identical to that of β_I and β_{II}. No label was seen in the supporting cells (*s*). The axon bundles (*ax*) deep in the sub-epithelial tissue contained bright speckles of label.

β_{III} ~~was not~~ appeared to be virtually absent from detected in the respiratory epithelium (Figure 3B). In fact, as shown in the figure, the labeling ~~stopped~~ appeared to abruptly at the junction between olfactory sensory epithelium (*se*) and the respiratory epithelium (*re*).

{insert Figure 3 near here}

4. β_{IV}

β_{IV} was very prominent in the kinocilia layer of the sensory epithelium (Figure 4A). ~~No~~ Almost no label was observed in the remainder of the sensory epithelium (*se*), or in the axons.

In the respiratory epithelium (Figure 4B), β_{IV} was almost entirely found in ~~limited to~~ the kinocilia. The label in respiratory kinocilia was very bright compared to the label in olfactory kinocilia. No label was present elsewhere in the respiratory epithelium (*re*), which may be compared to the sensory epithelium (*se*).

{insert Figure 4 near here}

COMMENT #3

Discussion

β Tubulin isotypes in cells of the nasal epithelium

The results of this study are summarized in Table 1 and depicted in Figure 5. Olfactory neurons were found to express all four isotypes studied. However, the distribution of the isotypes within the cell differed. The dendrites, soma and axons of olfactory neurons contained three isotypes (β_I, β_{II} and β_{III}) while the receptor kinocilia layer contained β_I, β_{III} and β_{IV}. This suggests that olfactory neurons are able to sort β tubulin isotypes into different cellular compartments. In the respiratory epithelium, the outermost kinocilia layer contained β_I and β_{IV}. No significant label was found in the cell bodies of respiratory epithelial cells.

All isotypes found in sensory neuron soma were always also found in basal cells, which are embryonic developing neurons. Thus it is likely that the distribution of β tubulin isotypes in olfactory neurons is unchanged (apart from the kinocilia) throughout the 40 to 60 day life of the neurons. This is unlike the olfactory marker protein (OMP; Margolis, 1972) which is expressed in mature sensory neurons only. Thus it is unlikely that expression of OMP is linked to β tubulin isotypes in any significant way.

{insert Figure 5 near here}

The label in the kinocilia layer of sensory neurons appears to be in the kinocilia themselves rather than in the dendritic bulbs. Each olfactory neuron bears 10-25 fine kinocilia that together appear as a dense mat (Morrison and Costanzo, 1992). If label were present only in the dendritic bulbs, we would expect a more punctate appearance to the label. We also do not believe that the label in the kinocilia layer represents non-specific binding due to contamination by olfactory mucus. The sharp transition between β_{III} labeled sensory kinocilia and unlabeled respiratory in Figure 3B argues strongly against the existence of non-specific label in kinocilia layers of these specimens.

We did not see label for any β tubulin isotype in the supporting cells of olfactory sensory epithelium, or in the cell body of respiratory epithelial cells. Undoubtedly these cells have at least some microtubules, although they may be few in number. It is possible that faint label from one of our antibodies may have been obscured by the relatively bright label in other cells, or that other isotypes may be present.

β Tubulin isotypes in kinocilia

The variety of isotypes expressed in a single organelle type, the kinocilium, is most intriguing. It is not surprising that β_{IV} should be so prominent in kinocilia since, of all the vertebrate β isotypes, β_{IV} is the one that comes closest to having a functional assignment, as the β isotype of axonemes. β_{IV} has been localized by immuno-electron microscopy to the axonemal microtubules of bovine retinal rod cells and bovine tracheal ~~kino~~cilia (Renthal et al., 1993). It is also the only one of the four isotypes found in oviduct epithelial ~~kino~~cilia (Roach et al., 1998), and mouse sperm flagella (Lu et al., 1998). The presence of β_{IV} in axonemes is also consistent with the prediction of Raff et al. (1997) who postulated that, for a β isotype to be in an axonemal microtubule, it must have the sequence EGEFEEE near its C-terminus. β_{IV} (both β_{IVa} and β_{IVb}) is the only vertebrate isotype that contains this sequence (Ludueña, 1998). This speculation seemed to be confirmed by the finding of only β_{IV} in vestibular hair cell kinocilia (Perry et al. 2001). However, olfactory sensory kinocilia are here shown to contain β_{I}, β_{III} and β_{IV}, and olfactory respiratory epithelial kinocilia contain β_{I} and β_{IV}. The underlying structure of these three kinocilia types is similar – each contains the familiar 9+2 arrangement of axonemal microtubules – but the functions of the kinocilia are nonetheless altogether different. The single kinocilium of vestibular hair cells is rigid and connects a mechanically-responsive membrane (the otolithic membrane in macular organs, the cupula in ampullary organs) to the mechanically-sensitive stereociliary bundle of the hair cell. In contrast, the multiple kinocilia of olfactory sensory neurons are flexible and provide a

surface for the olfactory receptor molecules. Further, the short, motile kinocilia of olfactory respiratory epithelial cells function to move mucous around the organ, and are therefore perhaps the only kinocilia in this study to contain the motile protein dynein.

Table 2 presents these findings in summary form. Every type of kinocilium so far examined has a different β tubulin isotype composition. The only common feature ~~of the isotype composition~~ is the presence of β_{IV}. While it remains to be seen what might be the function of each isotype, or combination of isotypes, it is clear from these studies that cells can exquisitely tailor the isotype composition of even such a stereotypical structure as the axoneme in order to meet their needs.

The multi-tubulin hypothesis

The multi-tubulin hypothesis proposes that multiple tubulin isotypes exist in separate pools within the same cell, and are differentially expressed between cell types of the same tissue, due to their specific physiologic functions (Ludueña 1998). We saw evidence of compartmentalization of tubulin isotypes in olfactory neurons, as well as in the respiratory epithelial cell. In olfactory neurons, three of the four isotypes studied were present in the kinocilia, whereas a different three isotypes were present in the dendrite, soma and axon. Thus this study provides strong support for the existence of separate pools of β tubulin isotypes within olfactory neurons.

In its original formulation, the multi-tubulin hypothesis (Fulton and Simpson 1976) envisaged specific functions for each isotype. The complexity of the isotype expressions patterns that have so far been observed, in which even neighboring cells of apparently similar function in the same organ express different isotype panels (Roach et al. 1998, Hallworth and Ludueña 2000, Perry et al. 2001), seemingly refutes this form of the hypothesis. In the cochlea, for example, it is almost the case that no two cell types express the same panel of isotypes (Hallworth and Ludueña 2000). Only the adjacent inner and outer pillar cells in the cochlea express the same isotypes (β_{II} and β_{IV}); even the inner and outer hair

cells express different isotypes (β_I and β_{IV} versus β_{II} and β_{IV}, respectively). In vestibular hair cells, β_I, β_{III} and β_{IV} are found, while in the adjacent supporting cells the isotypes seen are β_I, β_{II} and β_{IV}. Thus, ascribing a single function to a single isotype has proved impossible, at least at our present level of understanding about function. The fact remains, however, that cells purposely select a panel of β tubulin isotypes to express from the seven isotypes, and even sort the isotypes to separate within-cell pools. The function of this selectivity remains obscure but intriguing.

(Bergeron, 2001)

Acknowledgments

Supported by N.I.H. grant CA26376 and Welch Foundation grant AQ-0726 to R.F.L. and N.I.H. grant DC02053 to R.J.H. We thank Joseph Kaeller and Heather Jensen for technical assistance, Stan McGruff for initial assistance in the preparation of olfactory epithelium, and Laurence Dryer for sage advice.

) Army grant DAMD17-98-1-8246)

References

Banerjee A, Roach MC, Wall KA, Lopata MA, Cleveland DW, Ludueña RF (1988) A monoclonal antibody against the type II isotype of β-tubulin. Preparation of isotypically altered tubulin. J. Biol. Chem. 263:3029-3034.

Banerjee A, Roach MC, Trcka P, Ludueña RF (1990) Increased microtubule assembly in bovine brain tubulin lacking the type III isotype of β-tubulin. J. Biol. Chem. 265:1794-1799.

Banerjee A, Roach MC, Trcka P, Ludueña RF (1992) Preparation of a monoclonal antibody specific for the class IV isotype of β-tubulin. Purification and assembly of $\alpha\beta_{II}$, $\alpha\beta_{III}$, and $\alpha\beta_{IV}$ tubulin dimers from bovine brain. J. Biol. Chem. 267:5625-5630.

Burton PR (1992) Ultrastructural studies of microtubules and microtubule organizing centers of the vertebrate olfactory neuron. Micros. Res. And tech. 23:142-156.

Fulton C, Simpson PA (1976) Selective synthesis and utilization of flagellar tubulin. The multi-tubulin hypothesis. In: Goldman R, Pollard T, Rosenbaum J. (eds) Cell Motility, vol. 3. Cold Spring Harbor Laboratory Press, New York, NY, pp. 987-1005.

Graziadei PPC (1973) The ultrastructure of vertebrates olfactory mucosa. In Friedmann I (ed) The ultrastructure of sensory organs. North Holland, Amsterdam, pp 267-305.

Hallworth R, Ludueña RF (2000) Differential expression of β tubulin isotypes in the adult gerbil organ of Corti. Hear. Res. 148:161-172.

Lu Q, Moore GD, Walss C, Ludueña RF (1998) Structural and functional properties of tubulin isotypes. Adv. Struct. Biol. 5:203-227.

Ludueña RF (1998) The multiple forms of tubulin: Different gene products and covalent modifications. Int. Rev. Cytol. 178:207-275.

Margolis F (1972) A brain protein unique to the olfactory bulb. P.N.A.S. 69:1221-1224.

Morrison EE, and Costanzo RM (1992) Morphology of olfactory epithelium in muman and other vertebrates. Microsc. Res. And Tech. 23:49-61.

Perry BP, Ludueña RF, Hallworth R (2001) Localization of β Tubulin Isotypes in Vestibular Tissues. Assoc. Res. Otolaryngol. Abs. P. 17.

Raff EC, Fackenthal JD, Hutchens JA, Hoyle HD, Turner FR (1997) Microtubule architecture specified by a β-tubulin isoform. Science 275:70-73.

Renthal R, Schneider BG, Miller MA, Ludueña RF (1993) β_{IV} is the major β-tubulin isotype in bovine cilia. Cell Motil. Cytoskeleton 25:19-29.

Roach MC, Boucher VL, Walss C, Ravdin, PM, Ludueña RF (1998) Preparation of a monoclonal antibody specific for the class I isotype of β-tubulin:The β isotypes of tubulin differ in their cellular distributions within human tissues. Cell Motil. Cytoskeleton 39:273-285.

Woo K, Ludueña RF, Hallworth R (2001) Localization of β Tubulin Isotypes in Nasal Epithelia. Assoc. Res. Otolaryngol. Abs. p. 111.

Figures

Figure 1. A) Section of olfactory sensory epithelium stained for β_I tubulin, showing label in the somas (*sn*) and dendrites (*d*) of sensory neurons, in basal cells (*b*), in the axons of sensory neurons (*ax*), and in the kinocilia (*kc*). No label is present in the nuclei of supporting cells (*s*). B) Section of respiratory epithelium (*re*) stained for β_I tubulin, showing label in the kinocilia only (*kc*). Scale bar = 25 μm.

Figure 2. A) Section of olfactory sensory epithelium stained for β_{II} tubulin, showing label in the somas (*sn*) and dendrites (*d*) of sensory neurons, in basal cells (*b*), and in the axons of sensory neurons (*ax*). No label is present in the nuclei of supporting cells (*s*). Note the absence of label in the kinocilia. B) Section showing transition between sensory epithelium (*se*) and respiratory epithelium (*re*) stained for β_{II} tubulin, showing complete absence of label in respiratory epithelium. Scale bar = 25 μm.

Figure 3. A) Section of olfactory sensory epithelium stained for β_{III} tubulin, showing label in the somas (*sn*) and dendrites (*d*) of sensory neurons, in basal cells (*b*), in the axons of sensory neurons (*ax*), and in the kinocilia (*kc*). No label is present in the nuclei of supporting cells (*s*). B) Section showing transition between sensory epithelium (*se*) and respiratory epithelium (*re*) stained for β_{III} tubulin, showing complete absence of label in respiratory epithelium. Scale bar = 25 μm.

Figure 4. A) Section of olfactory sensory epithelium stained for β_{IV} tubulin, showing absence of label in the sensory epithelium (*se*), except for the kinocilia (*kc*). B) Section showing transition between sensory epithelium (*se*) and respiratory epithelium (*re*) stained for β_{IV} tubulin, showing strong label in the respiratory kinocilia (*kc*). Scale bar = 25 μm.

Figure 5. Diagram of the distribution of β tubulin isotypes in the microtubule compartments of olfactory epithelial cells and olfactory neurons, based on the results of this study.

Table 1

Summary of the results of this study.

Sensory Epithelium

	β_I	β_{II}	β_{III}	β_{IV}
Kinocilia	✓	x	✓	✓
Dendrites	✓	✓	✓	x
Somas	✓	✓	✓	x
Axons	✓	✓	✓	✓
Support cells	x	x	x	x

Respiratory Epithelium

	β_I	β_{II}	β_{III}	β_{IV}
Epithelial kinocilia	✓	x	x	✓
Epithelial cells	x	x	x	x

Table 2

Distribution of β tubulin isotypes in kinocilia of various kinds.

Source	β_I	β_{II}	β_{III}	β_{IV}	Function of kinocilium
Vestibular hair cells	x	x	x	✓	Attach motion detection membrane (cupula, otolithic membrane) to the stereocilia bundle for transduction
Olfactory sensory neurons	✓	x	✓	✓	Bear olfactory receptor molecules for transduction
Olfactory respiratory epithelial cells	✓	x	x	✓	Motile – move olfactory mucous

Figure 1

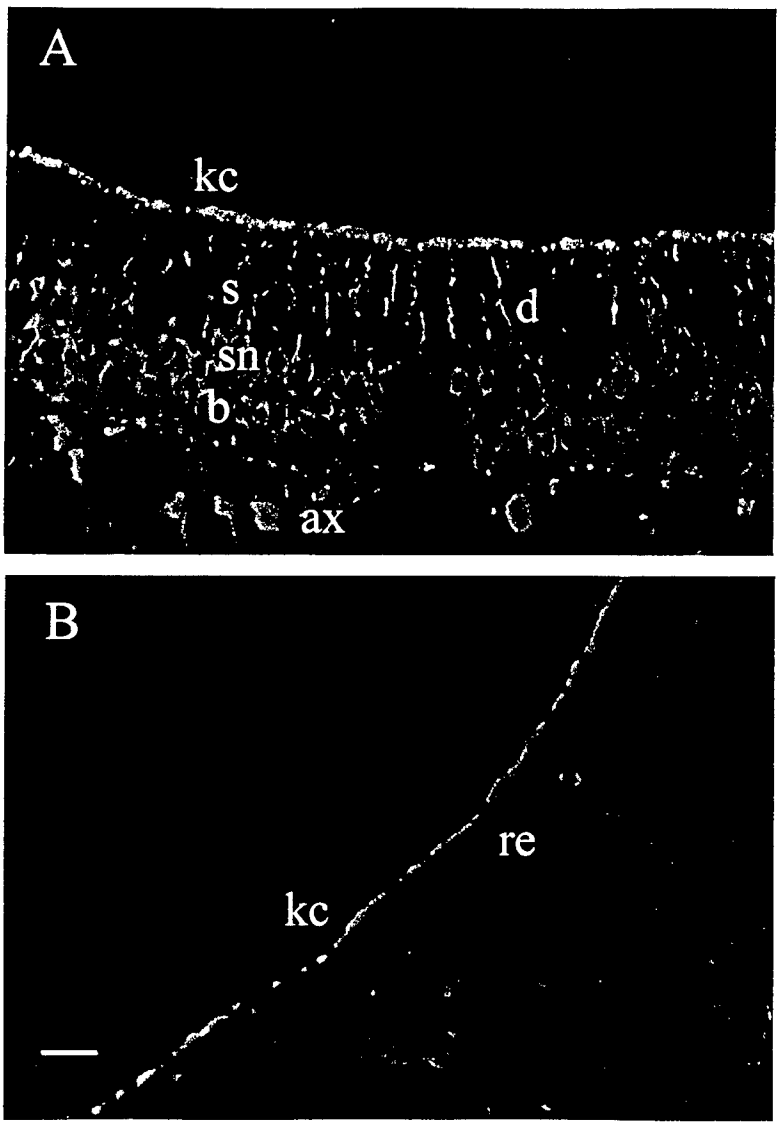

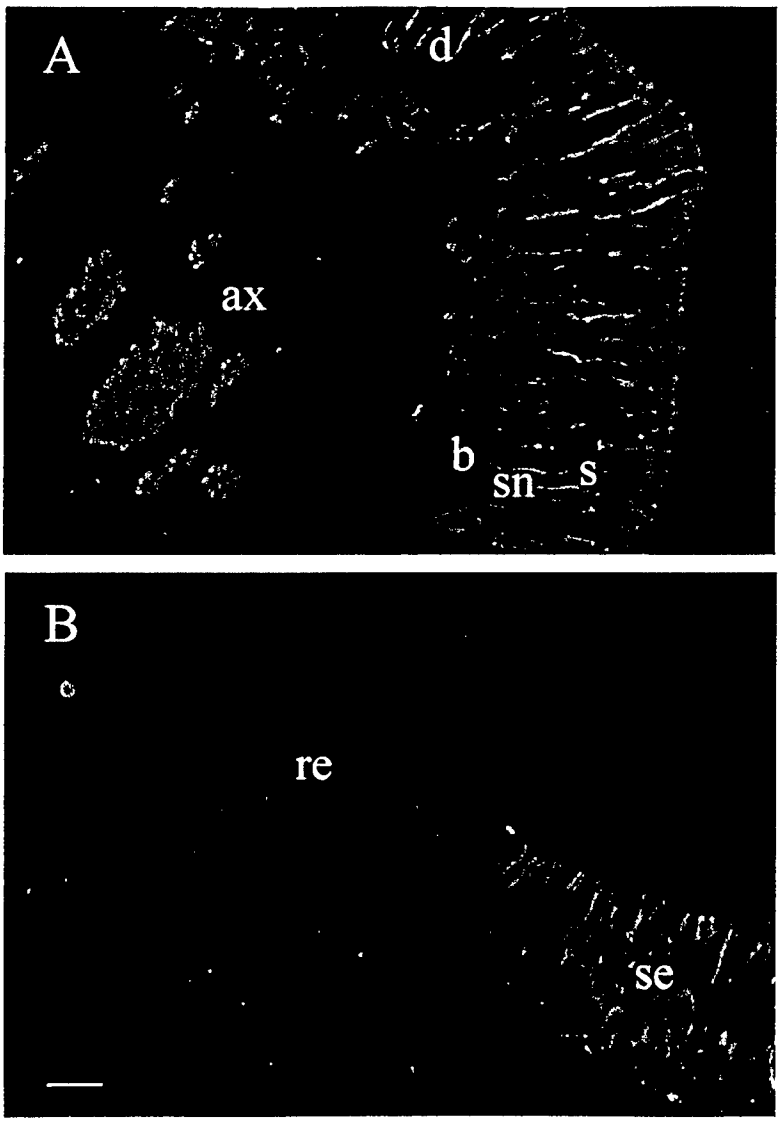
A
d
ax
b
sn
s
B
re
se

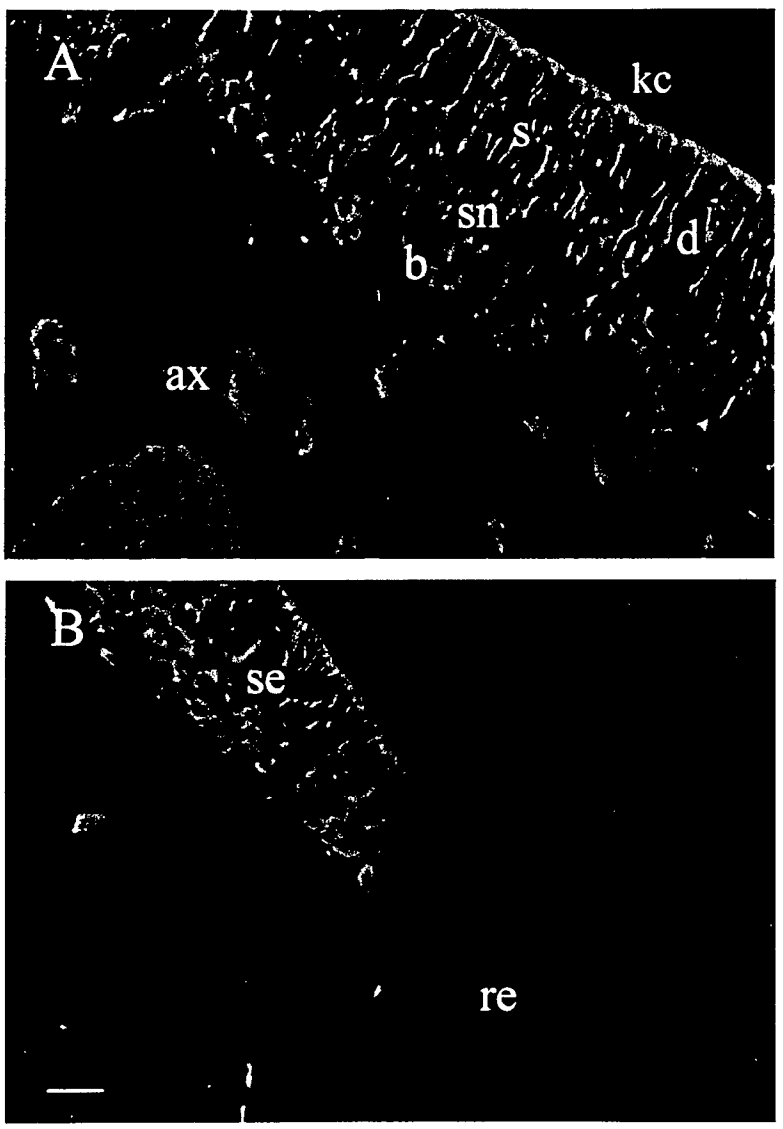
A
kc
s
sn
d
b
ax
B
se
re

Figure 4

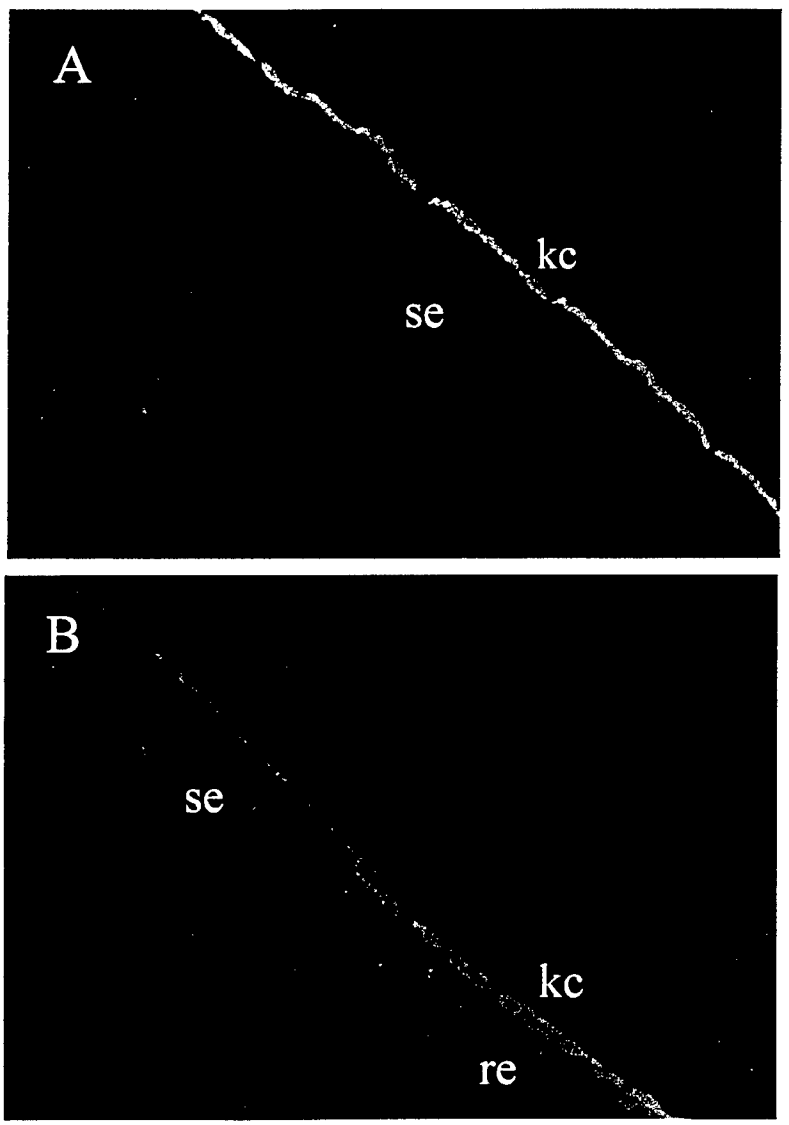

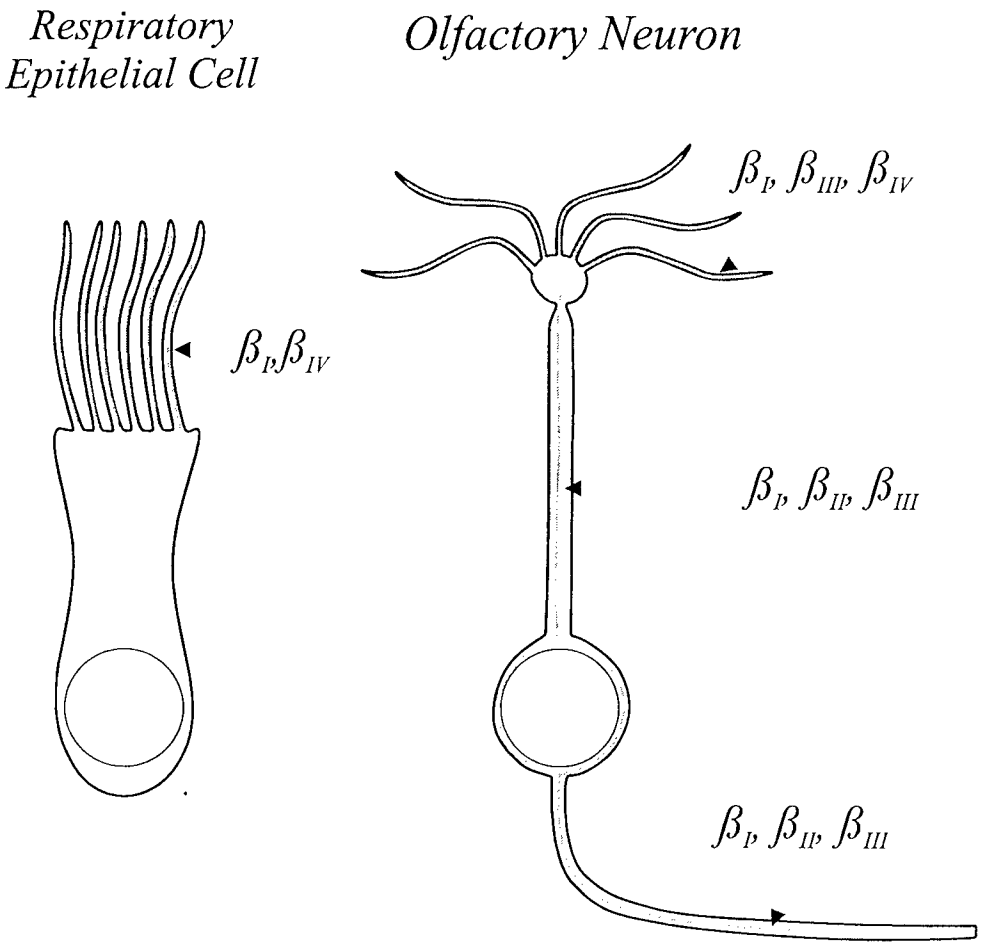
Respiratory Epithelial Cell
Olfactory Neuron
β_I, β_{IV}
$\beta_I, \beta_{III}, \beta_{IV}$
$\beta_I, \beta_{II}, \beta_{III}$
$\beta_I, \beta_{II}, \beta_{III}$

Richard F. Ludueña, Ph.D.
DAMD17-98-1-8246

Appendix 9

Abstracts

#905 TUBULIN CONTENT AND β-TUBULIN ISOTYPE DISTRIBUTION IN CELL LINES USED IN THE NCI IN VITRO DRUG SCREEN. Pascal Verdier-Pinard, Ruoli Bai, Richard F Luduena, Asok Banerjee, Edward A Sausville, and Ernest Hamel, *National Cancer Inst, Frederick, MD, National Cancer Institute-FCRDC, Frederick, MD, S A I C-Frederick, Frederick, MD, and Univ of Texas Health Sci Ctr, San Antonio, MD*

We have undertaken the characterization of the tubulin content and β-tubulin isotype distribution of the cell lines used in the NCI drug screen, using a competitive ELISA assay, as part of the molecular characterization of these cell lines. An additional goal was to determine whether total tubulin content and/or isotype distribution play a role in the differential cytotoxicity pattern observed with anti-tubulin drugs. As of October 1999, we have examined a first set of cytosolic extracts from 34 cell lines for their content of total β-tubulin and of isotypes II, III and IV. These data were analysed in terms of possible correlation between tubulin or β-tubulin isotype content and the relative potency of five antimitotic drugs in these cell lines. We found that β-tubulin content could be a sensitivity marker for antimitotic drugs in melanoma cells, that β_{IV}-tubulin content in leukemia cells and that β_{III}-tubulin content in melanoma cells, as well as in lung and CNS tumor cells, could be such markers. So far, neither total β-tubulin nor isotype content were such markers in ovarian and breast cancer cell lines. We are currently performing a large scale ELISA study with a second set of cytosolic extracts from each of the 60 cell lines to extend our first set of data. An initial study on γ-tubulin content has been launched. Status reports will be presented.

#3522 NUCLEAR TUBULIN AS A POSSIBLE MARKER FOR BREAST CANCER CELLS. Consuelo Wales, P. Barbier, M. Banerjee, M. C Bissery, R. F Luduena, and A. Fellous, *Lab de Pharmacologie Experimentale et Clin, Paris, France, Rhone-Poulenc Rorer S A, Vitry sur Seine, France, and Univ of Health Sci Ctr, San Antonio, TX*

Tubulin has generally been thought to be entirely a cytosolic protein, but a recent study (Walss et al., *Cell Motil. Cytoskeleton* **42,** 274, 1999) found the β_{II} isotype of tubulin, in non-microtubule form, in the nuclei of cultured rat kidney mesangial cells. Here we show, by immunoperoxidase staining, that β_{II}-tubulin localizes to the nuclei of breast tumor cells *in situ* whereas the non-tumor cells which surround the cancerous tissue lack nuclear tubulin. Immunofluorescence microscopy shows the presence of substantial amounts of β_{II} in the nuclei of MCF-7 breast cancer cells while the non-transformed MCF10-F cells have variable amounts of nuclear β_{II}, ranging from similar levels to MCF-7 cells to undetectable. We also observed nuclear β_{II} in tumor tissue obtained from mice which had been implanted with Calc 18 breast cancer cells. We have also found β_{II} in the nuclei of prostate cancer cells. These results suggest that transformation may lead to localization of β_{II} in cell nuclei, serving an as yet unknown function, and that nuclear β_{II} may be a useful marker for detection of breast tumor cells *in situ.* [Supported by grants to R.F.L. from the US Army (DAMD17-98-1-8246), the NCI (CA26376) and the Welch Foundation (AQ-0726) and to A.F. from the Société des Amis des Sciences].

NUCLEAR βII-TUBULIN AS A MARKER AND THERAPEUTIC TARGET IN BREAST CANCER

Ludueña, R.F., Banerjee, M., Moore, M., Walss, C., Barbier, P., Bissery, M.C. and Fellous, A.

Department of Biochemistry, University of Texas Health Science Center, San Antonio, TX, Laboratoire de Pharmacologie Expérimentale et Clinique, 75 Paris, France, and Rhône-Poulence-Rorer S.A., 94 Vitry sur Seine, France
luduena@uthscsa.edu

Using immunofluorescence microscopy, we have observed that the βII isotype of tubulin is located in the nuclei of a variety of cancer cells, including breast cancer cells. We have specifically seen βII in the nuclei of MCF-7 cells, Calc-18 cells and in breast tumor cells in situ. Interestingly, breast cancer cells lacking estrogen receptors sometimes have less βII in their nuclei. Using confocal microscopy, we also find that the βI, βIII, and βIV isotypes, all of which are expressed in MCF-7 cells, are not localized to the nuclei, but are restricted to the cytosol. In the case of βIV, much of it is concentrated in the perinuclear region, although not in the nucleus itself. The function of nuclear βII-tubulin is as yet unknown; we are attempting to use it as a target for anti-tumor drugs. We have designed a fluorescent peptide, containing a nuclear localization sequence; we have found that the peptide can efficiently enter the nucleus. We will be attaching the peptide to a derivative of colchicine, a drug that binds to tubulin and inhibits microtubule function. We have also synthesized an estradiol-colchicine derivative, which should also target the nucleus and we will compare the sensitivity to this compound of cancer cells with and without estrogen receptors.

The U.S. Army Medical Research and Materiel Command under DAMD17-98-1-8246 supported this work.

984

Effect of Taxol and Vinblastine on the βII Isotype of Tubulin in the Nuclei of Normal and Transformed Cells.

Consuelo Walss[1], Keliang Xu[1], Veena Prasad[1], Vivek Kasinath[1], Richard F. Luduena[2], [1]Univ of Texas Health science center, [2]Biochemistry, Univ of Texas Health Science Center, 7703 Floyd Curl Drive, San Antonio, Texas 78284

We have previously found that the βII isotype of tubulin is present in the nuclei of various cells, including rat mesangial cells and a variety of tumor cells. Taxol and vinblastine represent two different classes of drugs that target tubulin but have separate binding properties with different mechanisms of action. We investigated their effects on nuclear βII tubulin in different cell lines by immunofluorescence microscopy. With increasing concentrations of vinblastine and taxol, βII tubulin appears to move out of the nucleus. Normal mesangial cells require only low concentrations of vinblastine and taxol to see the effect whereas we need higher concentrations for prostate and breast cancer cells. Although vinblastine and taxol have different mechanisms of action on microtubules, the similar effect on nuclear βII may give an insight into the role of βII tubulin in the nucleus. (Supported by grants CA26376 from the N.I.H, DAMD17-98-1-8246 from the US army BCRP, and AQ-0726 from the Welch Foundation to R.F.L.)

Back
2177

Occurrence of the β II Isotype of Tubulin in the Nuclei of Ovarian Cancer Cells

Richard F. Luduena, Mohua Banerjee, Victoria Centonze, I-Tien Yeh, Oredius Pressley, University of Texas Health Science Center at San Antonio, San Antonio, TX.

Tubulin is a major target for anti-tumor drugs. We have previously found the beta-II isotype of tubulin in the nuclei of rat kidney mesangial cells and breast cancer cells. We have now searched for it in cultured SKOV3 ovarian cancer cells and in excisions of ovarian tumors. SKOV3 cells contained beta-II in their nuclei as well as in the cytoplasm. However, they contained the beta-I, beta-III and beta-IV isotypes only in the cytoplasm. Treatment of these cells with vinblastine caused changes in the nuclei, including the intra-nuclear distribution of beta-II, but did not appear to affect the cytoplasmic microtubules made of beta-II. Examination of 13 ovarian tumor biopsies showed 10 out of 13 contained nuclear beta-II. Out of 6 Stage I tumors, 1 had beta-II only in the cytoplasm, 3 had it in both cytoplasm and nuclei and 2 had it in the nuclei only. Out of 2 Stage 2 tumors, one had beta-II only in the nucleus and one only in the cytoplasm. Out of 5 Stage 3 tumors, 4 had beta-II only in the nucleus and 1 only in the cytoplasm. Another way of looking at the data is by cell type of origin. 9 out of 10 tumors of epithelial origin contained nuclear beta-II. Out of 3 tumors of non-epithelial origin, only 1 contained nuclear beta-II, and that only faintly. Normal epithelial cells visible in some of the biopsies appeared to contain beta-II only in the cytoplasm. Our results are consistent with a model whereby transformation, particularly in epithelial cells, is accompanied by movement of beta-II tubulin from the cytoplasm into the nucleus, with this movement being completed in Stage 1. Our results also raise the possibility that antitumor drugs may exert an effect on nuclear beta-II. It is intriguing that two of the most successful tubulin-targeting antitumor drugs, taxol and vinblastine, favor binding to the beta-II isotype. (Supported by grant DAMD17-98-1-8246 from the US Army BCRP and Welch Foundation grant AQ-0726 to R.F.L.)

From the Proceedings of the AACR, Vol. 42, March 2001.

Online Publication Date: February 27, 2001.
DOI: 10.1158/010101.

PB14

Effect of Taxol on the β_{II} Isotype of Tubulin in the Nuclei of Cancer Cells.

K. Xu and **R. F. Ludueña**.
University of Texas Health Science Center, San Antonio, Texas USA.

The β_{II} isotype of tubulin, which was thought to exist only in the cytoplasm of cells, has recently been observed in the nuclei of some cancer cells and hypothesized to play an important role in the proliferation and survival of cancer cells, raising the possibility that nuclear β_{II} tubulin may be a valuable target in cancer chemotherapy. In this study, nuclear β_{II} tubulin was also observed in rat C6 glioma cells, human T98G glioma cells, and human MCF-7 and MDA-MB-435 breast cancer cells. Given the fact that taxol is an anti-tumor drug with high specificity for β_{II} tubulin, the C6, MCF-7, and MDA cells were treated with taxol at different concentrations for 24 hours. As a result, β_{II} tubulin was observed to disappear in a dose-dependent manner from the nuclei of these cells, apparently moving into the cytoplasm. In contrast, nuclear β_{II} in these cells was not affected by treatment with nocodazole. These results support the hypothesis that nuclear β_{II} tubulin may play an important role in cancer cells and be a worthwhile target for cancer chemotherapy. Therefore, it may be a promising strategy to design new anti-tumor drugs with higher specificity for β_{II} tubulin. (Supported by US Army BCRP grant DAMD 17-98-1-8246, NIH grant CA26376, and Welch Foundation grant AQ-0726).

DEPARTMENT OF THE ARMY
US ARMY MEDICAL RESEARCH AND MATERIEL COMMAND
504 SCOTT STREET
FORT DETRICK, MARYLAND 21702-5012

REPLY TO
ATTENTION OF:

MCMR-RMI-S (70-1y) 26 Aug 02

MEMORANDUM FOR Administrator, Defense Technical Information Center (DTIC-OCA), 8725 John J. Kingman Road, Fort Belvoir, VA 22060-6218

SUBJECT: Request Change in Distribution Statement

1. The U.S. Army Medical Research and Materiel Command has reexamined the need for the limitation assigned to technical reports written for this Command. Request the limited distribution statement for the enclosed accession numbers be changed to "Approved for public release; distribution unlimited." These reports should be released to the National Technical Information Service.

2. Point of contact for this request is Ms. Kristin Morrow at DSN 343-7327 or by e-mail at Kristin.Morrow@det.amedd.army.mil.

FOR THE COMMANDER:

Encl

PHYLIS M. RINEHART
Deputy Chief of Staff for
Information Management

ADB274369
ADB256383
ADB264003
ADB274462
ADB266221
ADB274470
ADB266221
ADB274464
ADB259044
ADB258808
ADB266026
ADB274658
ADB258831
ADB266077
ADB274348
ADB274273
ADB258193
ADB274516
ADB259018
ADB231912
ADB244626
ADB256677
ADB229447
ADB240218
ADB258619
ADB259398
ADB275140
ADB240473
ADB254579
ADB277040
ADB249647
ADB275184
ADB259035
ADB244774
ADB258195
ADB244675
ADB257208
ADB267108
ADB244889
ADB257384
ADB270660
ADB274493
ADB261527
ADB274286
ADB274269
ADB274592
ADB274604

ADB274596
ADB258952
ADB265976
ADB274350
ADB274346
ADB257408
ADB274474
ADB260285
ADB274568
ADB266076
ADB274441
ADB253499
ADB274406
ADB262090
ADB261103
ADB274372